INFORMATION TO USERS

This manuscript has been reproduced from the microfilm master. UMI films the text directly from the original or copy submitted. Thus, some thesis and dissertation copies are in typewriter face, while others may be from any type of computer printer.

The quality of this reproduction is dependent upon the quality of the copy submitted. Broken or indistinct print, colored or poor quality illustrations and photographs, print bleedthrough, substandard margins, and improper alignment can adversely affect reproduction.

In the unlikely event that the author did not send UMI a complete manuscript and there are missing pages, these will be noted. Also, if unauthorized copyright material had to be removed, a note will indicate the deletion.

Oversize materials (e.g., maps, drawings, charts) are reproduced by sectioning the original, beginning at the upper left-hand corner and continuing from left to right in equal sections with small overlaps.

Photographs included in the original manuscript have been reproduced xerographically in this copy. Higher quality 6" x 9" black and white photographic prints are available for any photographs or illustrations appearing in this copy for an additional charge. Contact UMI directly to order.

Bell & Howell Information and Learning
300 North Zeeb Road, Ann Arbor, MI 48106-1346 USA

UMI®
800-521-0600

IDENTIFICATION AND CHARACTERIZATION OF RABBIT HEPATIC RECEPTORS FOR THROMBIN-ANTITHROMBIN COMPLEXES

By

Michael John Wells, B.Sc.

A Thesis

Submitted to the School of Graduate Studies

in Partial Fulfilment of the Requirements

for the Degree

DOCTOR OF PHILOSOPHY

SCIENCE

McMaster University

HEPATIC RECEPTORS FOR THROMBIN-ANTITHROMBIN

DOCTOR OF PHILOSOPHY (1996)
(Science)

McMaster University
Hamilton, Ontario

TITLE: Identification and Characterization of Rabbit Hepatic Receptors for Thrombin-Antithrombin Complexes

AUTHOR: Michael John Wells, B.Sc. (University of Guelph)

SUPERVISOR: Dr. M.A. Blajchman

NUMBER OF PAGES: xxi, 216

ABSTRACT

Antithrombin (AT)-mediated inhibition of thrombin is important in the maintenance of hemostasis. This importance is emphasised by the fact that people with AT deficiencies are at greater risk of developing thrombophilia. AT inhibits thrombin by forming a covalent 1:1 stoichiometric thrombin-antithrombin complex (TAT) and such formed complexes rapidly are removed from the circulation by hepatic receptors. The main aim of my doctoral thesis project has been to identify and characterize these hepatic receptors.

Competitive radioligand binding experiments demonstrated a low-affinity ^{125}I-TAT binding site on hepatic membranes. Ligand-blotting on rabbit liver plasma membranes was used to identify TAT-binding polypeptide(s). These experiments showed that ^{125}I-TAT interacted specifically with a 45 kDa protein which was identified as cytokeratin 18 (CK18) by amino acid sequencing. The biological relevance of this unusual interaction was verified by the presence of CK18 on the surface of rat and human hepatoma cells and the ability of anti-CK18 IgG, but not preimmune IgG, to inhibit TAT binding and internalization by these cells. Finally, the increased binding of ^{131}I-anti-CK18 IgG over ^{125}I-preimmune IgG to perfused rabbit livers supported the possibility that CK18 is expressed on the surface of hepatocytes in vivo. As a whole, these data indicate

a novel biological role for cytokeratins as cellular receptors.

The secondary aim of my thesis was to examine the metabolism of TAT when contained in a ternary complex with vitronectin (VN-TAT). Plasma clearance experiments revealed that VN-TAT was removed rapidly from the circulation by hepatic binding sites. Binding to these sites was found to be heparin-sensitive such that either heparin or protamine sulfate extends the VN-TAT clearance time ($t_{½\alpha}$) ten to fifteen fold. Similarly, *in vitro* radioligand binding studies on hepatoma cells indicate that VN-TAT binds to low affinity heparinoid sites. Furthermore, heparin greatly reduced the internalization and degradation of VN-TAT by HepG2 cells. These data demonstrate for the first time that VN-TAT, at least partially, is cleared by hepatic sites which are most likely heparan sulfate in nature.

ACKNOWLEDGEMENTS

I would like to thank my supervisor Dr. Mo Blajchman for believing in me and taking me on as his student, sharing his wealth of knowledge, for his generosity, and for his optimism and support, which helped me through many hard times. I would also like thank all the members of my supervisory committee for their guidance, especially Dr. Mark Hatton for his support and enlightening conversation. A special mention also goes to Dr. Bill Sheffield who patiently fielded my persistent barrage of questions and stimulating my scientific interest. Thanks also goes to the Heart and Stroke Foundation of Canada for their financial support.

I have to acknowledge a large number of people who have put up with my insanity all these years and always supported me. Firstly, I would like to thank all the great people that have been in the laboratory during my tenure. I wish you all the best in the future. A special thanks goes to Mr. Myron Kulczyky for all his technical help, both scientific and automotive. Thanks to both Summer Syed and Mike Cunningham for being good friends and also Rob, Scott, and Tim, for being the best friends in the world. To all the many people at McMaster who have come and gone, I won't forget you and all the good times you brought. I can't thank my parents and family enough, for all the love and support they have given me over the years, without you none of this would have been possible. Finally, I would like to thank my girlfriend Lori who has always supported me, through good and bad, I love you very much.

TABLE OF CONTENTS

LIST OF FIGURES

LIST OF TABLES

LIST OF SYMBOLS AND ABBREVIATIONS

a_n	clearance rate constant
α	alpha
α-AC	alpha$_1$-antichymotrypsin
α-AT	alpha-antithrombin
α-MEM	alpha-minimum essential medium medium
α-PI	α_1-proteinase inhibitor
α_2-AP	α_2-antiplasmin
α_2M	alpha$_2$-macroglobulin
α_2M*	methylamine-modified alpha$_2$-macroglobulin
Ala	alanine
AP	alkaline phosphatase
apoE	apolipoprotein E
APS	ammonium persulphate
Arg	arginine
Asn	asparagine
Asp	aspartic acid
AT	antithrombin
AT-ß	ß-isoform of antithrombin
AT-II	antithrombin-II
AT-III	antithrombin-III
ATP	adenosine 5'-triphosphate

ß	beta
BCIP	5-bromo-4-chloro-3-indolyl phosphate
ß-D-xyloside	p-nitrophenyl ß-D-xylopyranoside
BHK	mouse fibroblast cell line
5% blotto	tris-buffered saline containing 5% (w/v) non-fat dry milk
BSA	bovine serum albumin
cDNA	complementary deoxyribonucleic acid(s)
C_n	clearance constant
$CaCl_2$	calcium chloride
CHO	Chinese hamster ovary
CK	cytokeratin(s)
CK8	cytokeratin 8
CK18	cytokeratin 18
CNBr	cyanogen bromide
COS	transformed African green monkey kidney cells
C-terminal	carboxyl terminal
Cys	cysteine
Da	Dalton(s)
°C	degrees Celsius
DCI	dichloroisocoumarin
dd H_2O	deionized and distilled water
DEAE	diethyl aminoethyl

DMEM	Dulbecco's modified eagle medium
DMSO	dimethyl sulphoxide
DNA	deoxyribonucleic acid(s)
dpm	disintegrations per minute
EBS	epidermolysis bullosa simplex
EDTA	ethylenediaminetetraacetic acid
EH	epidmermolytic hyperkeratosis
ELISA	enzyme-linked immunosorbent assay
EPPK	epidermolytic palmoplantar keratoderma
F	free radioligand concentration
FBS	fetal bovine serum
FVFLM	phenylalanine-valine-phenylalanine-leucine-methionine
γ	gamma
g	gram(s)
Gln	glutamine
Glu	glutamic acid
GPI	glycosyl phosphatidyl inositol
gp330	glycoprotein 330/megalin/Heymann nephritis antigen/ LRP 1
HEPES	N-2-hydroxyethylpiperazine-N'-2-ethanesulfonic acid
HepG2	human hepatocellular carcinoma cell line
His	histidine
h	hour(s)

HCII	heparin cofactor II
HCl	hydrochloric acid
HBS	hepes-buffered saline
HBSB	hepes-buffered saline containing 0.5% (w/v) bovine serum albumin
HPLC	high pressure liquid chromatography
HSPG	heparan sulphate proteoglycan
HTC	rat hepatoma cell line
HT29	human colonic carcinoma cells
HUVECs	human umbilical vein endotheliai cells
IC_{50}	concentration at which 50% inhibition occurs
IF	intermediate filament(s)
IgG	immunoglobulin G
K_d	dissociation constant
K_i	inhibition constant
kDa	kiloDalton(s)
l	litre(s)
Leu	leucine
LDL	low density lipoprotein
LRP	low density lipoprotein receptor-related protein/ alpha$_2$-macroglobulin receptor/ LRP
LRP2	low density lipoprotein receptor-related protein/ alpha$_2$-macroglobulin receptor
Lys	lysine

μCi	microcurie(s)
μg	microgram(s)
μl	microlitre(s)
μm	micrometre(s)
μM	micromolar
M	molar
Met	methionine
mg	milligram(s)
$MgCl_2$	magnesium chloride
min	minute(s)
ml	millilitre(s)
mM	millimolar
mm	millimetre(s)
mRNA	messenger ribonucleic acid(s)
mVN	multimeric vitronectin
NBT	nitro blue tetrazolium
ng	nanogram(s)
NIH-3T3	hamster kidney cell line
nM	nanomolar
NMR	nuclear magnetic resonance
N-terminal	amino terminal
N	Nitrogen

p	percent specifically bound
PAGE	polyacrylamide gel electrophoresis
PAI-1	plasminogen activator inhibitor-1
PAI-2	plasminogen activator inhibitor-2
PBS	phosphate buffered saline
Phe	phenylalamine
pM	picomolar
PMSF	phenylmethylsulfonyl fluoride
PN-I	protease nexin I
PPACK	D-phenyl-L-prolyl-L-arginyl-chloromethylketone
Pro	proline
PVDF	polyvinylidene difluoride
RAP	receptor-associated protein
RCL	reactive centre loop
RFLP	restriction fragment length polymorphisms
rpm	revolutions per minute
RT	room temperature
SBTI	soybean trypsin inhibitor
SEC	serpin-enzyme complex
SECR	serpin-enzyme complex receptor
SEM	standard error of the mean
SDS	sodium dodecyl sulphate

SDS-PAGE	sodium dodecyl sulphate polyacrylamide gel electrophoresis
Ser	serine
serpin	serine proteinase inhibitor
SP	sulfo-propyl
STEP	solution buffered with 10 mM Tris-HCl (pH=7.4) and containing 0.25 M sucrose, 1 mM EDTA, and 1 mM phenyl-methylsulfonyl fluoride
$t_{½}$	half-life
$t_{½\alpha}$	half-life of alpha-clearance phase
$t_{½\beta}$	half-life of beta-clearance phase
TAT	thrombin-antithrombin complex
TBS	tris-buffered saline
TBST	tris-buffered saline with tween-20
TCA	trichloroacetic acid
TF	tissue factor
TFPI	tissue factor pathway inhibitor
Thr	threonine
tPA	tissue-plasminogen activator
TPA	tissue polypeptide antigen
TRAP	trypsin-alpha$_1$-proteinase inhibitor complex
Tris	tris(hydroxymethyl)aminomethane
Trp	tryptophan
UV	ultraviolet

μg	microgram(s)
μM	micromolar
V	volt(s)
Val	valine
VN	vitronectin
VN-TAT	vitronectin-thrombin-antithrombin complex
v/v	volume:volume ratio
uPA	urokinase plasminogen activator
uPAR	urokinase plasminogen activator receptor
U937	human monocytoid cell line
w/v	weight:volume ratio
WISH	cell line derived from human amnion tissue

1. INTRODUCTION

Serine proteinases are a family of proteins which hydrolyze peptide bonds using an active site serine residue. This large and ancient family of enzymes contains many members whose functions include roles in digestion, blood coagulation, fibrinolysis, and the complement system. One of the most studied members of this family is the penultimate coagulation enzyme α-thrombin. Although α-thrombin has a wide variety of physiological functions it is classically known for its role in coagulation and the formation of a fibrin clot. The coagulation system consists of a complex series of enzymatic reactions culminating in the formation of the fibrin clot. During these reactions there is a successive conversion of inactive zymogens into active serine proteinases, leading to the ultimate end-product of the coagulation cascade, α-thrombin. α-Thrombin then proteolytically cleaves soluble fibrinogen to form insoluble fibrin, subsequently forming the cross-linked fibrin clot.

To ensure that these proteinases do not continue to act unchallenged and therefore cause excessive damage in the host organism, nature has evolved a system of proteins to regulate the enzymatic activity of the serine proteinases. The largest group of proteins to control the serine proteinases are members of the serine proteinase inhibitor family, or *serpins*. The serpin family includes both inhibitory proteins, which inhibit their cognate proteinases, and proteins with no

known inhibitory function. The inhibitory serpins are suicide inhibitors which inhibit serine proteinases through the formation of a 1:1 stoichiometric covalent serpin-enzyme complex (SEC). The inhibitory serpins include antithrombin (AT), α_1-proteinase inhibitor (α-PI), α_1-antichymotrypsin (α-AC), heparin cofactor II (HCII), plasminogen activator inhibitors (PAI) I and II, α_2-antiplasmin (α_2-AP) and proteinase nexin I (PN-1) (Carrell *et al.*, 1987). In plasma, the main physiological inhibitor of thrombin is the serpin, AT. AT inhibits thrombin activity by forming a covalent 1:1 stoichiometric complex with thrombin (TAT).

SECs are not stable and can break down resulting in the release of cleaved inhibitor and active proteinase. Physiologically, it is important to remove these complexes quickly before they can degrade and release active enzyme. Plasma elimination studies of various radiolabelled SEC, including TAT, have revealed that they are rapidly removed from the circulation mediated mainly by hepatic receptors. In the following pages I give an overview on AT and the serpins, what is currently known about different candidate SEC receptors, and report on data acquired from my studies identifying cytokeratin 18 as a TAT-binding protein.

1.1 Antithrombin: Historical Background

The term 'antithrombin' was first used by Morowitz (1905) who described a circulating plasma or serum substance that inhibited thrombin. Later, the

anticoagulant nature of heparin was found to be dependent upon the presence of an unidentified plasma component, which was termed heparin cofactor (Brinkhous *et al.*, 1939). When several different antithrombin activities were found, a numerical classification scheme for the antithrombotic activities was devised by Seegers *et al.*(1954). Antithrombin-I was described as the ability of a fibrin clot to absorb thrombin. Antithrombin-II (AT-II) was described as the heparin cofactor activity, and Antithrombin-III (AT-III) represented the plasma or serum component responsible for the progressive inhibition of thrombin. The description of a family with recurrent venous thromboembolism shed light on the nature of AT-II and AT-III (Egeberg, 1965). Affected members of this family showed a partial loss of both heparin cofactor and progressive AT activity, indicating that AT-II and AT-III were possibly the same. Further support for this possibility came from Abilgaard (1967; 1969), who isolated an α_2-globulin that had both progressive and heparin cofactor activities. It was not until Rosenberg and Damus (1973) first isolated large quantities of this protein, that convincing evidence was provided that the proteins possessing progressive and heparin cofactor activities were indeed identical. This protein was designated AT-III. In 1993 a subcommittee of the Scientific and Standardization Committee of the International Society of Thrombosis and Haemostasis was formed to study AT-III nomenclature (Lane *et al.*, 1993). Although no consensus was found at this meeting, the bulk of AT investigators favoured the name AT for AT-III, and it is now the officially accepted term for AT-III.

1.2 The Biochemistry of Antithrombin

1.2.1 Structure of Antithrombin

Human AT is a single-chain plasma glycoprotein with a molecular mass of ~60 kDa (Rosenberg and Damus, 1973; Petersen *et al.*, 1979). Human plasma AT is composed of 432 amino acids (Bock *et al.*, 1982; Prochownick *et al.*, 1983a; Stackhouse *et al.*, 1983) with three disulfide linkages, between cysteine residues 8 and 128, 21 and 95, and 247 and 430 (Petersen *et al.*, 1979; Sun and Chang, 1989). AT has four N-linked biantennary glycosidic side chains, which comprise 9-15% of the molecular mass of AT, at asparagine (Asn) residues 96, 135, 155, and 192 respectively (Petersen *et al.*, 1979; Franzen *et al.*, 1980; Mizuochi *et al.*, 1980). Biochemical analysis of the glycosidic side chains revealed them to be complex biantennary oligosaccharides with terminal sialic acid residues (Danishefsky *et al.*, 1977; Franzen *et al.*, 1980). The isoelectric point of purified AT ranges from 4.7 to 5.2 and is a reflection of charge heterogeneity in the terminal sialic acid residues of the glycosidic side chains (Borsodi and Narasimhan, 1978; Daly and Hallinan, 1985). Approximately 10% of plasma AT is found lacking the glycosidic side-chain at Asn 135 and is denoted as being AT-ß (Petersen and Blackburn, 1985; Brennan *et al.*, 1987). The tertiary structure, deduced by analogy to the three-dimensional crystal structure of cleaved α_1-proteinase inhibitor (α-PI) (Loeberman *et al.*, 1984: Carrell *et al.*, 1987a,b) and by peptide modelling on the amino acid sequence (Villanueva, 1984), consists of

31% α-helix, 16% ß-sheet, 9% ß-turn, and 44% random coil. Since then the crystal structures of cleaved bovine AT (Mourey *et al.*, 1990), dimeric human AT (Schreuder *et al.*, 1994; Carrell *et al.*, 1994), and AT complexed with a heparin-derived pentasaccharide (Carrell *et al.*, 1997) have been defined and support the modelling data. From these strudies AT has been determined to contain three ß-sheets, designated sheets A, B, and C, and 9 α-helices, designated from A to I. A model of these structures is shown in Figure 1., using the crystal structure of dimeric-AT as a model for native AT.

1.2.2 Molecular Biology of AT

Molecular biological techniques have revolutionized the biochemical analysis of AT. Molecular cloning allowed the elucidation of the AT cDNA and the AT gene. The human AT gene is located on the long arm of chromosome 1, in the region 1q23-25 (Kao *et al.*, 1984; Bock *et al.*, 1985b). The human AT gene is composed of 13,477 base pairs from the 5' transcription start site to the 3' polyA tail (Olds *et al.*, 1993). In all, the gene is composed of 7 exons and 6 introns (Prochownick *et al.*, 1983; Jagd *et al.*, 1985; Bock *et al.*, 1988). The cloning of the AT cDNA was accomplished by three independent groups in the years 1982 and 1983 (Bock *et al.*, 1982; Prochownick *et al.*, 1983a; Stackhouse *et al.*, 1983). The coding region of the human AT cDNA has an open reading frame of 1392 nucleotides. The first 96 nucleotides of the open reading frame encode a 32 amino acid signal peptide with the final 1296 nucleotides encoding the mature protein. cDNAs for rabbit and mouse have been isolated and characterized by

FIGURE 1. Three-dimensional structure of AT adapted from Whisstock *et al.*(1996). The nine α-helices are coloured blue. The A, B, and C β-sheets are coloured red, green, and yellow respectively. The reactive centre loop is indicated in purple. The reactive centre residues P1 and P1' are indicated and the pre-inserted residues P14-P15, which are expelled upon heparin binding, are also indicated. The location of the putative serpin-enzyme complex receptor-binding pentapeptide (FLVFI) is also indicated. This figure was reprinted from Whisstock *et al.* (1996) (Copyright ©1996, Wiley-Liss Inc.) with permission of John Wiley & Sons, Inc.

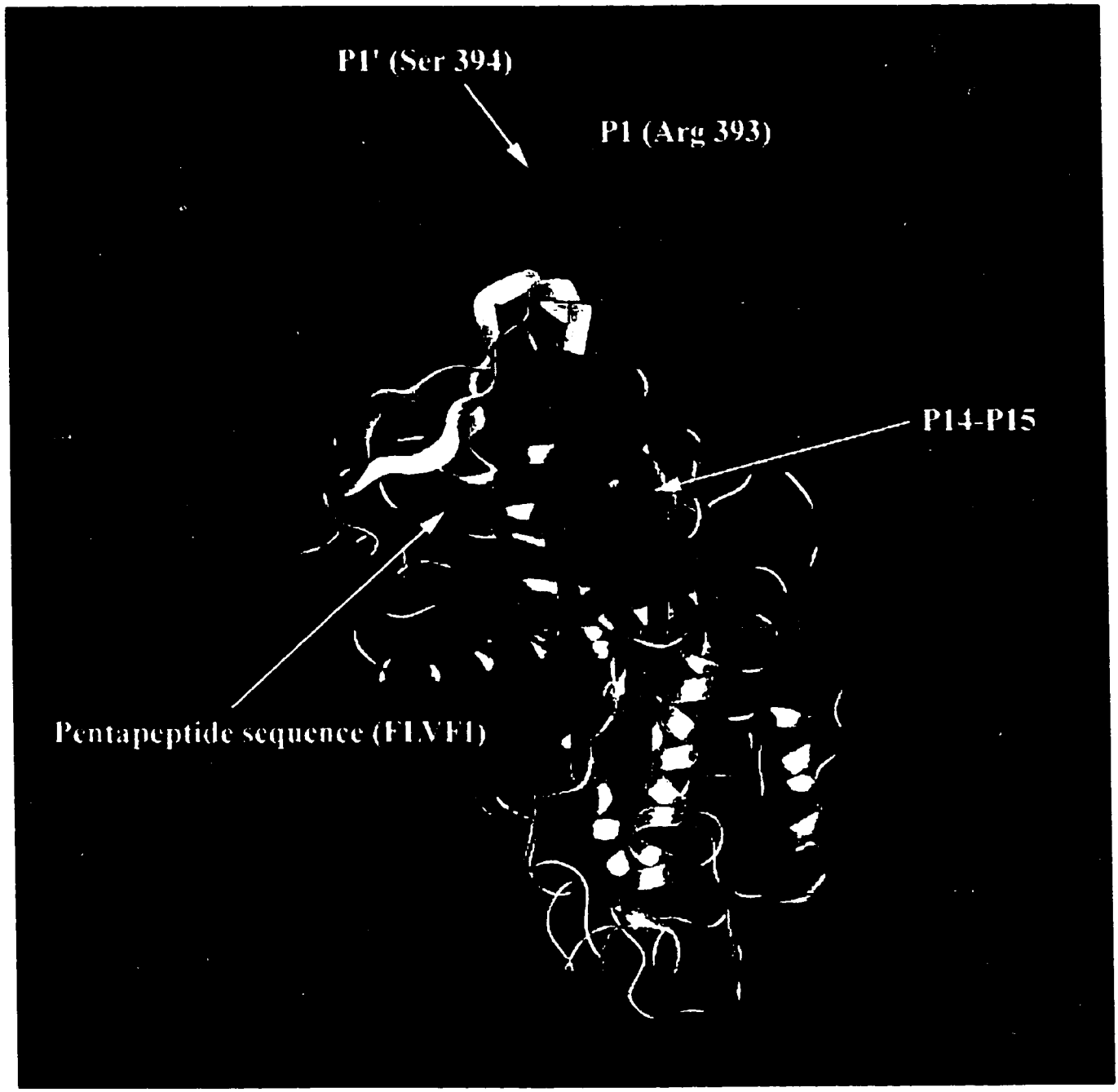
P1' (Ser 394)
P1 (Arg 393)
P14-P15
Pentapeptide sequence (FLVFI)

Dr. Blajchman and colleagues (Sheffield *et al.*, 1992; Wu *et al.*, 1992). The rabbit cDNA is 1359 nucleotides in length and encodes for a mature protein of 433 amino acids while the mouse cDNA is 1398 nucleotides in length and encodes a full length protein of 433 amino acids. Additionally, the cDNAs for sheep (Niessen *et al.*, 1992) and chicken AT (Tejada and Deeley, 1995) have also been resolved.

1.2.3. Homology Between the AT From Different Species

The complete primary amino acid sequence has been determined from cDNAs derived from human (Bock *et al.*, 1982; Prochownick *et al.*, 1983a; Stackhouse *et al.*, 1983), rabbit (Sheffield *et al.*, 1992), mouse (Wu *et al.*, 1992), chicken (Tejada and Deeley, 1995), and sheep sources (Niessen *et al.*, 1992). The complete amino acid sequence for porcine (Tokunaga *et al.*, 1994) and bovine AT (Medjoub *et al.*, 1991), and a partial sequence for rat AT (Tokunaga *et al.*, 1979), have been determined by amino acid sequencing. Relative to the human protein, the other mammalian antithrombins have 84-91% amino acid sequence identity, while chicken AT has 69% amino acid sequence identity. Although the amino acid sequences of human, rabbit, mouse, and pig AT encode for proteins of identical mass, SDS-PAGE analysis of the purified proteins shows that the ATs of the different species are of dissimilar mass (Koide, 1979; Wu *et al.*, 1992). These differences are assumed to be due to the different degrees of glycosylation on the different polypeptides (Wu *et al.*, 1992). In all species, AT contains four conserved potential glycosylation sites, except the chicken, which has a potential

glycosylation site at Asn 164 instead of 96 (Tejada and Deeley, 1995). Additionally, purified rabbit plasma AT, like human AT, has also been shown to be found in two isoforms; 90% α and 10% ß (Carlson and Atencio, 1982; Brennan *et al.*, 1987). Finally, the six cysteines are conserved in all species indicating their structural necessity for AT function.

1.2.4. Biosynthesis of AT

AT is synthesized and secreted by the liver (Watada *et al.*, 1981; Leon *et al.*, 1983) and other tissues, such as endothelium (Lee *et al.*, 1979). The liver is the major site of AT production, a fact supported by the fact that individuals with liver disease have greatly reduced AT plasma levels (Ratnoff, 1982; Lechner *et al.*, 1977). Furthermore, the human hepatoma cell line, HepG2, has been shown to synthesize and secrete AT with similar size and behaviour as plasma derived AT (Fair and Bahnak, 1984). AT protein has also been reported to be secreted by cultured endothelial cells (Chan and Chan, 1981) and mRNA encoding AT has been detected in human leukocytes (Perry and Carrell, 1992), rat kidney (D'Souza and Mercer, 1987), and human brain (white and grey matter) (Kalaria *et al.*, 1993). However, work done in our laboratory suggests that neither rabbit (Sheffield *et al.*, 1992) nor human kidneys contain AT transcripts (personal communication from Dr. W.P. Sheffield, unpublished data). Although the liver is the major source of AT production, other tissues appear to have the capability to produce small amounts of AT, which may play important roles in regulating local proteolytic events. Finally, the biosynthesis of the ß-AT isoform has been

examined (Picard *et al.*, 1995). The presence of serine instead of threonine in the glycosylation consensus sequence, asn-X-ser/thr/cys, results in partial glycosylation at Asn 135 of AT polypeptides.

1.2.5. Distribution and Metabolism of AT

Human AT is found in the plasma at a concentration of 2-3 μM (150 - 200 mg/l) (Chan *et al.*, 1979; Conard *et al.*, 1983). AT is found in very low levels in the cerebrospinal fluid at a concentration between 80 and 400 nM (Bleyl, 1981). Bleyl (1981) also found that AT is excreted in the urine, in an inactive form, at a concentration of 30 to 50 μg/day. AT has also been found associated with platelets (Gursoy and Ulutin, 1983; Alhenec-Gelas *et al.*, 1985). Stimulated platelets were found to release AT which was biologically active and immunologically similar to plasma AT. However, the biological relevance of this observation is unknown, since the concentration of AT within the platelets was found to be only 1.5 pM, which is 10^6 lower than plasma levels.

The *in vivo* metabolism of AT has been found to be best described by a three-compartment model, in both rabbits (Carlson *et al.*, 1984) and humans (Knot *et al.*, 1986). The half-life of AT has been found to be ~ 2.8 days ($t_{½\beta}$) in normal humans (Collen *et al.*, 1977; Knot *et al.*, 1986) and ~ 2.3 days in rabbits (Vogel *et al.*, 1979). Examination of the half-life of AT in AT deficient patients gave a similar value of ~ 2.6 days (Menache *et al.*, 1990) and was not significantly different in patients orally anticoagulated with coumarin and those not. Heparin, has been shown to reduce the half-life of AT in a small number of patients with

deep vein thrombosis and treated with heparin compared to AT clearance in normal individuals or patients not on heparin (Collen *et al.*, 1977). de Swart *et al.* (1984) found that co-administration of heparin and AT in normal individuals resulted in an increased clearance of AT in humans. In baboons, a small bolus of heparin was found not to alter the clearance of either ^{131}I-AT or ^{125}I-HCII (Sie *et al.*, 1986). In contrast, Carlson (1989) found that co-injection of AT and heparin resulted in the decreased clearance of AT in rabbits. The observed differences might be accounted for by different doses of heparin administration, species variations, and the physical state of the animal or person.

1.3. The Physiological Function of AT

The physiological function of AT is the irreversible inhibition of various serine proteinases. AT forms 1:1 stoichiometric complexes with various proteinases including plasma clotting factors IIa (thrombin), IXa, Xa, XIa, as well as plasmin, trypsin, and kallikrein (Sheffield *et al.*, 1995). Of these, the interaction with thrombin, factor Xa, and possibly factor IXa appear to be the most physiologically relevant. The inhibition of thrombin and factor Xa is slow in the absence of heparin but is greatly accelerated in its presence (Olson *et al.*, 1992). This property of heparin accounts for its widespread clinical use as an anticoagulant and antithrombotic agent (Hirsh, 1991). More recently, AT has also been found to inhibit the factor VIIa/tissue factor complex, although the rate of

factor VIIa/TF inhibition by AT in solution is very slow (Lawson *et al.*, 1993). Recent evidence indicates that AT, in the presence or absence of heparin, can inhibit cell-surface factor VIIa/tissue factor, which is further enhanced in the presence of factor Xa and IXa (Rao *et al.*, 1996; Hamamoto *et al.*, 1996). These observations support the concept that AT has a physiological role in factor VIIa inhibition and suggests that AT inhibition of coagulation proteinases occurs at various levels of the coagulation cascade.

1.3.1. Interaction with Thrombin

AT forms an irreversible 1:1 molar complex with thrombin through the interaction of its reactive centre with the active site of thrombin (Rosenberg and Damus, 1973). The AT reactive centre residues involved in forming the covalent complex have been determined to be Arg^{393}-Ser^{394} (Jornvall *et al.*, 1979; Bjork *et al.*, 1981; Bjork *et al.*, 1982) (see Figure 1). Complex formation is initiated when thrombin cleaves the peptide bond between Arg^{393}-Ser^{394} (Fish *et al.*, 1979; Bjork *et al.*, 1982). These two residues are designated as P1 and P1' using the nomenclature of Schechter and Berger (1967). In this labelling system residues N-terminal from the scissile bond are numbered successively (ie P1, P2, P3 etc) while residues C-terminal to the scissile bond are enumerated (ie P1', P2', P3' etc). In the three-dimensional structure of AT, the reactive centre is contained within an exposed mobile loop, called the reactive centre loop (RCL), rising from the main body of the protein, presenting the reactive centre in an ideal substrate conformation (see Figure 1) (Carrell *et al.*, 1991; Schreuder *et al.*, 1994; Carrell

et al., 1994).

The cleaved complex is stabilized by the formation of an acyl ester bond between the carboxyl group of Arg^{393} and the hydroxyl side group of the reactive site serine of thrombin (Owen *et al.*, 1975; Longas *et al.*, 1980; Bjork *et al.*, 1982). This acyl-bond is then protected from hydrolysis through a large conformational change in the TAT complex caused by insertion of the RCL into the A ß-sheet (discussed further in Section 2.2.1). The covalent nature of TAT is supported by the fact that it is resistant to breakdown in the presence of SDS and also by the greatly reduced affinity of AT for ß-anhydrotrypsin, a form of trypsin which has its active site serine blocked (Olson *et al.*, 1995).

If AT is not present in sufficient excess over thrombin then the formation of cleaved AT, proteolyzed at the reactive centre, occurs (Bjork *et al.*, 1981). Cleaved AT is also found *in vivo* and is a marker for thrombin generation and activation of the coagulation system (Lindo *et al.*, 1995). Additionally, during TAT formation *in vitro* there are additional smaller SDS-stable complexes seen on SDS-PAGE analysis. The amounts and rate of formation of these smaller complexes is dependent upon the molar ratios of the inhibitor and proteinase used in complex formation, and they are increased with excess levels of thrombin. Western blotting has revealed that these smaller complexes contain both AT and thrombin, and are most likely to be AT complexed with the thrombin autoproteolytic products, ß and γ thrombin (Witmer and Hatton, 1991).

The importance of the reactive centre residues is indicated by natural and

engineered mutants which demonstrate that both residues confer specificity for thrombin (Stephens *et al.*, 1987; Stephens *et al.*, 1988; Erdjument *et al.*, 1988; Theunissen *et al.*, 1993; Olson *et al.*, 1995). A number of mutations within the RCL have been found and affect the ability of AT to inhibit thrombin. Mobility of the RCL appears to be essential for AT-thrombin interaction as mutations within the RCL that reduce this mobility lead to severe dysfunction of AT (Carrell and Evans, 1992; Sheffield *et al.*, 1995). However, other mutations outside the RCL have also been found to result in reduced or abolished thrombin inhibition, indicating the sensitive relationship between AT protein structure and function (Perry, 1994).

1.3.2. Interaction with Heparin

Heparin is a highly sulfated heterogeneous linear polysaccharide. In its absence, AT inhibits thrombin in a relatively slow fashion but in the presence of heparin the reaction is accelerated several thousand fold (Jordan *et al.*, 1980; Olson and Bjork, 1991). Two different models have been proposed as to how heparin catalyzes the AT inhibition of thrombin and Xa. For AT inhibition of thrombin, heparin acts as a bridge, binding to both thrombin and AT (Griffith, 1982). In this case, a long chain heparin (at least 18 monosaccharide units long) is required, that contains a high affinity pentasaccharide sequence necessary for optimal catalysis of AT inhibition of thrombin (Choay *et al.*, 1983; Atha *et al.*, 1984). For factor Xa inhibition, heparin induces a conformational change in AT that enhances its inhibition of factor Xa (Olson *et al.*, 1992) In this case, the

pentasaccharide is sufficient to optimally catalyze factor Xa inhibition (Lane *et al.*, 1984; Olson *et al.*, 1992).

The heparin binding site on AT has been mapped from chemical modification studies (Peterson *et al.*, 1987) and from natural and site-directed AT mutants with diminished heparin binding (Lane *et al.*, 1993; Sheffield *et al.*, 1995). These studies have implicated positively charged asparagine and lysine residues in the N-terminus of AT that form the A and D α-helices (Huber and Carrell, 1992; Carrell, 1992). The recently determined crystal structures of AT have shed light on how heparin catalyzes AT inhibition of proteinases. From these structures the positively charged residues are clustered into a defined region on α-helices A and D, similar to the model mentioned above (Schreuder *et al.*, 1994; Carrell *et al.*, 1994). In these structures there is a partial insertion of the RCL residues, P14 and P15, into the A ß-sheet (Figure 1). This structural feature fits in with a recently proposed model of heparin activation of AT (van Boekel *et al.*, 1994). In this model, heparin is proposed to act by causing a conformational change in the D-helix that is transmitted to the RCL, resulting in expulsion of the RCL from the A ß sheet, and therefore, moving AT into a more suitable inhibitory conformation . This model is supported by increased fluorescence in a P14 serine to tryptophan AT variant, upon heparin binding, indicating the exposure of the tryptophan preinserted into the A ß-sheet (Huntington *et al.*, 1996).

1.4 The Serpin Superfamily of Proteins

AT is a member of the superfamily of proteins named the serine proteinase inhibitors, or *serpins* (Carrell and Travis, 1985). The existence of this superfamily of proteins was first proposed by Hunt and Dayhoff who recognized the resemblance of the primary amino acid sequences between ovalbumin, AT, and α-PI (Hunt and Dayhoff, 1980). Since then there has been an explosion in the discovery of new members of the serpin family, such that now there are over a 100 proteins in this family if species variants and gene products, represented by cDNA sequences, are included (Gettins *et al.*, 1996).

Interestingly the term "serpin" is somewhat of a misnomer since there are a number of non-inhibitory serpins, including not only ovalbumin, but angiotensinogen (Doolittle, 1983), corticosteroid-binding globulin (Hammond *et al.*, 1987), thyroxine-binding globulin (Flink *et al.*, 1986), the more recently discovered maspin (Zou *et al.*, 1994), and others. Furthermore, there are even serpins whose cognate proteinases are not serine proteinases, but are cysteine proteinases. These include the cowpox viral protein CrmA (Komiyama *et al.*, 1994), a squamous cell carcinoma antigen (Takeda *et al.*, 1995), and an α-A-C-ke protein (Hook *et al.*, 1993).

Recently a subfamily has been proposed within the serpin family (Remold-O'Donnell, 1993). This proposed subfamily is based on protein and gene similarities to ovalbumin. These physical similarities include higher than usual

sequence identity (40-60%) compared to the rest of the serpin family, the absence of a cleavable hydrophobic signal sequence, and related gene intron and exon organization.

The serpins are an ancient family of proteins, having descended from a common ancenstral gene 500 million years ago (Dayhoff and Hunt, 1980; Bao *et al.*, 1987). Serpins are found in a wide range of species, in man and other mammals, in birds, in fish, in amphibians, in plants, even down to the level of viruses (Gettins *et al.*, 1996). Human plasma serpins have been the main focus of study and are the best characterized serpins. The plasma serpins provide an excellent example of positive Darwinian selection such that individual serpins have evolved in parallel with their cognate proteinases (Carrell *et al.*, 1989; Goodwin *et al.*, 1996). All serpins contain a core domain of ~ 400 amino acids and over time N and/or C-terminal extensions have evolved resulting in the development of specialized functions, such as heparin binding to AT. The relationship between serpins in this core domain is not a reflection of high primary sequence homology, since there is only ~ 30% homology between serpin members, but is through the translation of this core domain into homologous tertiary architecture (Gettins *et al.*, 1996). In this regard, all serpins have a homologous tertiary, structure composed of three ß-sheets and nine α-helices.

1.4.1. Mechanism of Proteinase Inhibition By Serpins

The simplest mechanism describing the interactions of inhibitory serpins (I) with serine proteinases (E) is that of a two branched mechanism (Rubin *et al.*,

1990; Patston *et al.*, 1991). In this scheme the serpin reactive centre forms an initial low affinity reversible complex with the active site of the proteinase, called a Michaelis complex (E-I). Following formation of the initial encounter complex the proteinase and serpin form an intermediary complex which is the branchpoint for complex or substrate formation (O'Malley *et al.*, 1997). This branchpoint complex has been proposed to be an initial tetrahedral intermediate formed by the active site serine attack on the P1 carbonyl group. From this complex, the pathway proceeds to form a stable-complex or cleaved-serpin.

An important structural feature for serpin-proteinase interactions is the RCL. Although there is controversy about the structural conformation of the RCL in the native serpin, the recent crystal structure of the α-PI RCL has demonstrated that it is in a "canonical" form similar to other non-serpin serine proteinase inhibitors (Elliot *et al.*, 1996). Non-serpin inhibitors contain a reactive centre (p3-p3') that is in the optimal proteinase binding, or canonical, conformation. Thus the term "lock and key" fit is used to describe proteinase-inhibitor interactions. Unlike inhibitors, substrates have more flexible conformations and their interaction with a proteinase results in large conformational changes within the proteinase. In this case the mechanism is defined as an "induced fit". Thus, if the α-PI RCL conformation is consistent throughout the serpins, then the serpins represent a unique hybrid mixing the efficiency of binding of non-serpin inhibitors and the ability to act as substrate. Therefore the canonical RCL form allows the rapid interaction of serpin and

proteinase, with the subsequent formation of a tetrahedral intermediate as in a typical substrate reaction, and it is at this stage that the pathway banches to form a substrate or stable-covalent complex.

The key to the inhibitory pathway is the insertion of the RCL into the A ß-sheet. Crystal structure analysis of latent and cleaved serpins has revealed that the RCL can insert into the A ß-sheet and that this transforms the serpin from a stressed, or metastable, state to a more thermodynamically favourable state. A number of lines of evidence support the premise that complex formation is dependent upon the insertion of the RCL into the A ß-sheet. In the cleaved structure of the non-inhibitory serpin, ovalbumin, called plakalbumin, there is no insertion of the RCL into the body of the protein (Wright *et al.*, 1990). This suggests that insertion of the RCL is particular to the inhibitory serpins and is necessary for their function. Furthermore, in natural and engineered mutants of the hinge region of the RCL, which are believed to prevent or slow down RCL insertion, the serpin acts as a substrate instead of an inhibitor (Holmes *et al.*, 1987; Hood *et al.*, 1994; Hopkins *et al.*, 1993; Hopkins *et al.*, 1995). The most compelling evidence comes from studies using peptides corresponding to the insertable RCL residues (P14-P1), on native AT (Bjork *et al.*, 1992; Bjork *et al.*, 1992b) and α-PI (Schulze *et al.*, 1992), which resulted in the serpins being converted from inhibitory to exclusively substrate molecules. Thus, loop insertion is a requirement for the inhibitory mechanism of serpins.

The degree of RCL insertion is still unknown. Biochemical studies, three-

dimensional modelling of complexes, and the observation of natural mutants suggests that the partial insertion of the hinge region (P8-P15) up to at least P12 is necessary for inhibition (Whisstock, *et al.*, 1996; Hopkins *et al.*, 1997). Hopkins *et al.* (1997) note that hinge mutations (including P12 mutants) result in serpins being changed from inhibitors to substrates by slowing the RCL insertion and thereby reducing the rate at which stable complexes form. Based on this observation these investigators suggest that the insertion of the hinge region, up to P12, is the rate-limiting step in complex formation and precedes interaction with the active site of proteinase. This presumably occurs because insertion would place the RCL in a more permissive conformation for interaction with proteinase. However, evidence against this concept comes from examining AT structure-function. In AT the RCL hinge region is already in a partially inserted conformation and it has a much reduced rate of complex formation compared to other serpins. In fact, heparin interaction exposes the buried residues, placing AT into a more active inhibitory conformation (Huntington *et al.*, 1996).

How does insertion stabilize the complex? The insertion of the RCL, and the resultant conformation changes in the serpin-enzyme complex, are hypothesized to protect the acyl-enzyme bond from hydrolysis by solvent nucleophiles (Wright and Scarsdale, 1995). However, the insertion rate is important in determining down which pathway the reaction will proceed. If loop insertion is slow then the normal substrate pathway will occur, resulting in complete cleavage of the serpin and the deacylation of the acyl-enzyme bond.

Thus insertion is the decisive step determining complex formation.

1.4.2. Conformational Changes in the Serpin-Complexed Proteinase

Examination of various biochemical studies of the proteinase, in its serpin-complexed form, raises further questions about the mechanism of serpin inhibition of serine proteinases. Recent evidence demonstrates that, like the serpin moiety, the proteinase in serpin-enzyme complexes undergoes conformational changes. Proton NMR studies demonstrated that complexed chymotrypsin has a conformationally altered active site in the complex with α-AC than compared with the native proteinase (Plotnick *et al.*, 1996). These data support the hypothesis that alterations in the proteinase active site might result in a catalytically challenged proteinase in the complex, thereby vastly reducing the ability for the deacylation of the acyl-bond, and hence lowered ability to release cleaved substrate. Furthermore, complexed chymotrypsin can undergo proteolysis by elastase when in the complexed form with α-AC, but is resistant in uncomplexed state, indicating that conformational changes occur in the proteinase during serpin inhibition (Stavridi *et al.*, 1996). Interestingly, proteolysis of the complexed chymotrypsin increases the stability of the complex and might aid in clearance of complexes (Cooperman *et al.*, 1993; Stavridi *et al.*, 1996). Studies have found that active proteinase and inactive serpin can dissociate from serpin-enyzme complexes over time, including TAT (Jesty, 1979; Vercaigne-Marko *et al.*, 1987; Cooperman *et al.*, 1993; Griffith and Lundblad, 1981). Since proteolysis of complexes releases only inactive proteinases and serpins, proteolysis might represent a physiological

process to ensure that active enzyme is not released and that the more stable complexes can be removed by cellular receptors (discussed below).

1.4.3 Tertiary Structure of Serpin-Enzyme Complexes

To date no crystal structures of serpin-enzyme complexes have been reported. However, modelling studies, using the crystal data from a variety of serpins and serine proteinases, have been performed for elastase-αPI (Wright and Scarsdale, 1995) and for TAT, in its Michaelis complex (Schreuder *et al.*, 1994). The inhibitory complex of elastase-α-PI is consistent with biochemical studies, with elastase flipped to the opposite pole of α-PI, satisfying the necessity for RCL insertion into the A ß-sheet. However, more recent modelling has been performed for TAT and α-PI complexed with trypsin, elastase, and thrombin (Whisstcock *et al.*, 1996). These authors modelled the complexes to maintain more biochemically defined characteristics such as the property of loop-insertion, adoption of the RCL scissile bond region (P3-P3') to a conformation similar to non-serpin inhibitors (ie such as bovine pancreatic trypsin inhibitor, see above), and a lack of steric hindrance of the proteinase docking to the serpin. Interestingly, they found that the proteinase is not at the opposite end of the serpin but is off to one side (see Figure 2). Additionally, in their models strand 1C is pulled out of the C ß-sheet to allow insertion of the RCL into the A ß-sheet. The importance of mobility in the C ß-sheet for inhibition is demonstrated by pathologies associated with a number of natural mutants in AT, α-PI, and C1-inhibitor (summarized in Stein and Carrell, 1995). In contrast, mutational

FIGURE 2. Modelled three-dimensional structure of TAT adapted from Whisstock *et al.* (1996). Thrombin is the green coloured molecule on the upper left. The reactive centre is shown inserted as the new strand 4 in the A β-sheet. This figure was reprinted from Whisstock *et al.* (1996) (Copyright © 1996, Wiley-Liss Inc.) by permission of John Wiley & Sons, Inc.

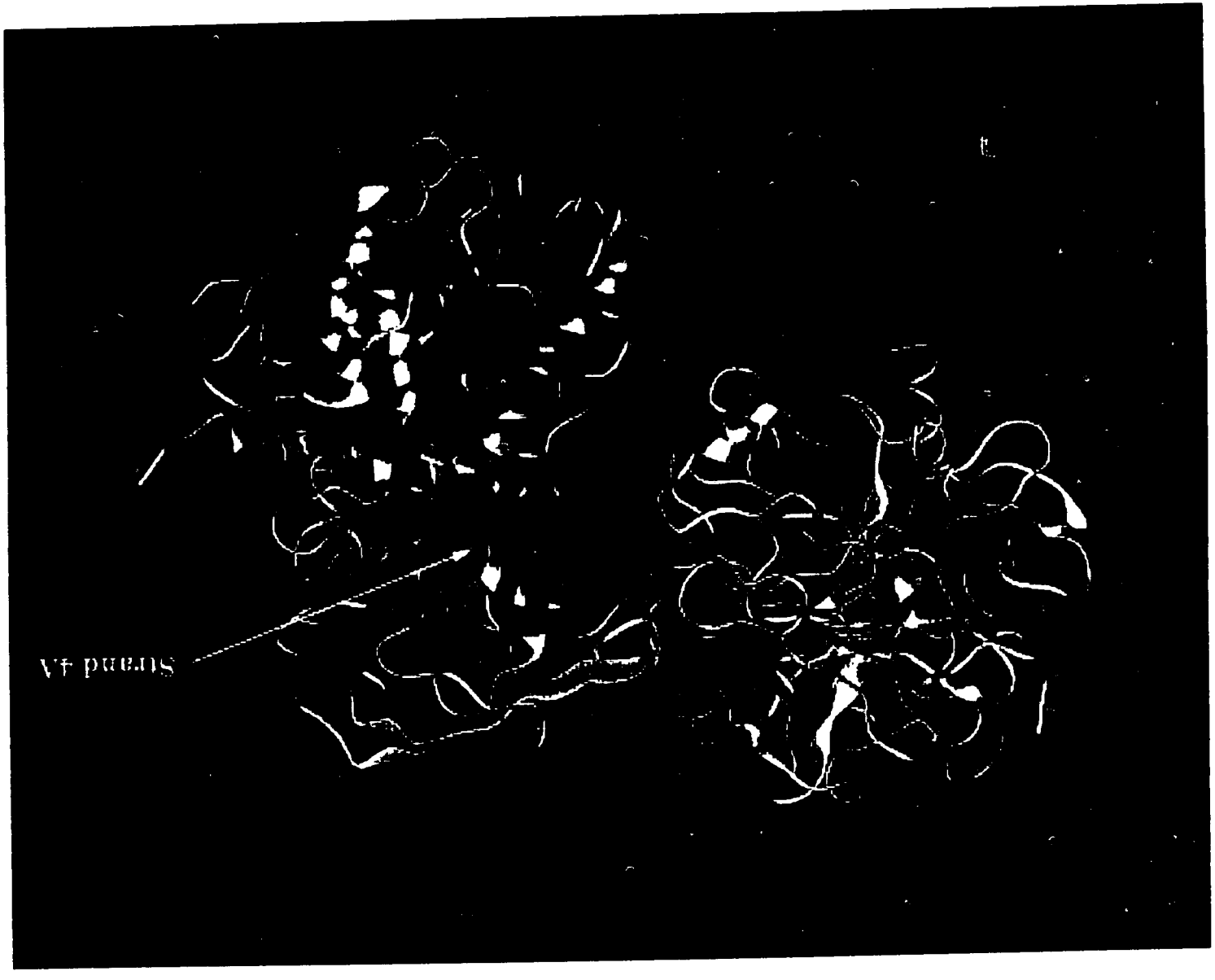
strand 4A

replacement of α-PI residues Pro^{361} and Ser^{283} with cysteine, resulting in disulfide-dependent immobilization of strand 1C through linkage between strands C1 and C2, did not abrogate its inhibitory ability (Hopkins *et al.*, 1997). However, recombinant C ß-sheet mutants, in C1 inhibitor, resulted in native inhibitor with thermodynamic stability similar to cleaved or complexed C1 inhibitor (Eldering *et al.*, 1995). Furthermore, these C1 inhibitor mutants were recognized by a monoclonal antibody specific for cleaved or complexed C1 inhibitor, but not normal intact inhibitor. These data support the concept of C sheet movement concurrent with RCL insertion. Relating the clinical and biochemical data to three-dimensional SEC interactions is strictly theoretical and only when a SEC is crystallized will the true structural interactions between proteinase and inhibitor be known.

1.5 Metabolism of Serpin-Enzyme Complexes

The first studies examining the metabolic fate of SECs were performed by Ohlsson, when he studied the clearance of α-PI-trypsin complexes in the circulation of dogs (Ohlsson, 1971; Ohlsson *et al.*, 1971). Since then a large volume of data has accumulated examining the metabolism of SECs, both *in vivo* and *in vitro*. More recently, studies have implicated a number of different receptor proteins in SEC removal. In the following sections the in vivo and *in vitro* data for SEC clearance is reviewed and the different candidate receptor

proteins for SEC and, more specifically, TAT removal summarized.

1.5.1. SEC Clearance In Vivo

The bulk of the in vivo data are from plasma elimination experiments in which the metabolic clearance of radiolabelled proteins is followed. These experiments have been performed in humans, dogs, rabbits, rats, guinea pigs, and mice using various SECs, with the preponderance of data coming from murine studies. In human studies, native serpins typically have half-lives greater than 24 hours, but when in complexed form, this is reduced to a few hours; indicating the existence of a specific removal pathway for SECs (Ohlsson and Laurell, 1976; Collen and Wiman, 1979). This concept was further refined in mice using different SECs. AT, α-PI, HCII, α-AC, and α_2-AP-enzyme complexes were all found to be removed very rapidly ($t_{½}$ ≈ 5 minutes) compared to the native serpins ($t_{½}$ > 60 minutes) (Fuchs *et al.*, 1982; Gonias *et al.*, 1982; Shifman and Pizzo, 1982; Pratt *et al.*, 1988; Pizzo *et al.*, 1988). The plasma elimination data for the different complexes is summarized in Table 1. Interestingly, the use of homologous human SECs demonstrated an almost identical clearance behaviour as that of murine SECs. Competition experiments demonstrated that α-PI, AT, HCII, and α-AC-enzyme complexes are all removed by the same pathway but that α_2-AP-enzyme complexes are removed by a distinct pathway. The clearance of enzymatically-cleaved serpins has been found to closely resemble native serpins and competition of SEC with cleaved serpins did not alter their clearance rate (Mast *et al.*, 1991; de Smet *et al.*, 1993; Malek *et al.*, 1996). However, unlike

SERPIN-ENZYME COMPLEX	*HALF-LIFE (α OR β)*	*COMPETITION DEMONSTRATED WITH*	*ANIMAL MODEL*	*REFERENCE*
α_1-PI-trypsin	α= 15-20 min	TAT, AT-trypsin	mouse	Fuchs et al., 1982
α_1-PI-trypsin	α ≈ 45 min		dog	Ohlsson, 1970
α_1-PI-trypsin	α ≈ 5 min	α_1-PI-trypsin; asialo-α_1-PI	rat	Gan, 1979
α_1-PI-neutrophil elastase	α= 5 min		mouse	Pizzo, 1989
α_1-PI-porcine pancreatic elastase	α= 1 min		mouse	Pizzo, 1989
TAT	α= 3 min	α_1-PI-trypsin	mouse	Shifman and Pizzo, 1982
TAT	β= 7.25 h		rabbit	Vogel et al., 1979
AT-trypsin	α= 5 min	α_1-PI-trypsin	mouse	Fuchs et al., 1984
AT-Factor IXa	α= 1.5 min	α_1-PI-trypsin	mouse	
HCII-thrombin	α= 10 min	TAT, α_1-PI-neutrophil elastase	mouse	Pratt et al., 1988
α_1-AC-chymotrypsin	α= 12 min	α_1-PI-trypsin	mouse	Pizzo et al., 1988
α_1-AC-cathepsin G	α= 12 min		mouse	Pizzo et al., 1988
C1-inhibitor-proteinases (C1s, kallikrein, or βXIIa)	α= 20, 32, 47 min respectively		rat	de Smet et al., 1993
C1-inhibitor-proteinases (C1s, kallikrein or βXIIa)	α not calculated, but <10 min; β ranging from 3 to 4.8 h		guinea pig	Malek et al., 1996
Factor XIa-serpins (C1-inhibitor, α_2-AP, AT, or α_1-PI)	α= 19, 18, 15, and 98 min respectively		rat	Wuillemin et al., 1996
α_2-AP-plasmin	α= 20 min	α_2-AP-plasmin; None with excess α_1-PI-trypsin	mouse	Gonias et al., 1982
α_2-AP- trypsin	α= 14 min		mouse	Gonias et al., 1982
α_2-AP-plasmin	α= 0.8 - 0.92 days		humans	Collen and Wiman, 1979
t-PA-PAI-1	α= 9.7 min; β= 7 h		perfused rat livers	Wing et al., 1991

TABLE 1. Summary of reported plasma elimination studies of various serpin-enzyme complexes. These clearance experiments were fitted typically to a two-compartment model describing clearance, where the α half-life represents the clearance half-life for the initial rapid clearance due to receptor-binding and the β half-life represents the half-life for the second slower phase of clearance.

cleaved AT, α_2-AP, and α-AC, the clearance rates of cleaved C1-inhibitor and α-PI were found to be intermediate to that of native or complexed C1-inhibitor or α-PI (Mast *et al.*, 1991; de Smet *et al.*, 1993; Malek *et al.*, 1996). Nevertheless, these data indicate the expression of receptor-binding domains present only in the complexes. Enghild *et al.* (1994) found that complexes of serpin and 3,4-dichloroisocoumarin (DCI)-inactivated serine proteinase were cleared from the murine circulation faster than native serpin. However, further studies indicated that the DCI-proteinase complex could decay, releasing active proteinase which could then covalently complex with the serpin (Gettins *et al.*, 1996).

Previously, the serpin moiety of the complex was believed to confer the receptor binding epitopes (Pizzo, 1990). However, the clearance data of various factor XIa-serpin (Wuillemin *et al.*, 1996) and C1-inhibitor-enzyme complexes (Malek *et al.*, 1996), combined with the demonstration that complexed proteinases undergo conformational changes (Stavridi *et al.*, 1996), indicate that both moieties of the SEC likely confer sites for receptor binding.

1.5.2. Tissue and Receptor Specificity *In Vivo*

Post-mortem analysis of different tissues following clearance studies revealed that the large majority of the radiolabelled SEC was contained within the liver, indicating a liver-specific mechanism of removal (Fuchs *et al.*, 1982; Pizzo, 1990; Xiong *et al.*, 1991). Autoradiographic analysis of the liver from ^{125}I-TAT clearance, at the electron microscopic level, revealed that the removal mechanism was associated with hepatocytes and not non-parenchymal cells (Shifman and

Pizzo, 1982). Competition experiments demonstrated that the SECs were being removed by novel hepatic receptors. Competition experiments, with receptor-specific ligands, demonstrated that the α_2-macroglobulin receptor (also known as the low density lipoprotein receptor-related protein (LRP)), the asialoglycoprotein receptor, and thrombin receptors are not involved in the removal of SECs (Shifman and Pizzo, 1982; Fuchs *et al.*, 1982). Furthermore, the inability of macroalbumin (heat denatured albumin) to block removal of TAT indicated that TAT was not being cleared by the reticuloendothelial system cell receptors (Shifman and Pizzo, 1982). However, more recent elimination data supports the possibility that LRP plays a role in TAT clearance, since competition using an LRP antagonist, the receptor associated protein (RAP), resulted in an increased half-life for TAT clearance (Kounnas *et al.*, 1996).

1.5.3. *In Vitro* Studies on SEC-Receptor Interactions

The studies that have been conducted to examine SEC-receptor interactions have been a mixture of quantitative and qualitative radioligand binding studies, and functional assays with cultured cells or with purified proteins. A summary of the quantitative SEC radioligand binding studies are shown in Table 2. Further investigations of these interactions have lead to the identification of a number of different putative receptor and cofactor proteins involved in the metabolism and biological effects of SEC. These proteins include the serpin-enzyme complex receptor (SECR), LRP, gp330 (also known as megalin or LRP1), urokinase plasminogen activator receptor (uPAR), vitronectin (VN),

	LIGAND	K_D AND B_{MAX}	REFERENCE
HepG2 cells	TAT	247nM/ 5.19×10^5 sites	Fair and Plow,1985
U937 cells	TAT	68nM/ 79,000 sites	Takeya et al., 1994
HUVECs	VN-TAT	16nM/ 1.7×10^5 sites	de Boer et al., 1992
Spinal cord astrocytes	α_1-AC-cathepsinG	80nM/ 2.2×10^6 sites	Chen et al., 1993
HepG2 cells	HCII-thrombin	19-32nM/ $0.6\text{-}2.6\times10^5$ sites	Maekawa and Tollefsen., 1996
HepG2 cells, neutrophils	α_1PI-elastase/ peptide 105Y	40nM/ 4.5×10^5sites; 40 nM/ $0.13\text{-}5\times10^5$ sites	Perlmutter et al., 1990b; Joslin et al., 1992
gp330(LRP1/megalin)	uPA-PAI-1	$\approx$ 1.0 nM	Stefansson et al., 1995
LRP1 (gp330); LRP2	thrombin-PAI-1	3.3 nM; 13nM	Stefansson et al., 1996

TABLE 2. Summary of reported radioligand binding studies with different serpin-enzyme complexes.

and from my studies, CK18. These will be discussed individually below.

More specifically, TAT complexes have been found to interact with the human hepatoma cell line HepG2 (Fair and Plow, 1986; Joslin *et al.*, 1991a; Joslin *et al.*, 1993), mouse hepatocytes (Bauer *et al.*, 1982; Fuchs *et al.*, 1984; Kovacs *et al.*, 1987; Spolarics *et al.*, 1989), the human monocytoid cell line U937 (Takeya *et al.*, 1994), fibroblastic cell lines (Kounnas *et al.*, 1996), bovine aortic and corneal endothelial cells (Savion and Farzame, 1986; Knoller and Savion, 1991), and human umbilical vein endothelial cells (HUVEC) (de Boer *et al.*, 1992). Quantitative binding data for TAT binding to cells are included in Table 2.

1.5.4. The Serpin-Enzyme Complex Receptor (SECR)

To date, the receptor protein that most parallels the *in vivo* SEC recognition pattern is a receptor protein designated the SECR (Perlmutter *et al.*, 1990). The first evidence of a signalling receptor, sensitive to α-PI, came from studies examining the neutrophil chemotactic abilities of α-PI-elastase complexes and the C-terminal peptide released from reactive site cleaved α-PI (Banda *et al.*, 1988a; Banda *et al.*, 1988b). Furthermore, elastase was found to induce up-regulation of α-PI mRNA and protein production in cultured human monocytes. It was speculated that these effects were receptor-mediated through complexes formed from elastase inhibited by secreted α-PI (Perlmutter and Punsal, 1988; Perlmutter *et al.*, 1988).

Perlmutter and associates identified the SECR on HepG2 cells, monocytes, and neutrophils which demonstrated ligand specificity consistent with that seen

from the *in vivo* studies (Perlmutter *et al.*, 1990; Joslin *et al.*, 1992). These investigators conducted radioligand binding experiments which identified residues in the C-terminus of α-PI that could bind to SECR. An α-PI carboxy-terminal peptide (peptide 105Y), corresponding to residues 359-374 (P'1- P'16), was found to bind specifically to a single set of sites on HepG2 cells, monocytes and neutrophils (Perlmutter *et al.*, 1990a; Joslin *et al.*, 1992). The affinity of peptide 105Y for SECR was determined to be ~40nM and bound to ~ 450,000 sites per cell. The binding of peptide 105Y was competed by a variety of SECs, including α-PI-elastase, TAT, α-AC-cathepsin G complexes, weakly with C1-inhibitor-C1 esterase complexes, but not by the native serpins or proteinases. Furthermore competitive radioligand binding experiments demonstrated cross-competition binding to HepG2 cells with TAT, thrombin-HCII, tPA-PAI-I, and α-PI-elastase complexes (Joslin *et al.*, 1993). However, unlike the behaviour of cleaved serpins seen from *in vivo* clearance studies, Joslin *et al.* (1993) found that proteolytically cleaved α-PI could bind to SECR, and that its binding could be inhibited by peptide 105Y as well as α-PI-enzyme complexes. Another similarity to the *in vivo* receptor was the observation that α-PI-trypsin complexes were internalized and degraded via SECR and that peptide 105Y could inhibit the internalization of these complexes (Perlmutter *et al.*, 1990b). Since then SECR has been found to be on a variety of other cell types including monocytoid cell lines U937 and HL-60 cells, intestinal epithelial cell line Caco2, mouse fibroblast L cells, mouse kidney cell line Cos, rat neuronal cell line PC12, and human glial cell line

U373MG (Perlmutter, 1994).

Further studies revealed that SECR-ligand interaction resulted in similar effects seen in the seminal experiments using neutrophils and monocytes. Peptide 105Y was found to be a chemoattractant for neutrophils similar to that of α-PI-elastase complexes (Joslin *et al.*, 1992). SECR ligands have been found also to up-regulate α-PI synthesis in HepG2 cells and monocytes (Perlmutter *et al.*, 1990; Joslin *et al.*, 1991a; Joslin *et al.*, 1991b; Joslin *et al.*, 1993). α-PI up-regulation experiments showed that α-PI-elastase, TAT, and α-AC-cathepsin G complexes all stimulated α-PI synthesis but that none of the complexes resulted in an increase in α-AC or AT synthesis (Joslin *et al.*, 1993). A similar inability to stimulate hepatocyte AT synthesis by TAT was also reported by Hoffman *et al.*(1986). Also, C1-inhibitor-enzyme complexes had no effect on C1-inhibitor synthesis by HepG2 cells or U937 cells (Patston *et al.*, 1993). The ability of SEC-SECR interaction to up-regulate α-PI levels would seem to implicate some form of signal transduction. Although this possibility has not been examined in any depth, pentapeptide (FVFLM; see directly below) binding to neutrophil-like HL-60 cells resulted in a pertussis toxin-sensitive increase in intracellular calcium and suggests that these responses could be mediated by G-proteins (Takenouchi and Munekata, 1995).

Mapping studies revealed that a pentapeptide sequence (FVFLM) within peptide 105Y, contained the minimal necessary residues for α-PI binding to SECR (Joslin *et al.*, 1991a). Alterations in the pentapeptide sequence, by mutation,

deletion, or scrambling, demonstrated that SECR recognition was sequence specific. Furthermore, this pentapeptide demonstrated cross-competition sensitivity with α-PI-enzyme complexes and was found to stimulate up-regulation of α-PI protein in monocytes. Examination of other serpin members revealed that this pentapeptide sequence is homologous (based on semi-conservative changes) to the corresponding sequences in other serpins. The corresponding C-terminal peptides of AT, α-AC, and PAI-1 competed for binding of ^{125}I-peptide 105Y to HepG2 cells indicating that the same pentapeptide sequence could be important for all SEC binding (Joslin *et al.*, 1993). In contrast, a number of investigators have found no inhibition of SEC binding to cells by the SECR-binding pentapeptide, including TAT (Chen *et al.*, 1993; Conese *et al.*, 1994: Takeya *et al.*, 1994). Indeed, inhibitory pentapeptide-binding alterations in the pentapeptide consensus sequence for HCII had no effect on HCII-thrombin complex binding to HepG2 cells (Maekawa and Tollefsen, 1996).

Interestingly, similar pentapeptide sequences were found in various bioactive peptides including ß-amyloid protein, bombesin, substance P, and other tachykinins (Joslin *et al.*, 1991b). Cross-competition radioligand binding experiments revealed that all of these ligands were binding solely to SECR on HepG2 cells (Joslin *et al.*, 1991b). This was verified in cross-linking eperiments in which the cross-linking of ^{125}I-peptide 105Y to an ~80 kDa polypeptide was inhibited by competition with bombesin, ß-amyloid peptide, substance P, peptide 105Y, and α-PI-trypsin complexes. Furthermore, in similar fashion to that of α-

PI-elastase, peptide 105Y, and the pentapeptide, substance P demonstrated a specific and concentration-dependent up-regulation of α-PI protein. Studies revealed that the homologous pentapeptide sequence in soluble ß-amyloid peptide, residues 31-35 (IIGLM), were critical for binding to SECR and that SECR mediated the internalization and degradation of the ß-amyloid peptide by a neuronal cell line, PC12 (Boland *et al.*, 1995). These data are particularly interesting since this region of ß-amyloid is responsible for its neurotoxicity in Alzheimer's disease (Yankner *et al.*, 1990). Additionally, the serpins AT, PN-1, and especially α-AC are found within the amyloid plaques of Alzheimer's patients (Kalaria *et al.*, 1993; Rosenblatt *et al.*, 1989; Abraham *et al.*, 1988). Studies have found that ß-amyloid must be in an insoluble and aggregated form to have its neurotoxic effects (Yankner *et al.*, 1990; Pike *et al.*, 1995). Boland *et al.* (1996) found that only the non-toxic soluble form of ß-amyloid bound to the SECR and the insoluble neurotoxic form did not. This raises questions as to the role, if any, SECR may have in the pathogenesis of Alzheimer's disease.

1.5.5. Low Density Lipoprotein Receptor-Related Protein (LRP)

Plasma elimination studies in dogs first gave an indication that α_2-M-enzyme complexes were removed from the circulation by hepatic receptors (Ohllson *et al.*, 1971; Ohllson, 1971). The α_2-M receptor has been affinity purified and found to be identical to LRP (Moestrup *et al.*, 1989; Jensen *et al.*, 1989; Ashcom *et al.*, 1990; Strickland *et al.*, 1990; Kristensen *et al.*, 1990). LRP is a member of the endocytic LDL-receptor family of proteins which includes the low

density lipoprotein receptor, the very low density lipoprotein receptor, and gp330 (megalin/Heymann Nephritis Antigen) (Strickland *et al.*, 1995).

Both LRP and gp330 proteins are more highly characterized compared to SECR, with LRP much more characterized than gp330. LRP is expressed in a variety of tissues including the liver, brain, placenta, intestines, and lung (Moestrup *et al.*, 1992; Zheng *et al.*). Within these tissues LRP is expressed within certain cell types such as hepatocytes, Kupfer cells in the liver, fibroblasts, and macrophages. More recently, LRP has also been found to be expressed on endothelial cells (Luoma *et al.*, 1994; Lupu *et al.*, 1994). By comparison, gp330 is found in specialized absorptive epithelia of the brain, kidneys, and lungs (Zheng *et al.*, 1994). LRP is an endocytic receptor which is recycled back to the surface after releasing bound ligand in endosomal compartments. (Kowal *et al.*, 1989). LRP is synthesized initially as a single chain precursor but is cleaved enzymatically in the *trans* Golgi to a 515 kDa heavy chain (α subunit) and a light chain of 85 kDa (ß subunit) (Herz *et al.*, 1990). The α subunit associates non-covalently with the ß subunit; the latter contains a single transmembrane spanning domain. The 50 amino acid residue cytoplasmic domain of the LRP ß chain contains two Asn-Pro-X-Tyr sequences (NPXY) that are required for the efficient internalization of ligand-bound LRP by clathrin-coated pits (Chen et al., 1990; Schwartz, 1995). LRP contains 22 epidermal growth factor-like repeats and 31 cysteine-rich complement-type repeats which are formed into four different clusters. Six cysteine residues in the complement-type repeats have been shown

to form three conserved disulfides necessary for stabilizing ligand-binding sites in LRP, especially when releasing ligand in the acidic endosomal compartments (Goldstein *et al.*, 1985). Both subunits of LRP contain complex N-linked glycosidic sidechains with glycosylation representing up to 90 kDa of the larger α subunit and up to 20 kDa for the smaller ß-subunit (Jensen *et al.*, 1992). Additionally, both subunits appear to contain small amounts of O-linked glycosidic sidechains. LRP and gp330 bind a large number of similar, although not identical ligands (such as α_2-M-complexes). These include various lipoproteins, methylamine-modified α_2M (α_2M*), lactoferrin, lipoprotein lipase, thrombospondin, tissue factor pathway inhibitor (TFPI), and different serpin-enzyme complexes (reviewed in Strickland *et al.*, 1995). Interestingly, a small subset of high-affinity LRP sites has been identified which are coupled to G-proteins and which have different ligand-binding properties than endocytic LRP receptors (Howard *et al.*, 1996a).

One of the defining characteristics of LRP, and other members of the LDL receptor family, is their interaction with the antagonist receptor-associated protein (RAP). RAP was first identified when it co-purified with LRP (Strickland *et al.*, 1990; Kristensen *et al.*, 1990). RAP binds to LRP with high affinity (K_d=4nM) and its ability to block LRP-ligand interactions has made it a powerful biochemical tool (Williams *et al.*, 1992). *In vivo* RAP is found within the endoplasmic reticulum and Golgi-apparatus while LRP is found within endosomes and on the plasma membrane (Bu *et al.*, 1994a; Biemesderfer *et al.*, 1993).

What is the physiological relationship between RAP and LRP? Examination of transgenic mice and transfection experiments have revealed that RAP is a specialized chaperonin protein necessary for LRP expression (Bu and Rennke, 1996; Willnow *et al.*, 1996). RAP has been proposed to function in LRP expression in two ways: 1) by binding to LRP it protects LRP from the premature binding of ligands and 2) it aids in the proper folding of LRP by ensuring intradomain disulfide bond formation.

Both LRP and gp330 have been demonstrated to bind various SEC. LRP and gp330 have both been found to bind t-PA-PAI-1 (Willnow *et al.*, 1992; Bu *et al.*, 1993), uPA-PAI-1 (Steffanson *et al.*, 1995), endocytose thrombin-PAI-1 complexes (Stefansson *et al.*, 1996) and PN-1-thrombin complexes (Knauer *et al.*, 1997). Recently, purified LRP has been demonstrated to bind TAT, α-PI-trypsin, and HCII-thrombin complexes (Kounnas *et al.*, 1996). Binding analyses revealed that these complexes interacted with LRP with relatively low affinity (half saturation estimated at 80-120 nM), although the binding data was incomplete and the reactions had extended incubation times (18 hours at 4°C). Endocytosis experiments with the different SECs using normal and LRP-deficient fibroblasts were more convincing, demonstrating definitively that LRP was indeed the vehicle of internalization. From the same studies, *in vivo* clearance experiments demonstrated that excess RAP could increase the clearance time for TAT in rats, supporting the role of LRP in TAT clearance (Kounnas *et al.*, 1996).

Like the SECR, LRP possibly plays a role in Alzheimer's disease. LRP and

a number of its ligands have been found to be associated directly, or in close proximity, to the senile plaques of Alzheimer's patients (Rebeck *et al.*, 1995). These ligands include apolipoprotein E (apoE), t-PA, uPA, PAI-1, and lipoprotein lipase. Interestingly, genetic studies have indicated that inheritance of the 4 allele of apoE as a risk factor in Alzheimer's disease (Stritmatter *et al.*, 1993). Furthermore, Kounnas *et al.* (1995) showed that a secreted from of ß-amyloid precursor protein, which contains the plaque forming ß-amyloid peptide sequence, could bind to LRP and be internalized. In all, these data suggest the importance of LRP in the pathophysiology of Alzheimer's disease, since it converges with a variety of Alzheimer's-associated proteins in a common metabolic pathway.

LRP and SECR demonstrate similar ligand specificity and tissue expression and suggests that perhaps SECR and LRP are the same. However discrepancies in the reported data make this assumption inconclusive. Joslin *et al.* (1991b), using cross-linking, found that SECR was 78-84 kDa, a similar mass to the light chain of LRP (85 kDa). However, using ligand-blotting and cross-linking, others have found that the heavy chain of LRP is the ligand binding subunit for α-PI-elastase, uPA-PAI, and tPA-PAI-1 complexes (Poller *et al.*, 1995; Orth *et al.*, 1992). Poller *et al.* (1995) compared the degradation of α-PI-elastase and α-AC-cathepsin G complexes by various cell types known to express, or not express, LRP and/or gp330. These studies found that α-PI-elastase bound to LRP in ligand-blotting experiments and that degradation of these complexes was through LRP. Conversely, neither LRP expressing nor LRP-deficient fibroblasts degraded

α-AC-cathepsin G, but a cell line expressing gp330 degraded these complexes. However, HepG2 cells, which lack gp330, also efficiently degraded α-AC-cathepsin G complexes indicating that a receptor distinct from LRP was degrading these complexes, possibly the SECR. Moreover, discrepancies in cell-type expression have been found. SECR has been determined not to be expressed on CHO cells, by radioligand-binding studies, (Boland *et al.*, 1995; Perlmutter, 1995) and yet LRP has been demonstrated to be expressed on these cells (Berryman and Bensadoun, 1995; Willnow *et al.*, 1996). Interestingly, Takeya *et al.* (1994) provided evidence for ^{125}I-TAT binding to U937 cells which suggests that neither SECR or LRP, but another protein, is involved in TAT binding to these cells. Furthermore, although a homologous pentapeptide sequence has been identified in SECR-binding ligands (Joslin *et al.*, 1991a), different, non-homologous cell-binding site sequences have been determined for the binding of α-macroglobulins (Nielsen *et al.*, 1996; Howard *et al.*, 1996b) and PN-1 to LRP (Knauer *et al.*, 1997).

1.5.6 Urokinase-Plasminogen Activator Receptor (uPAR) and Vitronectin

uPAR is a single chain 55-60 kDa glycoprotein composed of 313 amino acids (reviewed in Behrendt *et al.*, 1995). After post-translational modifications, the mature protein of 283 residues is anchored to the plasma membrane by a glycosyl-phosphatidylinositol moiety. Possessing five putative N-linked glycosylation sites, uPAR shows heavy and heterogeneous glycosylation. uPAR is found on the surface of monocytes, U937 cells, granulocytes, fibroblasts, and

tumor cells (Bu *et al.*, 1994b; Christensen *et al.*, 1996). uPAR binds pro-uPA, active uPA (two-chain uPA), and diisopropylfluorophosphate inhibited two-chain uPA (Vassalli *et al.*, 1985). Moreover, binding to uPAR is dependent upon residues within an amino-terminal fragment of pro-uPA (residues 1-135) and more specifically within a growth factor domain (residues 4-43) (Appella *et al.*, 1987; Mazar *et al.*, 1992). Interestingly, the u-PA clearance studies have shown that the liver is the main site of removal and that this association is independent of the u-PA amino terminal fragment, suggesting interaction with another receptor protein (Stump *et al.*, 1987; Kuiper *et al.*, 1992). More recently van der Kaaden *et al.* (1997) proposed that LRP was the u-PA binding protein *in vivo*, although the inability of huge excesses of RAP to increase the clearance makes their data less convincing. uPAR-bound uPA is not protected from inhibition by PAI-1 and PAI-2 (Ellis et al., 1990) and the ternary uPAR-uPA-PAI complexes have been shown to be internalized through interaction with LRP (Nykjaer *et al.*, 1992; Herz *et al.*, 1992; Conese *et al.*, 1995) or gp330 (Moestrup *et al.*, 1993). Similarly, uPA-PN-1 complexes have also been found to remain bound to uPAR and to be endocytosed through LRP (Conese *et al.*, 1994).

VN may also play a role in SEC removal, specifically via complexes formed with thrombin or factor Xa. VN is a 78 kDa liver-synthesized glycoprotein found in the blood at a concentration of 200-400 μg/ml (Tomasini and Mosher, 1986). VN plays key roles in the attachment of cells to their surrounding matrix (Preissner and Jenne, 1991; Tomasini and Mosher, 1990) and has also been found

to have various functions in proteolytic cascades. For example, VN stabilizes the major inhibitor of fibrinolysis PAI-1 (Mimuro and Loskutoff, 1989), inhibits the complement system (Podack *et al.*, 1977; Dahlback and Podack, 1985), and neutralizes the heparin catalysis of AT inhibition of thrombin and factor Xa (Podack *et al.*, 1986; Preissner and Muller-Berghaus, 1987).

The interaction between VN and TAT complexes was first described by Ill and Ruoslahti (1985) who found that VN in serum had a different electrophoretic mobility from plasma VN because, in serum, it was associated with TAT. Since then, more extensive studies have identified the presence of VN-TAT in human plasma and the molecular mechanism of VN-TAT formation (de Boer *et al.*, 1993). Non-reducing SDS-PAGE analysis, in combination with Western blot analysis, revealed that the VN-TAT forms multimers with the monomer having a M_r of ~ 160 kDa. Under reducing conditions the monomeric and multimeric VN-TATs breakdown to smaller products. As indicated by SDS-PAGE, the covalent nature of the ternary complex is through disulfide bridge formation between the thrombin and VN and this is supported by the inability of ternary complexes to form in the presence of the thiol-alkylating compound N-ethylmaleimide. Furthermore, ammonia is known to dissociate TAT. When VN-TAT is treated with ammonia only AT is released further supporting the concept of a covalent interaction between VN and thrombin. The use of monoclonal antibodies, against different portions of VN, found that the amino-terminal region of VN is important in forming ternary complexes (de Boer *et al.*, 1993). These

authors speculated that an acidic region within the amino-terminus of VN interacts with the basic anion exosite of thrombin. Other VN-SEC have been identified also: VN-thrombin-HCII (Preissner and Sie, 1988; Liu *et al.*, 1995); VN-thrombin-PN-1 (Rovelli *et al.*, 1990); VN-Xa-antithrombin (Gouin-Thibault *et al.*, 1996); VN-thrombin-PAI-1 (van Meijer *et al.*, 1997); VN-thrombin-Protein C inhibitor, and ternary complexes of VN and thrombin with the mutant α-$PI_{Pittsburg}$ (Preissner *et al.*, 1996).

What is known about the interaction between VN-TAT and receptor proteins? Radioligand binding experiments have shown that VN-TAT binds to proteoglycans on HUVEC with a $K_d \approx 16$ nM. This binding appears to be mediated by the C-terminal heparin-binding domain of VN (de Boer *et al.*, 1992), although other heparin-binding domains might exist in VN (Liang *et al.*, 1997). Furthermore VN-TAT was found to be internalized and translocated, without degradation, to the subendothelial matrix by HUVEC (de Boer *et al.*, 1995). Whether these proteoglycans are the major binding sites or are intermediary binding sites on HUVEC remains to be determined. Interestingly, studies suggest that both uPAR and LRP might play a role in VN-TAT metabolism. Proteoglycans have been implicated in the binding of a number of LRP ligands, including thrombospondin (Mikhailenko *et al.*, 1995) and TFPI (Warshawsky *et al.*, 1996). From these and other studies it has been hypothesized that heparan sulphate proteoglycans bind ligands and present them to LRP for endocytosis. In this regard it is interesting to note that the heparin-binding domain of VN has

been found to bind to a highly conserved sequence in complement proteins C6, C7, C8, C9, as well as perforin (Tomasini and Mosher, 1990). This sequence is composed of negatively charged amino acids and contains 3 intradomain disulfide bridges and it has been shown to be homologous to the ligand-binding domain of the LDL receptor (Sudhof *et al.*, 1985). The corresponding sequence is also found in LRP indicating that it might be involved in binding to VN-SEC complexes. This is supported by studies indicating that VN promotes the LRP-dependent removal of thrombin-PAI-1 complexes (Steffanson *et al.*, 1996). In plasma, 98% of VN is found in native monomeric form with 2% found in a multimeric form which has high heparin-affinity (Izumi *et al.*, 1989). The conformation of multimeric VN (mVN) is reportedly similar to that of VN in ternary complex with TAT (Tomasini and Mosher, 1988; Stockmann *et al.*, 1993). mVN has been found to bind to uPAR on HUVEC (Kanse *et al.*, 1996). In all, these data indicate the possible interactions of VN, uPAR, proteoglycans, and LRP in mediating TAT binding and removal.

1.5.7. Are Other Proteins Involved in SEC Binding?

The accumulated data has not provided unequivocal evidence that LRP and/or other SECR proteins are solely responsible for the *in vivo* clearance of SEC. Discrepancies in the literature indicate that other proteins may be involved in mediating SEC removal. For example, Perlmutter and associates have defined the SECR as binding a conserved pentapeptide sequence of serpins. However, as mentioned above, a number of investigators have reported that the pentapeptide

sequence appears not to compete for binding of different SECs to cellular binding sites. Indeed, AT residues 253-314 were identified to contain the cellular binding domain for bovine corneal endothelial cells (Knoller and Savion, 1991). Additionally, amino terminal residues 39-66 of HCII were found to have significant chemotactic activity for monocytes and neutrophils (Church *et al.*, 1990). Neither of these sequences contains the SECR-binding pentapeptide binding sequence, so what is the nature of the site(s) these peptides are binding to? Recently a PN-1 peptide was found to be a potent inhibitor of PN-1-thrombin internalization by LRP but did not inhibit PN-1-thrombin binding to the cell surface, supporting the possibility of TAT binding to another receptor protein (Knauer *et al.*, 1997). Furthermore, α-AC-chymotrypsin complexes have been shown to associate directly with NADPH-oxidase and inhibit superoxide production (Schuster *et al.*, 1992). During my doctoral research I have identified that TAT interacts with CK18, an intermediate filament protein. In the following section I therefore discuss the intermediate filament family of proteins and CK18 in particular.

1.6 Cytokeratin (CK18) and the Intermediate Filament (IF) Family of Proteins

Cytokeratins (CKs) are members of the intermediate filament (IF) family of proteins which are found primarily in epithelial tissues (Abe *et al.*, 1990, Moll *et al.*, 1982). IFs mesh together to form filamentous cytoplasmic networks that

run from the surface of the nucleus to the plasma membrane (Okanoue *et al.*, 1985; French *et al.*, 1989). IFs derive their name from the diameter of the filaments they form. The 10 nm IF filaments are intermediate in diameter to the 6 nm thin actin filaments and the larger 23 nm microtubular filaments (Fuchs and Weber, 1994). Together, these three forms of filaments comprise what is known as the cytoskeleton. In contrast to the actins and tubulins, there is low sequence identity amongst the IFs, which can share as little as 20% homology. However, the ~ 50 member IF protein family can be placed into six subtypes based on sequence homology, gene structure, and their ability to co-polymerize to form filaments (reviewed in Fuchs and Weber, 1994; Klymkowsky, 1995). Futhermore, despite the low family-wide homology, all IFs possess a unifying protein structure composed of a central α-helical rod domain which is flanked by non-helical head and tail domains (Fuchs and Weber, 1994; Coulombe, 1993; Steinert, 1993 for reviews). Figure 3 shows a diagram demonstrating the common secondary structure for IFs.

At least 30 different CK proteins are found in epithelial tissues and carcinomas, and these are grouped into two main types of cytokeratin; type I which are acidic and type II which are neutral-basic proteins (Fuchs and Weber, 1994). Unlike other IF proteins, cytokeratins are obligate heteropolymers, requiring the presence of both a type I and type II protein to form filaments (Steinert *et al.*, 1976). Thus at least one member of both types of CKs are found coordinately expressed in epithelial tissues, for example CK18 and CK8 is the pair

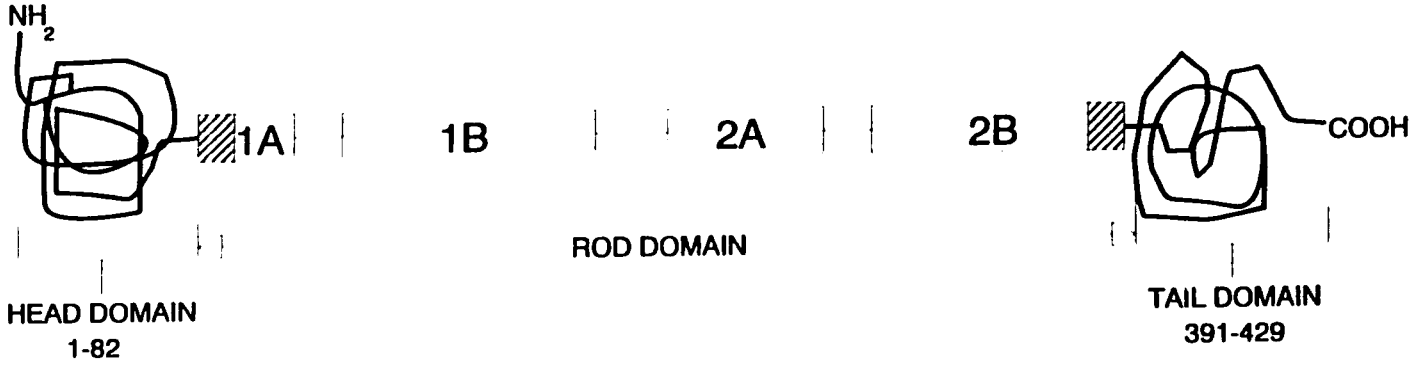

Figure 3. Schematic representation of the common structural domains of intermediate filaments. All intermediate filaments are composed of non-helical head and tail domains of varying lengths with a central α-helical rod domain. The head domain of CK18 is composed of amino acids 1 to 82, as indicated, and contains serine residues that are sites for phosphorylation or O-glycosylation with N-acetylglucosamine. The central rod domain is composed of four α-helical regions, labelled 1A, 1B, 2A, and 2B,.which are connected by non-helical linker domains. The hatched regions of the 1A and 2B domains are amino acids highly conserved in intermediate filaments. The conserved 1A domain is the site of helix initiation and is a mutational hot-spot that results in a variety of epidermal diseases (see Discussion, section 1.6.1, 1.7.3). The tail domain of CK18 begins at residue 391 and goes to the C-terminal residue (amino acid 429).

found in most simple epithelia, such as liver (Van Eyken and Desmet, 1993). CK18 protein is also found in other simple glandular epithelia such as the kidney (tubular epithelia), lung, pancreas, intestine, trachea, bladder urothelium, uterus, and mammary tissue (Moll *et al.*, 1982; Abe and Oshima, 1990). CK18 has also been detected in certain stratified epithelia such as esophagus (Bosch *et al.*, 1988; Abe and Oshima, 1990). CK18 is not found in the bulk of the brain, the heart, and muscle. The literature reports that CKs are not found in endothelial cells. However, CK1 expression in HUVECs has recently been described (Schmaier, 1997) and CK8 and CK18 is apparently found in endothelial cells *in vivo* (personal communication with Bryan Hewlett, Histopathology Laboratories, Department of Pathology, McMaster University). CK18 is also found in a variety of tumor cells (Moll *et al.*, 1982) *in vitro* and *in vivo*. Clinical relevance of tissue CK identification comes from the fact that CK tissue-specific expression has been found to be maintained in cells even after neoplastic transformation (Sundstrom and Stigbrand, 1994; Van Eyken and Desmet, 1993). This allows the lineage of tumors to be traced, thus aiding in classification of a particular tumor type.

Within each type of CK there is high homology (50-99% identity) in the α-helical rod domains which drops to $< 30\%$ when comparing proteins between the types. However, even within types there is notable diversity in the end domains (Hanukoglu and Fuchs, 1982; Hanukoglu and Fuchs, 1983). Despite this diversity in the end domains, all CKs form similar morphological filaments, which implies the importance of the α-helical domains in filament formation. The divergence

in the end domains, along with the diversity of tissue expression of the CKs, could indicate that individual CKs might have specialized functions within cells, besides forming filaments (Fuchs and Weber, 1994; Steinert, 1993).

1.6.1 IF Structure and Formation

The 310-350 amino acid central α-helical rod domain is composed of four α-helical regions (1A, 1B, 2A, 2B) joined by three linker domains (L1, L1-2, L2) (see Figure 3). The α-helical rod domains are characterized by repeating heptads of amino acids (abcdefg) (Coloumbe, 1993; Steinert, 1993; Fuchs, 1994a; Fuchs and Weber, 1994). Within these repeats a common motif is that the first and fourth residues (a, d) are apolar residues. Furthermore, a series of zones of alternating basic and acidic residues exist possibly to stabilize intrachain interactions through salt bridge formation (Fuchs and Weber, 1994). Monomers of IFs align in parallel (ie N-terminus to N-terminus) to form dimers with the α-helical rod domains wrapping around each other to form a coiled-coil structure. Dimerization, and the formation of higher oligomers, is thermodynamically favoured as it protects the heptad hydrophobic residues from the aqueous environment (Downing, 1995). Dimers then associate in an antiparallel fashion to form tetramers. Sucrose velocity gradient sedmentation studies have found that the tetramer is the smallest IF subunit found *in vivo* (Soellner *et al.*, 1985; Franke *et al.*, 1987; Chou *et al.*, 1987). Based on such data, it has been proposed that the tetramer is the basic unit of filament formation (Fuchs and Weber, 1994) and that tetramers form rapidly after synthesis of the IF proteins (Bachant and

Klymkowsky, 1996).

Unlike other IF proteins, CKs form obligate heteropolymers. On the basis of cross-linking studies, it has been proposed that CKs form heterodimers before polymerizing into higher forms. However, recent modelling studies suggest that CKs, like other IFs, also form homodimers before forming higher order oligomers (Downing, 1995). This possibility is supported by the observation that *in vitro* homodimers of CKs can be formed and be incorporated into filaments, but cannot form filaments by themselves (Steinert, 1990). This is further supported by the observation that analogous vimentin-desmin filaments are built from homopolymers of vimentin and desmin (Traub *et al.*, 1993). Other evidence suggests however, that homodimeric CKs cannot be found within cells (Steinert, 1990; Pang *et al.*, 1993). The structural interactions between dimers is not truly known with both staggered and in register interactions found (Meng *et al.*, 1996; Coloumbe and Fuchs, 1990; Steinert, 1991).

The rod domains are obviously central for filament formation but the roles of specific regions, including the head and tail domains, have also been examined using molecular mutagenesis and deletion studies (reviewed in Fuchs, 1994; Fuchs and Weber, 1994; Fuchs, 1996). Tail-less IFs form normal filaments although they tend to break down, indicating a possible stabilizing role for the tail domains (Bader *et al.*, 1991; Fuchs and Weber, 1994). The head domain appears to be more important in filament formation, with putative roles in both lateral and end-end interactions (Fuchs and Weber, 1994). Recent *in vitro* evidence suggested no

role in filament formation for either end domain (Meng *et al.*, 1996). It is interesting to note that headless CK14 has been shown able to form filaments with wild-type CK5 (Coulombe *et al.*, 1990) but headless CK5 is unable to form filaments with wild-type CK14 (Wilson *et al.*, 1992). This fact underscores once again that structural differences in CKs can lead to functional differences. The sequence identity of all IFs is especially high at the beginning of rod 1A and the end of rod 2B (see Figure 3) (Fuchs, 1996). CK14 deletion mutants, in either one of these regions, resulted in drastic alterations in the endogenous CK filaments in transfected cells, resulting in punctate keratin aggregates in the cells (Albers and Fuchs, 1989). Similarly, microinjection of mimetic peptides from helix initiation 1A domain into cultured fibroblasts resulted in rapid disassembly of IF networks (Goldman *et al.*, 1996). Furthermore, *in vitro* filament assembly was altered with these mutants, such that the filaments formed were considerably shorter than wild-type filaments (Coulombe *et al.*, 1990). Site-directed mutagenesis studies of the N-terminus of helix 1A or the C-terminus of helix 2B found that these regions are very sensitive to mutation, with even conservative changes resulting in dramatic changes in the formation of 10 nm filaments (Loewinger and McKeon, 1988; Hatzfeld and Weber, 1991).

1.7 Biochemistry of CK18

1.7.1 Protein Structure of CK18 and Post-Translational Modifications

Human CK18 is a single chain phosphoglycoprotein of 429 amino acids with an electrophoretic mobility corresponding to a molecular mass of 45 kDa (Oshima *et al.*, 1986; Leube *et al.*, 1986; Van Eyken and Desmet, 1993). Human CK18 is 89.7% identical to the mouse homolog (Endo B) and contains an extra seven amino acids (Oshima *et al.*, 1986). Interestingly, the slightly smaller murine protein has a slower mobility (49 kDa) than human CK18 (Van Eyken and Desmet, 1993). CK18 is a type I (acidic) CK with an isoelectric point of 5.8 (Moll *et al.*, 1982). The *in vivo* half-life of mouse liver CK18 was determined to be between 98 and 104 h, from pulse-labelling experiments (Denk *et al.*, 1987). Similar half-life values obtained for CK8 indicate the coordinate synthesis and degradation of these two proteins. In HT29 cells (human colonic carcinoma cells) pulse labelling experiments revealed little change in CK18 levels over 70 h, indicating possible differences in CK metabolism in cell culture, or between different tissues (Chou *et al.*, 1992).

CK18 undergoes two main post-translational modifications: glycosylation and phosphorylation. CK18 has been demonstrated to contain single O-linked N-acetylglucosamines attached to serine residues 29, 30, and 48, all of which are found in the head domain (Chou *et al.*, 1992; Ku and Omary, 1995). The nature of the glycosylation is a dynamic one with the turnover rate of the carbohydrate

much higher than that of the polypeptide. CK18 also undergoes dynamic phosphorylation with serine 52 having been identified as the major phosphorylation site of CK18 *in vivo* and *in vitro* (Ku and Omary, 1994). Nevertheless, other sites in the head domain also appear to be phosphorylated (Liao *et al.*, 1995). *In vitro* phosphorylation of Ser52 is accomplished by S6 kinase, calcium/calmodulin-dependent kinase, and protein kinase C (Ku and Omary, 1994). Interestingly, glycosylation and phosphorylation appear not to occur on the same molecule, indicating that these different modifications each have their own biological effect, or might even regulate each other. However, at this point in time there is no clear function related to either CK glycosylation or phosphorylation. It was hypothesized that glycosylation/phosphorylation could be important in forming soluble CK fractions (~ 5% of total CK) seen in various cell lines (Chou *et al.*, 1993) and from rat livers (Sayhoun *et al.*, 1982). Studies found that the levels of both glycosylation and phosphorylation were the same for soluble or insoluble CKs indicating that neither plays a role in CK solubility (Chou *et al.*, 1993). Futhermore, glycosylation does not appear to be important in filament formation as CK18 glycosylation mutants formed similar-looking filaments as wild-type CK18 in BHK (mouse fibroblast) and NIH-3T3 (hamster kidney) cells (Ku and Omary, 1995).

Other studies suggest that CK phosphorylation plays a role in filament disassembly and reorganization. Increased phosphorylation of CK18 is seen concurrent with filament disassembly and reorganization in cultured cells, as they

go through the S and G_2/M cell cycle phases (Liao *et al.*, 1995). Subsequently, there is a decrease in phosphorylation coinciding with filament reformation as cells enter the G_1 phase. Another implied function of phosphorylation is to guide CK cellular localization in tissues. Phosphoserine 52-CK18 has been shown to be localized specifically to the basolateral domains of hepatocytes and the apical domains of pancreatic cells *in vivo* (Liao *et al.*, 1995). Still, a large amount of work remains to be done and it will be interesting to see what other effects these post-translational modifications have on CK function and localization.

1.7.2 The Molecular Biology of CK18

The human CK18 gene has been isolated and sequenced (Kulesh and Oshima, 1988; Kulesh and Oshima, 1989). The coding region is 3791 base pairs in length and is contained in seven exons with six introns. The deduced exons were found to be identical to the CK18 cDNA, which had been isolated previously (Oshima *et al.*, 1986). The murine Endo B gene (Endo B ß-1) has also been isolated and sequenced (Ichinose *et al.*, 1988; Oshima *et al.*, 1988). Southern hybridization experiments have revealed that the human genome contains 15-20 homologous genes while in mice there are five homologous genes (Trevor and Oshima, 1985). Expression of the Endo B gene appears to be sensitive to methylation and to nucleases such that in non-expressing cells, like fibroblasts, the gene is in a methylated and DNAase-resistant state (Oshima *et al.*, 1988). However, murine embryonal carcinoma cells do not express Endo B, even though the gene is not methylated and is DNAase-sensitive, indicating that other factors

play a role in murine CK18 expression. The cDNAs of both human (Oshima *et al.*, 1986) and mouse CK18 (Singer *et al.*, 1986) have been isolated. The human cDNA is 1428 base pairs in length an encodes for a protein of 429 amino acids while the mouse cDNA is 1466 base pairs in length and encodes for a protein of 422 amino acids. The cDNAs are 85.3% identical and encode for a protein lacking a signal-sequence.

1.7.3 Functions of CKs

The main function of CKs has been assumed to be that of maintaining the mechanical integrity of cells. This hypothesis is supported by the discovery of the first known IF-mutant-associated pathology (reviewed in Fuchs, 1994; Fuchs, 1996). The generation of truncated-CK14 mutant transgenic mice lead to the discovery that CKs play important roles in known epidermolytic pathology. The role of CK14 in epidermolysis bullosa simplex (EBS) in human patients was identified in transgenic mice which produced a similar phenotype (Vassar *et al.*, 1991). Since then further molecular defects in epidermal CKs have been found to result in epidermolysis bullosa simplex (EBS), epidermolytic hyperkeratosis (EH), epidermolytic palmoplantar keratoderma (EPPK), and other skin diseases (Cadrin and Martinoli, 1995; Fuchs, 1994b, Fuchs, 1996). In these diseases, gene mutations in epidermal CKs 1, 5, 9, 10, 14, 16, and 17 are manifested in the formation of aberrant filaments with the resulting clinical presentation of blistering at sites of physical stress. Analogous to the *in vitro* data, it was found that mutations in the helix 1A and helix 2B domains resulted in the most severe

phenotypes in affected individuals. In all, these observations relate epidermal cytokeratin function with maintenance of cell and tissue integrity.

Other transgenic animal models have shed light on CK function in the liver. Ku *et al.* (1995) created transgenic mice expressing mutant human CK18 (hCK18) (Arg89 to Cys) or wild-type hCK18. The mutant hCK18 resulted in striking disruption of CK filaments, increased phosphorylated and glycosylated soluble CK18 forms which resulted in increased hepatocyte fragility, as demonstrated by a marked decrease in hepatocyte viability after collagenase perfusion. The mutant hCK18 mice also have been found to be more susceptible to drug hepatotoxicity (Ku *et al.*, 1996). These data give support to the concept that CK18 has a role in maintaining cell integrity, as shown for the epidermal keratins. However, CK8 double knockout transgenic mice resulted in less obvious pathology. CK8 -/- targeting was found to be embryonically lethal in C57B1/6 129SV mice with 94% penetrance (Baribault *et al.*, 1993). Interestingly, viable mice showed no gross tissue problems or defects in liver function. When this transgenic line was backcrossed to another mouse strain (FVB/N) the embryonic lethality was less, such that 55% escaped embryonic lethality (Baribault *et al.*, 1994). In these surviving mice, the females were sterile and both sexes developed colorectal adenomatous hyperplasia, resulting in rectal prolapse. Interestingly, although the liver lacked CK filaments there were no apparent morphological problems with the liver, except that the degenerative lesions usually associated with old age (> 1 year) appeared much earlier (3 months). Similarly, liver functions also

appeared to be normal. However, the same collagenase experiments performed on CK18 mutant livers was not performed on CK8 -/- mice livers and therefore increased cell fragility cannot be excluded. Intriguingly, the surviving mice from the CK8 -/-embryonic lethal strain displayed the FVB/N phenotype. This suggests that strain-specific alleles can enhance or suppress the effects from lacking CK8 (Klymkowsky, 1995).

Although the data supporting a mechanical role for epidermal CKs is strong there remains uncertainty about the functions of the other non-epidermal CKs. Cells in culture do not require cytoplasmic CKs for growth, unlike their need for microfilaments, microtubules, or the nuclear lamins. (Fuchs, 1994). Furthermore, although cells possess various CKs during development, differentiated tissues express specific CK pairs coincident with their cellular specialization (Marceau and Loranger, 1995). These observations indicate that the functions of different CKs are tailored to the specific tissue and that CKs have functions besides maintaining cell integrity. For example CKs have been implied to have roles in the movement of organelles and the secretion and internalization of proteins and dyes (Albers *et al.*, 1996; Kawahara *et al.*, 1990; Bendayan, 1985; French *et al.*, 1989). CKs also appear to play roles in tumourigenesis, either by altering functions or assuming new ones (Klymkowsky, 1995). For example CK8 and CK18 have been shown to increase tumour cell motility and invasiveness (Chu *et al.*, 1996; Chu *et al.*, 1995), play a role in tumour progression (Caulin *et al.*, 1992) as well as conferring resistance to a number of anti-cancer drugs (Bauman

et al., 1994). Since oncogenic proteins can activate CKs, it remains to be determined if CKs alone are causal for the effects observed (Pankov *et al.*, 1994).

CKs have also been found to be expressed on the surface of cultured cells where they act as cellular receptors. For example, CK8 has been demonstrated to be expressed on the surface of hepatocytes, HepG2 cells, and breast carcinoma cells where it acts as a plasminogen receptor (Hembrough *et al.*, 1995; Hembrough *et al.*, 1996a). Furthermore, CK1 has also been reported to be found on the surface of human endothelial cells where it acts as a receptor for high molecular weight kininogen (Schmaier, 1997). These findings are not without precedence. Recently other proteins, previously believed to have solely intracellular localization, have been found on the external surface of cells where they have been shown to act as cellular receptors for various plasma proteins. A list of these proteins and their ligands is seen in Table 3. In this regard, I will present my data supporting CK18 as a TAT-binding protein and also present data examining the *in vivo* and *in vitro* metabolism of VN-TAT.

RECEPTOR PROTEIN	*LIGAND(S)*	*CELL TYPE(S)*	*REFERENCE(S)*
cytokeratin 8	plasminogen, t-PA	HepG2 cells, mammary carcinoma cells, primary hepatocytes	Hembrough *et al.*, 1995 Hembrough *et al.*, 1996 Hembrough *et al.*., 1997
cytokeratin 8 and 18	mAb COU-1	colon cancer cells	Ditzel *et al.*, 1997
cytokeratin 1	high molecular weight kininogen	endothelial cells	Schmaier, 1997
actin	factor Va, angiogenin, plasminogen, t-PA, and lipoprotein (a)	endothelial cells	Moroianu *et al.*, 1993 Furmiak-Kazmierczak *et al.* 1995 Dudani and Ganz, 1996
α-actinin	thrombospondin	platelets	Dubernard *et al.*, 1995
nucleolin	apoE and apoB containing lipoproteins	HepG2 cells	Semenkovich *et al.*, 1990
annexin II	plasminogen	endothelial cells	Hajjar *et al.*, 1994

Table 3. Listing of intracellular proteins which have been reported to act as external cellular receptors for various plasma proteins [LIGAND(S)], their cell-type expression, and the appropriate references.

2. MATERIALS AND METHODS

2.1 Materials

2.1.1 Source of Chemicals and Reagents

The diphosphate salt of chloroquine, molecular biological grade sucrose, cyanogen bromide, 5-bromo-4-chloro-3-indolyl phosphate (BCIP), nitroblue tetrazolium (NBT), cyclic adenosine monophosphate (cAMP), thymidine-5'-mono-phospho-p-nitrophenylester, methylamine, phenyl-methyl-sulfonyl fluoride (PMSF), bovine serum albumin (BSA), heparinase (heparin lyase 1 from *flavobacterium heparinum*), pepsin, p-nitrophenyl ß-D-xylopyranoside (ß-D-xyloside), protamine sulfate (grade X, from salmon), and heparin (grade 1-A, from porcine intestines) were purchased from Sigma Chemical Co.(St. Louis, MO). The tissue freezing medium, OCT compound, was purchased from Bayer Canada (Etobicoke,ON).

Coomassie brilliant blue R-250, bromophenol blue, nitrocellulose membranes, polyvinylidene difluoride (PVDF) membranes, Bio-Rad Protein Assay, Triton X-100, Tween-20, and various SDS-PAGE molecular weight protein standards were purchased from Bio-Rad (Mississauga, ON). IODO-GEN and the bicinchoninic acid protein assay (BCA assay) were purchased from Pierce

Chemical Co. (Rockford, IL). Sulfo-propyl (SP)-Sephadex C-50, heparin-Sepharose, and cyanogen-bromide pre-activated Sepharose 4B were all purchased from Pharmacia Biotech Inc. (Baie D'Urfe, Que). Polyethylene glycol (molecular weight 20,000) and 2-octanol were purchased from Fisher Scientific Ltd.(Nepean, ON).

Cell culture media (α-Minimal Essential Media (α-MEM) and Dulbecco's Modified Eagle Medium (DMEM)) and phosphate-buffered saline (PBS) were purchased from the Depament of Pathology at McMaster University. Other cell culture reagents including: penicillin-streptomycin, fetal bovine serum, and cell culture grade 1X trypsin-EDTA (0.05% trypsin; 0.53 M EDTA), were purchased from Gibco-BRL (Mississauga, ON). Additionally, N,N,N',N'-tetramethylethylenediamine (TEMED) and soybean trypsin inhibitor (SBTI) were also purchased from Gibco-BRL.

Electrophoretically pure human α_2-macroglobulin and bovine trypsin, as well as D-phenylalanyl-L-prolyl-l-arginine-chloromethylketone (PPACK) (>99% active), were purchased from Calbiochem (San Diego, CA). Human α-thrombin (> 2000 U/mg > 99% active) was the generous gift of Dr. J. Fenton (New York State Division of Biologicals, Albany, NY). Purified bovine CK18 was purchased from Research Diagnostics Inc. (Flanders, NJ). Arvin (Ancrod) was purchased from Knoll Pharmaceuticals Canada Inc. (Markham, ON). Human serum was the generous donation of the Hamilton Centre of the Canadian Red Cross Society. Non-fat dry milk was purchased at Foino's Grocery Store (Hamilton, ON).

Purified rat liver plasma membrane preparation was a generous gift of Dr. E. Roegeczi (Depament of Pathology, McMaster University). The HPLC purified pentapeptide, FVYLI, was purchased from Enzyme Research Laboratories (South Bend, IN). All other chemicals and reagents used were of the highest quality available.

2.1.2 Radiochemicals

Carrier free ^{125}Iodine (sodium iodide in 0.1 M NaOH, 99.95% radiochemical purity; 629 GBq/mg) was purchased from Dupont Canada Inc (Mississauga, ON).

2.1.3 Rabbits

Male New Zealand White rabbits (weight 2.2-2.7 kg) used in the various experiments of this project were purchased through the Central Animal Facility (CAF) at the McMaster University Medical Centre. The animals were cared for in the CAF in accordance with the Canadian Animal Ethics guidelines.

2.1.4 Antibodies

Anti-human CK18 Monoclonal antibodies, CY-90 and KS-B17.2, were purchased from Sigma Chemical Co. (St.Louis, MO). CAM 5.2 monoclonal anti-human cytokeratin was purchased from Becton Dickinson Canada Inc. (Mississauga, Ontario). Alkaline phosphatase and horseradish peroxidase (HRP)-conjugated rabbit anti-chicken IgG, alkaline phosphatase-conjugated rabbit anti-sheep IgG, and alkaline phosphatase-conjugated goat anti-rabbit-IgG were purchased from Jackson Laboratories (Mississauga, ON). Biotinylated goat anti-

mouse IgG and streptavidin-HRP were purchased from Dako Diagnostics Canada Inc. (Mississauga, ON). Rabbit anti-human VN antibodies were purchased from Celsus Laboratories Inc.,(Cincinnati, OH). Goat anti-human HCII serum was purchased from Diagnostica Stago through Murex Diagnostics (Guelph, ON). Sheep anti-human VN antibodies were the generous gift of Dr. T. Podor (Depament of Pathology, McMaster University). Affinity-purified sheep anti-human α-thrombin and chicken anti-rabbit AT has been previously isolated by Mr. Myron Kulczyky, a technologist working for my supervisor, Dr. M.A. Blajchman.

2.1.5 Cell Lines

HepG2 cells, purchased from the ATCC (Rockville, MD), were grown in αMEM, supplemented with 10% fetal calf serum and 100 units/ml of penicillin-streptomcyin. The rat hepatoma cell line, HTC, was a generous gift of Dr. T. Podor (Depament of Pathology, McMaster University). These cells were grown in DMEM supplemented with 10% fetal calf serum and 100 units/ml penicillin-streptomcyin. LTK- fibroblasts were a kind gift of Dr. P. Chang (Depament of Pediatrics, McMaster University) and were cultured in DMEM containing 10% fetal calf serum and 100 units/ml penicillin-streptomycin.

2.2 Purification and Modification of Proteins

2.2.1 Purification of Rabbit AT

AT was purified by chromatographic separation of plasma proteins on

heparin-Sepharose. The heparin-Sepharose used was either purchased from Pharmacia or heparin was conjugated to Sepharose 4B using cyanogen bromide according to the procedure outlined by Miller-Andersson *et al.* (1974). Rabbit plasma (100 ml) was applied to the heparin-Sepharose column (~ 35 ml heparin-Sepharose) and the column was then washed with 0.5 M NaCl buffered with 0.05 M Tris-HCl (pH=7.4) until the O.D.< 0.03. Rabbit AT was batch eluted using 0.05M Tris-HCl (pH=7.4) containing 2.0 M NaCl and dialyzed against 0.025 M Tris-HCl (pH=7.4) containing 0.150 M NaCl and 0.02% Na azide (TBS) overnight. AT concentration was determined spectroscopically using the $E^{1\%280\ nm}$ value of 6.5 (Atha *et al.*, 1984b). The purity of AT and its functional ability to inhibit α-thrombin (see below section 2.2.6) were determined by SDS-PAGE as described by Laemmli (1970).

2.2.2. Purification of Bovine α-Thrombin

Bovine thrombin was purified from Thrombostat (Parke-Davis Co., Detroit, MI) by cation exchange chromatography on SP-Sephadex (Pharmacia, Uppsala, Sweden) as described by Hatton *et al.* (1978). Two vials of Thrombostat (10,000 NIH units/vial) were resuspended in 0.05 M phosphate, pH=6.5, and applied to a 30 ml SP-Sephadex column equilibrated in the same buffer. The column was washed with the same buffer until the O.D. < 0.03. The column was then washed with 0.1 M phosphate, pH=6.5 until the O.D. < 0.03. Bound thrombin was eluted with a gradient from 0.1 M phosphate, pH=6.5 to 0.3M phosphate pH=8.0. The presence of thrombin in the different fractions was detected by clotting assay on

human plasma and verified by SDS-PAGE. Fractions with high clotting activity were pooled and dialyzed against 0.15 M NaCl buffered with 25 mM phosphate, pH=7.4 overnight at 4°C. The dialyzed protein was then concentrated using polyethylene glycol at 4°C. The concentration of the thrombin was determined spectroscopically using the $E^{1\%}_{280\ nm}$ = 16.2 (Atha *et al.*, 1984b).

2.2.3 Purification of VN-TAT

VN-TAT was purified on heparin-Sepharose from human serum according to the method of de Boer *et al.* (1992). The protein concentration of the purified VN-TAT was determined with the Bio-Rad Protein Assay kit.

2.2.4 Preparation of Chicken Anti-CK18 and Preimmune Antibodies

Antibodies against bovine CK18 were generated by injecting laying hens with 40 μg of purified bovine CK18 in complete Freund's Adjuvant, followed by three weekly injections with 40 μg of bovine CK18 in incomplete Freund's Adjuvant. The chicken IgG was purified as described (Polson, 1990).

The reactive IgG was purified by affinity chromatography on a column in which a liver-cytoskeletal protein extract had been coupled to Sepharose 4B. The cytoskeletal proteins (mainly CK8 and CK18) were semi-purified according to the procedure of Meiklejohn *et al.* (1990) except that the proteins were solubilized in a 0.1 M sodium bicarbonate, pH=8.3 containing 9 M urea. This mixture was then coupled to pre-activated Sepharose 4B according to the manufacturer's protocol (Pharmacia Biotech Inc., Baie D'Urfe, Quebec).

Total chicken IgG was loaded onto the affinity-column which was

equilibrated in TBS buffer. Non-specifically bound IgG was removed with 50 mM Tris-HCl, pH=7.4 containing 1M NaCl. Specifically bound IgG was then eluted by using 0.1 M sodium citrate (pH=4.0) into tubes containing 2 M Tris base, to neutralize the acid. The IgG was then dialyzed overnight against TBS containing 0.02% sodium azide and stored at 4°C. Preimmune IgG was fuher purified from total IgG on DEAE-Sephadex using the procedure of Gassmann *et al.* (1990). DEAE-Sephadex was equilibrated in 0.015 M phosphate, pH=8.0. ≈ 15 mg of IgG in 3 ml of the same buffer, was loaded onto the column. A gradient was then run from 0.015 M phosphate, pH=8.0 to 0.2 M phosphate, pH=8.0. The gradient was 100 ml in total and 2 ml fractions were collected. The fractions were checked by SDS-PAGE and the most homogeneous IgG fractions were pooled, dialzyed against PBS, and concentrated. Anti-CK18 and preimmune Fab fragments were made from purified IgG by the method of Harlow and Lane (1988) using pepsin.

2.2.5 Radiolabelling of Proteins

For radioiodination of all proteins, IODO-GEN-coated glass vials were used as described in the method of Fraker and Speck (1978). IODO-GEN was solubilized in chloroform (10μg/100μl) and left to dry in glass vials in a fumehood overnight. Typically 100 μg of thrombin was radiolabelled in a volume of 300 μl of chilled PBS for 3 min in the vials while stirring at . To remove free ^{125}I, the ^{125}I-thrombin was then immediately dialyzed against an initial 500 ml of chilled PBS in a packed ice-bucket, while stirring, for 2-3 h at room temperature. Fuher free ^{125}I was then removed by extensive dialysis overnight at 4°C.

Methylamine-modified α_2M (α_2M*; see below, section 2.2.6), VN-TAT, AT, anti-CK18 IgG, and chicken preimmune IgG were all radiolabelled in an identical fashion with labelling being carried out with protein concentrations ranging from 50 to 200 μg. All ^{125}I-protein samples were measured for radioactivity using a Packard MINAXIγ autogamma 5000 series gamma counter. VN-TAT had a specific activity of 1400-2800 dpm/ng, AT had a specific activity of 4400 dpm/ng, anti-CK18 and preimmune IgG had specific activities of 700-1400 dpm/ng, and α_2M* had a specific activity of 12000 dpm/ng.

2.2.6 The Formation of TAT, TRAP, and α_2M*

TAT was formed by reacting thrombin, or ^{125}I-thrombin, in a 1:3 molar ratio with AT at 37°C for 30 min. To inhibit any residual active thrombin PPACK was added to the reaction at a final concentration of 100 μM and left at 37°C for 5 min. The TAT was then dialyzed against cell-radioligand binding buffer overnight (see below, section 2.4.2) and then aliquoted and stored at -70 °C. ^{125}I-TAT was immediately aliquoted and stored at -70°C. The formation of TAT and ^{125}I-TAT were verified by analysis on 10% SDS-PAGE gels and visualized by staining with Coomassie blue or by autoradiography. TRAP was formed in an identical fashion except that any remaining active trypsin was inhibited by the addition of PMSF, solubilized in dimethyl sulfoxide, to a final concentration of 1 mM.

α_2M* was formed according to the method of Wu and Pizzo (1996). Briefly, 10 mg of α_2M was reconstituted in 2 ml double distilled water. 600 μl of

1M methylamine, solubilized in double distilled water, was mixed with 1.8 ml α_2M and water added to give a final methylamine concentration of 200 mM. The reaction was left for 18 h in the dark then the mixture was dialyzed against PBS at 4°C overnight. The molecular mass of α_2M* used for these experiments was 720 kDa. For radioligand binding experiments on cultured cells the different ligands were dialyzed against the corresponding cell media (i.e. DMEM for HTC and fibroblasts), lacking fetal calf serum and penicillin-streptomcyin, but buffered with 10 mM HEPES, pH=7.4.

2.2.7 Preparation and Purification of Rabbit Liver Plasma Membranes

Rabbit liver plasma membranes were purified as described (Hubbard *et al.*, 1983a) with minor modifications. Briefly, young male New Zealand White rabbits (1.5 kg each) were starved overnight, and anesthetized with Na pentobarbital prior to euthanization by exsanguination. The livers were exposed and perfused through the poal vein with warm (22 °C) buffer at pH 7.4 containing 0.25 M sucrose, 10 mM Tris-HCl, 1 mM EDTA, and 1 mM PMSF (STEP). The perfused livers were then excised and immersed in cold STEP, then homogenized using a Polytron homogenizer (Brinkmann, Switzerland) at high power for two cycles of 30 s each. Rabbit platelets were prepared as described previously (George, 1978). Rabbit platelet membranes were isolated by lysing the platelets in double distilled water, at ambient temperature, after which the membranes were recovered from the soluble components by centrifugation at 16,000 × g for 10 min. The protein concentration of the final plasma membrane preparations was determined using

the BCA assay.

2.3 Analysis of Proteins by Western and Ligand-Blotting Assays

2.3.1 Electroblotting of Proteins onto Membranes

For the electroblotting of proteins from SDS-PAGE gels, onto either nitrocellulose or PVDF membranes, the Bio-Rad Mini-Protean II electroblotter was used and was performed as follows, unless indicated. After SDS-PAGE, the gels were equilibrated in 25 mM Tris (pH=8.3) containing 192 mM glycine for 30 min at room temperature by gentle shaking. During this time nitrocellulose and Whatman #3 chromatography paper were equilibrated in the same buffer without shaking. The gel, Whatman paper, and nitrocellulose were placed together according to the instructions from the manufacturer. The proteins within the gels were then electroblotted onto nitrocellulose at 0.4A, 4°C, 1 h (4 h for ligand-blot gels) in pre-chilled equilibration buffer. After electroblotting the non-specific sites on the blots were blocked by incubating the blots overnight with 5% (w/v) non-fat dry milk in TBS (5% blotto) at room temperature.

2.3.2 Western Blot Analyses

For Western blots the pre-blocked blots were incubated with primary antibodies in 5% blotto at room temperature for one h. The dilution of antibodies used for Western blots are given in the appropriate figure legends. The blots were then washed by gentle shaking, 3 times for 5 min each, with TBS

containing 0.1% Tween-20. The alkaline-phosphatase conjugated secondary antibodies were used at 1/5000 dilution, unless otherwise indicated, and were incubated with the blots in 1% blotto for one h at room temperature. The blots were washed as described above and the bound antibodies recognized by development with BCIP (0.165 mg/ml final; 50 mg/ml stock solution in N,N-dimethylformamide) and NBT (0.33 mg/ml final; 50 mg/ml stock in 70% N,N-dimethylformamide) in TBS, pH=9.5 containing 5 mM $MgCl_2$. Colour development was stopped by rinsing the blots in tap water. The blots were dried between two pieces of #3 Whatman chromatography paper and stored in the dark.

To determine the presence of CK18 in rabbit tissues, the organs were freshly removed from anaesthetized rabbits, poions were excised, and immediately homogenized for 1 to 2 min at room temperature in 100 ml of TBS containing 10mM EDTA and 1mM PMSF using a polytron homogenizer (Brinkmann, Switzerland). To separate any non-homogenized materials from the homogenized tissue, samples were removed (~ 1 ml) into microcentrifuge tubes and then spun at 1000 RPM for 5 min and 300 μl of the supernatants removed. The amount of protein in the supernatants was determined by BCA assay. Samples were solubilized in 4X reducing SDS-sample buffer and a total of 20 μg, in 20μl, of each tissue sample was loaded per well on 10% SDS-PAGE gels. For the detection of CK18, 1 μg/ml chicken anti-CK18 IgG was used as the primary antibody.

For the detection of CK18 in fibroblasts and HTC cells cells Western blot analyses were performed. Cells grown in 24 well culture dishes were solubilized with 100 μl SDS-PAGE sample buffer and then passed through a 20 gauge needle with a 1 ml syringe to shear the DNA. When the mixture was able to be pipetted easily it was placed into a microcentrifuge tube which was put into boiling water for 3 min, cooled to room temperature, and centrifuged for 30 s. For blotting purposes, 32 and 16 ng quantities of CK18 were loaded onto a 10 % SDS-PAGE gels along with 20 and 10 μl of HTC cell extract and 20 μl fibroblast cell extract. However the fibroblast extract tube broke in the centrifuge and I was forced to use residual extract found in the syringe, therefore the amount of electrophoresed protein was much lower for the fibroblast extract than for the HTC cell extract.

2.3.3 Ligand-Blotting Assay

For ligand-blot assays, 32 μg of rabbit liver plasma membranes, rat liver plasma membranes, total platelet membranes, or 1 μg of purified CK18, were separated on 10% SDS-PAGE gels and electroblotted onto nitrocellulose as discussed above. The radioligand solution was composed of 10 nM ^{125}I-TAT, with or without competitors, in 5% Blotto containing 2 mM $MgCl_2$ and 1 mM $CaCl_2$. The blots and 10ml of the ^{125}I-TAT solution were placed together in plastic hybridization bags and were rocked gently at 37°C for 40 min in a hybridization oven. The blots were then removed and washed 4 times for one hour each with 300 ml of TBS buffer containing 1% skim milk powder and 0.3% Tween-20. The blots were then air dried and exposed to Kodak X-Omat XAR-1 film at -70°C,

usually for 24 h, before developing.

2.3.4 Isolation and Identification of the 45 kDa TAT-Binding Protein

7 ml of ice-cold TBS was added to 500 μl of rabbit liver plasma membranes (17.5 mg/ml), mixed, and was pelleted in a Ti70 rotor at 16,500 RPM (20,000 g) for 10 min at 4°C. The supernatant was removed and the pellet washed gently two times with 10 ml ice-cold TBS. The pellet was then resuspended in 1750 μl of ice-cold TBS and 18 μl of Triton X-100 added. This was mixed by voexing and left on ice for 30 min. The pellet was then spun down at 16,500 RPM (20,000 g) for 10 min at 4°C. The supernatant was removed and the pellet washed two times with 1 ml ice-cold TBS and then resuspended in 1750 μl ice-cold TBS. 875 μl was then placed into a microcentrifuge tube and 292 μl of reducing 4X SDS-PAGE sample buffer added. The solution was voexed briefly and then placed into boiling water for 4 min.

400 μl of the SDS-solubilized material was then electrophoresed on a 1.5 mm thick 12% acrylamide SDS-PAGE gel made with a preparative comb. The gels were stained with 0.3 M $CuCl_2$ for 5 min according to the method of Lee *et al.* (1987). The TAT-binding band and other control bands were excised with a scalpel and then destained by washing three times in 0.25 M Tris, pH=9.0 containing 0.25 M EDTA, for 10 min each. The gel pieces were then equilibrated in a buffer of 25 mM Tris base containing 192 mM glycine and 0.1% SDS for 20 min by gently rocking the gel pieces in the solution. The proteins were then eluted from the slices in the same buffer using a Bio-Rad (Mississauga, ON)

electroeluter according to the manufacturer's instructions. The condition of the eluted bands was checked by SDS-PAGE and Coomassie blue staining. The ability of the eluted proteins to bind ^{125}I-TAT was verified by ligand-blot assay and compared to rabbit liver plasma membranes (see Results section 3.1.5).

For amino acid sequencing, 670 μl of the purified TAT-binding protein were electrophoresed again on 1.5 mm thick 12% acrylamide SDS-PAGE gels and electroblotted onto PVDF in a solution of 25 mM Tris base containing 192 mM glycine, 0.01% SDS, and 20% methanol at 0.4 A, in ice, for 3 h. The blot was rinsed in double distilled water and stained with Ponceau S. The blot was then placed in 1% acetic acid and the TAT-binding protein band was cut out. This piece of blot was then voexed in double distilled water and the water removed. The piece of blot was then sent to Harvard Microchem (Cambridge, MA) for protein digestion, HPLC peptide separation and isolation, and amino acid sequencing. Amino acid homology to other proteins was determined using the NCBI BLASTN protein homology search program.

2.4 Radioligand Binding Experiments

2.4.1 Binding to Rabbit Liver Plasma Membranes

Binding experiments with rabbit liver plasma membranes were done in a total volume of 125 μl of 1% BSA in TBS with various amounts of rabbit liver plasma membranes containing the desired amount of ^{125}I-TAT and competitors.

All binding reactions were done in microcentrifuge tubes pre-coated with 5% BSA in TBS. In all experiments the membranes were resuspended in TBS such that 10 μl contained the desired amount of total membrane protein per reaction tube. The membranes were stored on ice in a microcentrifuge tube until the experiment was to sta. At this point the membranes were voexed before adding them to three different tubes (triplicates) making up each reaction point. The different binding reactions were staggered at two min intervals and the stock membrane tube voexed each time before addition. The reaction tubes were also voexed and added to a shaking water bath at 37°C to keep the membranes in solution. Initial association experiments revealed that steady-state for ^{125}I-TAT binding to rabbit liver plasma membranes occurred by 40 min and this was the length of time chosen for all following radioligand binding experiments to rabbit liver plasma membranes. Immediately after this incubation 1 ml of cold TBS was added to the tubes and the tubes centrifuged at 16,000 g for 2 min. The pellets were washed three times and the tips of the microcentrifuge tubes were cut off and the bound radioactivity was determined. Competitive binding curves were obtained by analyzing the data by non-linear regression analysis using the analytical graphics programme, Fig.P (Biosoft, Ferguson, MO.).

2.4.2 Radioligand Binding Experiments With Cultured Cells

For cell binding experiments, cells were grown on 24 well plates at a final density of ~ 4.5 $\times$ 10^5 cells/well. Binding experiments were performed in cell binding buffer. This was composed of either αMEM (for HepG2 cells) or DMEM

(for HTC cells) containing 0.5% BSA and buffered with 10 mM HEPES, pH=7.4. Cells were washed in binding buffer and then incubated with the ligand (either ^{125}I-TAT, ^{125}I-VN-TAT, or ^{125}I-IgG), with or without competitors, in binding buffer at 4°C for two h. The reaction solution was aspirated and the cells were washed three times with 10 mM HEPES (pH=7.4) containing 0.15 M NaCl, 1 mM $CaCl_2$, 2 mM $MgCl_2$, and 0.5% BSA (HBSB). The cells and associated radioactivity were solubilized by incubation with 2 M NaOH overnight before counting for radioactivity. Competitive binding curves were obtained by analyzing the data by non-linear regression analysis using the analytical graphics programme, Fig.P.

For experiments on HepG2 cells using ß-D-xyloside the cells were trypsinized and re-plated on 24 well culture dishes in the presence of a final concentratioin of 2.5 mM ß-D-xyloside in the cell culture media for 3 days before conducting the binding experiment. This reagent was made up in dimethyl sulfoxide (DMSO) and an equal volume of DMSO was added to control wells.

In experiments using heparinase-treated HepG2 cells, the cells were first washed twice with αMEM buffered with 10mM HEPES (pH=7.4). The heparinase was then added in the same buffer, for 2.5 h at 37°C, at a final concentration of 30 units/ml.

2.4.3 Radioligand Binding to Fixed and Fixed-Permeabilized Cells

The protocol for fixation-permeabilization of all cell types was the same. For fixation of cells 3.7% formaldehyde in buffered phosphate (pH= 7.6) was used. This solution was made as follows: 87 ml of 1.0 M sodium phosphate was

added to 750 ml of double distilled water; 40 g of paraformaldehyde was added to this and mixed under gentle heat; when dissolved 13 ml of 1.0 sodium phosphate (monobasic) was added and the volume was brought to 1 l with double distilled water.

Cells were fixed with cold formaldehyde at room temperature for 15 min. The cells were then washed once with a solution buffered with 10 mM HEPES (pH=7.4) containing 150 mM NaCl (HBS). Next, the cells were incubated with 0.1 M glycine in HBS at Room temperature for 10 min to quench the fixation reaction, the solution was aspirated off and the cells washed once with HBS. To permeabilize fixed cells 0.1% Triton X-100 in HBS was added to cells for 5 min. This solution was aspirated off and the cells washed twice in HBS before beginning the binding experiment. The binding experiments were then conducted exactly as done with intact cell monolayers described above (section 2.4.2).

2.4.4 Binding of ^{125}I-TAT and ^{125}I-Anti-CK18 IgG to Trypsinized HepG2 Cells

The media from confluent HepG2 cells in 24-well cell culture dishes was removed and the cells were washed twice with HepG2 cell-binding buffer. Then 50μl HepG2 cell-binding media, or 50 μl of 2.5 mg/ml bovine trypsin in HepG2 cell-binding media, was added to each well for 5, 10, or 15 min at 37°C. To the trypsinized wells 50 μl of 2 mg/ml SBTI (this is a two-fold molar excess required to inhibit the trypsin) was added at 37°C for five min. To the control wells 50 μl of binding media was added or the 50 μl of media removed and 100 μl of pre-formed trypsin-SBTI complexes added, equivalent to the amounts of complex that

would form in the culture wells. 100 μl of ^{125}I-TAT or ^{125}I-anti-CK18 IgG, in binding media, were then added to the cells at 4°C for 2 h. The intact cell monolayers were washed three times with HBSB and 500 μl of 2M NaOH added to the wells to remove the cells and the associated radioactivity for γ-counting. The trypsinized cells were carefully aspirated off and added them to microcentrifuge tubes. Fresh 200 μl of binding media was placed back into the wells to ensure that all the cells and radioactivity were aspirated off. 1 ml of binding media was added to the tubes and they were centrifuged at 16,000 g for 2 min. The media was removed and the cell pellets were washed two times with 1 ml binding media on each occasion. The tips of the tubes were cut off and measured for associated radioactivity.

2.4.5 Solid-Phase Binding to CK18

Purified bovine CK18 (500 ng in 0.1 M phosphate (pH=8.0)), was dried onto the wells of Immulon 4 ELISA plates (Dynatech Labs, Chantilly, VA) by incubation overnight at 37°C. The wells were washed two times with TBST (0.1% tween-20) before blocking the non-specific sites with 1.5% BSA in TBS at 4°C for two h. The wells were then washed with TBST and incubated with desired concentrations of ^{125}I-preimmune or anti-CK18 IgG at 37°C for 40 min. The wells were then washed three times with TBST and the individual wells were separated and subjected to gamma-counting.

2.5 Cell Receptor-Mediated Endocytosis Experiments

2.5.1 Internalization Assay

^{125}I-TAT internalization assays were performed on HTC cells at ~ 80% confluency. The cells were first washed three times with pre-warmed binding buffer before adding the rection mixture. The reaction mixture, 200 μl in total, contained 50 nM ^{125}I-TAT, in the absence or presence of 2.5 μM unlabeled TAT, 100 μM chloroquine, 850 nM anti-CK18 Fab, or 850 nM preimmune Fab fragments in HTC-cell binding buffer which was pre-warmed at 37 °C. The reaction took place at 37°C in a cell incubator (95% CO_2/5% O_2) over a period of five h. The binding media was then removed and the cells were incubated with ice-cold 5 mg/ml proteinase K at 4°C for 30 min. The cells and supernatant were then aspirated from the culture wells, placed into microcentrifuge tubes, and centrifuged at 16,000 g for 5 min at room temperature. The supernatant was aspirated off and the tips of the microcentrifuge tubes cut off and the cell pellet-associated radioactivity was counted. In other experiments, the anti-CK antibody CAM 5.2 was used to inhibit ^{125}I-TAT internalization. The antibodies were first concentrated using Millipore Ultrafree concentrators (10 kDa cutoff)(VWR Canlab, Mississauga, ON) down to a concentration of 72.5 μg/ml. The antibodies were then dialyzed into DMEM buffered with 10 mM HEPES, pH=7.4 overnight at 4°C. For each experiment 10.9 μg of CAM 5.2 and control IgG were used in the reaction mixtures and the experiment conducted as described above.

2.5.2 VN-TAT Degradation Assay

For these experiments, the concentration of ^{125}I-VN-TAT and α_2M* used was 10 nM final in a total volume of 200 μl. All competitors were either dialyzed or solubilized in DMEM buffered with 10mM HEPES, pH=7.4. Cells were washed three times with sterile filtered (0.2 μM filters) HBS containing 2 mM $MgCl_2$ and 1 mM $CaCl_2$. The reaction media which contained the radioligand in the absence or presence of 775 nM α_2M*, heparin (100 units/ml final), or chloroquine (100 μM final) was then added to the cells. The radioligands in the reaction buffer were added to 24-cell culture wells, that had been pre-incubated with normal HTC cell media, to control for non-cellular mediated protein degradation over the experiment. At the appropriate time points (0, 1, 4, and 17 h) media was removed from the wells and 100 μl of the media was added to 100 μl of 20% trichloroacetic acid (TCA) to precipitate out non-degraded proteins (any protein or peptide > 10 kDa). To determine true cell-mediated degradation of proteins, the total TCA-soluble counts from the control wells were subtracted from the TCA-soluble counts in the experimental wells.

2.6 Immunohistochemical Experiments

2.6.1 Tissue Preparation

Tissues were prepared for either paraffin-embedding or were flash frozen. In brief, for paraffin-embedding small pieces (~ 5 mm thick) were cut from livers

of anaesthetized rabbits and immediately placed into 3.7% formaldehyde overnight. The next day the pieces were sequentially placed into 50%, 60%, and finally 70% ethanol for at least one hour each. The pieces were then processed and paraffin-embedded by the Histology Laboratory, (Depament of Pathology, McMaster University Medical Centre). For the frozen sections, tissue was cut from the livers of anaesthetized rabbits and placed into small open containers made of foil wrap containing small amounts of OCT compound. These were then dropped into a beaker of isopentane cooled in liquid nitrogen. When the OCT became frozen solid the foil containers were twisted closed and dropped into the liquid nitrogen, and then stored at -70°C. All sections cut from the liver blocks, prepared by either technique, were 5 μm thick and mounted on aptex slides (prepared by the Histology Laboratory) and dried overnight at Room temperature.

2.6.2 Immunocytochemistry

Slides were first baked at 60°C for 45 min. The paraffin-embedded sections were then de-paraffinized as follows: 1) three separate incubations in xylene for 15 min each; 2) three successive washes in 100% ethanol, by agitating for 10 s, followed by a 1 minute incubation in each; 3) 30 min in freshly prepared 200 ml methanol containing 5 ml of 30% hydrogen peroxide and 0.5 ml concentrated HCL; 4) transfer to 100% ethanol, to 95% ethanol, to 70% ethanol by a 10 second agitation then 1 minute incubation in each; 5) then a five minute wash in running tap water; and finally 6) a rinse in distilled water. The slides

were kept moist at all times and immunostained as quickly as possible. Frozen sections were prepared for immunostaining by incubating in acetone for 10 min, air dried, and then immunostained.

Identification of primary antibody (monoclonals) was done by using a streptavidin-biotin system from Dako Diagnostics Canada Inc.(Mississauga, ON) described below. Additionally, at this stage some paraffin sections were incubated with 0.1% trypsin in TBS with 0.1% $CaCl_2$ at 37°C for twenty-five min to expose antigenic epitopes which might be blocked by fixation. The slides were then incubated with TBS diluted 10-fold with distilled water for 15 min and placed in a humid chamber. The slides were then incubated for 15 min with 2-3 drops of a protein blocking agent containing normal swine serum from Dako. Each slide was then drained and wiped and primary antibody added, after appropriate dilution in Dako dilution buffer, overnight in a sealed humid chamber. The antibody dilutions used for staining the paraffin sections were 1/500 and 1/100 for the monoclonal antibodies CY-90 and KS-B17.2 respectively, while chicken anti-CK18 antibodies were used at a concentration of 1 μg/ml. For staining the frozen sections the monoclonal antibodies were used at a 1/1000 dilution while the chicken anti-CK18 antibody was used at 0.1 μg/ml. The slides were also stained with equivalent amounts of preimmune IgG as a negative control.

The following morning the slides stained with the monoclonal antibodies were washed three times with TBS for five min each. They were then incubated with optimally diluted biotinylated antibodies from Dako at Room temperature

for 45 min in the humid chamber and then washed as above (3× 5 min with TBS). The slides were incubated with an optimally diluted streptavidin-horseradish peroxidase conjugate (from Dako) for a fuher 45 min. Chicken IgG stained slides from the overnight incubation were washed as above and incubated with a horseradish peroxidase-conjugated rabbit anti-chicken IgG at a dilution of 1/500 in Dako dilution buffer for one hour in the humid chamber. The slides were then washed as above. The slides were then incubated with 0.05 M sodium acetate (pH=5.0) for 5 min and immmediately placed into aminoethylcarbazole (AEC) substrate solution for 15 min. This solution was made immediately prior to use by adding 5 ml of stock AEC solution (4 mg/ml in N,N-dimethylformamide) to 0.05 M sodium acetate buffer, mixed, filtered through Whatman paper #1, and 1 drop of 30% hydrogen peroxide added to the solution. The slides were washed with running tap water for 5 min and rinsed in distilled water before counterstaining with haematoxylin for 5 min, washing in TBS, rinsing in distilled water, and mounting onto slides with glycerin gelatin.

2.7 Liver Perfusion Experiments

Purified antibodies were differentially radiolabelled, ^{131}I for anti-CK18 IgG and ^{125}I for preimmune chicken IgG, using IODO-GEN as described above. The purity of the radiolabelled antibody preparations were checked by SDS-PAGE. The perfusion of rabbit livers and the analysis of the removal of radiolabelled IgG

from the perfusate was done as reported previously (Hatton *et al.*, 1994). The data were analyzed using a two-sample t-test and values reported as the mean ± standard error of the mean (SEM).

2.8 VN-TAT Formation in Plasma

To test the ability of TAT to form VN-TAT in plasma pre-formed ^{125}I-TAT was added to human or rabbit plasma or ^{125}I-thrombin to defibrinogenated human or rabbit plasma (see below). TAT formation, using either human or rabbit AT with either bovine or human thrombin, was done as described in section 2.2.6. The final concentration of each preparation of TAT complex was 0.329 mg/ml. A volume (1.5 μl) of the different ^{125}I-TAT complex preparation was added to 49 μl of either rabbit or human plasma (acid-citrate anticoagulated; final TAT concentration was 100 nM) for 30 min at 37°C. Aliquots were then removed and prepared for SDS-PAGE using both reducing and non-reducing SDS-PAGE sample buffers. Identical amounts were then electrophoresed on 6% acrylamide SDS-PAGE gels and the radioactivity visualized by autoradiography.

500 μl of human or rabbit plasma was defibrinogenated by adding 5 μl arvin (0.015 unit/ml) at 37°C for 10 min. The clot was pulled out and excess plasma squeezed out. These were then used as the plasma stocks for VN-TAT formation with thrombin. 2 μl of thrombin was then added to 48 μl of plasma (final concentration of 100 nM thrombin) at 37°C for 30 min. Aliquots were then

removed and prepared for SDS-PAGE using both reducing and non-reducing SDS-PAGE sample buffers. Amounts identical to the TAT experiments were then electrophoresed on 6% acrylamide SDS-PAGE gels and radioactivity visualized by autoradiography.

2.9 Plasma Elimination of ^{125}I-VN-TAT, ^{125}I-TAT, and ^{125}I-AT From Rabbits

Young male New Zealand White rabbits, weighing between 2.2 to 2.7 kg) were injected into the marginal vein with ^{125}I-VN-TAT (12.6-17.5 $\times 10^6$ dpm; 8 to 16 μg per animal), ^{125}I-TAT (3.4 $\times 10^6$ dpm; 3.5 μg), or ^{125}I-AT (12.6 $\times 10^6$ dpm; $\approx$ 2.9 μg) made up in 1 ml of saline. The heparin (10,000 units/ml) or protamine sulfate (65 mg/ml) used in the competition experiments were made up in sterile saline and ^{125}I-VN-TAT added directly to the solutions just prior to injection. For the two TRAP competition experiments 4.2 ml of TRAP (14.9 mg) was injected 5 min prior to ^{125}I-VN-TAT or ^{125}I-TAT infusion. One ml blood samples were removed at various timepoints from the auricular aery of the opposite ear into 200 μl of anticoagulant (CP2D from the Canadian Red Cross Society: containing 0.016 M citric acid, 0.09 M sodium citrate, 0.016 M sodium phosphate (monobasic), and 0.284 M dextrose), mixed and put into microcentrifuge tubes. The blood sample taken one minute after injection was designated as containing 100% blood radioactivity. The blood samples were centrifuged for 10 min at 16,000 g. Two 100 μl aliquots of the plasmas were removed to determine total radioactive

counts. 100 μl aliquots were removed and 100 μl of 20% TCA were added, voexed, and left on ice for 15 min. The TCA samples were then centrifuged at 16,000 g for 10 min and the supernatants removed to determine the radioactivity. The TCA-soluble counts were subtracted from the total counts to give only the protein-associated radioactivity.

2.9.1 Pharmacokinetic Analysis of Clearance Data

The clearance data was analyzed using the technique of curve stripping as described by Fleck (1985). Briefly, the logarithm of the percentage of protein-associated radioactivity remaining in the circulation was plotted versus time after injection. The terminal exponential phase of clearance was curve-fit by linear regression. To determine the initial phase of clearance the contribution of the terminal clearance phase was subtracted from it as follows: firstly, time points from the interval describing the initial clearance phase were substituted into the equation of the line for the terminal clearance curve and the calculated values were subtracted from their inital clearance values; and secondly, these corrected data were plotted and analyzed by linear regression to give the equation of the line for the initial phase of clearance. This analysis revealed a biphasic clearance curve for VN-TAT and TAT, indicating a two-compartment model of clearance (Carson and Jones, 1979). This two-compartment model is shown in Figure 4. This clearance is described by the following equation:

$$y(t) = C_1e^{-(a1)t} + C_2e^{-(a2)t}$$

where C_1 and C_2 are coefficients and a_1 and a_2 are rate constants. The half-lives

Figure 4. **Two Compartment Model of ^{125}I-VN-TAT Clearance.** In this model the two compartments are composed of the intravascular space (ie plasma, Compartment 1) and the extravascular space, which includes the endothelium (Compartment 2). Compartment 2 has been subdivided into two further compartments, represented by the liver and the extravascular compartment. "CLEARANCE" represents the large and rapid movement of ^{125}I-VN-TAT from the intravascular space. The large arrow represents the accumulation of ^{125}I-VN-TAT in the liver that makes up the α-phase of clearance while the smaller arrow represents the subsequent slower ß-clearance phase out of the plasma into the extravascular component (i.e. other organs). The "CATABOLISM" arrow indicates the movement of degraded ^{125}I-VN-TAT (^{125}I-monoiodotryosine) back into the intravascular space and its subsequent excretion in the urine. Note that over the experimental time frame the clearance of ^{125}I-VN-TAT is much greater than its catabolism.

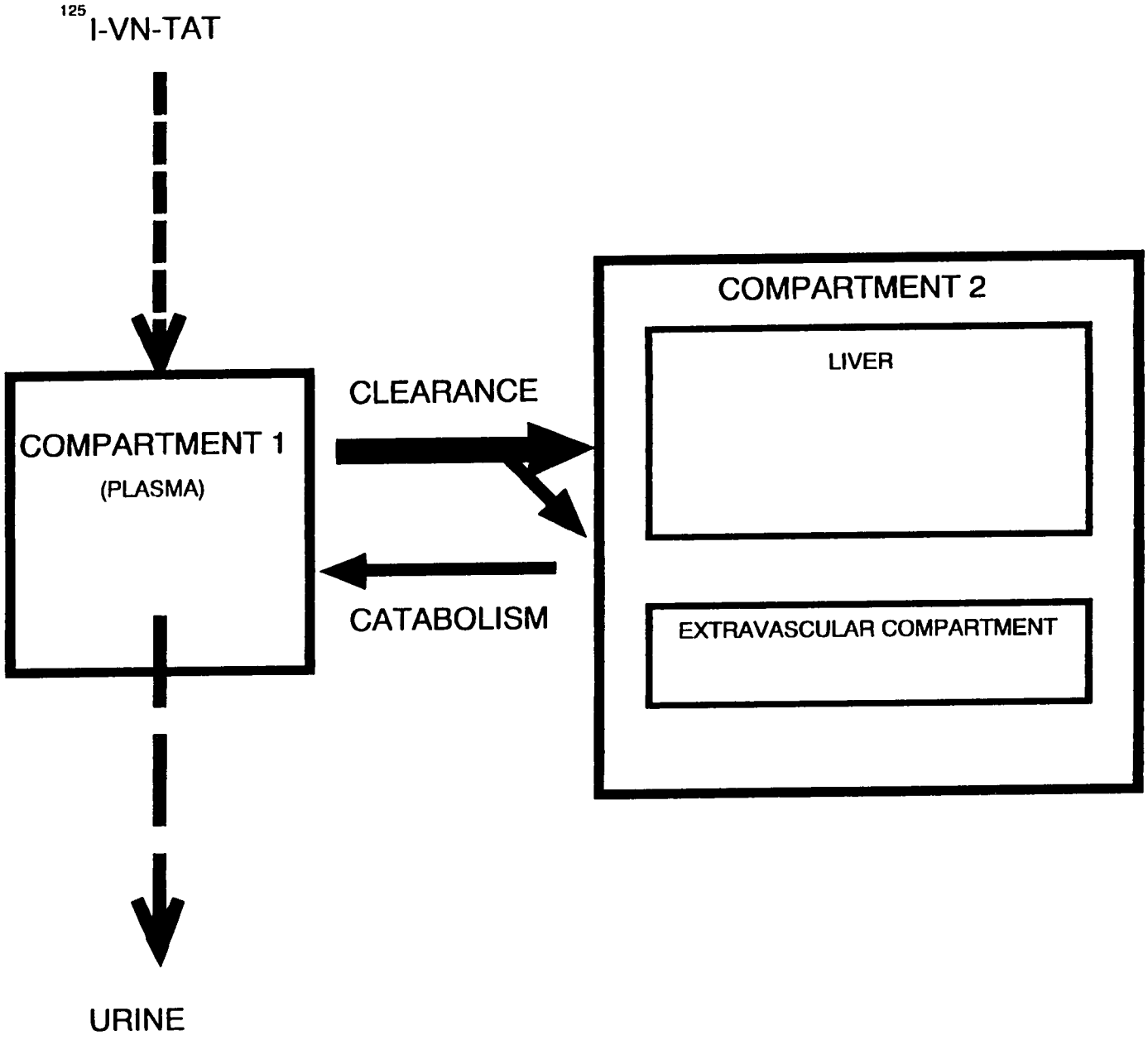
125 I-VN-TAT
COMPARTMENT 1
(PLASMA)
CLEARANCE
CATABOLISM
COMPARTMENT 2
LIVER
EXTRAVASCULAR COMPARTMENT
URINE

were determined from the C values. The data for the clearance of VN-TAT in the presence of heparin or protamine was best fit to a single-compartment model. The $t_{1/2}$ values were then analyzed using a two-sample t-test and values repoed as the mean $\pm$ SEM.

3.0 Organ Uptake of ^{125}I-VN-TAT In Vivo

To determine organ uptake, ^{125}I-VN-TAT (17.5×10^6 dpm; ~ 5.5 μg) was infused into each rabbit (n=3). At one hour the rabbits were anaesthetized, the femoral veins isolated, and 1 l of saline was perfused through each animal via a carotid aery cannula. The perfusion in all cases was judged to be successful by evidence of blanching of the liver and the lack of blood in the perfusate. The liver, lungs, kidneys, bladder, heart, and spleen were removed from each animal, weighed, and the values recorded. Each individual organ was then homogenized with a polytron homogenizer in TBS, with ~ 25 ml 2-octanol added to prevent foaming, for around 2 min, each at about 75% of the highest setting. The total volume was measured in a volumetric cylinder, the value recorded, and 2 ml removed to determine radioactivity. In separate experiments with ^{125}I-VN-TAT (~12.6×10^6 dpm), alone and in competition with heparin (10,000 units/ml) (n=3 for each), the incubation period was reduced to only 30 min and only the livers were removed and processed for determination of radioactive uptake. For these experiments the radioactivity in collected plasma samples was determined but were not TCA-corrected.

3. RESULTS

3.1 Characterization and Identification of CK18 as a TAT-Binding Protein

3.1.1 Purification and Radiolabelling of Rabbit AT and Bovine Thrombin and the Formation of TAT Complexes

Homogenous AT and α-thrombin were required to make TAT complexes. Since the animal model usually used in our laboratory is the rabbit, rabbit AT was used in forming TAT complexes. Heparin-Sepharose chromatography was utilized to purify AT and yielded large quantities (≈ 10-12 mg per 100 ml ACD plasma) of homogeneous AT, as determined by SDS-PAGE. A typical AT preparation is demonstrated in Figure 5, Lane 1. Although I wanted to maintain the use of rabbit-derived materials, the purification of rabbit thrombin proved to be tedious and resulted in low yields of pure rabbit thrombin (data not shown). Therefore, I decided to use bovine thrombin. Bovine thrombin was further purified from Thrombostat (Parke-Davis Co., Detroit, MI), a crude bovine thrombin preparation. Although this could bring species-dependent error into the experiments it has been found that homologous human complexes behaved very similarly to murine complexes in clearance experiments in mice, suggesting that the SEC of different species likely bind similarly to SEC receptors.

A cation exchange chromatogram of bovine thrombins purified on SP-

Figure 5. **Coomassie Blue Stained 10% SDS-PAGE of Rabbit AT, Bovine Thrombin, and TAT.** Lane 1, molecular weight markers (kDa). In Lane 2 is 2 μg of bovine thrombin. Lane 3 shows the mobility of 2 μg of AT on the same gel and Lane 3 shows the electrophoretic separation of TAT on the same gel after reacting 3 μg of AT with 0.6 μg of thrombin. The labels on the right indicate the mobility of the different proteins.

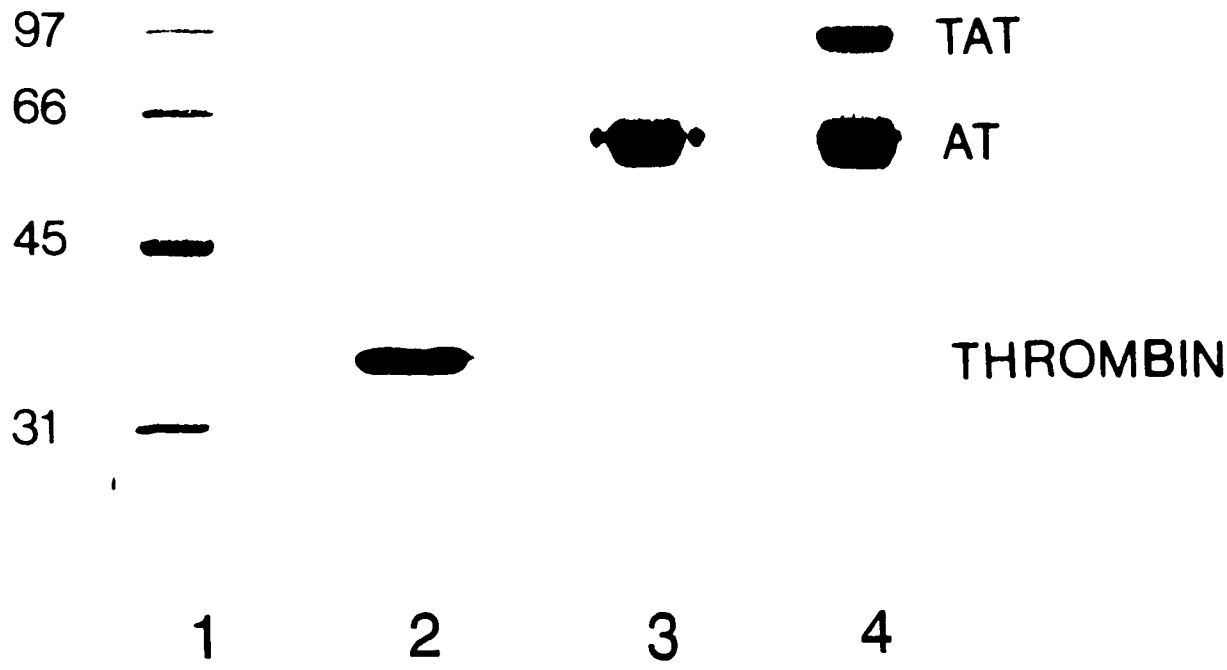
97
66
45
31
TAT
AT
THROMBIN
1
2
3
4

Figure 6. **Chromatogram of Thrombin Purification on SP-Sephadex.** 20,000 units of Thrombostat was run over SP-Sepadex-C50. Bound thrombin was eluted with a phosphate gradient (0.1 M, pH=6.5 to 0.3 M, pH=8.0) as detailed in the Materials and Methods section. The eluted protein was detected spectroscopically by absorbance at 280 nm (solid line). The presence of α-thrombin was detected by clotting assay (dotted line). Fractions tested for clotting activiity are indicated by the solid circles.

ABSORBANCE (280nm)
0
0.05
0.1
0.15
0.2
0.25
0.3
0.35
0.4
0.45
0.5
FRACTION NUMBER (5ml/fraction)
0
10
20
30
40
50
60
70
80
90
100
CLOTTING ACTIVITY (international units/ml)
0
100
200
300
400
500
600
700
800
900
—— = absorbance
..... = clotting activity

Sephadex from Thrombostat is shown in Figure 6. Thrombin is an autoproteolytic enzyme which acts on itself to form the smaller forms, known as ß and γ thrombin. A clotting assay was used to differentiate the α form of thrombin from the other forms, since only the α form has clotting activity (ie can cleave fibrinogen to yield fibrin). Performing the clotting assay on the different fractions (Figure 5) resulted in the identification of the most highly purified α-thrombin fractions and allowed the isolation of electrophoretically pure α-thrombin as demonstrated in Figure 5, Lane 2. The bovine thrombin preparations made typically gave an activity of > 2000 NIH U/mg as determined by clotting assay against standardized human thrombin preparations.

Iodogen-radiolabelling of ^{125}I-thrombin typically gave a specific activity of between 2100-7,000 dpm/ng of thrombin (see Figure 7, Lane 2). The functionality of the radiolabelled thrombin was determined by complexing assays with non-radiolabelled AT. To drive the formation of TAT complexes, with thrombin or ^{125}I-thrombin was reacted with an excess of AT, typically in a molar ratio of 1:3 at 37°C for thirty min. Densitometric analysis found that >95% of ^{125}I-thrombin formed TAT. The electrophoretic mobilities of TAT and ^{125}I-TAT on a 10% SDS-PAGE gel are shown in Figure 5, Lane 3 and Figure 7, Lane 1, respectively.

3.1.2 Determination of Assay Conditions for ^{125}I-TAT Binding to Rabbit Liver Plasma Membranes

The first experiments conducted were to determine whether to use 5% BSA or 5% blotto to reduce non-specific binding in the reaction mixtures. Single concentration (40 nM ^{125}I-TAT) competition experiments revealed that using 5%

Figure 7. **SDS-PAGE of ^{125}I-Thrombin and ^{125}I-TAT.** Lane 1 shows the electrophoretic separation of 7000 dpm of ^{125}I-TAT made with ^{125}I-thrombin and rabbit AT as described in Materials and Methods. Lane 2 demonstrates the autoradiograph of 7000 dpm of ^{125}I-thrombin electrophoresed on a 10% SDS-PAGE gel under reducing conditions. Molecular mass markers (as kDa) are indicated on the left.

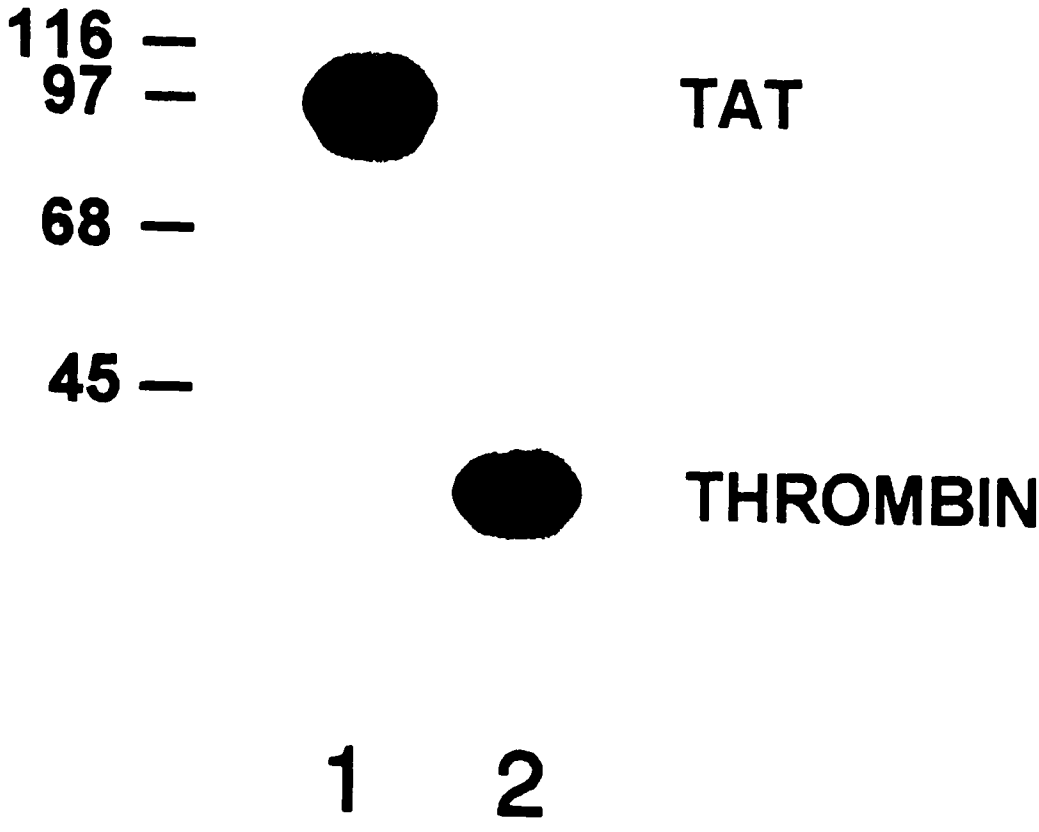
116
97
68
45
TAT
THROMBIN
1
2

BSA as blocker resulted in higher specific binding counts than that achieved with 5% blotto (data not shown). Furthermore, the amount of ^{125}I-TAT bound to the centrifuge tube was ≈ 10% that of ^{125}I-TAT bound when plasma membranes were present.

Constants derived from radioligand binding experiments are dependent upon the receptor-ligand interaction taking place under conditions of equilibrium. Therefore, the first experiments performed were association experiments. These experiments allow the determination of the time when steady state occurs (i.e. when the specific binding of ^{125}I-TAT to the plasma membranes is saturated). The association of 33 nM ^{125}I-TAT to 200 μg of rabbit liver plasma membranes at 37°C is demonstrated in Figure 8A. From this experiment it was determined that the incubation period for such experiments should be at least 40 min.

The next experiments conducted were to determine the tissue concentration to be used in the binding experiments. This is important as the apparent K_d is dependent upon the tissue receptor concentration (Bennet and Yamamura, 1985). Figure 8B shows the binding of 30 nM ^{125}I-TAT to increasing amounts of rabbit liver plasma membranes. This experiment indicated that the binding experiments should be done with 30 to 60 μg of liver plasma membranes.

3.1.3 Competitive Radioligand Binding Experiments With Rabbit Liver Plasma Membranes and Hepatoma Cells

First attempts at saturation experiments revealed that the affinity for ^{125}I-TAT binding sites is low on rabbit liver plasma membranes and that high concentrations of radioligand would be needed. Consequently, inhibition

Figure 8. **Determination of Conditions for ^{125}I-TAT Binding to Rabbit Liver Plasma Membranes. Panel A.** Association experiment examining the time for 33 nM ^{125}I-TAT to reach steady state binding to 200 μg of rabbit liver plasma membranes. Solid circles represent total binding, triangles non-specific binding, and open circles the specific-binding of ^{125}I-TAT. Each point is the mean ± SEM of triplicate determinations. **Panel B.** To determine the tissue concentration to use in radioligand binding studies the specific binding of 30 nM ^{125}I-TAT to increasing concentrations of rabbit liver plasma membranes at 37°C for 40 min was examined.

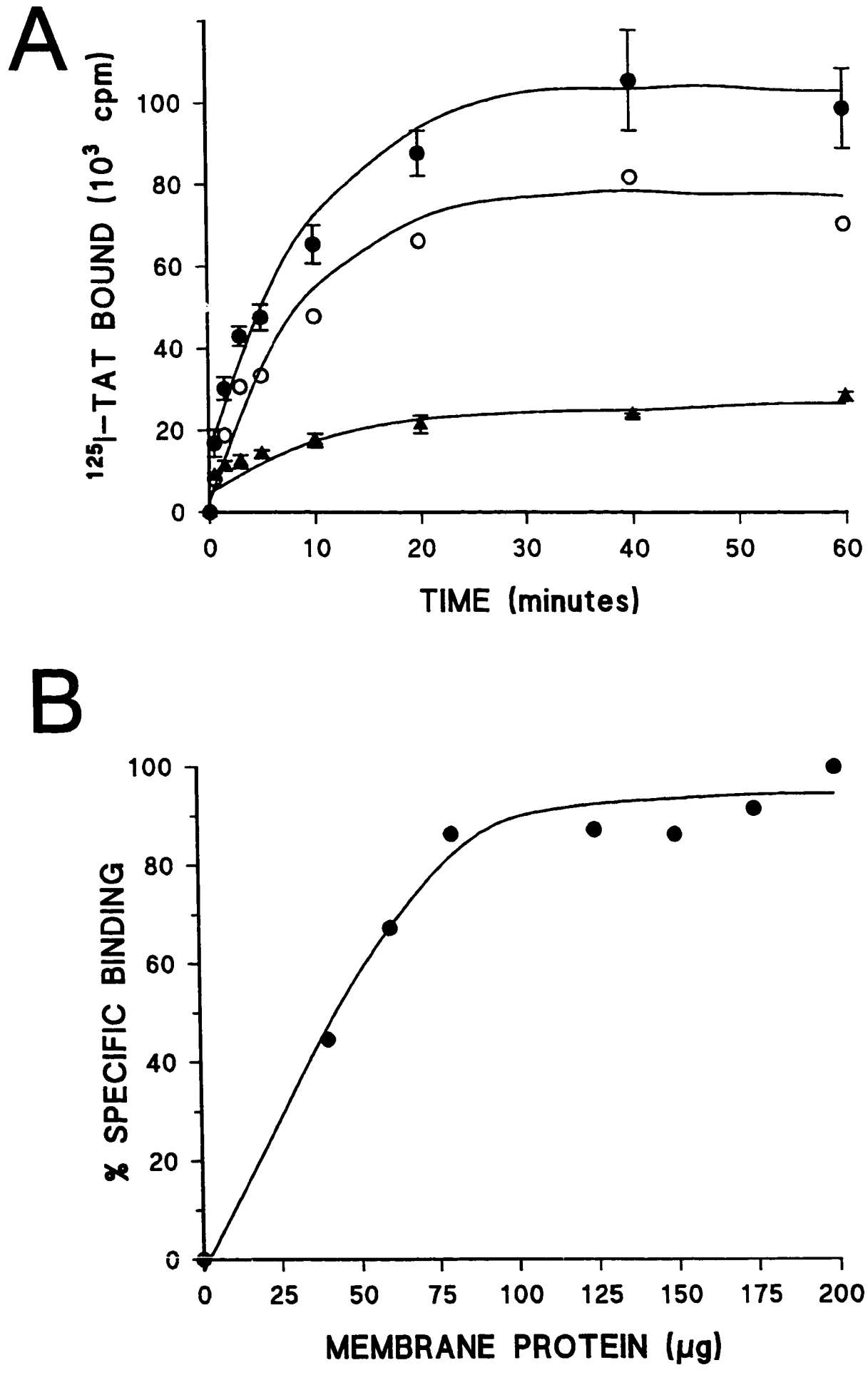
A
^{125}I–TAT BOUND (10^3 cpm)
0
20
40
60
80
100
0
10
20
30
40
50
60
TIME (minutes)
B
% SPECIFIC BINDING
0
20
40
60
80
100
0
25
50
75
100
125
150
175
200
MEMBRANE PROTEIN (μg)

experiments were done to preclude the need to use high quantities of radioactive ligand. The data from four different inhibition experiments were transformed into % specific bound and pooled and plotted as shown in Figure 9A. This data was further transformed into a logit plot (i.e. ln (p/100-p) vs log concentration inhibitor) as shown in the inset for Figure 9A. From this graph the IC_{50} was determined to be ~700 nM. Using the Cheng-Prusoff equation ($K_i=IC_{50}/(1+F/K_d)$) the apparent K_d was found to be ~ 680 nM (Cheng and Prusoff, 1973). The Hill coefficient was determined to be 0.93 which indicates that ^{125}I-TAT binds to a single set of sites on rabbit liver plasma membranes. Similar experiments were done on both HepG2 and HTC cells and gave similar K_ds, ~300 and 100 nM respectively.

To demonstrate the specificity of ^{125}I-TAT binding to rabbit liver plasma membranes, competitive radioligand binding experiments were performed using an excess of either unlabeled TAT, AT, or PPACK-thrombin (Figure 9B). These data suggest that the specificity of TAT-binding to the rabbit liver plasma membranes is specific, as neither a 20-fold molar excess of unlabeled PPACK-thrombin or AT competed with ^{125}I-TAT. However, competition by a 20-fold molar excess of unlabeled TAT was clearly evident. Competition with either a 20-fold molar excess of TAT composed of rabbit AT, or human AT, with bovine thrombin competed equally well for the binding of ^{125}I-TAT to rabbit liver plasma membranes (data not shown). To determine if ^{125}I-TAT bound to the same SECR binding site on rabbit liver plasma membranes, as that described by Perlmutter

Figure 9. **Competitive ^{125}I-TAT Radioligand Binding to Rabbit Liver Plasma Membranes. Panel A.** The summation of four different experiments showing the reduction in binding of 50 nM ^{125}I-TAT to 50 μg of rabbit liver plasma membranes in the presence of increasing concentrations of unlabelled TAT. Each datapoint is the mean ± SEM. Inset is the logit transformation of the data showing the IC_{50} of ~700 nM for the combined experiments. **Panel B.** Binding of 50 nM ^{125}I-TAT to rabbit liver plasma membranes in the presence of a 20 fold molar excess (1 μM) of TAT, AT, PPACK-thrombin(THR), the SECR binding pentapeptide (FVYLI), or the pentapeptide plus TAT. Binding in the absence of the inhibitors was arbitrarily designated 100%. Binding was performed in triplicate and under the same conditions as in Panel A.

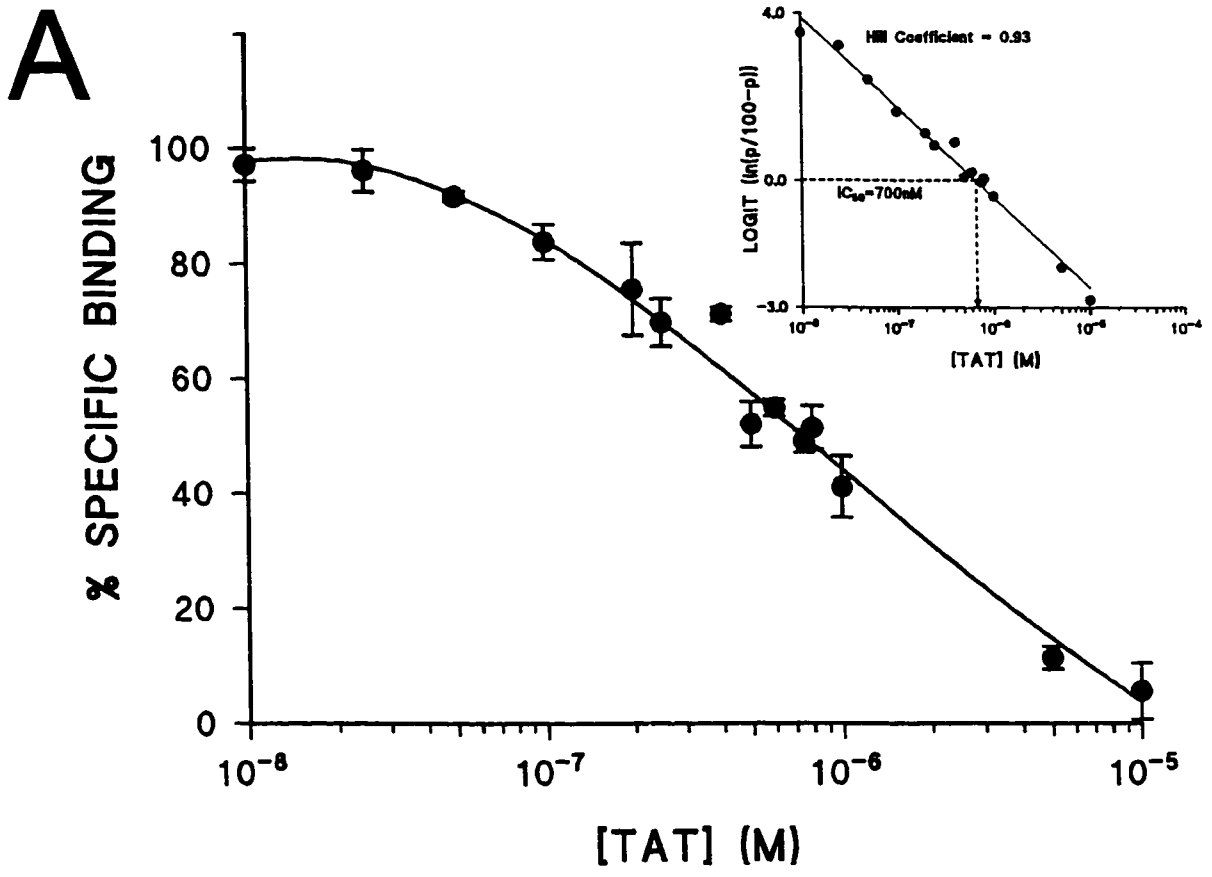
A
% SPECIFIC BINDING
100
80
60
40
20
0
10^{-8}
10^{-7}
10^{-6}
10^{-5}
[TAT] (M)
Hill Coefficient = 0.93
LOGIT (In(p/100-p))
4.0
0.0
-3.0
IC_{50}=700nM
[TAT] (M)

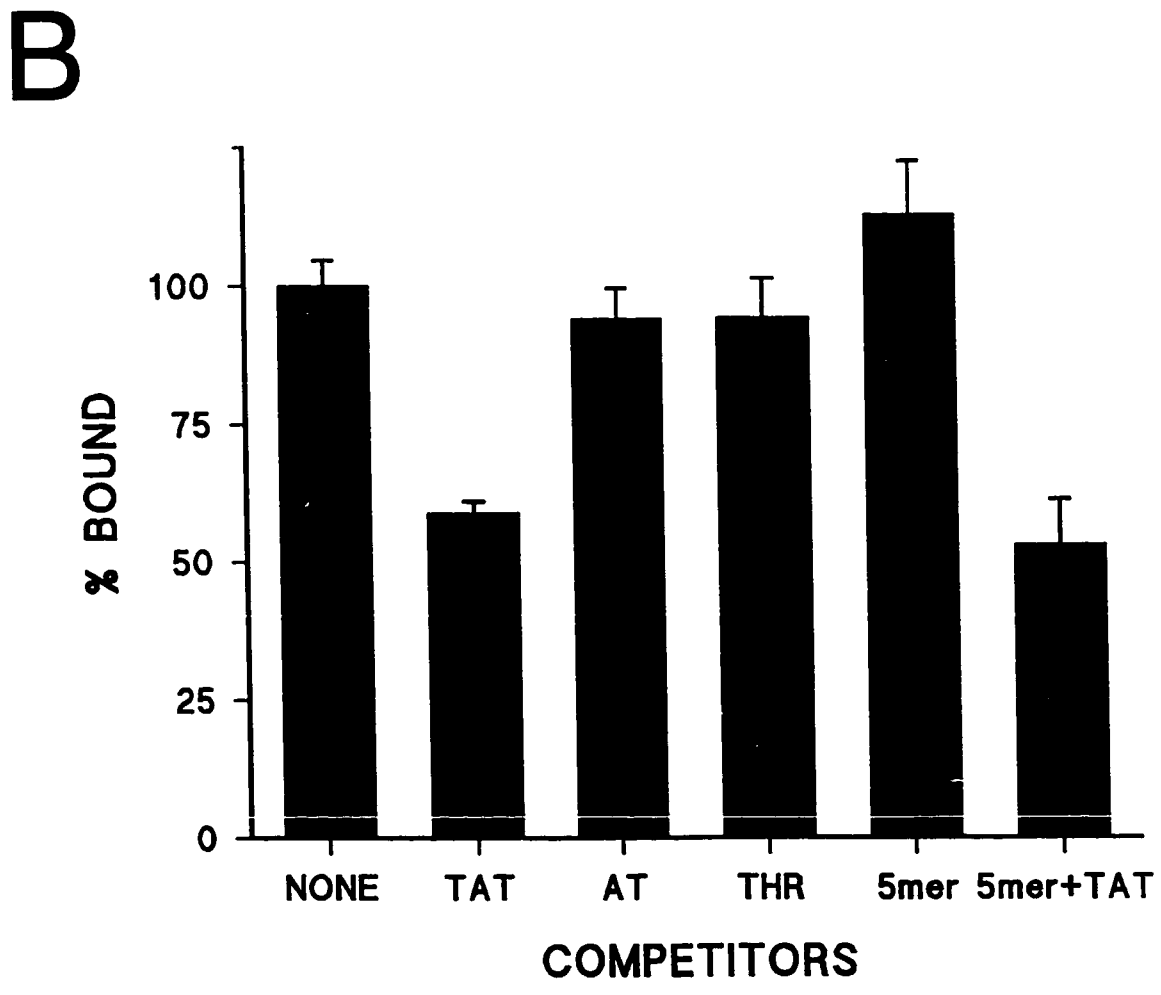
B
% BOUND
100
75
50
25
0
NONE
TAT
AT
THR
5mer
5mer+TAT
COMPETITORS

and associates (Perlmutter *et al.*, 1990), the SECR binding pentapeptide (FVYLI) was utilized in competitive radioligand binding experiments (Figure 9B). Unlike that obtained with excess TAT, a 20-fold molar excess of the pentapeptide did not inhibit TAT binding. A 20-fold molar excess of each of unlabeled TAT and pentapeptide together, reduced ^{125}I-TAT binding to the same extent seen with excess TAT alone. Similar molar excesses of TAT were found to inhibit the binding of α_1-PI-elastase, pentapeptide, and TAT binding to HepG2 cells to a comparable extent as in these studies (Perlmutter *et al.*, 1991; Joslin *et al.*, 1993).

3.1.4 Identification of a 45 kDa TAT-Binding protein

To identify any ^{125}I-TAT binding polypeptides from rabbit liver plasma membranes a ligand-blot assay was utilized. This assay has been used to identify and characterize membrane receptors including the erythropoietin receptor (Atkins *et al.*, 1991), murine interleukin 1 receptor (Bird *et al.*, 1988), LRP (Moestrup and Gliemann, 1991; Poller *et al.*, 1995) and many others. In initial experiments biotinylated TAT complexes were used to probe electroblotted rabbit liver plasma membranes but the background signal was too high, most likely due to endogenous biotin (data not shown). However, probing the electroblotted rabbit liver plasma membranes with ^{125}I-TAT resulted in the identification of a reactive band of 45 kDa (Figure 10A). The electrophoretic mobility of the 45 kDa polypeptide was identical when electrophoresed under non-reducing or reducing conditions. The recognition of this polypeptide was dose dependent in that increasing either the amount of ^{125}I-TAT or rabbit liver plasma membranes

Figure 10. **Identification and Isolation of a TAT-Binding Protein from Rabbit Liver Plasma Membranes. Panel A.** Rabbit liver plasma membrane proteins were electrophoresed on 10% SDS-PAGE gels, under reducing conditions, and electroblotted onto nitrocellulose. The blotted plasma membrane preparation was then probed with 10 nM ^{125}I-TAT in the absence (lane 1) or the presence of a 50 fold molar excess of TAT (lane 2), AT (lane 3), or PPACK-thrombin (lane 4) and visualized by autoradiography. **Panel B.** Rabbit liver plasma membranes were solubilized with 1% Triton X-100 and the soluble and the insoluble pellet fractions were analyzed by ligand-blotting with ^{125}I-TAT. Lane 1, Coomassie blue profile of soluble proteins; Lane 2, ligand blot of soluble proteins; Lane 3, Coomassie blue profile of insoluble proteins; Lane 4, ligand-blot of insoluble proteins. The 45 kDa protein was gel-purified (TATR) and identified by Coomassie blue staining of SDS-PAGE gels (lane 5), and its TAT-binding activity confirmed by ligand-blotting with ^{125}I-TAT (lane 6).

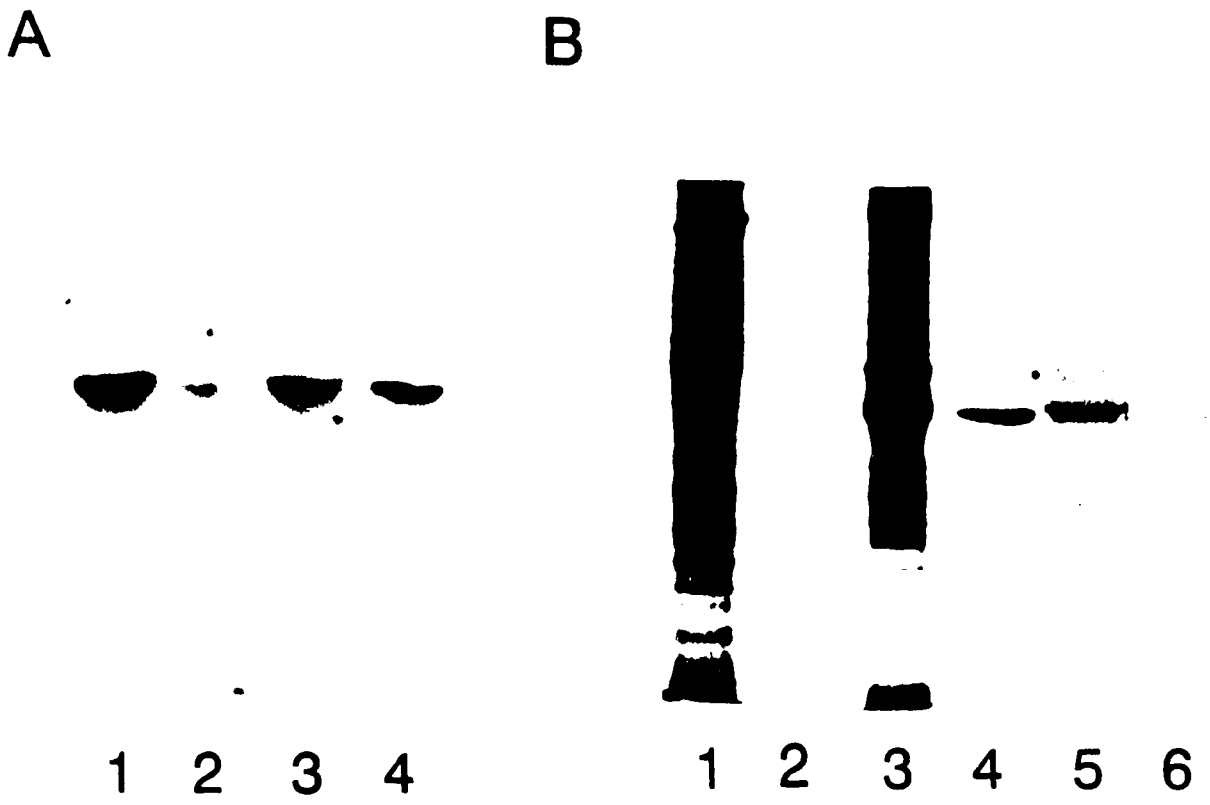
A
B
1 2 3 4
1 2 3 4 5 6

resulted in increased signal on autoradiographs (data not shown). Furthermore, the specificity of TAT binding was demonstrated by the ability of a 50-fold molar excess of unlabeled TAT to abrogate interaction of ^{125}I-TAT with the 45 kDa polypeptide (Figure 10A). In contrast a 50-fold molar excess of AT or PPACK-thrombin did not inhibit TAT interaction with the 45 kDa polypeptide. Further evidence supporting the specificity of the TAT-CK18 interaction is the observation that ^{125}I-TAT did not bind to either platelet membranes or aortic smooth muscle cell plasma membranes using the ligand-blot assay (data not shown). There have been no reports of TAT binding to either of these tissues and CK18 is known not to be found within them *in vivo*.

3.1.5 Identification of the 45 kDa Protein as CK18

Rabbit liver plasma membrane solubilization experiments with different detergents indicated that the 45 kDa band was insoluble in Triton X-100. Figure 10B, Lanes 1-4, shows the Coomassie blue stained protein profiles and the associated ^{125}I-TAT ligand-blots of the Triton X-100 soluble and insoluble fractions of rabbit liver plasma membranes. TAT-binding activity is clearly associated with the 45 kDa polypeptide which remained in the post-solubilization pellets (Figure 10B, Lane 4). Utilizing this biochemical property, the Triton X-100 insoluble TAT-binding polypeptide was solubilized in SDS and gel-purified by preparative SDS-PAGE. The purity of the isolated polypeptide was verified by SDS-PAGE, and its ability to bind ^{125}I-TAT verified by ligand-blot (Figure 10B, Lanes 5 and 6 respectively). The purified protein was electroblotted onto

polyvinylidene difluoride membranes, then digested with trypsin, and the resultant peptides purified by HPLC. Two peptides of 13 and 12 amino acids each were used to obtain amino acid sequence data. A homology search performed in the Genbank, using the NCBI BLASTN program, revealed that the sequences of both peptides had high homology to human CK18. Peptide #1, TFQSLEIDLESMK, was 76% identical to human CK18 and peptide #2, AQIFANSVDNAR, was 91% identical to human CK18. When semi-conservative amino acid substitutions were allowed, the identity was found to be 92% and 100% respectively.

3.1.6 Verifying CK18 as a TAT-Binding Protein

To exclude the possibility that CK18 was a contaminant in the gel-purified 45 kDa band from the rabbit liver plasma membranes, purified bovine CK18 was probed with ^{125}I-TAT in the ligand-blot assay (Figure 11A). ^{125}I-TAT was found to bind to purified bovine CK18 but not to any polypeptides in the rabbit platelet membranes (Figure 11A, Lanes 1 and 2, respectively). When purified bovine CK18 was added to the rabbit platelet membranes and probed with ^{125}I-TAT, the ^{125}I-TAT bound selectively to the CK18 (Figure 11A, Lane 3). The Coomassie blue stained protein profiles of the identical lanes are shown in Lanes 4 through 6 of Figure 11A. In addition, ^{125}I-TAT was found to interact with a 49 kDa polypeptide from purified rat liver plasma membranes which could be competed with excess cold TAT (Figure 11B, Lanes 2 and 3). This 49 kDa band corresponds to the rat homolog of CK18 as it was recognized with anti-CK18 IgG by Western blot analysis. Moreover its molecular mass (49 kDa) corresponds to

Figure 11. **Verifying CK18 as the TAT-Binding Protein. Panel A.** Ligand-blot analysis of ^{125}I-TAT binding to purified bovine CK18 (lane 1); rabbit platelet membranes (lane 2); and purified bovine CK18 added to rabbit platelet membranes (lane 3). Lanes 4, 5, and 6 are the corresponding Coomassie blue stained profiles for lanes 1,2, and 3, respectively. Molecular weight standards are in lane 7. **Panel B.** Ligand-blot of ^{125}I-TAT binding to rabbit liver plasma membranes (lane 1); purified rat liver plasma membranes (lane 2); or rat liver plasma membranes in the presence of a 90 fold molar excess of unlabelled TAT (lane 3).

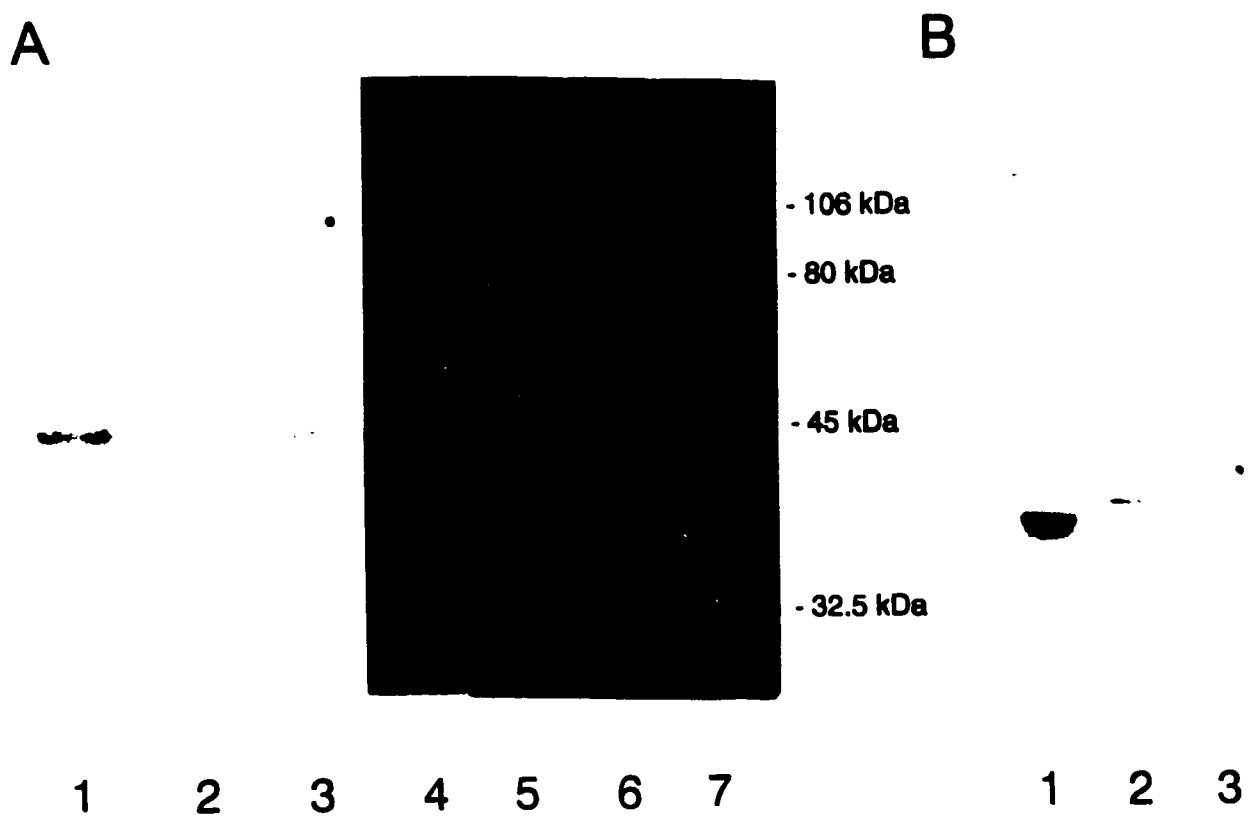
A
B
- 106 kDa
- 80 kDa
- 45 kDa
- 32.5 kDa
1 2 3 4 5 6 7
1 2 3

the reported electrophoretic mobility for the rat equivalent of CK18 (43). The presence of CK18 in both the rabbit and rat plasma membrane preparations is not unexpected as the association of CK18 with purified rat hepatocyte plasma membrane preparations has been reported previously (Hubbard and Ma, 1983).

3.1.7 Generation and Purification of Anti-CK18 IgG

To further characterize the interaction between CK18 and TAT, and for use in CK18 immunolocalization experiments, polyclonal antibodies to bovine CK18 were generated in chickens. Following immunization of laying hens with bovine CK18 antigen, the anti-CK18 IgG from egg yolks was purified to homogeneity by affinity chromatography. The preimmune chicken IgG retained a contaminant of approximately 60 kDa. The preimmune IgG was further purified on DEAE-Sephacel. The purity of ^{131}I-radiolabelled anti-CK18 and ^{125}I-chicken preimmune IgG is demonstrated by SDS-PAGE analysis in Figure 12A. Affinity-purified anti-CK18 IgG , whether or not labelled with ^{125}I, recognized purified bovine CK18 and CK18 from total rabbit liver homogenates and rabbit liver plasma membranes in Western blots, as a 45 kDa band (Figure 12B, Lanes 3, 4, 5 respectively). Conversely, the preimmune IgG, whether or not radiolabelled, did not react with any polypeptides from rabbit liver plasma membranes in Western blot analysis (data not shown). In binding experiments to purified bovine CK18 bound to ELISA wells, ^{125}I-anti-CK18 IgG bound to the CK18 while the ^{125}I-preimmune IgG did not (Figure 12C). The specificity of the anti-CK18 IgG was further indicated by the fact that it did not bind to BSA-coated wells.

Figure 12. **Purification and Characterization of Chicken Anti-CK18 IgG. Panel A.** Autoradiographs of SDS-PAGE analysis of ^{125}Iodine labelled purified IgG preparations: ^{131}I-anti-CK18, non-reduced (lane 1), reduced (lane 3); ^{125}I-preimmune IgG antibodies, non-reduced (lane 2); and reduced (lane 4). **Panel B.** Interaction between ^{125}I-anti-CK18 and rabbit liver homogenates and rabbit liver plasma membranes. Molecular weight markers (lane 1); Coomassie blue stained protein profile of total rabbit liver homogenate (lane 2); corresponding Western blot analysis of rabbit liver homogenate (lane 3); Western blot of 3.3 μg of plasma membranes using ^{125}I-anti-CK18 IgG (lane 4); and subsequent autoradiograph of the plasma membrane Western blot (lane 5). **Panel C.** The solid phase binding of increasing amounts of ^{125}I-anti-CK18 (circles) or ^{125}I-preimmune IgG (triangles) to 500 ng of purified bovine CK18. The plotted data represent the means of triplicate determinations $\pm$ SEM.

A

1 2 3 4

B

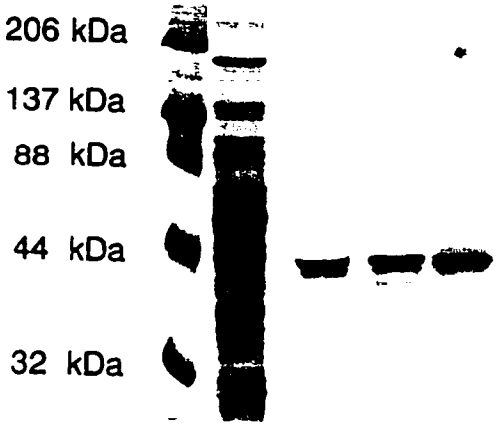

1 2 3 4 5

C

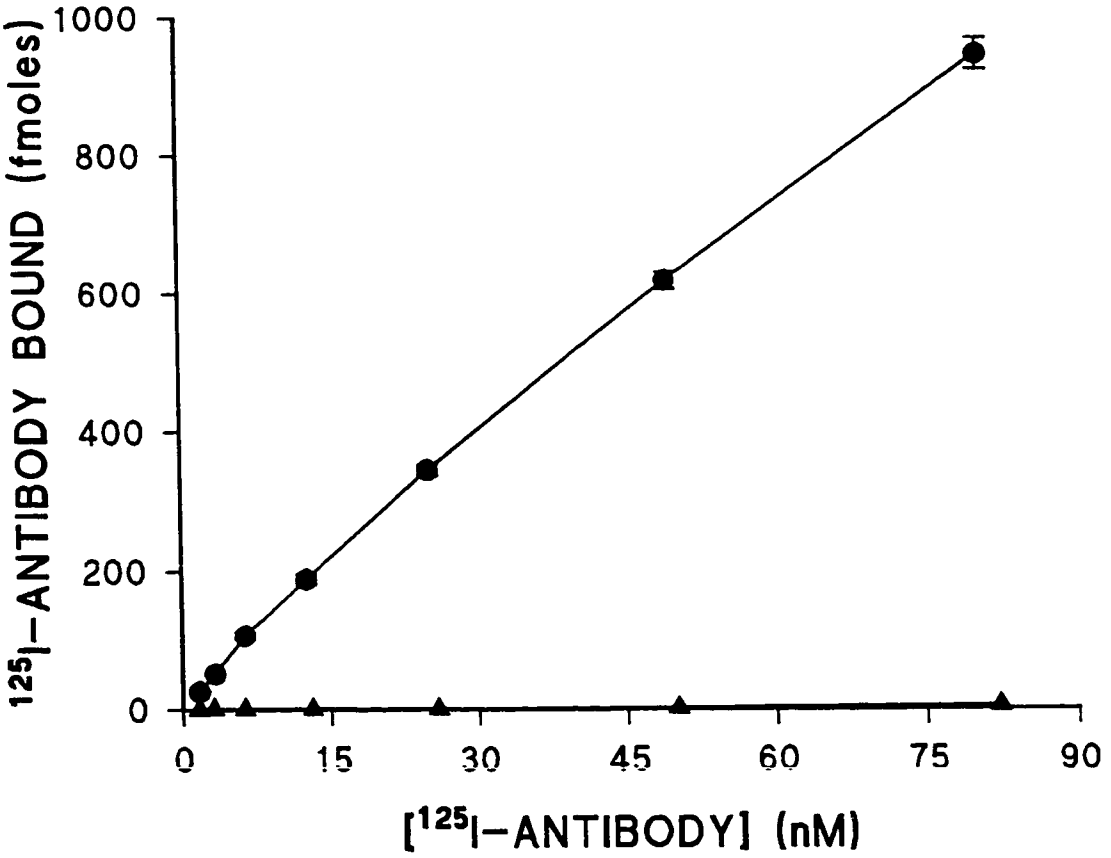

3.1.8 Determination of CK18 on the Surface of Hepatoma Cells

Since affinity-purified anti-CK18 IgG was highly specific for CK18 and retained the ability to bind CK18 even after being radiolabelled, ^{125}I-anti-CK18 IgG was used for binding to cultured hepatoma cells to determine if CK18 is expressed on their surface. To demonstrate this, the binding of ^{125}I-anti-CK18 to HepG2 cells and HTC cells was compared to that of ^{125}I-preimmune IgG (Figure 13). ^{125}I-anti-CK18 IgG bound to HTC cells to a much greater extent than that of preimmune IgG, and comparable results were obtained with HepG2 cells. Similar results were found when the experiment was performed using paraformaldehyde-fixed, but non-permeabilized, HTC and HepG2 cells (data not shown); demonstrating the presence of cell membrane CK18 epitopes even after cell fixation. To demonstrate that the anti-CK18 IgG bound specifically to the cells, anti-CK18 IgG binding to intact HTC cells was performed in the presence of an 80-fold molar excess of preimmune IgG. This excess of preimmune IgG only partially inhibited ^{125}I-anti-CK18 IgG binding to HTC cells, suggesting that the anti-CK18 IgG had both specific and non-specific binding. To substantiate the antibody specificity to CK18, HTC cells were fixed and then permeabilized with Triton X-100 to expose the bulk of the CK18 intermediate filaments. As expected, permeabilization increased antibody binding by approximately an order of magnitude at identical antibody concentrations (data not shown).

Figure 13. **^{125}I-Anti-CK18 IgG Binding to the Surface of Intact Hepatoma Cells.** Binding of increasing concentrations of ^{125}I-anti-CK18 (closed circles) or preimmune IgG (open circles) to HTC cells at 4°C for 2 h. The Plotted data represent the means of triplicate determinations ± SEM.

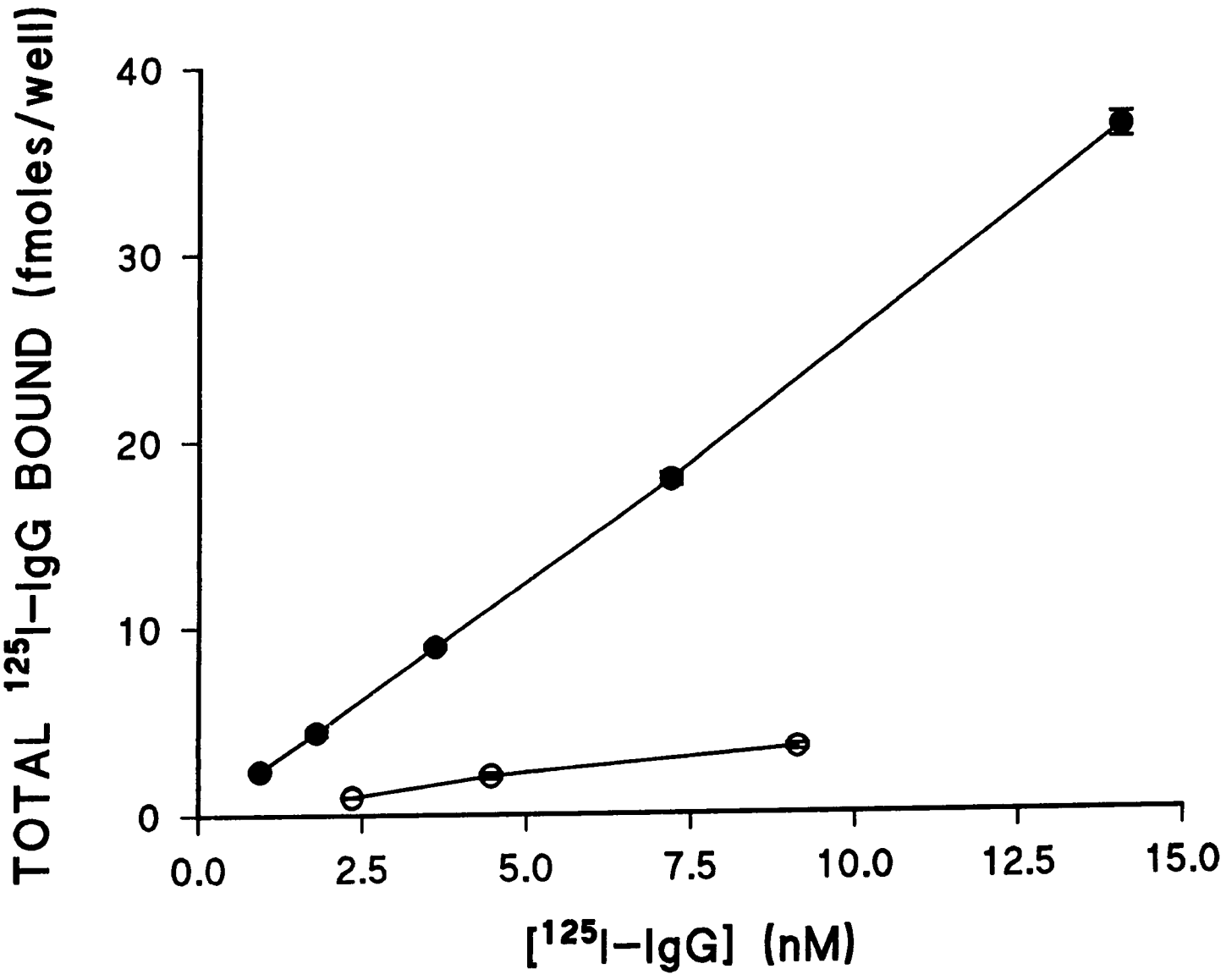
TOTAL ^{125}I–IgG BOUND (fmoles/well)
40
30
20
10
0
0.0
2.5
5.0
7.5
10.0
12.5
15.0
[^{125}I–IgG] (nM)

3.1.9 TAT Binding to Permeabilized Hepatoma Cells

If TAT interacts with CK18 then it might be expected that increased amounts of TAT would bind to the exposed CK cytoskeleton of permeabilized hepatoma cells. To determine this the binding of TAT to intact living hepatoma cells, formalin-fixed hepatoma cells, and fixed-permeabilized cells was investigated. In both cell types there was an increase in total TAT binding to fixed-permeabilized cells compared to that seen with intact or fixed cells (Figure 14, A and B). For HepG2 cells there was an ~ three-fold increase in TAT binding to fixed-permeabilized cells (~ 800 fmoles) than to fixed (~ 300 fmoles) or intact cells (~ 200 fmoles) respectively, at the highest TAT concentration used (122 nM) (Figure 14A). In the HTC cells the binding of ^{125}I-TAT was similar for both intact and fixed cells (~ 300 fmoles) but was only half of that bound to fixed-permeabilized HTC cells (~ 600 fmoles) (Figure 14B). Such data are consistent with the hypothesis that TAT binds specifically to CK18.

In a separate experiment the binding of 100 nM ^{125}I-TAT to intact HTC cells was compared to that for fixed and permeabilized HTC cells in the absence and presence of a 100 fold molar excess of cold TAT (10 μM) (Figure 15). In comparison to the previous experiments the amount of total binding to intact and fixed-permeabilized cells was nearly identical with that seen for fixed-permeabilized cells being ~ 5 fold greater than that to intact monolayers. Excess cold TAT reduced the binding of ^{125}I-TAT to intact cells by 47%. Such data are very similar to that seen in other binding experiments which indicate a high

Figure 14. **Binding of ^{125}I-TAT to Intact, Fixed, or Fixed-permeabilized Hepatoma Cells.** The binding of increasing concentrations of ^{125}I-TAT to either (Panel A) HepG2 cells or (Panel B) HTC cells. Circles represent non-treated cell monolayers, triangles represent fixed cells, and squares represent binding to fixed-permeabilized cells. All points represent the means of triplicate determinations ± SEM.

A

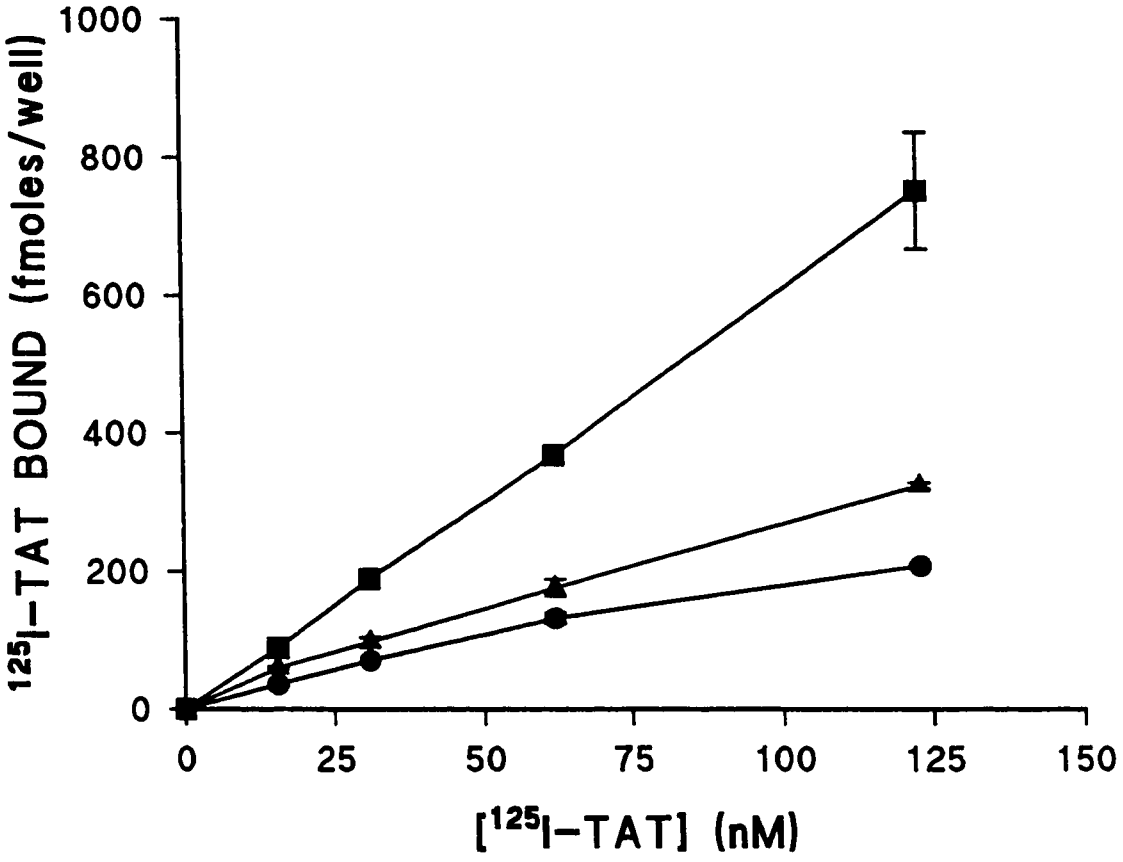
1000
800
600
400
200
0
^{125}I-TAT BOUND (fmoles/well)
0
25
50
75
100
125
150
[^{125}I-TAT] (nM)

B

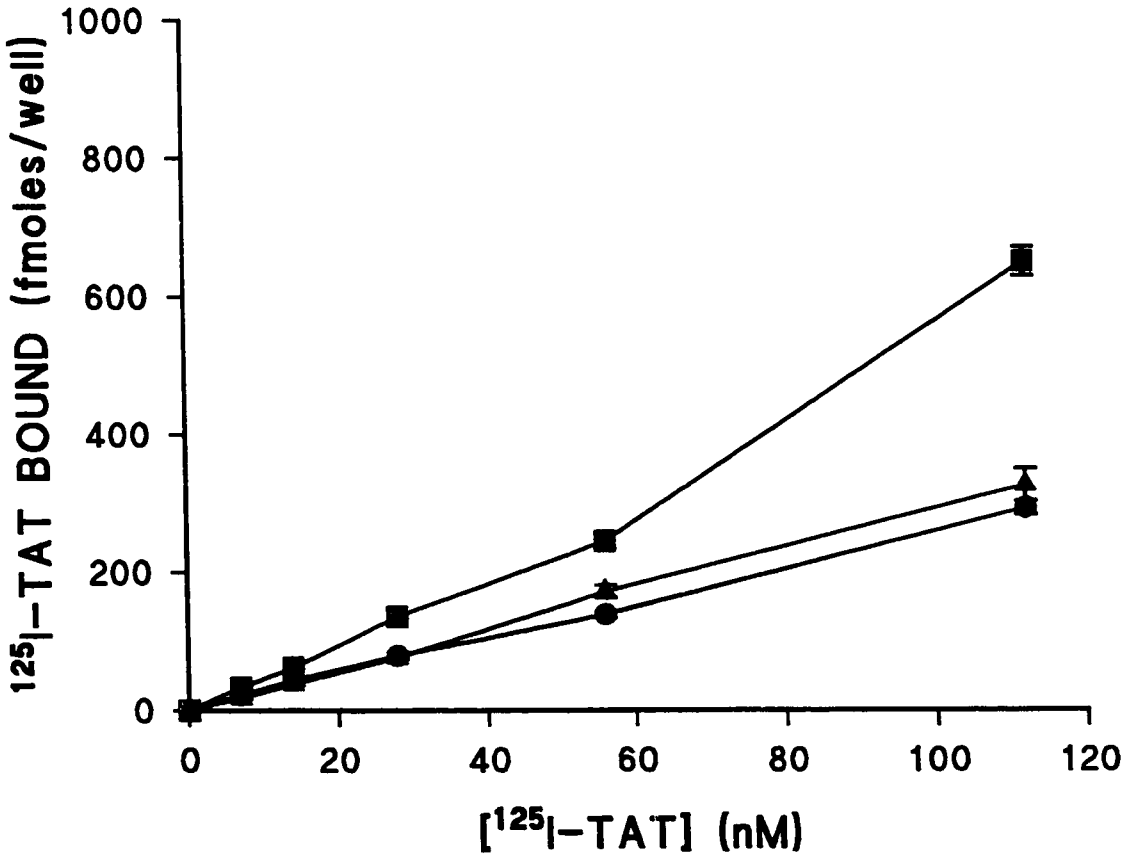
1000
800
600
400
200
0
^{125}I-TAT BOUND (fmoles/well)
0
20
40
60
80
100
120
[^{125}I-TAT] (nM)

Figure 15. **TAT Binding to Fixed-Permeabilized HTC Cells is Specific.** The binding of 100 nM ^{125}I-TAT was compared for non-treated HTC monolayers (NONE) and fixed-permeabilized monolayers (FIXED/PERM), in the absence and presence of 10 μM cold TAT. Solid bars represent the binding of ^{125}I-TAT alone and the hatched bars the binding in the presence of excess TAT. Each bar represents triplicate determinations ± SEM.

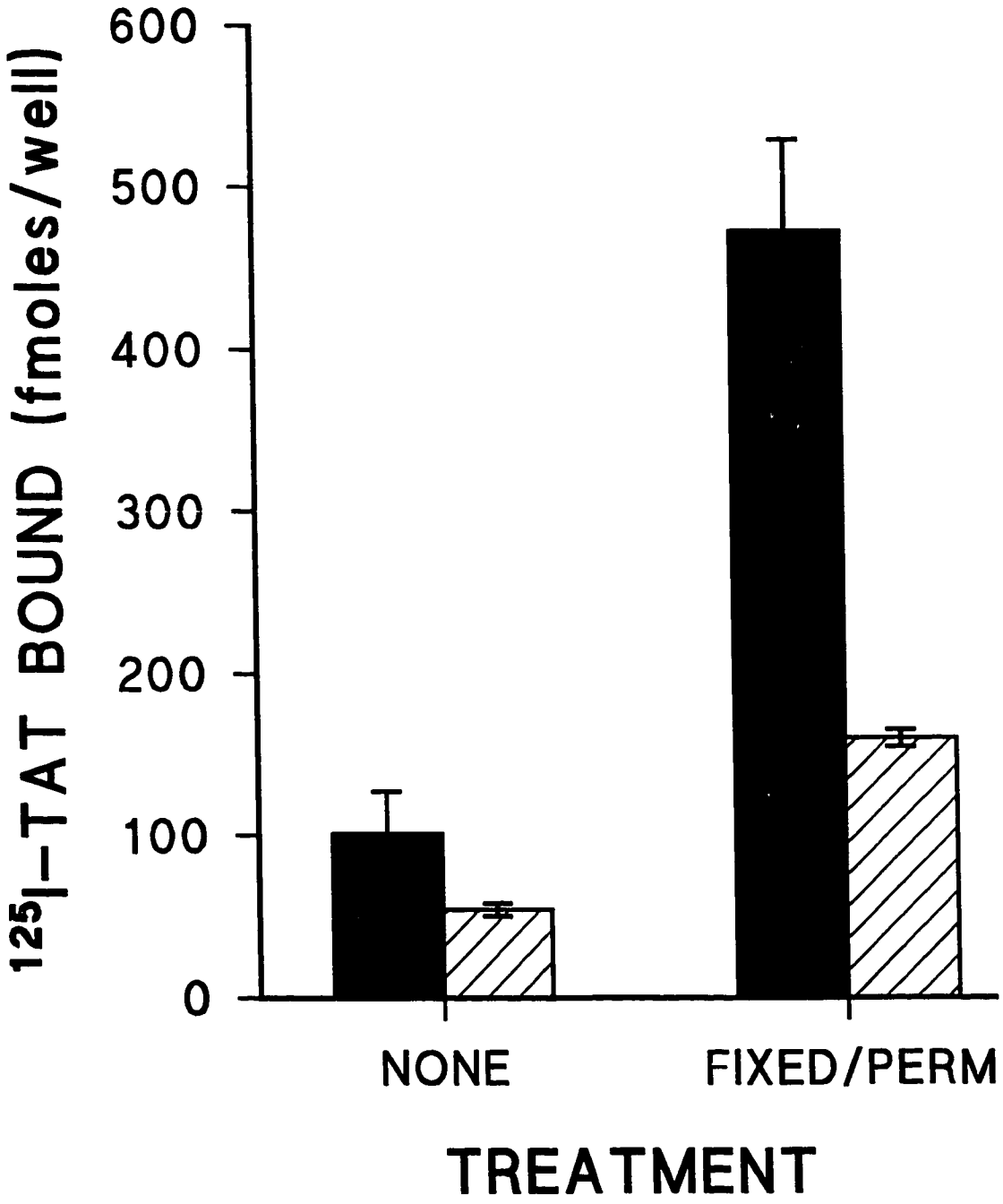
600
500
400
300
200
100
0
^{125}I–TAT BOUND (fmoles/well)
NONE
FIXED/PERM
TREATMENT

degree of non-specific binding to these cells. Cold TAT reduced the binding of ^{125}I-TAT to the fixed-permeabilized monolayers by 66%; giving an indication that TAT is binding specifically to proteins within the cells, most likely CK18.

3.1.10 TAT Interaction With Fibroblasts

TAT has been reported to bind to and be internalized by fibroblasts (Savion and Farzame, 1986; Kounnas *et al.*, 1996). An experiment was therefore performed to determine whether added CK18 would increase ^{125}I-TAT binding since to fibroblasts reportedly lack CK18. However, in these experiments there was no difference in total TAT binding to cells with and without CK18 added. These results could be due to either a lack of interaction with CK18 or because the CK18 did not bind to the cells (data not shown). To determine whether TAT was only binding to an external site, experiments examining binding on intact and fixed-permeabilized fibroblasts were done (Figure 16A). Interestingly, there was a greater than 5 fold difference in total binding of TAT to fixed/permeabilized cells than that seen with living monolayers. Fibroblasts have been reported to express CKs, spontaneously in culture (Knapp *et al.*, 1989). To determine if this was the case with these fibroblasts Western blot analyses were done. Figure 16B shows the interaction of anti-CK18 IgG with a protein of similar molecular mass (lane 5) to purified CK18 (lanes 1 and 2) in these fibroblasts. As a further control, total HTC cell protein was also probed and the rat homologue of human CK18 was recognized (Lanes 3 and 4). It should be noted that identical amounts of total protein were not loaded onto the wells such that there actually was less

Figure 16. **TAT Binding to Non-treated and Fixed-permeabilized LTK- Fibroblasts. Panel A.** The total binding (fmoles) of 100 nM ^{125}I-TAT to non-treated and fixed-permeabilized LTK- fibroblasts. Each bar represents triplicate determinations ± SEM. **Panel B.** Western blotting analysis for the presence of CK18 (or its rat homolog) was done on purified bovine CK18 (Lanes 1 and 2), HTC cell extracts (Lanes 3 and 4), and LTK- Fibroblast cell extracts (Lane 5), using chicken anti-CK18 IgG (5 μg/ml).

A

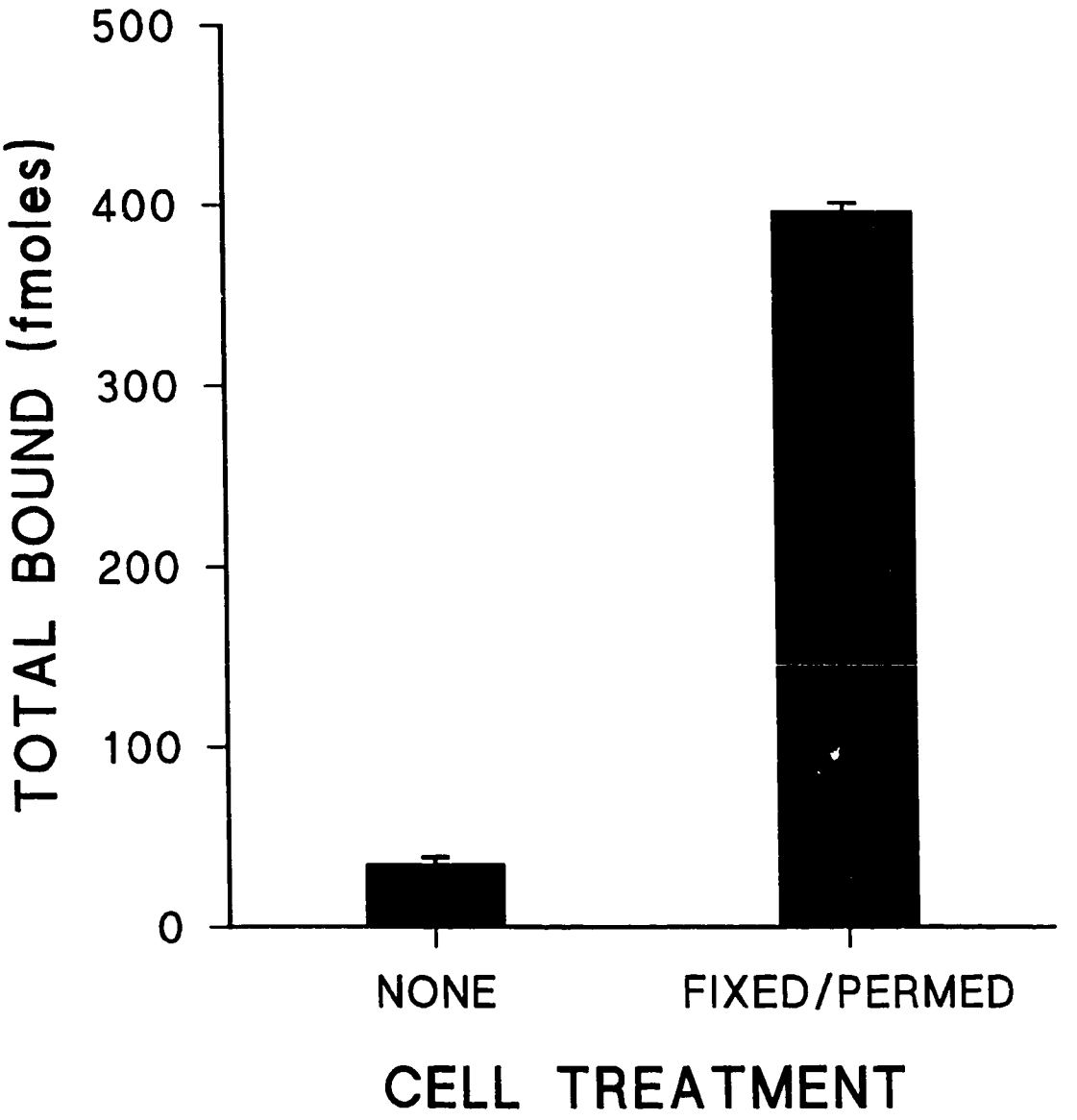
500
400
300
200
100
0
TOTAL BOUND (fmoles)
NONE
FIXED/PERMED
CELL TREATMENT

B

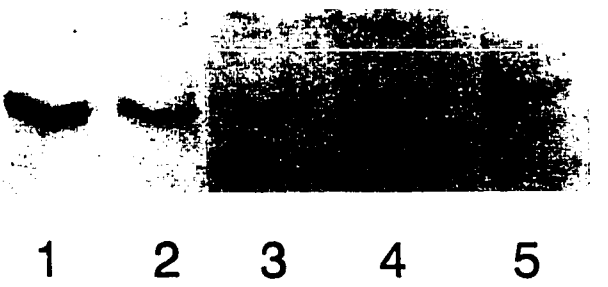
1
2
3
4
5

total fibroblast protein loaded than on than HTC cell protein. With this in mind it seems likely that there are substantial quantities of CK18 found in LTK- fibroblast cells.

3.1.11 Competition with Anti-CK18 IgG of TAT Binding to Hepatoma Cells

To further demonstrate that TAT binds to CK18 on the surface of hepatoma cells, the binding of ^{125}I-TAT to hepatoma cells was examined in competitive radioligand binding studies in the presence of anti-CK18 IgG. Figure 17 shows the binding of ^{125}I-TAT to HTC cells in the absence or presence of anti-CK18 IgG or preimmune IgG. With a 25-fold molar excess of anti-CK18 IgG, there was a ~ 40% reduction in TAT binding, while the binding was not reduced in the presence of a 25-fold molar excess of preimmune IgG. The extent of anti-CK18 IgG to inhibit TAT binding to fixed and permeabilized HTC cells was similar (Figure 17). There was a similar reduction in ^{125}I-TAT binding to fixed and permeabilized cells in the presence of a 100-fold molar excess of unlabeled TAT (data not shown).

3.1.12 Anti-CK18 Antibodies Inhibit ^{125}I-TAT Internalization

To determine whether CK18 has a functional role in ^{125}I-TAT uptake by hepatic cells internalization experiments were performed with HTC cells using anti-CK18 Fab fragments as competitor. The results of these experiments are shown in Figure 18. In the absence of competitor the amount of internalized ^{125}I-TAT corresponed to ~ 17 fmoles per 10^5 cells. In the presence of competing anti-CK18 Fab fragments, this was reduced by 41 %. Furthermore equivalent amounts

Figure 17. **Inhibition of ^{125}I-TAT Binding to HTC Hepatoma Cells by Anti-CK18 IgG.** Intact live HTC cells (hatched bars) or HTC cells fixed with 4% paraformaldehyde and permeabilized with 0.5% Triton X-100 (solid bars) were incubated at 4°C for two h with 50 nM ^{125}I-TAT in the the absence of IgG (none), in the presence of a 25 fold molar excess of preimmune IgG (pre), or in the presence of a 25 fold molar excess of anti-CK18 IgG (anti-CK18). The binding data shown represent the means ± SEM of triplicate determinations.

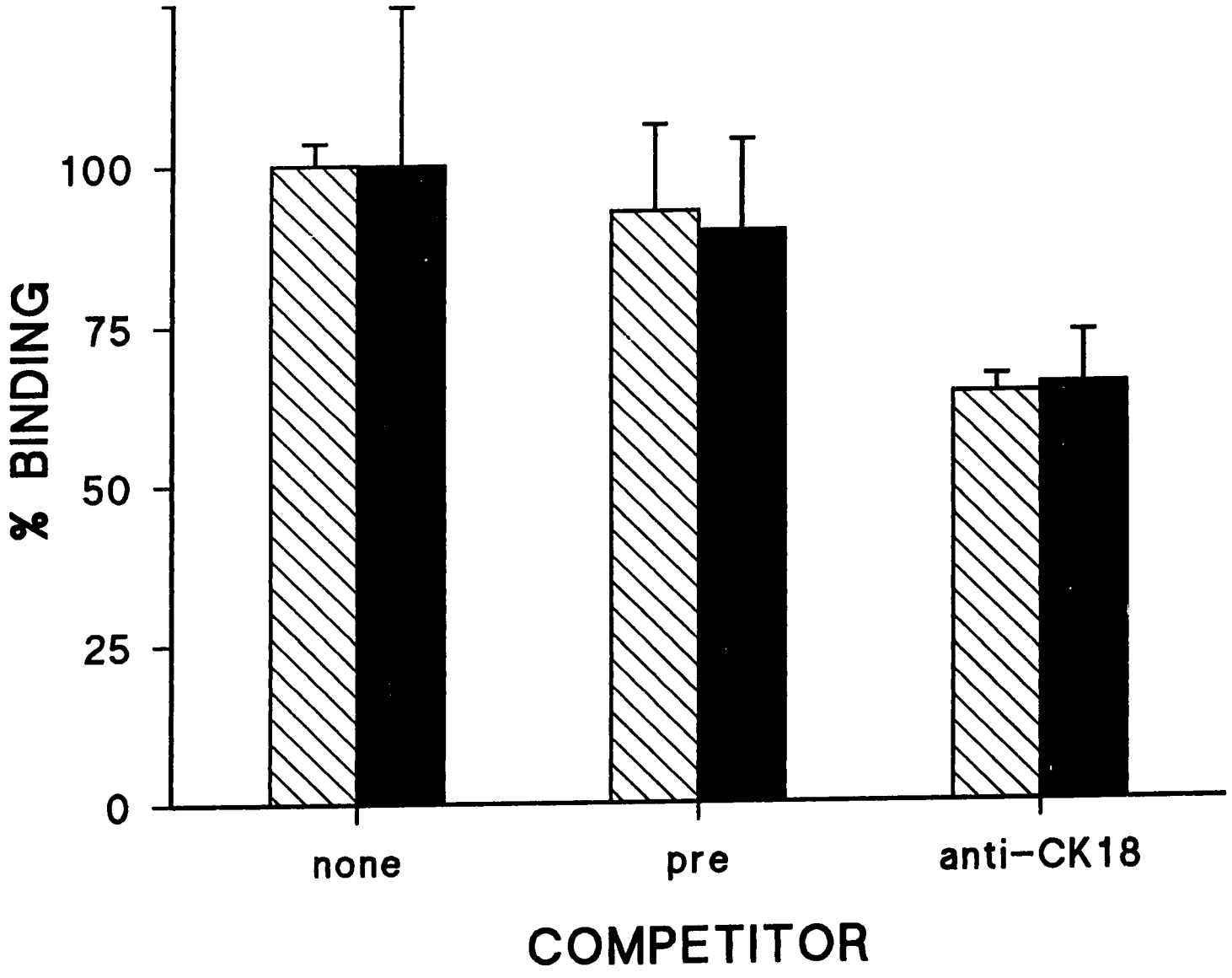
% BINDING
100
75
50
25
0
none
pre
anti-CK18
COMPETITOR

Figure 18. **Anti-CK18 Antibodies Inhibit ^{125}I-TAT Internalization by HTC Cells.** HTC cells were incubated with 50 nM ^{125}I-TAT, in the absence (NONE) or presence of 2.5 μM unlabeled TAT (TAT), 100 μM chloroquine (CHLOR), 850 nM anti-CK18 Fab fragments (αCK18), or 850 nM preimmune Fab fragments (PRE) and the amount of internalized protein was determined as described in Materials and Methods. Each bar represents the mean $\pm$ SEM of triplicate determinations.

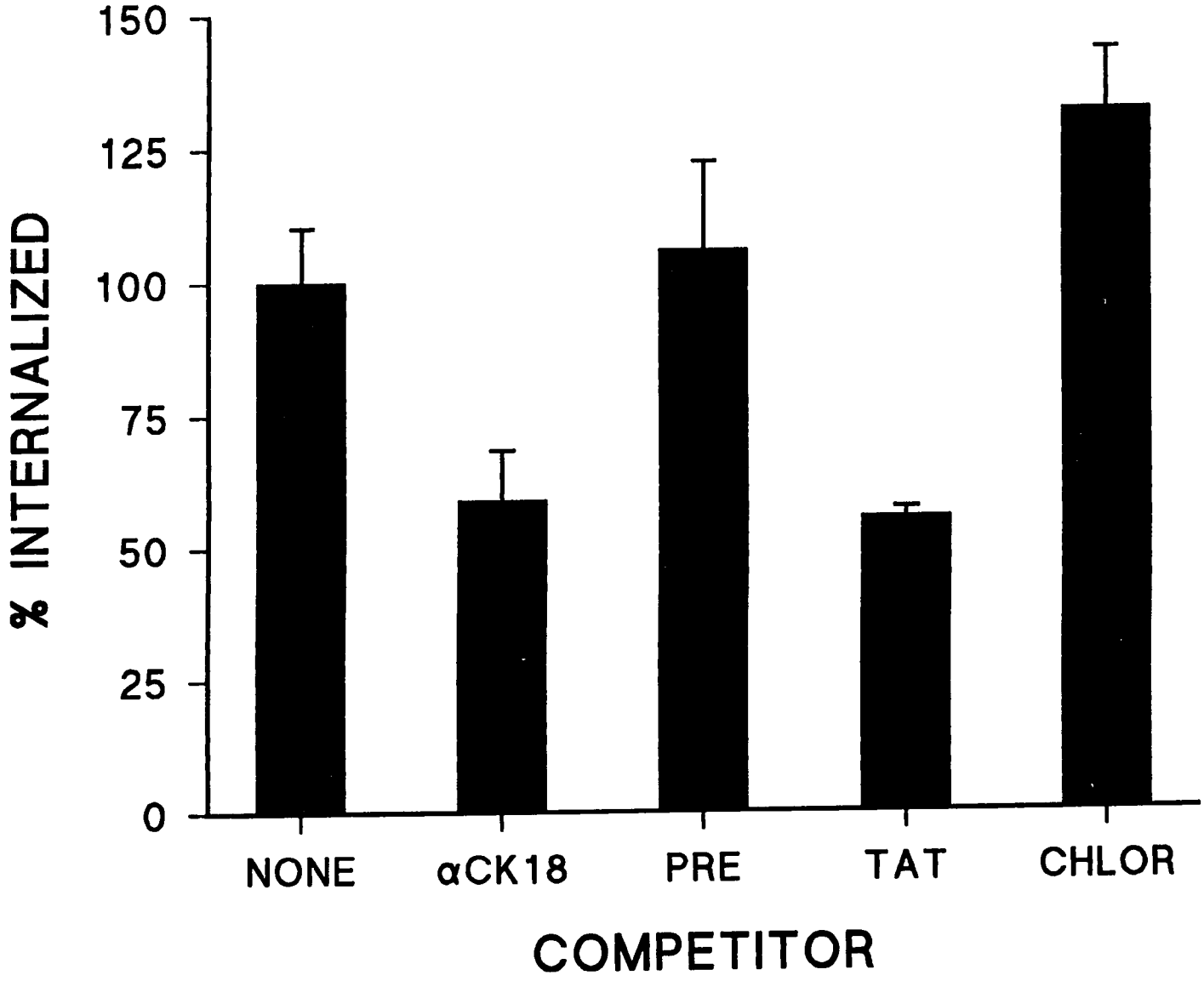
150
125
100
75
50
25
0
% INTERNALIZED
NONE
αCK18
PRE
TAT
CHLOR
COMPETITOR

of preimmune Fab fragments did not inhibit TAT internalization. A 50-fold molar excess of cold TAT also inhibited internalization by 45 %. These data support the binding data and further indicate that CK18 is the main TAT-binding protein on HTC cells. To determine whether internalized ^{125}I-TAT was degraded in lysosomes, 100 μM chloroquine, an inhibitor of lysosomal degradation, was used. Chloroquine resulted in the retention of 31 % more internalized ^{125}I-TAT than did control cells indicating that internalized TAT is degraded in lysosomes. In other internalization experiments the anti-CK monoclonal antibody CAM 5.2 was also used to compete for internalization of TAT. Similar to that seen with the chicken anti-CK18 Fab fragments, the monoclonal antibody CAM 5.2 also reduced internalization by 40 % over control cells.

3.1.13 Effects of Trypsin on ^{125}I-Anti-CK18 and ^{125}I-TAT Binding to Hepatoma Cells

To determine if proteinase treatment of hepatoma cells could remove TAT binding sites, the binding of ^{125}I-TAT to intact monolayers and to trypsinized cells was compared. Furthermore the effect this had on CK18 expression was followed by also probing the trypsinized cells with ^{125}I-anti-CK18 IgG. In these experiments 133 nM ^{125}I-TAT and 63 nM (9.33 μg/ml) ^{125}I-anti-CK18 were used for binding to both intact and trypsinized cells. The amount of ^{125}I-TAT binding to intact monolayers was approximately six-fold less than that with trypsinized cells (Figure 19). Anti-CK18 binding to trypsinized cells was increased (~ 60%). There appeared to be no effects of residual active trypsin on ligand binding since addition of pre-formed trypsin-SBPTI complexes resulted in identical binding to

Figure 19. **Binding of ^{125}I-TAT and ^{125}I-Anti-CK18 IgG to Trypsinized HepG2 Cells.** The binding to untreated and trypsinized HepG2 cells of 133 nM ^{125}I-TAT or 63 nM ^{125}I-anti-CK18 IgG. The solid bars represent the binding of ^{125}I-TAT and the hatched bars represent the binding of ^{125}I-anti-CK18 IgG. Each bar represents triplicate determinations ± SEM.

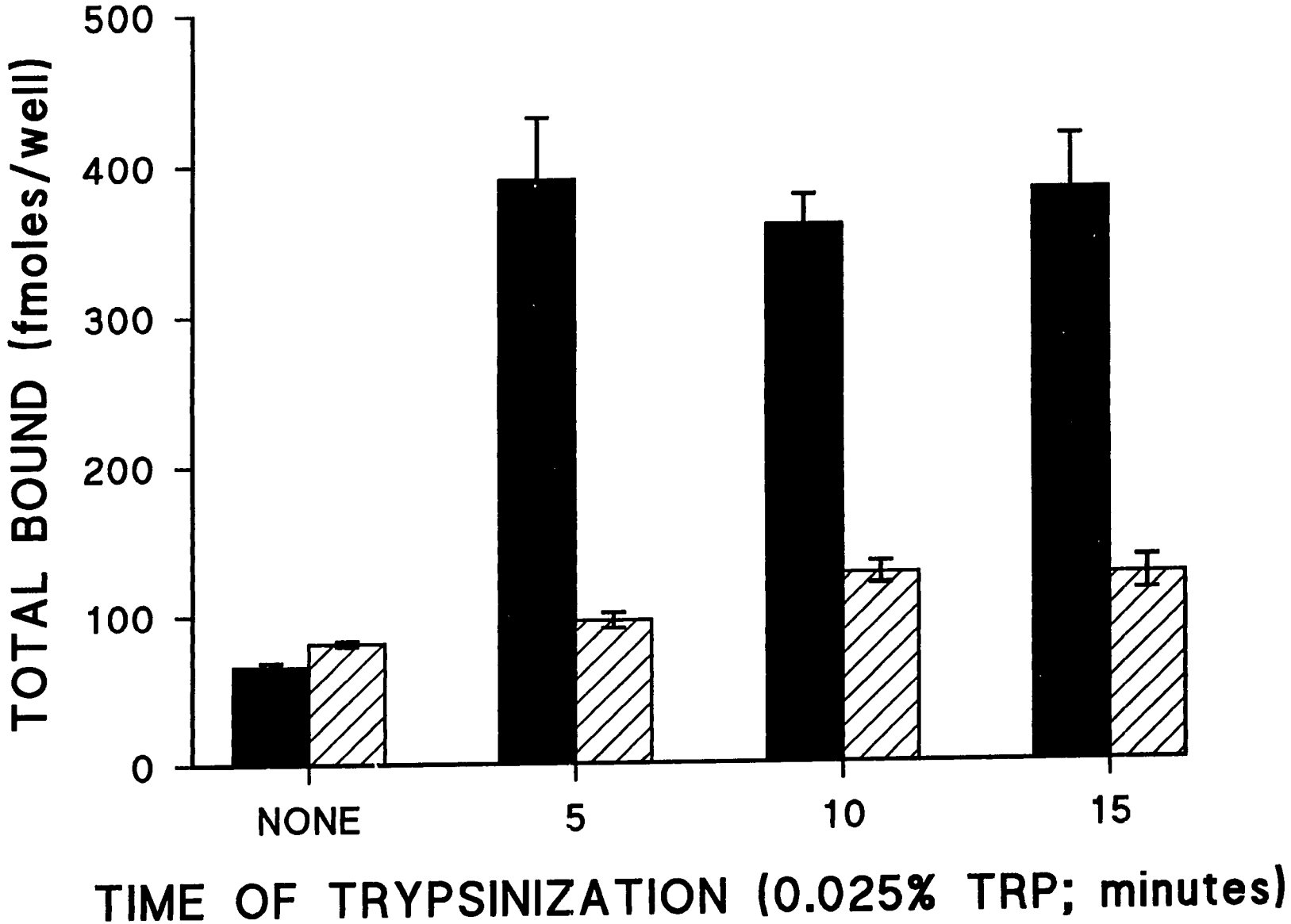
500
400
300
200
100
0
TOTAL BOUND (fmoles/well)
NONE
5
10
15
TIME OF TRYPSINIZATION (0.025% TRP; minutes)

wells when just the media was added. Although the increased binding of ^{125}I-TAT could be attributed to cell damage and therefore exposure of the CK cytoskeleton (see above; section 3.8) this seems unlikely since such damage and exposure would be expected to result in a large increase in anti-CK18 binding also. Therefore trypsinization appears to result in both increased TAT-binding sites and increased CK18 expression.

3.1.14 Tissue Expression of CK18

To determine the expression of CK18 in various organs, Western blot analysis on rabbit tissue homogenates was performed. Panel A of Figure 20 shows the Coomassie blue stained protein profiles of the different tissue homogenates and Panel B shows the immunodetectable CK18 protein expression in the tissues. Strong expression of 45 kDa CK18 is seen in bladder, liver, lungs, and the pancreas. Weaker expression is seen in the intestines (small intestine). There was also strong interaction with an unknown higher molecular weight protein of greater than 200 kDa in bladder, heart, intestines, kidneys, lungs, and pancreas which was absent from liver. There was also slight cross-recognition with a protein of slightly greater molecular mass than CK18 which could represent CK8. However, this protein band was weakly recognized by the Anti-CK18 IgG compared to the CK18 band. In addition the CK18 in liver appears to have a slightly faster mobility to CK18 in lung and pancreas indicating that CK18 in liver might be different than CK18 in other tissues.

Figure 20. **Tissue Expression of CK18 in Various Rabbit Tissues. Panel A.** Coomassie blue stained 10% SDS-PAGE gel of electrophoresed tissue homogenates. The tissue homogenates are designated as follows: B, bladder; H, heart; I, small intestines; K, kidneys; L, liver; Lu, lungs; Pa, pancreas; and S, spleen. **Panel B.** Western blot analysis was performed on the electroblot of an identical gel as seen in **Panel A.** The homogenates from the different rabbit tissues were probed using chicken anti-CK18 IgG (1 μg/ml).

A

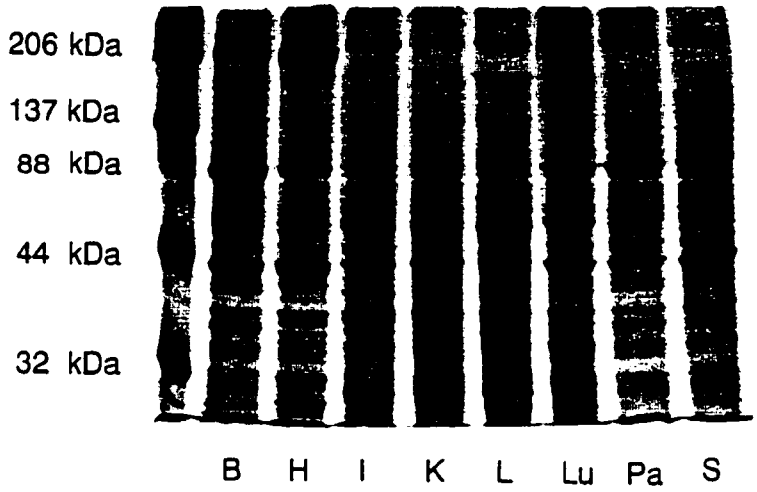
206 kDa
137 kDa
88 kDa
44 kDa
32 kDa
B H I K L Lu Pa S

B

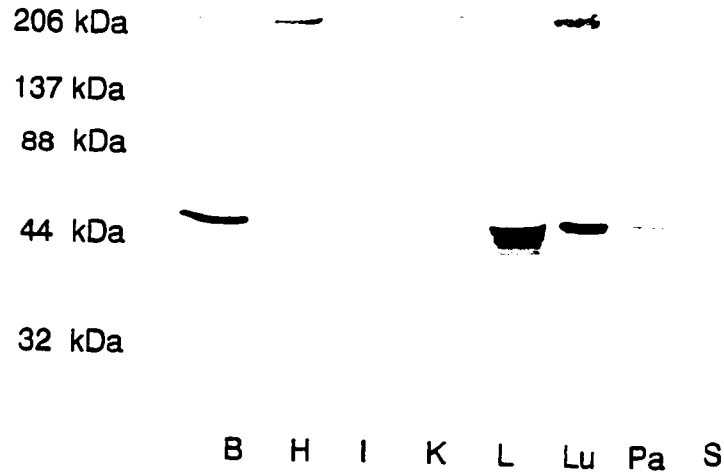
206 kDa
137 kDa
88 kDa
44 kDa
32 kDa
B H I K L Lu Pa S

3.1.15 Immunocytochemical Analysis of Liver Tissue

Immunocytochemical techniques were used to determine the CK18 distribution in rabbit liver sections. Both paraffin embedded and frozen sections of rabbit liver revealed an acinar gradient of staining (Figure 21). Hepatocytes around the portal triads demonstrated striking pericellular staining (Figs. 21A, 21C, and 21E) with a progressive reduction of staining seen distally (Fig. 21B). Interestingly, there was also increased pericellular staining of the hepatocytes adjacent to the central veins, although not to the same extent as that seen around the portal triads (Figure 21D). This pattern of staining was seen consistently using the chicken anti-CK18 IgG and with two different monoclonal anti-CK18 antibodies, KS-B17.2 (bovine antigen) and CY-90 (human antigen); with both paraffin embedded sections and frozen cryosections (Figure 21A (KS-B17.2) and also 21C (chicken anti-CK18)). This staining pattern was also visualized on paraffin embedded human liver sections using the monoclonal anti-CK antibody, CAM 5.2 (human antigen). Mild trypsinization of paraffin-embedded sections resulted in a small increase in staining (data not shown).

3.1.16 Binding of Anti-CK18 IgG to Hepatocytes

Experiments were done to determine whether anti-CK18 IgG would bind to CK18 on the surface of hepatocytes in whole organ perfusion studies. A liver organ perfusion system was used to compare the clearance and binding of ^{131}I-anti-CK18 IgG and ^{125}I-preimmune IgG in isolated rabbit livers. Figure 22 shows the clearance data from six such liver perfusion experiments, expressed as a ratio

Figure 21. **Immunocytochemical Localization of CK18 in Rabbit Liver Sections.** All immunocytochemical work was done as described in Materials and Methods. **Panel A.** CK18 staining, with monoclonal KS-B17.2 of a frozen rabbit liver section, adjacent to the portal triad. Note the strong pericellular staining (arrows) of hepatocytes around the portal vein, designated p. **Panel B.** Corresponding CK18 staining pattern further into the liver lobule. Note the lack of pericellular staining. **Panel C.** Same sectional area as in **panel A** but stained with chicken polyclonal anti-CK18 IgG, again demonstrating pericellular staining. **Panel D.** Staining of central vein region (cv) with chicken polyclonal anti-CK18 IgG. **Panel E.** Staining of paraffin section, proximal to portal triad, with monoclonal KS-B17.2, again demonstrating strong pericellular staining of hepatocytes (arrow). Bar, 20μm in **Panels A., B., C.,** and **D.**; 10 μm in **Panel E.**

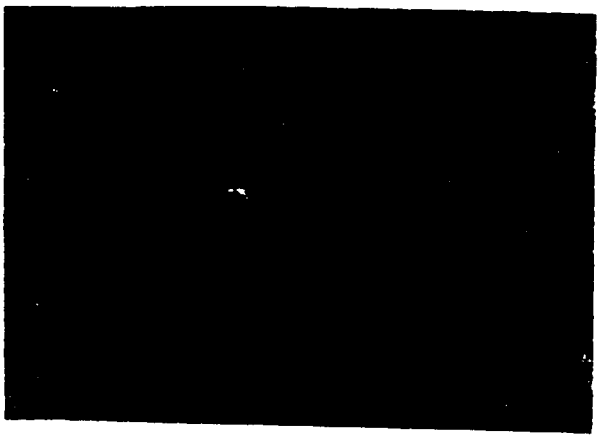

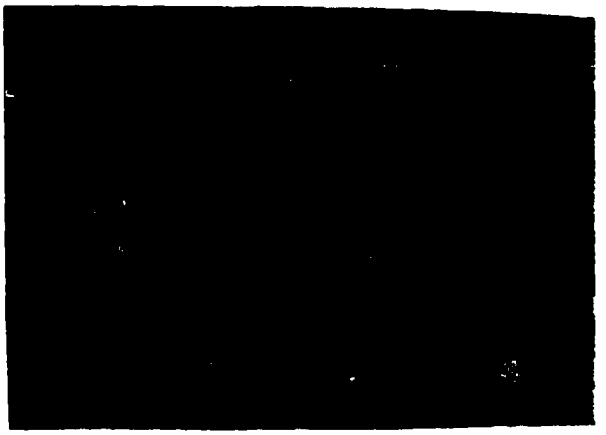

Figure 22. **Ratio of the Binding of ^{131}I-Anti-CK18 IgG Compared to ^{125}I-Preimmune IgG to Perfused Rabbit Livers.** Livers were isolated from anesthetized rabbits and perfused with 17.5×10^6 dpm of ^{125}I-preimmune IgG and equivalent amounts of ^{131}I-anti-CK18 IgG. The IgG clearance over time from the perfusate is represented as the means ± SEM of the ratios of anti-CK18 IgG to preimmune IgG for six different livers.

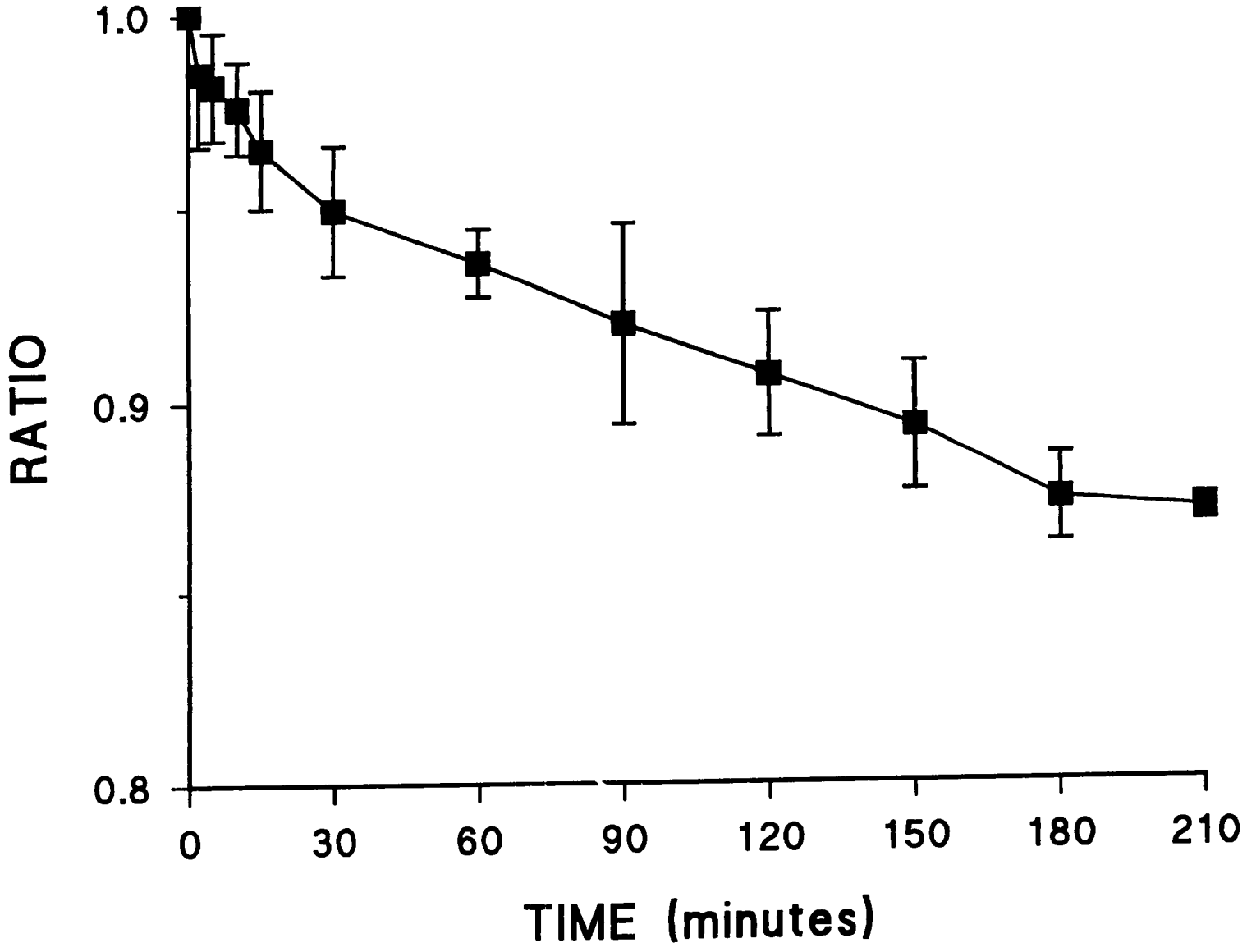
1.0
0.9
0.8
RATIO
0
30
60
90
120
150
180
210
TIME (minutes)

of the protein-bound radioactivities in the perfusate of ^{131}I-anti-CK18 IgG to ^{125}I-preimmune IgG, as a function of perfusion time. In all perfusion experiments the anti-CK18 IgG cleared at a faster rate than that observed with the preimmune IgG. This trend was reflected also in the ratio of bound anti-CK18 IgG to preimmune IgG bound to the liver. In all experiments, there was 1.6-fold more anti-CK18 IgG bound compared to preimmune IgG after 3.5 h of perfusion ($p=0.015$). It is important to note that over the course of these experiments the livers continued to release protons and glucose steadily into the perfusate indicating the viability of the hepatocytes in the liver.

3.2 The Metabolism of VN-TAT

3.2.1 Formation of VN-TAT in Rabbit Plasma

In 1992 and 1993, it was reported that TAT was found in human plasma as a ternary complex with VN and that VN-TAT could bind to a heparinoid-like moiety on HUVECs (de Boer *et al.*, 1992; de Boer *et al.*, 1993). Studies with rabbit plasma were done to determine if VN-TAT could be formed in rabbit plasma as in human plasma. To examine this question pre-formed ^{125}I-TAT complexes were added to plasma, or ^{125}I-α-thrombin was added to de-fibrinogenated plasma and the formation of VN-TAT was evaluated by SDS-PAGE and subsequent autoradiography. To determine if species differences played a role in the formation of VN-TAT, TAT complexes composed of ^{125}I-

bovine thrombin were used together with human and rabbit AT or ^{125}I-human thrombin with rabbit and human AT in both rabbit and human plasma. When these different TAT complexes were added to rabbit plasma (100 nM final; ACD plasma) no higher molecular weight species were seen on SDS-PAGE gels (see Figure 23A). Similarly, TAT composed of bovine thrombin and rabbit AT did not form higher molecular weight complexes in human plasma (Figure 23A, Lanes 7 and 8). However, almost all of the homogeneous human TAT formed a higher molecular weight complex in human plasma (~ 160 kDa); visible under non-reducing conditions (lane 10), but not under reducing conditions (Lane 9). When bovine or human α-thrombin was added to either de-fibrinogenated rabbit or human plasma directly, and analysed under reducing or non-reducing conditions, identical results were obtained (see Figure 23B). Adducts of ~ 160 kDa can be seen in the human plasma under non-reducing conditions when human thrombin was used (lane 10), while very slight ternary complex formation can be seen when bovine thrombin was used in human thrombin (Lane 8).

In other experiments 100 nM ^{125}I-TAT was added to plasma and the formation of VN-TAT was evaluated by SDS-PAGE and subsequent autoradiography. From these experiments the formation of VN-TAT was determined to be rapid with over 50% of the TAT moving into higher molecular weight adducts by 3 min (data not shown). Moreover, when the ability of VN-TAT to form in re-calcified human and rabbit plasma versus calcium-chelated plasma (ie anticoagulated with sodium citrate-phosphate) were compared there

Figure 23. **Formation of VN-TAT in Plasma. Panel A.** Different preparations of pre-formed ^{125}I-TAT complexes were incubated (100 nM final) in either rabbit (Lanes 1-6) or human (Lanes 7-10) plasma for 30 min before evaluation on 6% SDS-PAGE gels. Samples electrophoresed in all even-numbered lanes are under non-reducing conditions and odd-numbered lanes are in the presence of ß-mercaptoethanol (reducing). The following complexes were used: rabbit AT-bovine thrombin, Lanes 1,2,7, and 8; human AT-bovine thrombin, Lanes 3 and 4; and human AT-human thrombin, Lanes 5,6,9,and 10. **Panel B.** Human or bovine ^{125}I-thrombin was added to defibrinogenated rabbit or human plasma at 37°C for 30 min and the inhibitory complexes that formed were followed by 6% SDS-PAGE. Lane 1 is TAT formed with human AT and thrombin and Lane 2 is TAT formed with human AT and bovine thrombin, electrophoresed under non-reducing conditions. Otherwise samples in all even-numbered lanes were electrophoresed under non-reducing conditions and under reducing conditions in the odd-numbered lanes. Bovine thrombin was added to rabbit plasma (Lanes 3 and 4) or human plasma (Lanes 7 and 8) while human thrombin was added to rabbit plasma (Lanes 5 and 6) or human plasma (Lanes 9 and 10).

A

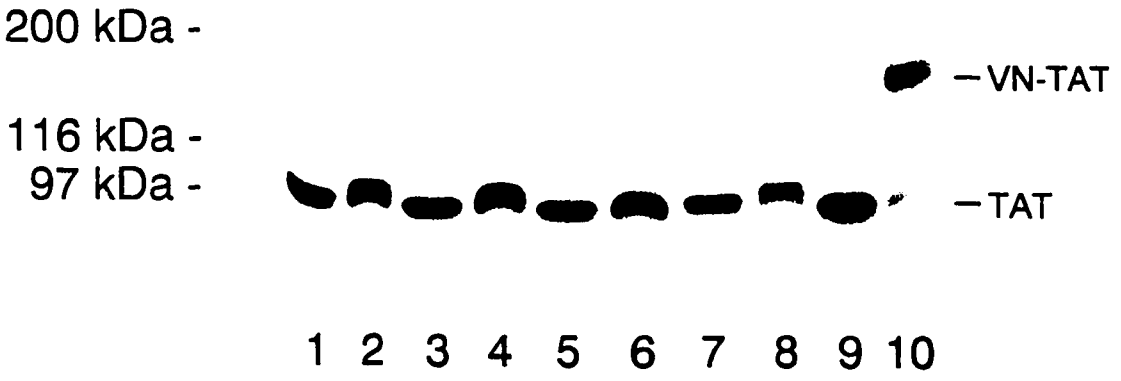
200 kDa -
116 kDa -
97 kDa -
VN-TAT
TAT
1 2 3 4 5 6 7 8 9 10

B

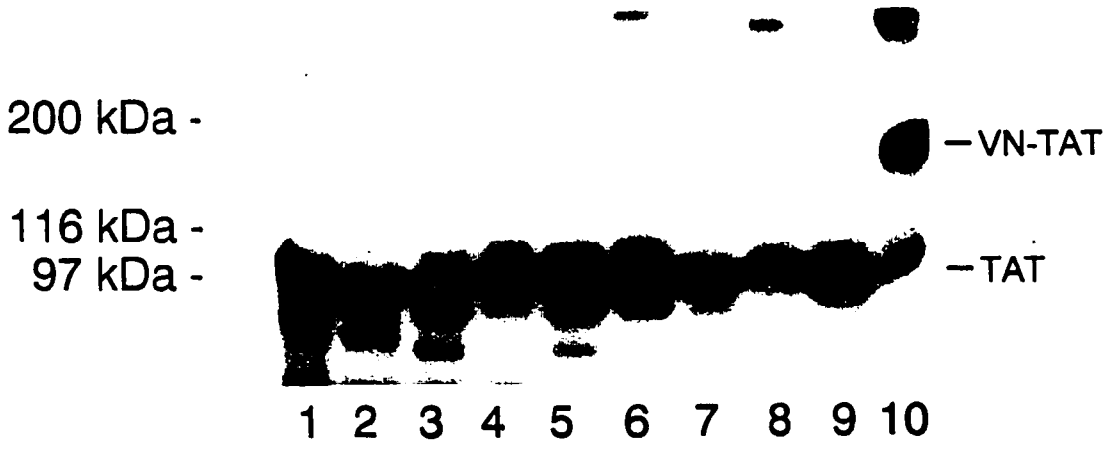
200 kDa -
116 kDa -
97 kDa -
VN-TAT
TAT
1 2 3 4 5 6 7 8 9 10

was no difference in the ability of VN-TAT to form. In all, these data suggest that VN-TAT formation in human plasma is dependent upon human thrombin, and possibly human vitronectin, since only TAT containing human thrombin formed VN-TAT in human plasma to a significant degree. This interaction is apparently mediated by disulfide bond formation between VN and thrombin as the higher molecular weight complexes broke down under reducing conditions on SDS-PAGE and is similar to that reported previously by de Boer *et al.* (1993).

3.2.2 Does VN-TAT Form in Rabbit Plasma or Serum?

The lack of *in vitro* VN-TAT formation in rabbit plasma prompted us to determine whether VN-TAT complexes can be formed in rabbit blood by performing Western blot analyses on rabbit serum and comparing the results to that seen with human serum. Figure 24 shows the localization of AT, VN, and thrombin detected by specific antibodies in human and rabbit serum. In all cases the individual components of VN-TAT were detected mainly at a molecular mass corresponding to monomeric VN-TAT but also as higher molecular mass, multimeric VN-TAT (see Figure 24). Anti-thrombin antibodies appear to be less reactive to thrombin in VN-TAT, possibly due to conformational changes in thrombin or steric hindrance of thrombin by AT and VN. The lower antibody reactivity to thrombin in VN-TAT was also seen by de Boer *et al.* (1993).

3.2.3 Purification and Radiolabelling of Human VN-TAT

In order to investigate the metabolism of VN-TAT *in vitro* and *in vivo*, VN-TAT was purified by heparin-Sepharose chromatography. Figure 25 (Panel A),

Figure 24. **Western Blot Analysis for VN-TAT in Rabbit and Human Serum.** Three μl of either human or rabbit serum were electrophoresed on 8% SDS-PAGE gels, under non-reducing conditions, and then electroblotted onto nitrocellulose. The headings indicate the species of serum probed and the individual proteins probed for are indicated underneath each lane. **Panel A.** For human serum the primary antibodies used were: for AT, sheep anti-human AT (5 μg/ml); for vitronectin, sheep anti-human VN (5 μg/ml); for thrombin, chicken anti-human thrombin (5 μg/ml). **Panel B.** For rabbit serum the primary antibodies used were: for AT, sheep anti-rabbit AT (5 μg/ml); for VN, sheep anti-human VN (5 μg/ml); and for thrombin, chicken anti-human thrombin (5 μg/ml). Reactive IgG bands were visualized using alkaline phosphatase conjugate secondary antibodies, at 1/2000 dilution.

A. HUMAN SERUM

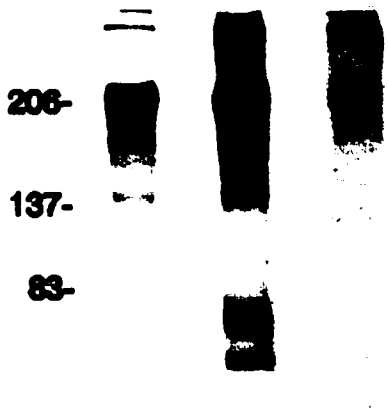

AT VN THROMBIN

B. RABBIT SERUM

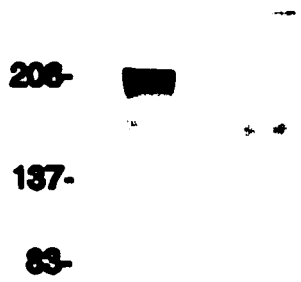

AT VN THROMBIN

lanes 2 and 3, shows purified VN-TAT electrophoresed on 10% SDS-PAGE gels under non-reducing and reducing conditions, respectively. As a comparison human TAT, electrophoresed under reducing conditions, is shown in lane 4. Under non-reducing conditions the majority of the VN-TAT is seen as an ~ 160 kDa monomer but also as higher molecular weight multimers. When VN-TAT is electrophoresed under reducing conditions it appears to breakdown to form TAT (~ 100 kDa) and VN (75 and 65 kDa bands) in comparison to a TAT preparation (~ 100 kDa) (upper band, Lane 4). This is consistent with VN-TAT being formed through a disulfide bond between VN and the thrombin in the TAT complex as previously reported (De Boer *et al.*,1993). Furthermore the bulk of the VN-TAT appears to be found as higher molecular weight multimers based on comparing the amount of protein in non-reduced monomeric VN-TAT versus the amount of protein in the TAT and VN bands when VN-TAT was analyzed under reducing conditions (Figure 25, panel A). Panel B of Figure 25 shows ^{125}I-VN-TAT and ^{125}I-TAT electrophoresed on 8% SDS-PAGE gels.

3.2.4 Composition of Purified VN-TAT

To demonstrate that purified VN-TAT is composed of AT, VN, and thrombin Western blot analyses were performed. Figure 26 shows the detection of VN (lane 2), AT (lane 3), and thrombin (lane 4). Once again all three proteins are detected in a major band of ~ 160 kDa (arrow) with the presence of higher molecular weight multimers also being detected. Interestingly, a lower molecular weight band is also detected and from Coomassie blue stained SDS-PAGE gels

Figure 25. **Electrophoreseis of Purified VN-TAT. Panel A.** Coomassie blue stained 10 % SDS-PAGE gel in which 6 μg of purified VN-TAT was electrophoresed under non-reducing conditions (Lane 2) or reducing conditions (Lane 3). For comparsion 3 μg TAT was run under reducing conditions (Lane 4). Molecular weight markers are shown in Lane 1. **Panel B.** Autoradiograph of ^{125}I-VN-TAT and ^{125}I-TAT electrophoresed, under reducing conditions, on 8% SDS-PAGE gels.

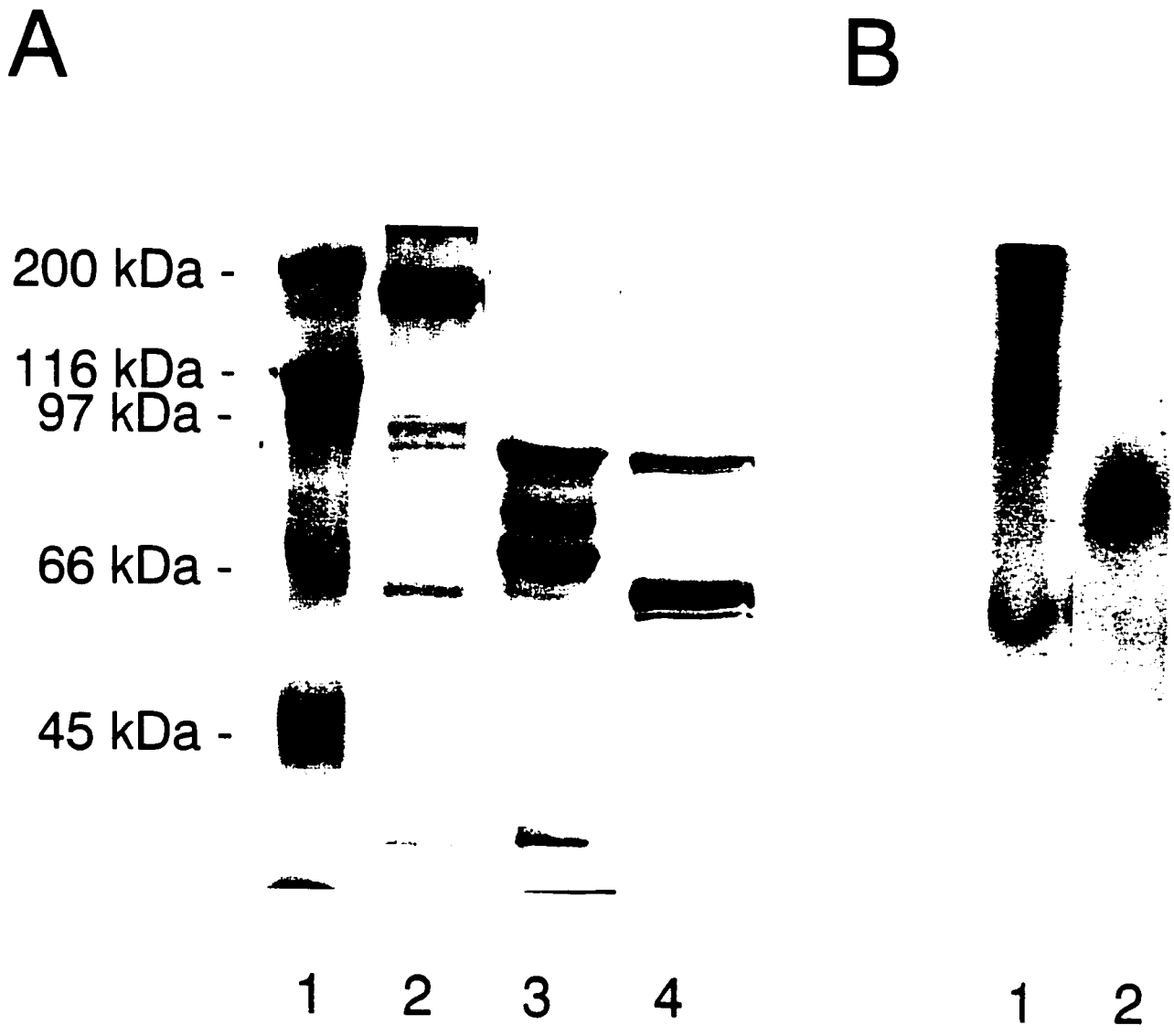
A
B
200 kDa -
116 kDa -
97 kDa -
66 kDa -
45 kDa -
1
2
3
4
1
2

Figure 26. **Protein Composition of VN-TAT.** 500 ng of purified VN-TAT was electrophoresed on 8% SDS-PAGE gels, under non-reducing conditions, and electroblotted onto nitrocellulose. The blots were then probed with the following primary antibodies: **Lane 1,** rabbit anti-human Vn (1/5000); **Lane 2,** sheep anti-human AT (7.2 μg/ml) ; **Lane 3,** rabbit anti-human HCII antiserum (1/50); or **Lane 4,** chicken anti-thrombin (10 μg/ml). The arrow indicates the location of monomeric VN-TAT (160 kDa), recognized by anti-VN, anti-AT, and anti-thrombin antibodies. The arrowhead shows the location of VN-TAT degradation products recognized by anti-VN, anti-AT, and anti-thrombin antibodies.


106 kDa -
80 kDa -
49.5 kDa -
1
2
3
4

corresponds to a molecular mass of ~ 60 kDa. This band most likely represents degradation of the ternary complex from free proteinases in the serum since antibodies against all three proteins recognize it. Thrombin also forms ternary complexes with vitronectin and the serpins HCII and PN-1 (Preissner and Sie, 1988; Liu *et al.*, 1995; Rovelli *et al.*, 1990). To determine if HCII ternary complexes are found in the VN-TAT preparation Western analysis was performed using anti-HCII anti-serum. Lane 3 shows that HCII is found in the preparation and its mobility coincides with that of VN, AT, and thrombin. VN-T-HCII complexes, like VN-TAT, appear to be composed of multimers with the majority of the complexes being found in the monomeric form. The monomers appear to have a slightly slower electrophoretic mobility than VN-TAT and is most likely due to the fact than HCII is a larger protein than AT (Figure 26 lane 3). Furthermore, there also appear to be more degradation products than that seen with VN-TAT, which are of higher molecular mass than VN-TAT degradation products. These lower mass bands are again most likely VN-T-HCII degradation products since they also recognized by antibodies against all three proteins.

3.2.5 Plasma Elimination of ^{125}I-VN-TAT, ^{25}I-TAT, and ^{125}I-AT

^{125}I-VN-TAT plasma elimination clearance experiments were done in rabbits to determine whether VN-TAT is metabolized in a similar fashion to TAT. The mean of TCA-corrected plasma clearance curves of ^{125}I-VN-TAT up to 60 min is shown in Figure 27 (n=3). Clearance parameters determined from VN-TAT clearance data are shown in Table 4. VN-TAT was cleared rapidly from the

Figure 27. **Plasma Clearance of ^{125}I-VN-TAT, ^{125}I-TAT, and ^{125}I-AT in Rabbits.** The plasma clearance of ^{125}I-VN-TAT (open circles; 12.6 x 10^6 dpm; 8 μg; n=3), ^{125}I-TAT (closed circles; 3.4 x 10^6 dpm; 3.5 μg; n=3), and ^{125}I-AT (closed triangles; 12.6 x 10^6 dpm; ~ 2.9 μg; n=2) was measured as described in the Materials and Methods section. Each datapoint is the mean ± SEM of TCA-corrected plasmas.

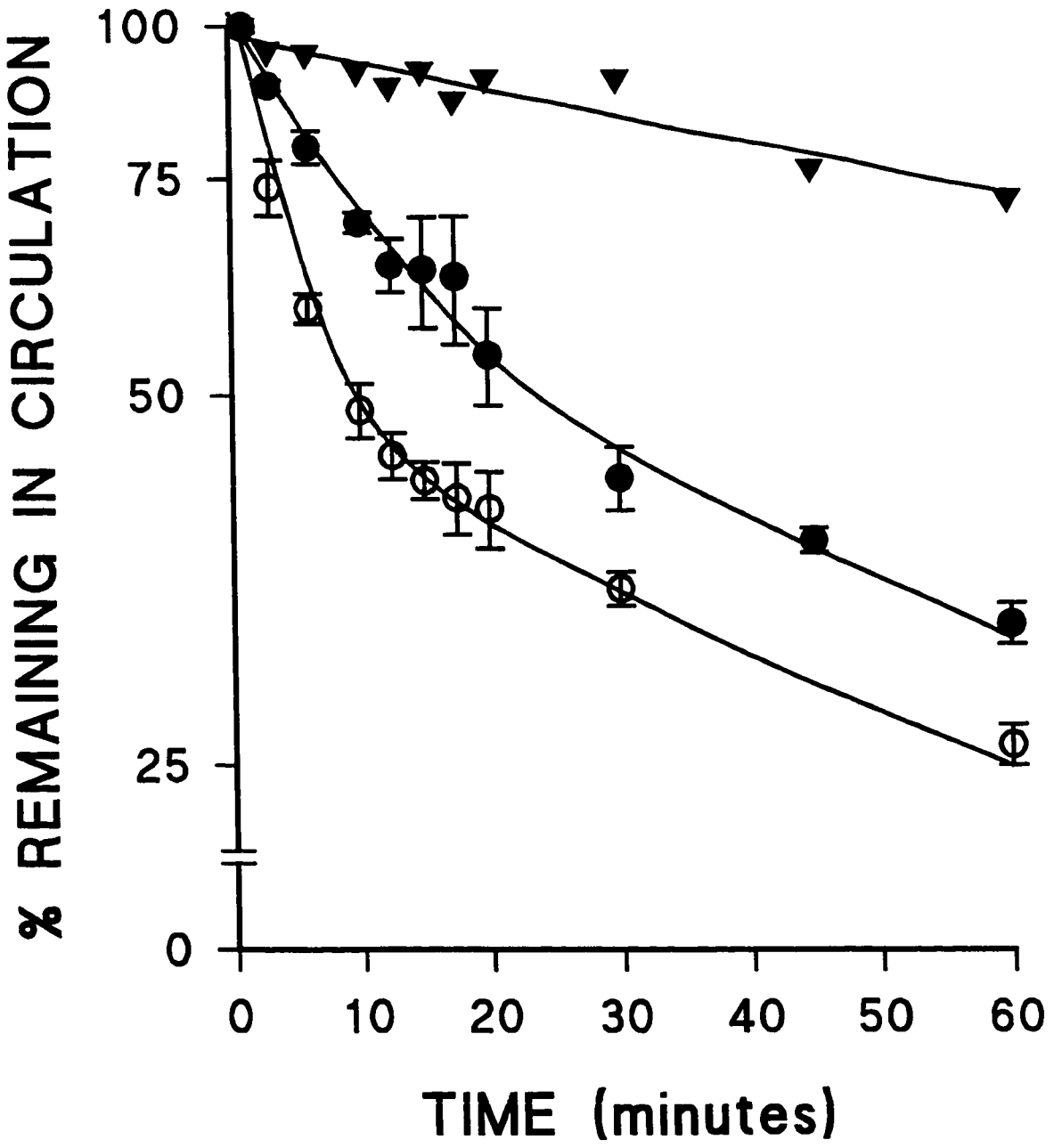
% REMAINING IN CIRCULATION
100
75
50
25
0
0
10
20
30
40
50
60
TIME (minutes)

CLEARANCE PARAMETERS	*VN-TAT ALONE (n=3)*	*VN-TAT PLUS HEPARIN (n=4)*	*VN-TAT PLUS PROTAMINE SULFATE (n=4)*	*TAT (n=3)*
half-life ($t_{0.5\alpha}$; min)	3.79 ± 0.49	61.77 ± 3.71 (p< 0.001)	49.44 ± 4.36 (p= 0.002)	5.25 ± 0.32
clearance rate constant (a_1; alpha phase)	0.189 ± 0.025	0.014 ± 0.001 (p=0.019)	0.011± 0.001 (p=0.019)	0.30 ± 0.18
C_1	0.585 ± 0.061	0.91 ± 0.008 (p=0.034)	1.03 ± 0.018 (p=0.02)	0.327 ± 0.10
half-life ($t_{0.5\beta}$; min)	85.35 ± 4.3			$t_{0.5\beta}$ = 42.78 ± 3.68 (p=0.005)
clearance rate constant (a_2; beta phase)	0.008 ± 0.000			0.016 ± 0.002
C_2	0.442 ± 0.042			0.718 ± 0.083

TABLE 4. Summary of clearance data for VN-TAT, VN-TAT plus heparin, VN-TAT plus protamine sulfate, and TAT from rabbits. Data were analyzed as described in the Materials and Methods Section. $t_{0.5\alpha}$ represents the half-life for protein clearance defined by a single-compartment model or for the initial phase of clearance in a multi-compartmental model of clearance. $t_{0.5\beta}$ represents the half-life for the second phase of clearance in a multi-compartment model of clearance. Clearance parameters showing significant differences from those of VN-TAT alone are indicated by the p-value in parentheses.

blood in a biphasic fashion. In the initial rapid phase the $t_{½\alpha}$ = 3.79 ± 0.49 min and the slower second phase of clearance revealed a $t_{½\beta}$ = 85.35 ± 4.3 min. Non-reducing SDS-PAGE analysis of plasma samples, taken up to 20 min after injection, followed by autoradiography, revealed that the ^{125}I-VN-TAT remained intact in the rabbit circulation. In Figure 27 the clearance curves of human TAT (n=3) and human AT (n=2) are shown. AT demonstrates a slow clearance and its disappearance from the plasma is essentially linear with only ~ 25% of the initially injected ^{125}I-AT cleared at the one hour point. In contrast, TAT clearance is more rapid than AT. The clearance parameters defining the removal of TAT from the circulation are shown in Table 4. Similar to VN-TAT, ^{125}I-TAT clearance is biphasic with an initial rapid phase of clearance ($t_{½\alpha}$ = 5.25 ± 0.32 min) which was not significantly different from that of VN-TAT. The half-life for the second phase ($t_{½\beta}$) was 42.78 ± 3.68 min and was significantly different from the $t_{½\beta}$ of VN-TAT (p=0.005). Finally, there was relatively little radioactivity associated with the cellular fraction of the blood samples collected from rabbits injected with either ^{125}I-VN-TAT or ^{125}I-TAT.

In other experiments either ^{125}I-VN-TAT or ^{125}I-TAT were co-injected with large excesses (1875 and 4300 fold molar excesses respectively) of trypsin-α-PI complexes (TRAP) (n=1 for both) to compare to the previously defined clearance experiments in mice and rats (Introduction, section 1.5.1). The presence of TRAP did not alter the clearance rate for either VN-TAT or TAT suggesting possible differences in clearance mechanisms in rabbits compared to that seen for murine

systems.

3.2.6 Tissue Distribution of ^{125}I-VN-TAT Clearance

To determine the organ localization of VN-TAT removal in rabbits ^{125}I-VN-TAT was injected into rabbits (n=3) and after one hour post mortem examination of radioactivity within different tissues was undertaken. The organs examined were the liver, lungs, kidneys, spleen, bladder, and heart (see Figure 28A). Over 80% of the total organ-associated radioactivity was localized in the liver. The kidney contained the next highest proportion of radioactivity (≈ 10% of total), possibly because it is the site of removal of free ^{125}Iodine and ^{125}I-tyrosine from the degraded protein fragments in the blood. Examining the amount of ^{125}Iodine per gram of tissues showed that the liver had the highest amount of radioactivity per gram of tissue (≈ 20,000 cpm/gm) (Figure 28B). Relatively high counts per gram were found in the kidneys and spleen (14221 cpm/gm and 14673 cpm/gm respectively). Again, the high counts in the kidneys most likely represent accumulation of free ^{125}Iodine from degraded fragments of ^{125}I-VN-TAT. This is most likely true since an approximately equal volume of blood flows through both the liver and kidneys. As the kidneys are of smaller total mass than the liver then the cpm/gm ratio would be expected to be higher in the kidneys than the liver if the former were specifically removing ^{125}I-VN-TAT.

3.2.7 Heparin Sensitivity of VN-TAT Clearance

De Boer *et al.* (1992) found that VN-TAT interacted with a heparinoid-like substance on the surface of HUVECs. Similarly, glycosaminoglycans have been

Figure 28. **Tissue Distribution of ^{125}I-VN-TAT.** The organ localization of ^{125}I-VN-TAT was determined by post-mortem examination of various organs one h after the injection of ^{125}I-VN-TAT (n=3). **Panel A.** The radioactivity associated with one organ, defined as the % radioactivity in one organ compared to the total radioactivity for all organs combined, is shown. **Panel B.** The radioactivity (cpm) per gram of tissue.

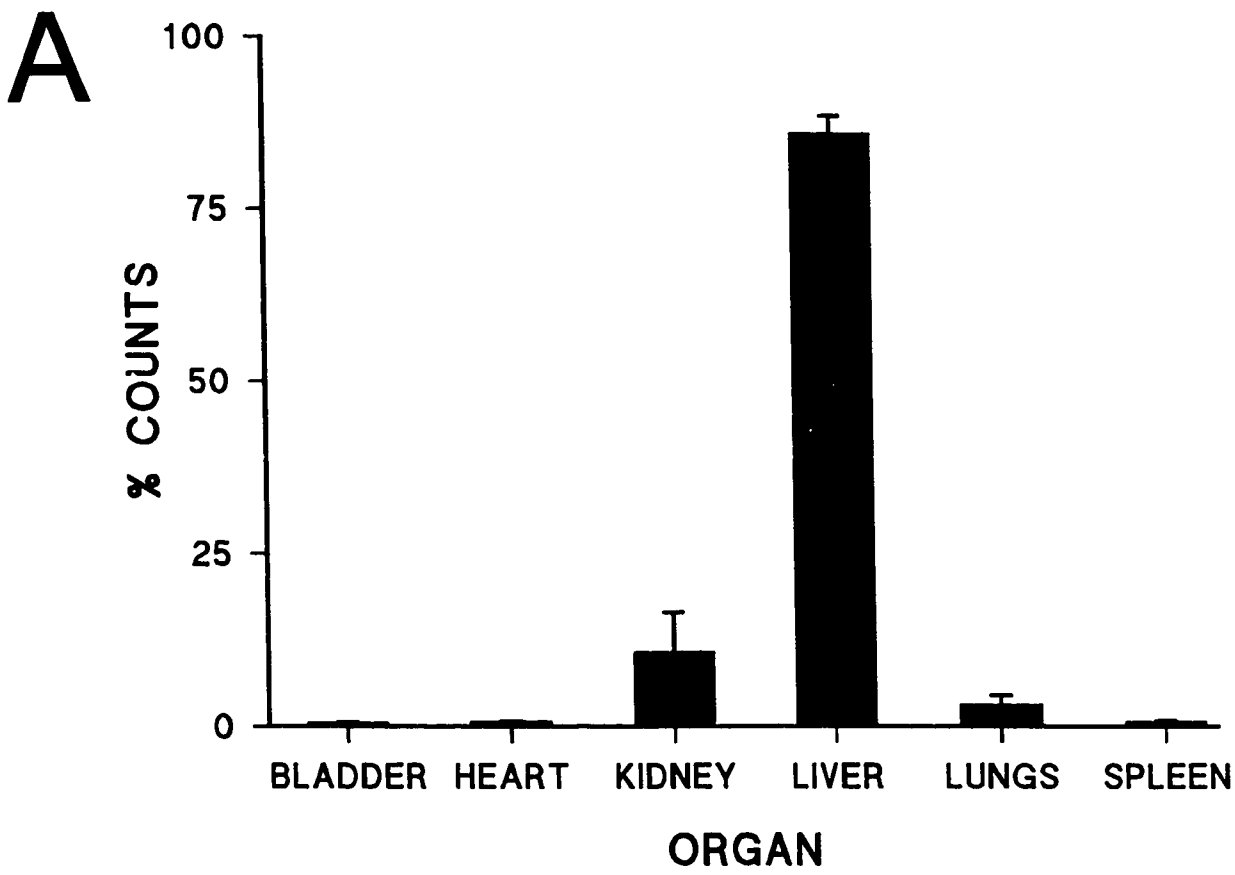
A
100
75
50
25
0
% COUNTS
BLADDER
HEART
KIDNEY
LIVER
LUNGS
SPLEEN
ORGAN

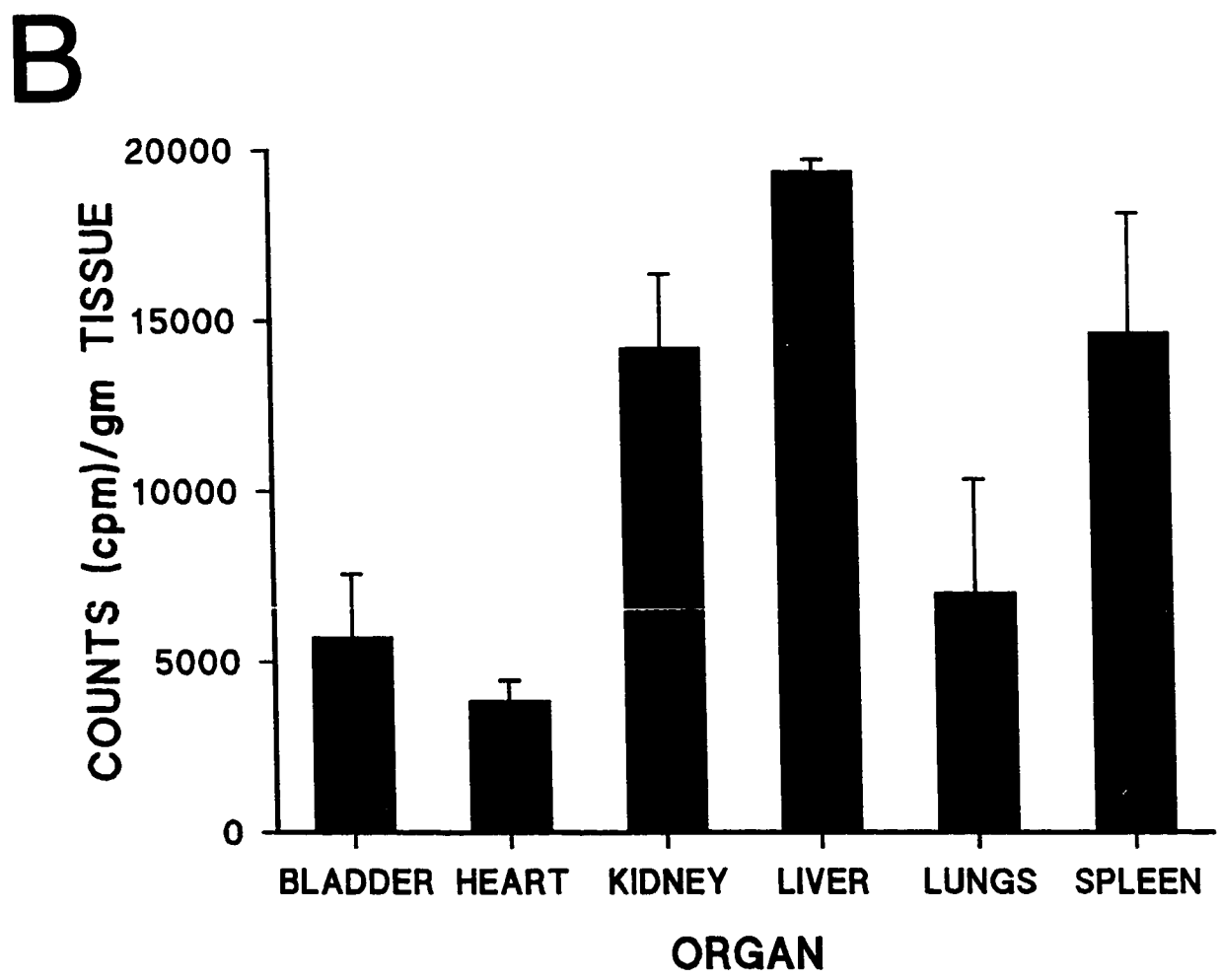
B
20000
15000
10000
5000
0
COUNTS (cpm)/gm TISSUE
BLADDER
HEART
KIDNEY
LIVER
LUNGS
SPLEEN
ORGAN

found to be involved in the metabolism of a number of LRP ligands (see Introduction, section 1.5.5). To determine if the binding of VN-TAT to liver receptors was heparin-sensitive, the plasma clearance of VN-TAT was observed under competition conditions with standard heparin. Figure 29 shows the mean clearance curve of ^{125}I-VN-TAT co-injected with a 10,000 Unit bolus of heparin (n=4), with the previous ^{125}I-VN-TAT clearance experiments from Figure 26 as a comparison. The clearance parameters determined from curve-fitting are shown in Table 4. In the presence of heparin, the clearance data best described by a single-compartment model in which the initial rapid clearance seen with VN-TAT alone was abolished. Thus, in the presence of high doses of heparin, the half-life for VN-TAT clearance ($t_{½\alpha}$) from the vascular space was 61.77 ± 3.71 min and was significantly different than the $t_{½\alpha}$ for VN-TAT (3.79 ± 0.49, $p<0.001$, Table 4). In the presence of heparin, the clearance of ^{125}I-VN-TAT resembled the second phase of ^{125}I-VN-TAT in the absence of heparin (85.35 ± 4.3 min). Non-reducing SDS-PAGE analysis of plasma samples, taken up to 20 min after injection, followed by autoradiography, revealed that the ^{125}I-VN-TAT remained intact in the rabbit circulation.

In further experiments the heparin-binding molecule protamine was co-injected (final concentration ≈ 500 μg/ml blood) with ^{125}I-VN-TAT (n=4). If heparin-like substances are involved in the removal of VN-TAT then protamine would be expected to reduce this clearance by binding to these substances and prohibiting their interaction with VN-TAT. The protamine competition clearance

Figure 29. **Heparin Sensitivity of ^{125}I-VN-TAT Clearance in Rabbits.** The clearance of ^{125}I-VN-TAT co-injected with either a 10,000 unit bolus of heparin (closed circles, n=4) or a bolus of protamine sulphate (65 mg/ml)(closed triangles, n=4) is shown. For comparison, the clearance curve of ^{125}I-VN-TAT alone from Figure 27 is shown (open circles). For all experimental groups each data point represents the mean of data from ± SEM.

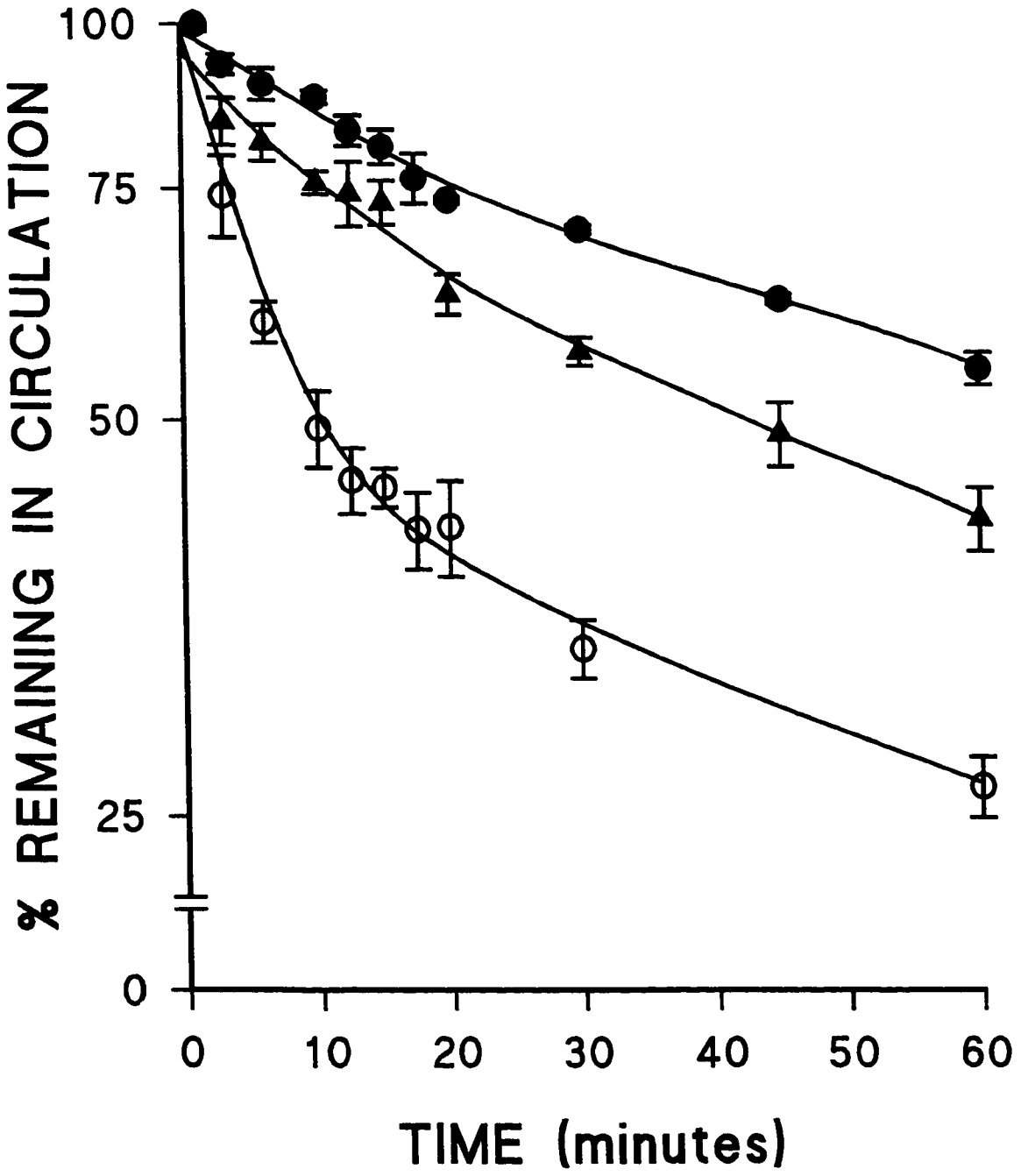
100
75
50
25
0
% REMAINING IN CIRCULATION
0
10
20
30
40
50
60
TIME (minutes)

data best fit to a single-compartment model and the clearance parameters determined from curve-fitting are summarized in Table 4. From Figure 29 it can be seen that protamine, like heparin, reduced the biphasic clearance of ^{125}I-VN-TAT to a single phase. Furthermore, competition with protamine significantly increased the $t_{1/2\alpha}$ of ^{125}I-VN-TAT clearance to 49.44 ± 4.36 min from 3.79 ± 0.49 min (p=0.002; see Table 4).

3.2.8 Heparin Reduces Liver-Specific Clearance of ^{125}I-VN-TAT

To determine whether heparin treatment affected liver-specific removal of VN-TAT further clearance studies were performed in rabbits and the liver-associated radioactivity was examined (n=3 for VN-TAT alone and n=3 for heparin co-injection group). Based on the above-mentioned clearance experiments the experimental clearance time was chosen as 30 min to maximize the differences in ^{125}I-VN-TAT accumulation between the two experimental groups. To ensure that the ^{125}I-VN-TAT cleared as previously found, samples were taken over the whole time course. The non-TCA-corrected clearance of ^{125}I-VN-TAT alone and in rabbits coinjected with heparin is demonstrated in Figure 30. As found previously the VN-TAT injected alone cleared rapidly while in the presence of heparin, 60% of ^{125}I-VN-TAT remained in the circulation even at 30 min.

The data from these experiments is summarized in Table 5. Comparing the amount of ^{125}I-VN-TAT in the livers of the two groups revealed that ~ 66% of cleared ^{125}I-VN-TAT at 30 min was associated with the liver (n=3). In the

Figure 30. **Heparin Reduces the Liver-Specific ^{125}I-VN-TAT Clearance.** In separate experiments the clearance of ^{125}I-VN-TAT alone (solid circles, n=3) or in competition with a 10,000 unit bolus of heparin (open circles triangles, n=3) was followed over 30 min. Each data point is the mean ± SEM from three animals and show the non-TCA-corrected plasma levels of ^{125}Iodine expressed as a % of the 1 min post-injection value.

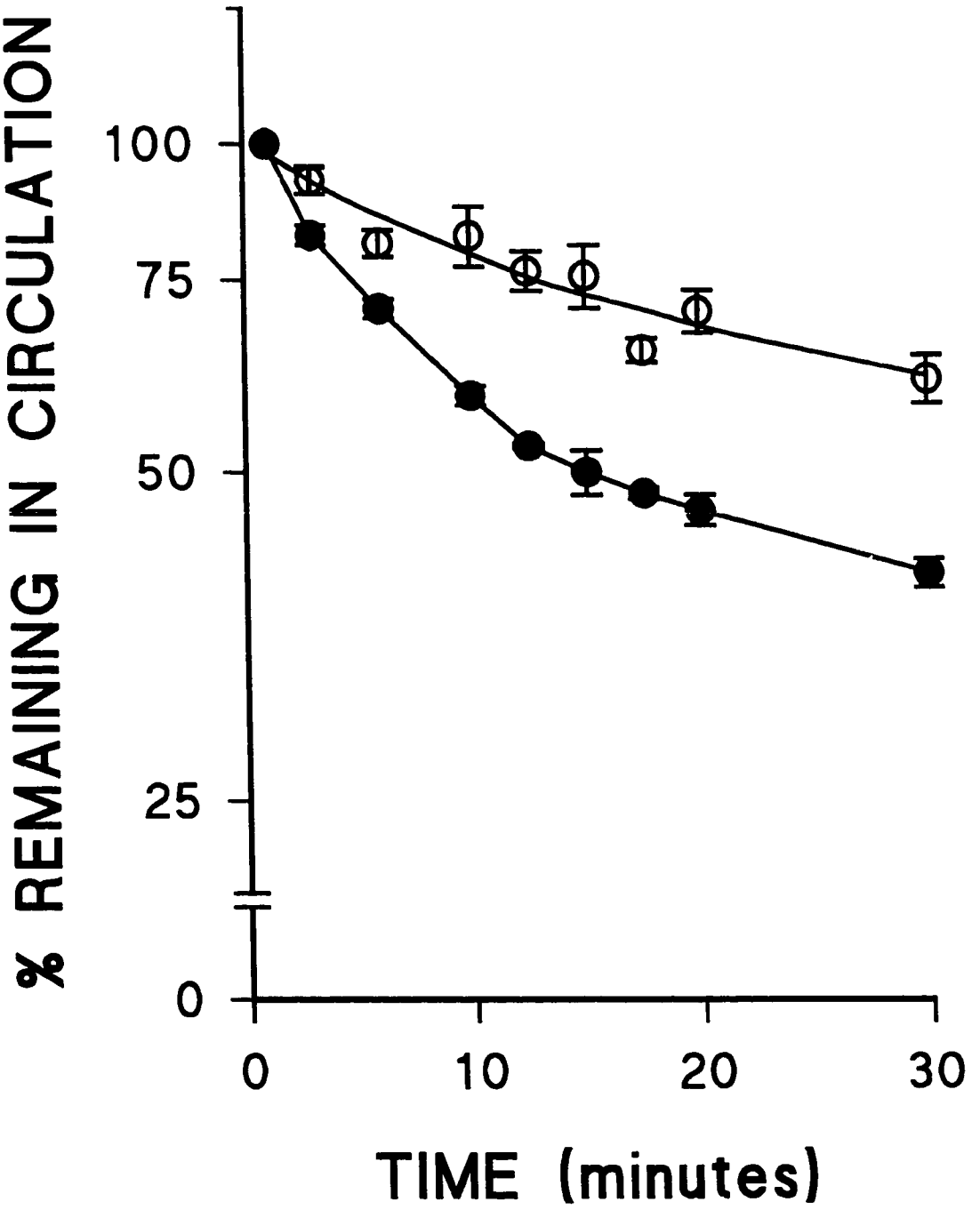
% REMAINING IN CIRCULATION
100
75
50
25
0
0
10
20
30
TIME (minutes)

LIGAND	*% ^{125}I-VN-TAT LEFT IN CIRCULATION (at 30 min)*	*TOTAL COUNTS IN LIVER (at 30 min)*	*COUNTS/GRAM OF LIVER (at 30 min)*	*% OF REMOVED ^{125}I-VN-TAT IN LIVER (at 30 min)*
VNTAT 1	42.8%	7968025	77813	77.4%
VNTAT 2	38.8%	6730762	67240	60.7%
VNTAT 3	39.9%	6488525	61444	59.6%
SUMMARY	*40.5%*			*65.9%*
VNTAT + HEPARIN 1	55%	2626635	30649	25.5%
VNTAT + HEPARIN 2	65%	2851183	36274	32.6%
SUMMARY	*61.2%*			*29.1%*
VNTAT + TRAP	42.3%	4775651	73698	45.7%

TABLE 5. Summary of the Effects of Heparin and TRAP on the Liver-specific Clearance of ^{125}I-VN-TAT. ^{125}I-VN-TAT was injected into rabbits alone or in the presence of heparin (10,000 units) or TRAP (≈ 15 mg). The amount of ^{125}I-VN-TAT left in the circulation is given as a % of the amount initially injected.

heparin-treated rabbits, only ~ 39% of cleared VN-TAT was liver-associated (n=2). Furthermore there was 50% less radioactivity per gram of liver tissue in the heparin-treated animals. This indicates that competition for heparin-binding sites within the liver drives the clearance of VN-TAT to other organs since the amount of liver-specific removal is reduced in the presence of heparin. Taken together these data support the hypothesis that the liver is the major site for VN-TAT removal and that heparinoid-like materials are important in VN-TAT clearance. Interestingly, although competition with an excess of TRAP did not effect the plasma clearance of ^{125}I-VN-TAT, it reduced the liver-specific uptake of ^{125}I-VN-TAT by ~ 50% (normal clearance =100%).

3.2.9 *In Vivo* Internalization and Degradation of VN-TAT

Figure 31A shows the appearance of TCA-soluble radioactivity in the plasmas of the rabbits injected with ^{125}I-VN-TAT. Examining the TCA-soluble ^{125}Iodine products in the plasma over 120 min indicates an initial decreased soluble radioactivity which most likely represents the clearance of free ^{125}Iodine from the blood. At 20 min the soluble radioactivity begins to increase and begins to plateau at 60 min at a level of 300% greater than that seen initially in the plasma. This increase in soluble radioactivity probably represents the degradation of internalized ^{125}I-VN-TAT. The small standard error indicate the consistency of the clearance experiments and that these data are highly representative for VN-TAT clearance in the rabbit. Figure 31B compares the *in vivo* ^{125}I-VN-TAT degradation data from Figure 31A with that of the ^{125}I-VN-TAT degraded in the

Figure 31. **Degradation of ^{125}I-VN-TAT In Vivo During Its Clearance. Panel A.** The appearance over time of TCA-soluble radioactivity in rabbit plasma is shown (closed circles) representing the mean ± SEM of plasma levels of TCA-soluble radioactivity from same three rabbits shown in Figure 26. The previous clearance data of ^{125}I-VN-TAT (from Figure 26) is also shown (open circles connected by the dashed line). **Panel B.** Comparison of the degradation of ^{125}I-VN-TAT in the absence (from Panel A, closed circles) or presence of heparin (open circles) or protamine (open triangles) over 60 min. All degradation data are from the clearance experiments shown in Figure 29.

A

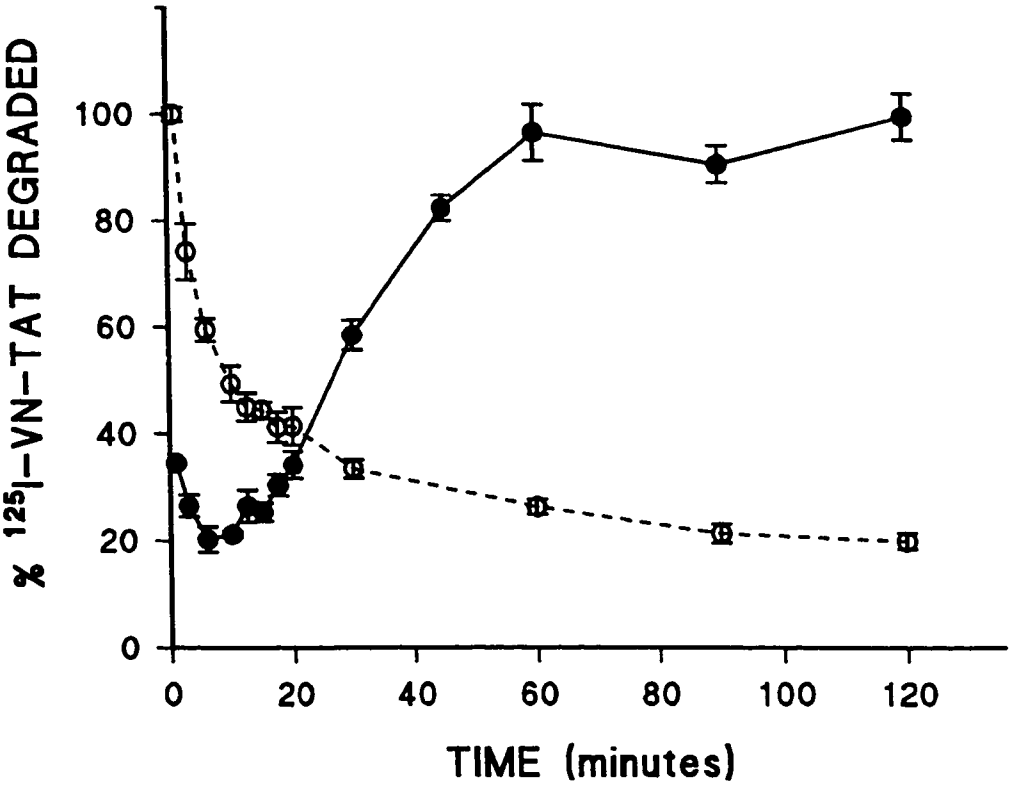
% 125I–VN–TAT DEGRADED
100
80
60
40
20
0
0
20
40
60
80
100
120
TIME (minutes)

B

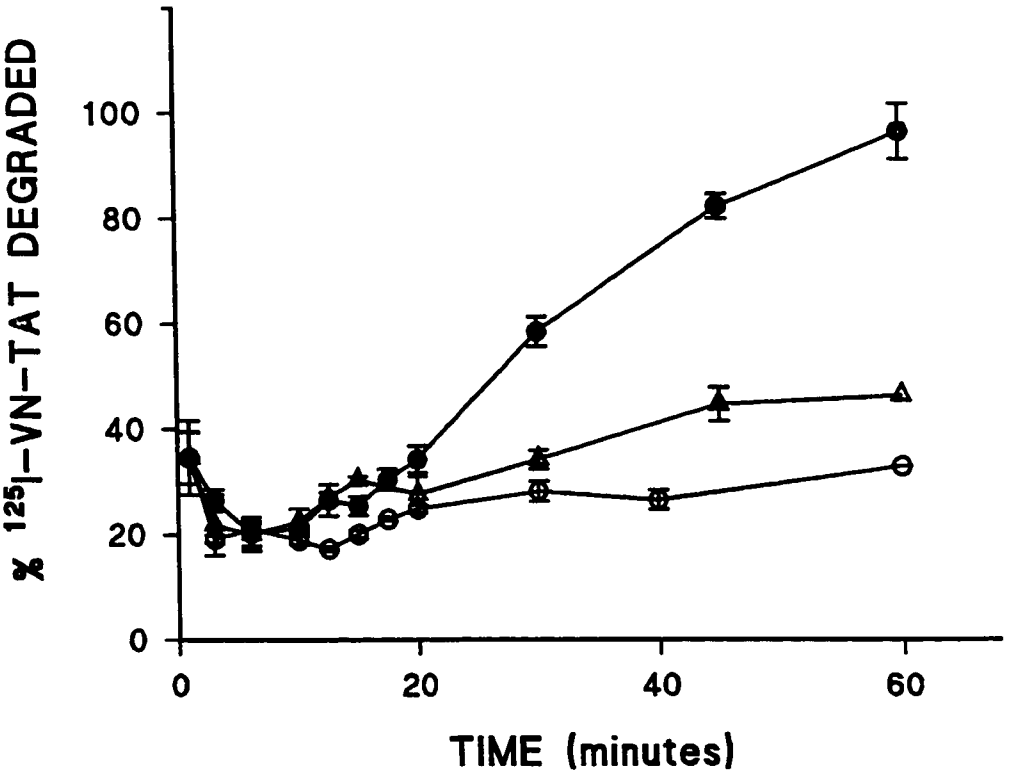
% 125I–VN–TAT DEGRADED
100
80
60
40
20
0
0
20
40
60
TIME (minutes)

rabbits coinjected with heparin or protamine. The initial values of degradation in the presence of heparin or protamine were normalized to the initial value of VN-TAT alone. The highest levels of degradation were reduced > 2.5 fold for VN-TAT competed with protamine or heparin than with VN-TAT alone. The initial levels of TCA-soluble counts were very similar up to ≈ 20 min for all three experimental groups and probably represent the level of free ^{125}I.

3.2.10 Radioligand Binding Studies with VN-TAT on Hepatoma Cells

To determine the appropriate incubation period for radioligand binding studies with VN-TAT an association (time-course) experiment was performed using HepG2 cells (data not shown). In this experiment a ^{125}I-VN-TAT concentration of 5 nM was used based on the dissociation constant of ≈ 16 nM derived for VN-TAT binding to endothelial cells by de Boer *et al.* (1992). From this experiment two h was chosen as the time frame for further binding experiments since saturation of specific-binding had occurred by this time.

To determine the affinity of VN-TAT for HepG2 cells a competitive radioligand binding experiment was performed. A competition curve from the data was obtained giving an IC_{50} value ≈ 1 μM (Figure 32). In further competitve radioligand binding experiments the ability of VN-TAT, TAT, and α_2M^* to compete for binding with ^{125}I-VN-TAT was examined. Figure 33A shows a single concentration competition binding experiment on HepG2 cells using 10 nM ^{125}I-VN-TAT in the absence or presence of a 240-fold molar excess of TAT or VN-TAT and a 76-fold molar excess of α_2M^*. As can be seen excess VN-TAT

Figure 32. **Competitive Radioligand Binding of ^{125}I-VN-TAT to HepG2 Cells.** The binding of 25 nM ^{125}I-VN-TAT (final) in the presence of increasing concentrations of cold VN-TAT at 4°C for 2 h. Each datapoint represents the mean ± SEM of triplicate determinations.

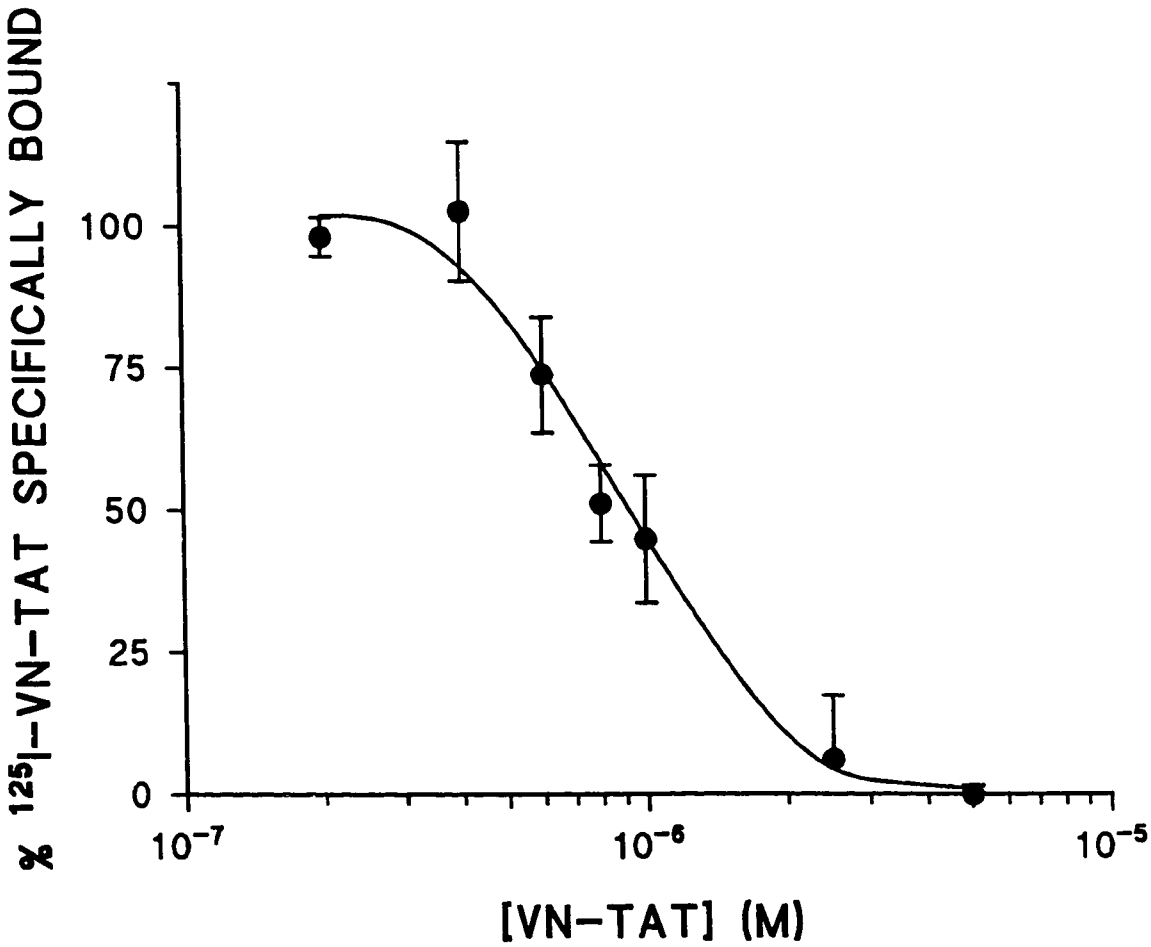
% 125I-VN-TAT SPECIFICALLY BOUND
100
75
50
25
0
10-7
10-6
10-5
[VN-TAT] (M)

Figure 33. **^{125}I-VN-TAT Binding to HepG2 Cells is Strongly Inhibited by VN-TAT or Heparin but not α_2M* or TAT. Panel A.** The inhibition of 10 nM ^{125}I-VN-TAT binding to HepG2 cells in the absence of inhibitors (NONE), 2.4 μM VN-TAT, 2.4 μM TAT, or 775 nM α_2M*. Each bar represents the mean ± SEM of triplicate determinations. **Panel B.** Inhibition of 10 nM ^{125}I-VN-TAT binding in the absence of competitors (NONE), 775 nM α_2M*, or 775 nM α_2M* with 500 units/ml heparin. Each bar is the mean ± SEM of triplicate determinations.

A

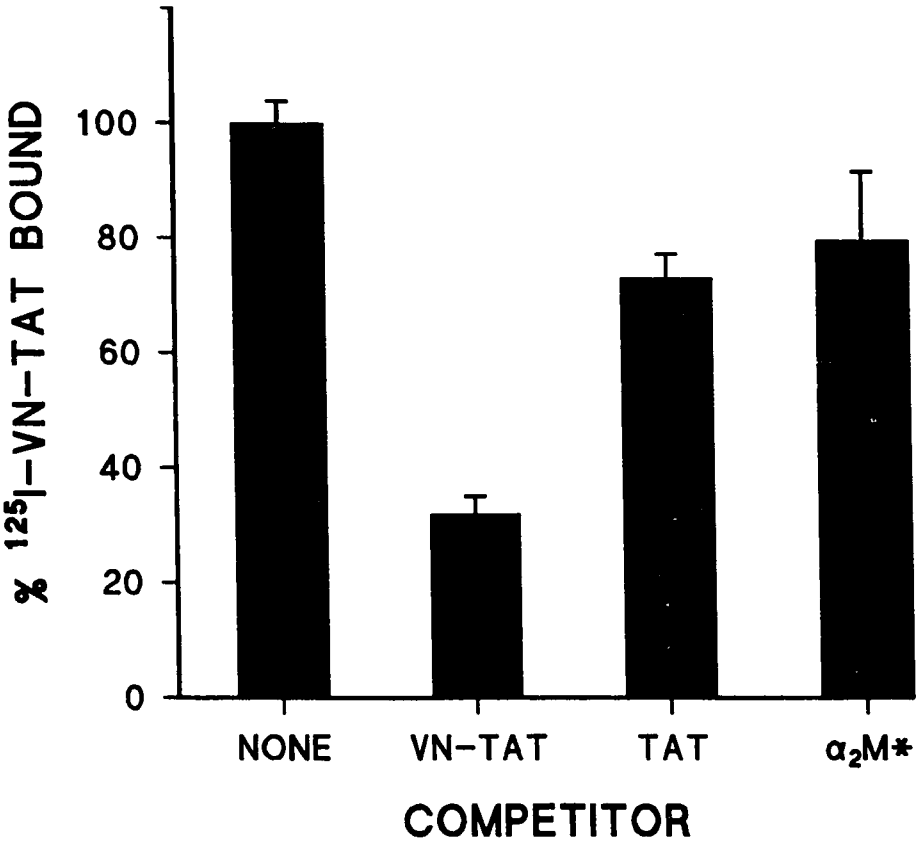
% 125I–VN–TAT BOUND
100
80
60
40
20
0
NONE
VN–TAT
TAT
α2M*
COMPETITOR

B

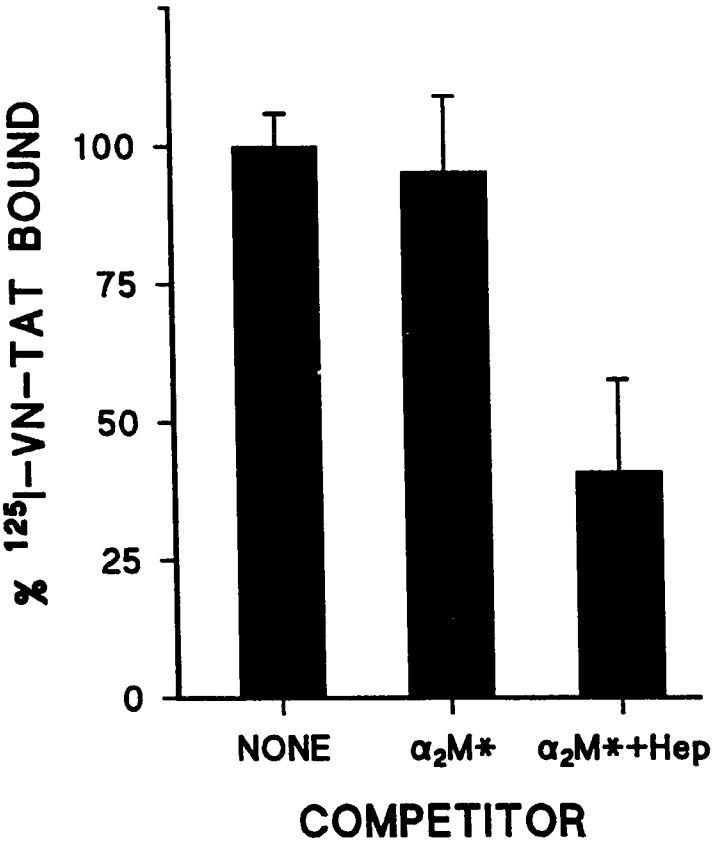
% 125I–VN–TAT BOUND
100
75
50
25
0
NONE
α2M*
α2M*+Hep
COMPETITOR

effectively competed with ^{125}I-VN-TAT binding, reducing its binding by 70%. However, TAT and α_2M* only modestly competed with VN-TAT binding, reducing its binding by only 25 and 20% respectively. This finding is similar to that found by de Boer *et al.* (1982) who reported that TAT only modestly competed with VN-TAT in binding to HUVECs. This indicates that the VN moiety in VN-TAT contains the residues involved in binding. Furthermore since vitronectin has been reported to mediate thrombin-PAI-1 complexes binding to HepG2 cells via LRP and gp330 (Steffanson *et al.*, 1996), the LRP ligand α_2M* was used in competition with ^{125}I-VN-TAT. Although the competing concentration of α_2M* was not as high as the other competing ligands the affinity of α_2M* is reportedly much higher (K_d~1-10nM) compared to that indicated from the present studies for VN-TAT. α_2M* was a poor inhibitor, an observation not unlike other reports that have found α_2M* unable to compete for binding to LRP with other known LRP ligands (Nykjaer *et al.*, 1992; Bu *et al.*, 1992).

Interestingly, the addition of heparin resulted in an ~60% reduction in VN-TAT binding compared to binding of ^{125}I-VN-TAT alone or even in the presence of α_2M* (Figure 33B). Moreover, comparable results were found with HTC cells such that a 165-fold molar excess of cold VN-TAT reduced 10 nM ^{125}I-VN-TAT binding by ~ 40% while competition with 775 nM α_2M* did not inhibit VN-TAT binding (see Figure 34). Competition with heparin alone or with α_2M* reduced the binding of VN-TAT by 40%. The effects of heparin on VN-TAT binding are discussed below.

Figure 34. **Inhibition of ^{125}I-VN-TAT Binding to HTC Cells by VN-TAT and Heparin but not by α_2M*.** The binding of 10 nM ^{125}I-VN-TAT to HTC cells was done in the absence of competitor (NONE) or in the presence of 165 μM VN-TAT (VN-TAT), 775 nM α_2M* (α_2M*), 775 nM α_2M* with 100 units/ml heparin (α_2M*+HEP), or with 100 units/ml heparin alone (HEPARIN). Each bar represents the mean ± SEM of triplicate determinations.

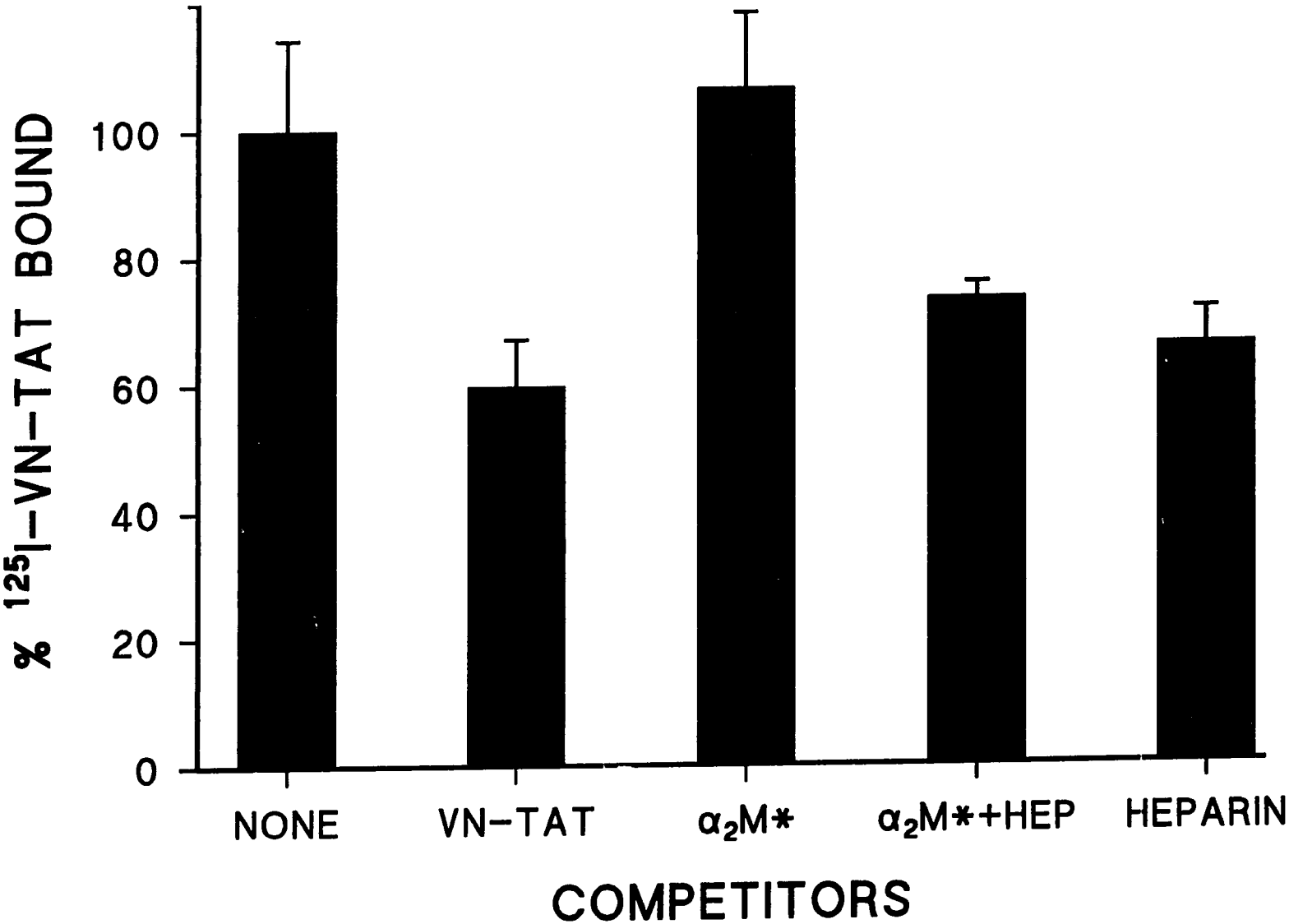
% 125I–VN–TAT BOUND
100
80
60
40
20
0
NONE
VN–TAT
α2M*
α2M*+HEP
HEPARIN
COMPETITORS

3.2.11 Heparin Competes For ^{125}I-VN-TAT Binding to Hepatoma Cells

Competitive radioligand binding experiments were conducted with HepG2 and HTC cells to further characterize the effects of heparin on the binding of 10 nM ^{125}I-VN-TAT binding to hepatic cells. Figure 35 shows a competitive radioligand binding experiment where the binding of 10 nM ^{125}I-VN-TAT to HepG2 cells was competed with increasing concentrations of heparin. An unusual inhibition curve was found with the binding of VN-TAT showing sensitivity to heparin at all concentrations of heparin used. At 1 U/ml (i.e. 1.2 μg of heparin in the reaction) there was a 72% decrease in VN-TAT binding to HepG2 cells, decreasing slightly less at higher heparin concentrations (up to 1000 U/ml). If this curve truly reflects the heparin-sensitivity of VN-TAT binding to cellular sites it could have interesting consequences on VN-TAT clearance in heparinized patients.

In other experiments the enzyme heparinase was used on HepG2 cells to see if this would reduce ^{125}I-VN-TAT binding. Heparinase is an enzyme that degrades heparin and heparan sulfate glycosaminoglycans (Ernst *et al.*, 1994). Heparinase treatment of HepG2 cells reduced ^{125}I-VN-TAT binding by 46% and is similar to the degree of inhibition observed by competition with a 30-fold molar excess of VN-TAT (Figure 36A). To further demonstrate that cell-synthesized proteoglycans are important for VN-TAT binding, HepG2 cells were treated with ß-D-xyloside, an inhibitor of glycosaminoglycan attachment to proteoglycans (Figure 36B). This treatment resulted in a 53% decrease in 50 nM ^{125}I-VN-TAT

Figure 35. **Competition of ^{125}I-VN-TAT Binding to HepG2 Cells in the Presence of Increasing Doses of Heparin.** The binding of 10 nM ^{125}I-VN-TAT was examined in the absence or presence or increasing concentrations of heparin. Each point represents the mean ± SEM of triplicate determinations.

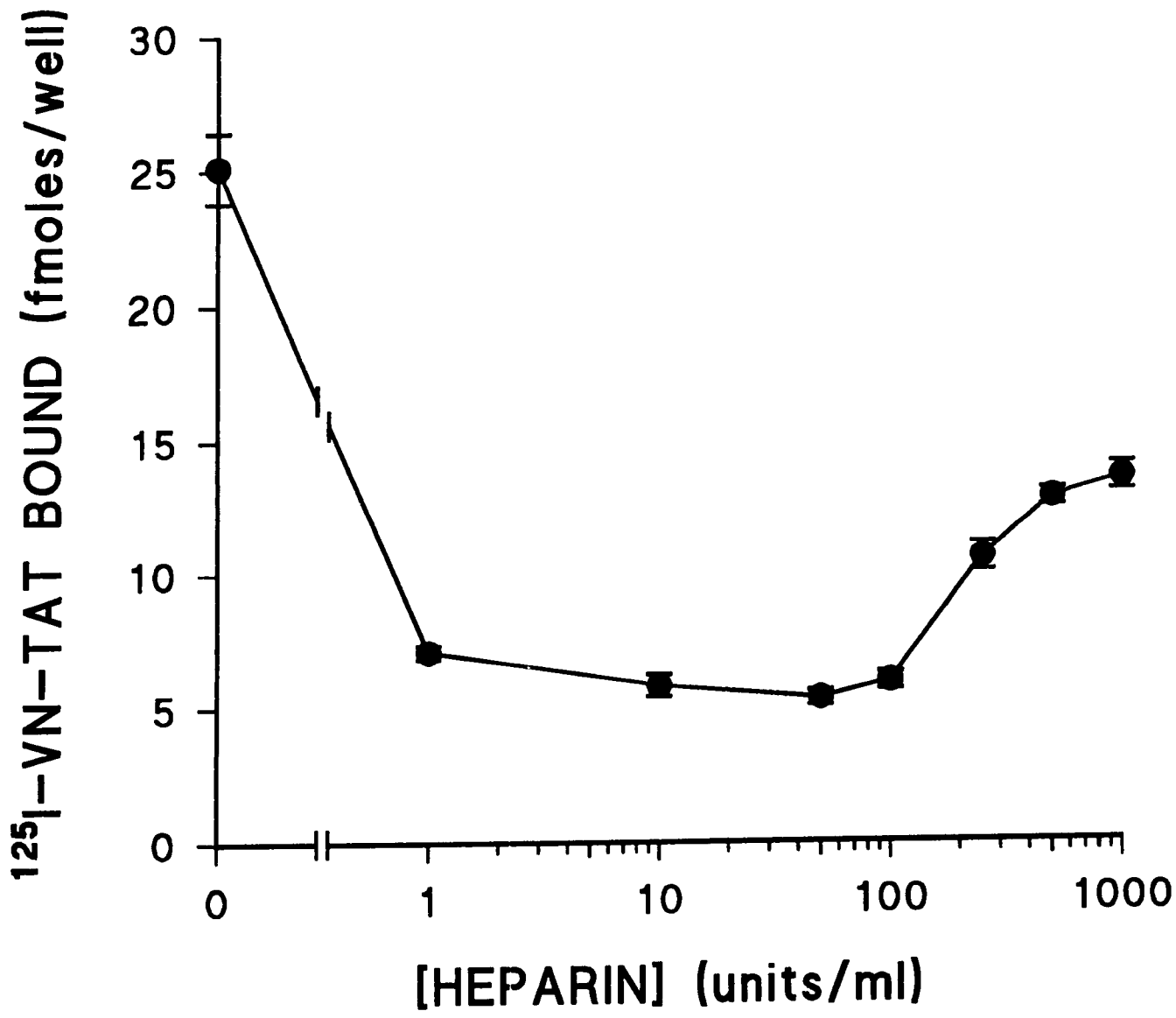
^{125}I–VN–TAT BOUND (fmoles/well)
30
25
20
15
10
5
0
0
1
10
100
1000
[HEPARIN] (units/ml)

Figure 36. **Proteoglycans Containing Heparan Sulphate Glycosaminoglycans are Important in VN-TAT Binding to HepG2 Cells. Panel A.** The binding of 50 nM ^{125}I-VN-TAT was performed with HepG2 cells in the absence of competitor (NONE), in the presence of 1.5 μM VN-TAT (VN-TAT), or to cells that had been pre-treated with 30 units/ml of heparinase (HEPARINASE) as described in the Materials and Methods section. Each bar represents the mean ± SEM of triplicate determinations. **Panel B.** HepG2 cells were treated with media containing DMSO (NONE) or with DMSO containing ß-D-Xyloside (ß-D-XYL; 2.5 mM final) for three days prior to the binding of 50 nM ^{125}I-VN-TAT. Each bar represents the mean ± SEM of six determinations.

A

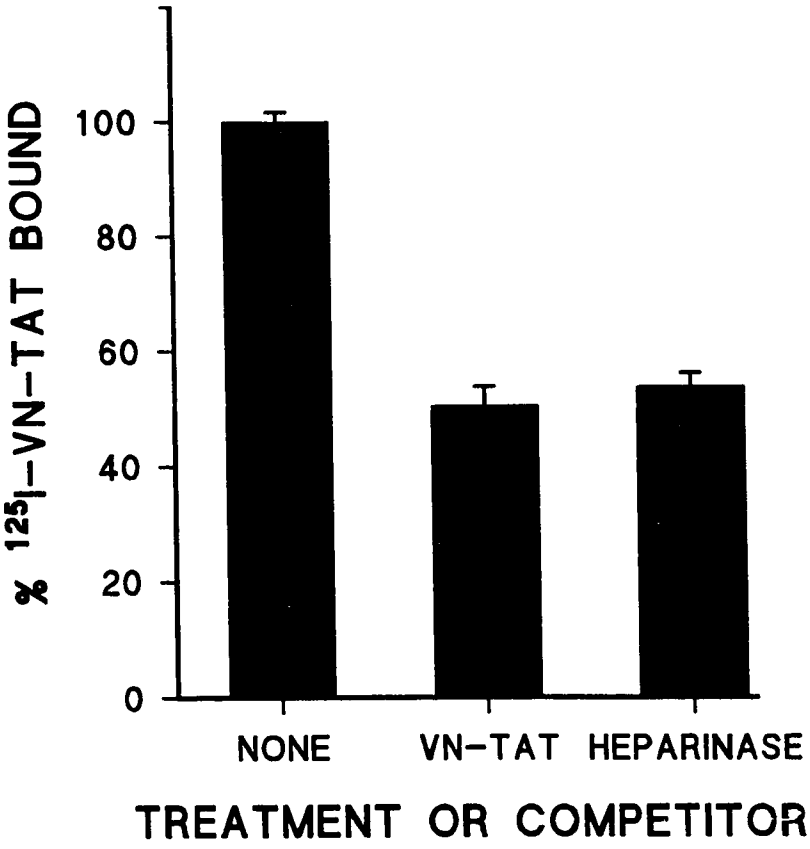
% 125I–VN–TAT BOUND
100
80
60
40
20
0
NONE
VN–TAT
HEPARINASE
TREATMENT OR COMPETITOR

B

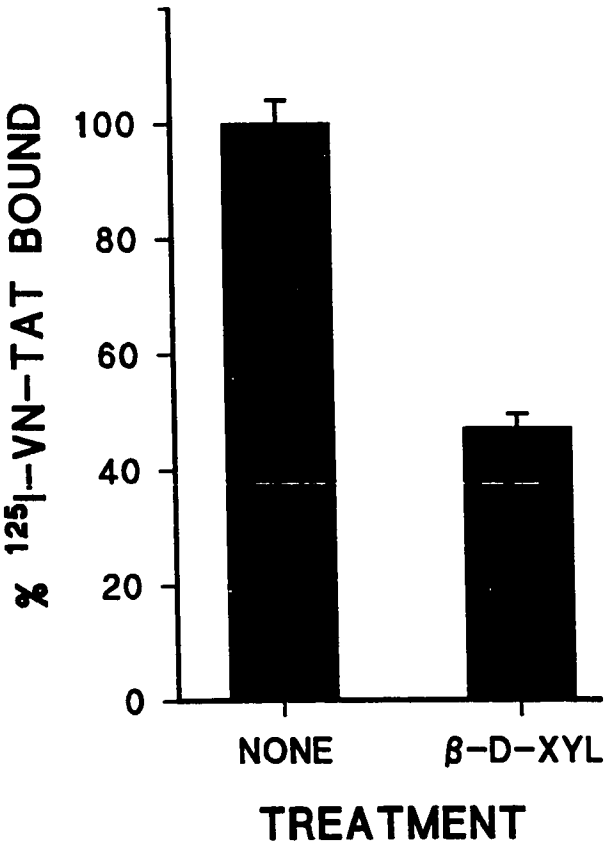
% 125I–VN–TAT BOUND
100
80
60
40
20
0
NONE
β–D–XYL
TREATMENT

binding. In all, the ability of competing heparin, heparinase, and the reduction of GAG containing proteoglycans to decrease VN-TAT binding support the hypothesis that HSPGs are important in VN-TAT binding to hepatic cells both *in vitro* and *in vivo*.

3.2.12 Heparin Inhibits the Degradation of VN-TAT by HepG2 cells

Different SEC have been found to be internalized and degraded after binding to receptors. To determine if VN-TAT could be internalized and degraded, and what effect heparin might have on this process, competitive internalization experiments of 10 nM ^{125}I-VN-TAT (final concentration) by HepG2 cells were performed. Fig 37A shows the amount of ^{125}I-VN-TAT degraded over time, determined from the TCA-soluble products, with maximal degradation products being 149 fmoles (~25 ng) at 17 h. This was reduced by heparin (100 U/ml, 558 μg/ml) which reduced the levels of degradation to only 33 fmoles (~ 5 ng) at 4 h and maintained this level even at 17 h. To show that the TCA-soluble counts were truly from receptor-mediated degradation, chloroquine, an inhibitor of lysosomal degradation was also used. In the presence of 200 μM chloroquine there were negligible amounts of TCA-soluble products such that the levels were very similar to those seen in control wells (autodegradation of VN-TAT seen in culture wells without cells). To determine whether other LRP ligands could affect this uptake excesses of α_2M* (77.5 ×; 775 nM final) and TRAP (200 ×; 2 μM final) were used. Neither of these competitors had any effect on VN-TAT internalization and degradation (data not shown). This might be due

Figure 37. **Internalization and Degradation of ^{125}I-VN-TAT by HepG2 Cells. Panel A.** The degradation of 10 nM ^{125}I-VN-TAT was measured in the absence of competitor (closed circles) or in the presence of 775 nM α_2M* (open squares), 2μM TRAP (open diamonds), 100 units/ml heparin (open circles), or 100 μM chloroquine (closed stars) as described in the Materials and Methods section. Each data point represents the mean of duplicate determinations. **Panel B.** The degradation of ^{125}I-α_2M* in the absence (close circles) or presence of 775 nM α_2M* (open circles) was determined from the TCA-soluble products as in Panel A. Each data point represents the mean of duplicate determinations.

A

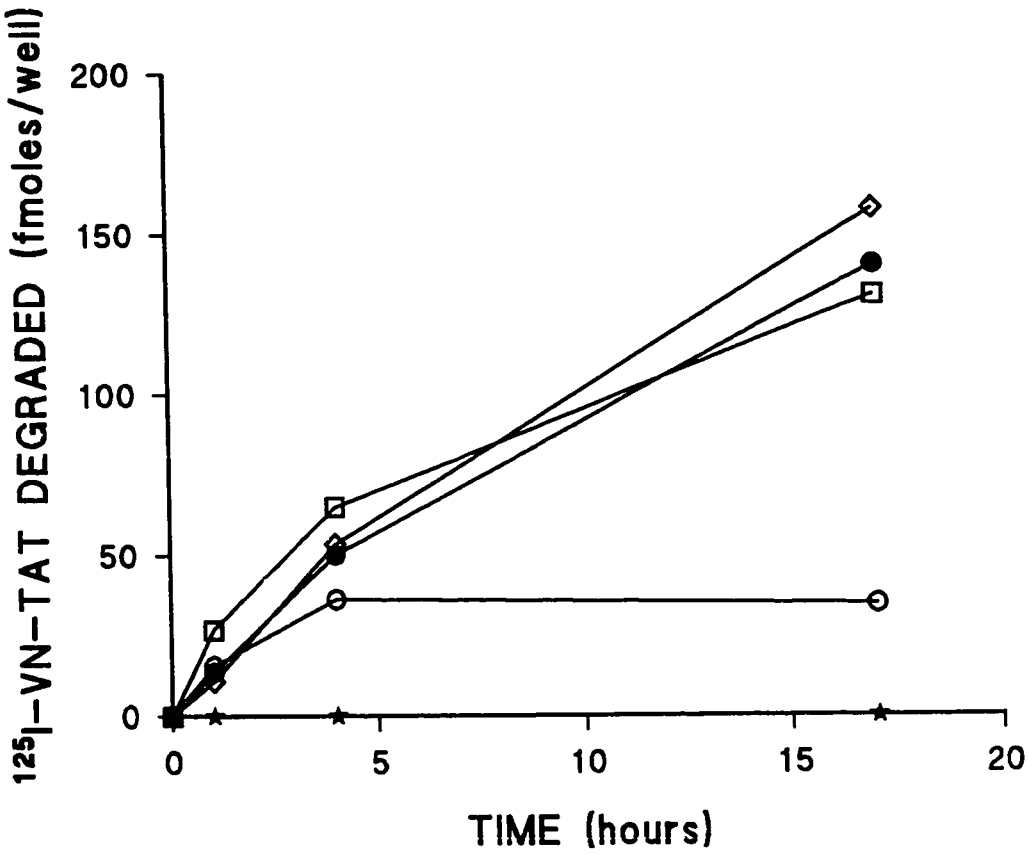
^{125}I–VN–TAT DEGRADED (fmoles/well)
200
150
100
50
0
0
5
10
15
20
TIME (hours)

B

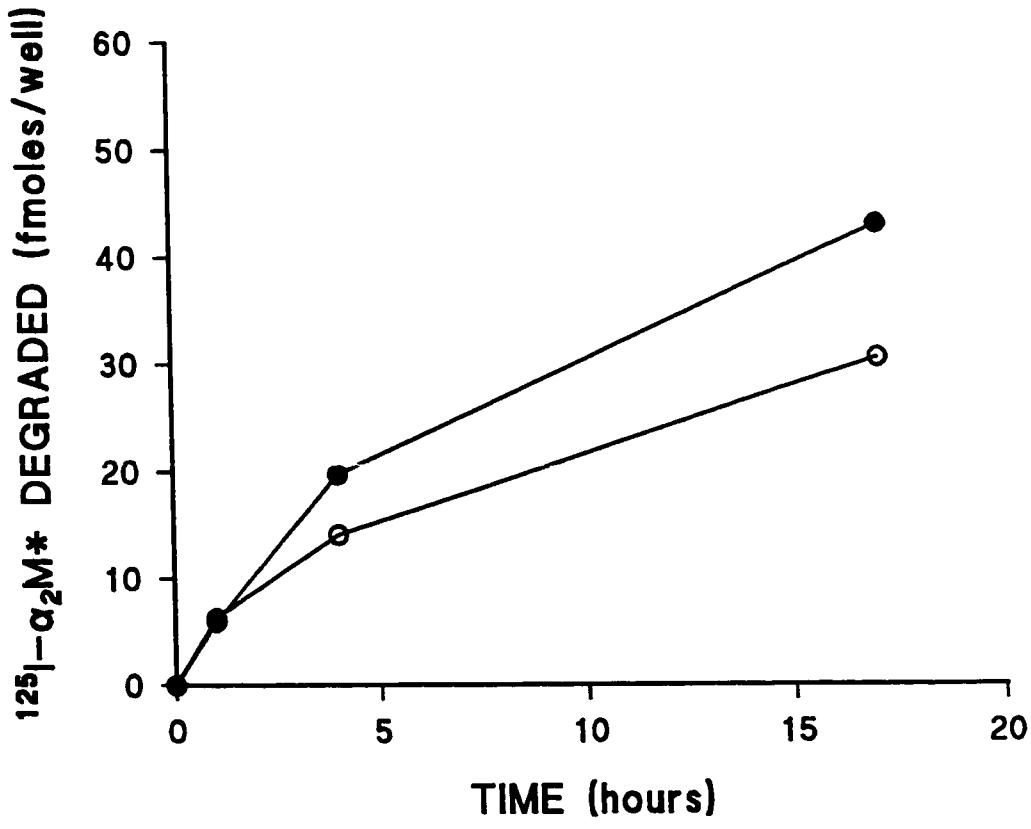
^{125}I–α_2M* DEGRADED (fmoles/well)
60
50
40
30
20
10
0
0
5
10
15
20
TIME (hours)

to not high enough amounts of competitor being present, or that they are internalized by a different protein, or that LRP can bind and internalize multiple ligands at once. As a positive control for internalization 10 nM ^{125}I-α_2M* was used and which is well known to be internalized through LRP. α_2M* was internalized to a much less degree with only 43 fmoles being degraded over 17 h (Figure 37B). This internalization appeared to be specific for α_2M* as the degradation of α_2M* was reduced to 22 fmoles in the presence of a 77-fold molar excess of cold α_2M*.

4. DISCUSSION

4.1 Identification of CK18 as a TAT-Binding Protein

The present studies were undertaken to identify the putative receptor(s) responsible for removal of TAT complexes from the circulation. During the course of these studies CK18 was identified as a TAT-binding protein associated with the plasma membranes of rabbit hepatocytes and cultured hepatoma cells. This conclusion was based on the following observations: (1) a TAT-binding protein from rabbit liver plasma membranes has high sequence homology to human CK18; (2) this TAT-binding protein has a similar electrophoretic mobility to CK18; (3) the insolubility of the TAT-binding protein in various detergents, a physical property of most IF proteins; and (4) there is increased specific binding of ^{125}I-TAT to fixed-permeabilized HTC cells. The potential physiological relevance of TAT interaction with CK18 is suggested by: (1) the inhibition of ^{125}I-TAT binding to cultured hepatoma cells by anti-CK18 antibodies; (2) the ability of anti-CK18 antibodies to inhibit ^{125}I-TAT internalization; (3) immunolocalization of CK18 on the surface of hepatoma cells in culture; and (4) the specific association, in perfusion experiments, of anti-CK18 antibodies with

rabbit livers.

Recently, the view that CKs, and other predominantly intracellular proteins, are confined solely to the cytosol has been challenged. Actin has been discovered on the external endothelial cell membrane surface (Moroianu *et al.*, 1990; Dudani and Ganz, 1993). CK8 has been detected on the cell membrane surface of MCF-7 breast carcinoma cells, primary hepatocytes, and HepG2 cells by immunofluorescence microscopy (Donald *et al.*, 1990; Hembrough *et al.*, 1995; Hembrough *et al.*, 1996a). Furthermore the cell surface expression of CK8 and CK18 was also supported by cell-surface radiodination of MCF-7 cells (Godfroid *et al.*, 1991). These results were however, later questioned (Riopel *et al.*, 1993). Additionally, CK1 also has been recently demonstrated to be present on the cell membrane surface of endothelial cells (Schmaier, 1997). Similarly, the present findings are difficult to reconcile with an exclusive intracellular localization of CK18.

Concurrent with these discoveries were the observations that a variety of intracellular proteins function as cell-surface receptors for plasma proteins (see Introduction 1.7.3; Table 3). Furthermore, intracellular proteins have also been found to be released into the media of cultured cells and to alter both protein and cell functions. For example proteolysed derivatives of CK18 and CK19 have been found to be released into the culture medium of MCF-7 cells (Chan *et al.*, 1986). Hembrough *et al.* (1996) found mainly intact CK8 in the culture medium of BT20 breast cancer cells which promoted the t-PA activation of plasminogen.

Moreover, calmodulin, found in the culture medium of HUVECs, binds to a specific-cell surface receptor on human monocytes (Houston *et al.*, 1997). Calmodulin binding to this receptor abrogated the ability of endotoxin to stimulate tumor necrosis factor release from the monocytes and resulted in the increased release of elastase.

4.1.1 Characterization of TAT-Binding to Hepatocytes

The interaction of serpin-enzyme complexes with four other cell surface membrane proteins has been reported previously. These include LRP; gp330; uPAR; and SECR. Of these, TAT has been reported to interact with LRP and SECR specifically (Perlmutter *et al.*, 1990; Joslin *et al.*, 1993; Kounnas *et al.*, 1996). In my study, TAT was found to bind specifically to a single set of sites on rabbit liver plasma membranes, believed to be CK18, as determined from the ligand-blotting experiments. Additionally, TAT bound to CK18 on rat HTC hepatoma cells and on HepG2 cells, as indicated by the anti-CK18 antibody inhibition experiments. The affinity of TAT for their CK18 hepatic binding sites appears to be low (with K_D's ranging from 100 to > 500 nM). However this is not dissimilar to the findings of other studies which predicted low affinity TAT binding to SECR (Perlmutter *et al.*, 1990; Joslin *et al.*, 1993), as well as purified LRP (Kounnas *et al.*, 1996). TAT bound to monocytoid cells specifically with a K_d~80nM (Takeya *et al.*, 1994), while TAT also bound to HepG2 cells with a K_d~247nM (Fair and Plow, 1986). Furthermore, the high proportion of non-specific binding of ^{125}I-TAT seen with the HTC cells, and to a lesser degree, with

the HepG2 cells, has also been reported for TAT binding to HepG2 cells (Joslin *et al.*, 1993), α-AC-cathepsin G binding to mouse spinal cord astrocytes (Chen *et al.*, 1993), and for PN-1-thrombin complex binding to fibroblasts (Knauer *et al.*, 1997).

To place TAT-binding to rabbit liver plasma membranes in the context of the reported TAT-SECR interaction, I used the SECR-binding pentapeptide in competition experiments. The use of a 20-fold molar excess of the pentapeptide did not inhibit ^{125}I-TAT binding to rabbit liver plasma membranes while a 20-fold molar excess of cold TAT inhibited binding by ~ 50%. Although these are not high levels of competition, other studies using similar molar excesses of cold TAT demonstrated a similar reduction in the binding of the SECR-binding pentapeptide, α_1-PI-elastase, and TAT to Hep-G2 cells (Perlmutter *et al.*, 1990; Joslin *et al.*, 1993). The inability of the pentapeptide to inhibit TAT and other SEC binding to cellular sites is not unique to the present studies. The SECR-pentapeptide also failed to inhibit the binding of TAT or α-AC-cathepsin G complexes to moncytoid cells and spinal cord astrocytes, respectively (Takeya *et al.*, 1994; Chen *et al.*, 1993). Indeed, alterations in the SECR-binding pentapeptide consensus sequence for HCII have been shown to have no effect on HCII-thrombin complex binding to HepG2 cells (Maekawa and Tollefsen, 1996).

4.1.2 Relationship Between CK18 and Other Putative SEC Receptors

As mentioned above, LRP and SECR have both been implicated in TAT-binding and clearance. How does CK18 fit into the picture of TAT clearance in

the context of these receptors? Controversy exists about whether SECR and LRP are the same protein and a comparison of these two receptors can be found in the Introduction (section 1.5.5).

Despite its low affinity for TAT, LRP has been shown to be the vehicle for TAT internalization into fibroblasts and in vivo in rats (Kounnas *et al.*, 1996). In addition to TAT having low apparent affinity for LRP, its binding to purified LRP appears very slow (an 18-hour incubation was used in binding experiments) (Kounnas *et al.*, 1996). This slow binding is not in keeping with the known very rapid removal rate for TAT observed in vivo. Moreover, some investigators have found no evidence for TAT binding to purified LRP (Takeya *et al.*, 1994).

However, although LRP has been shown to be involved in the internalization of TAT and other SEC, data exist which suggest that other proteins may likely be the initial binding sites for such complexes. Thus, recently a PN-1 peptide was found to be a potent inhibitor of PN-1-thrombin internalization by LRP, but this peptide was found not to inhibit PN-1-thrombin binding to the cell surface; thus supporting the hypothesis that TAT could bind first to a receptor protein before interacting with LRP (Knauer *et al.*, 1997). This scenario is not unprecedented as uPA-PAI and PN-1-uPA complexes have been shown to bind to uPAR before being internalized through interaction with LRP (Conese *et al.*, 1994; Conese *et al.*, 1995). Indeed, heparan sulfate proteoglycans have been found to bind thrombospondins 1 and 2 to mediate their internalization through LRP (Mikhailenko *et al.*, 1995; Godyna *et al.*, 1995; Chen *et al.*, 1996).

Further support for this hypothesis comes from the examination of the LRP expression in vivo and comparing it to the removal sites from SEC plasma clearance. Plasma clearance studies of different SEC (reviewed in section 1.5.1) reveal that the liver is the major removal site of such complexes but that LRP is expressed in a wide variety of tissues, including endothelial cells (Simon *et al.*, 1995; Warshawsky and Schwartz, 1996) monocytes, and neutrophils (Jardi *et al.*, 1996; Li *et al.*, 1997). If LRP alone was responsible for the binding of different SEC then high amounts of SEC would be expected to be found in the lungs, where the large majority of endothelial cell surface is found, and to monocytes in the blood. For example, if LRP and SECR are indeed the same protein then based on the findings of Joslin *et al.*(1992) of $\sim 4.5 \times 10^5$ sites/monocyte then, assuming 5×10^5 monocytes/ml, there would be $\sim 2 \times 10^{11}$ TAT binding sites/ml human blood. Thus if LRP by itself is a TAT-binding protein then the clearance of ^{125}I-TAT would be expected to be much slower since TAT would remain bound to monocytes and neutrophils in the circulation. The fact that complexes are cleared rapidly and mainly by the liver supports the hypothesis that other liver-specific proteins likely are involved in initial SEC binding or that liver-LRP may be found in a multi-protein association or complex.

Is there evidence to link CK18 to LRP? An unidentified plasma membrane glycoprotein of 85 kDa was co-immunoprecipitated with CK18 from a variety of epithelial cell lines (Chou *et al.*, 1994). This unidentified protein could represent the ß subunit of LRP, as it had a similar molecular mass and glycosylation profile.

As mentioned above, uPAR appears to facilitate the LRP mediated clearance of uPA-PAI-1 and PN-1 complexes. Coincidentally, CK8 and CK18 have been reported to be found in a complex with uPAR and protein kinase C in the plasma membranes of WISH cells (Busso *et al.*, 1994). Since uPAR is a GPI-linked protein, then either another transmembrane protein would have to be involved in mediating the interaction with CK8 and CK18 or the CKs would have to penetrate the cell membrane to interact directly with uPAR. The latter hypothesis cannot be ruled out since no intermediary membrane protein was found (Busso *et al.*, 1994).

VN appears to play an important role in TAT catabolism since TAT is found mainly in the form of a ternary complex with VN in plasma (see Introduction, section 1.5.6). VN also has been found to have strong links to uPAR, LRP, and CKs. For example, VN appears to play a role in mediating the binding and internalization of PAI-1-thrombin complexes to LRP and gp330 (Stefansson *et al.*, 1996). Furthermore, VN has been demonstrated to bind to cytokeratins (Hintner *et al.*, 1989) and mVN to bind to uPAR (Kanse *et al.*, 1996). This is particularly interesting since mVN is in a conformation very similar to VN in ternary complex with TAT (Stockmann *et al.*, 1993). Taken together, these reports support the hypothesis of a complex association occurs between LRP, uPAR, CK18, VN, and TAT. Although the histochemical experiments that I have done do not provide direct evidence of CK18 expressed on the cell surface in vivo, they provide an intriguing coincidental pattern of expression with that seen for

LRP, in that LRP is also preferentially expressed in hepatocytes proximal to the portal triads (Bu *et al.*, 1994; Voorschuur *et al.*, 1994). Finally, much of the characterization of LRP-ligand interactions, including the binding of TAT, has been done using fibroblast cell lines (Knauer *et al.*, 1997; Kounnas *et al.*, 1996; Poller *et al.*, 1995; Willnow *et al.*, 1992). It is interesting therefore that substantial amounts of CK18 were found to be expressed in LTK- fibroblasts in the present studies. This finding is not unusual as other fibroblast cell lines have been reported to express CKs 8 and 18 spontaneously (Knapp *et al.*, 1989), even though the CK expressing cells were present in low frequency. Although this data does not directly support the possibility of an interaction between CK18 and LRP, it once again illustrates interesting coincidences concerning the two proteins. In this regard, it would be interesting to see whether CK18 is expressed in the same fibroblast cell lines which express LRP, and, if so, whether the two proteins co-localize. Taken together, these observations provide compelling evidence which support the hypothesis that CK18 may be the initial TAT-binding protein on hepatocytes, leading to subsequent interaction with LRP.

Where does SECR fit into the present study? As mentioned earlier there is controversy as to whether SECR and LRP represent the same protein. Unfortunately there are no published reports on the primary sequence of the SECR protein, its cDNA, or its gene. Furthermore, it is unfortunate that neither group of investigators (ie the SECR group and/or the LRP group) has used available biochemical tools to try to deal with this issue. For example, why have

they not determined whether RAP affects pentapeptide binding to HepG2 cells? Nevertheless, the SECR binding pentapeptide has been shown to not compete for the binding of TAT or other SECs to plasma membranes of hepatic cells, monocytoid cells, and astrocytes. In this context, Perlmutter and associates demonstrated cross-competition between α-PI-enzyme complexes and the pentapeptide and also that different SECs competed for the binding of the pentapeptide to HepG2 cells. They also demonstrated cross competition between α-AT-elastase complexes and TAT for binding to HepG2 cells. Interestingly, AT and α-AC C-terminal peptides, containing the homologous pentapeptide sequence, were found to inhibit α-PI pentapeptide binding to HepG2 cells; implying that the same sequences in both AT and α-AC could be involved in binding of SEC containing them. So why does the pentapeptide not compete for SEC binding in this and other studies? A plausible explanation for the lack of inhibition by the pentapeptide in this present study might be the following: 1) that different SEC contain different sequences for binding to the SECR; 2) the native SEC after binding might alter the conformation of the receptor through a different portion of the complex; and 3) since the pentapeptide is small it can still bind to the SECR but might not be able induce a conformational change in the SECR that would result in the inhibition of further binding of other SECs. This hypothesis is supported by a number of facts including the observation that α_2-macroglobulin-methylamine was found to bind to a different area of LRP compared to t-PA-PAI complexes (Willnow *et al.*,1992). This is further supported by the work of Takeya

et al. (1994) who found that although both the pentapeptide and TAT bound specifically and saturably to monocytic U937 cells, the pentapeptide did not inhibit TAT binding (Takeya *et al.*, 1994). Furthermore Savion *et al.* (1990) found that TAT could bind to, and be endocytosed by, bovine corneal endothelial cells. These investigators determined that the binding domain of AT was between residues 253-314, a region of AT not containing the SECR-binding pentapeptide. Although Perlmutter *et al.* (1990) showed inhibition of pentapeptide binding using C-terminal peptides from different serpins it should be noted that the AT peptide did not inhibit nearly as well as the other peptides and that an α_1-PI C-terminal peptide *not* containing the pentapeptide inhibited the binding of the pentapeptide to a significant degree. Finally, although no SEC crystal structures have been reported to date, the surface expression of the pentapeptide on SEC has been questioned based on the known crystal structures of intact and cleaved serpins (Schulze *et al.*, 1994). It appears that the pentapeptide sequence may not be readily accessible from structural modelling of SEC (Whisstock *et al.*, 1996).

4.1.3 Mechanism of CK18 Release From Cultured Cells

At this point in time there are no definitive answers as to how CKs are externalized. CKs lack a signal peptide typical for secreted proteins and, based on this, constitutive secretion of CKs is unlikely. As mentioned above, soluble CKs have been found in the culture medium of a variety of mammary carcinoma cells and also from normal mammary cells (Chan *et al.*, (1986); Hembrough *et al.*, 1996b). Chan *et al.* (1986) found that CK18 present in the culture medium of

MCF-7 cells was proteolytically degraded as determined by SDS-PAGE and sedimentation analysis. This degradation was inhibited by the addition of EDTA. Furthermore, azide poisoning experiments resulted in increased amounts of the proteolyzed CK18 being released into the medium. However, gel-exclusion chromatography showed that the CKs were in complexes > 100 kDa. Additionally, Hembrough *et al.* (1996b) found that CKs found in the culture medium of breast carcinoma cells were intact and were present in complexes ranging in size from > 150 kDa to ~1000 kDa. These complexes are most likely identical, or similar to, tissue polypeptide antigen (TPA) seen in the blood in vivo (see below). Interestingly, when the kinetics of CK release was followed, the highest rate of CK release was found to be during the first few h after the fresh culture medium was added to cells and which diminished over time (Chan *et al.*, 1986). This pattern of release did not correspond to that of steady-state release and the release pattern observed was ascribed to cell damage due to changing the culture medium or by being induced from factors present in fresh medium. However, the authors concluded that the amount of CK found in the medium was greater than could be attributed from the complete lysis of the number of dead cells seen by trypan blue staining. Cell blebbing is another possible mechanism for CK release. This process, also known as zeiosis, is the transient spherical outpouching of cell membrane from cells spreading on a substrate or on the leading edges of moving cells (Dainiak, 1991). Interestingly, membrane blebbing has been found to be increased by the addition of serum or α_2M to cultured cells

(Dixon *et al.*, 1987). This could represent a mechanism for the increased release of CKs from cell cultures when fresh medium is added, as reported by Chan *et al.* (1986). Furthermore, actin was found within these blebs demonstrating a mechanism by which other cytoskeletal proteins can be moved out of viable cells. However, once out of the cells the mechanism by which actin or other cytoskeletal proteins could be released from such bleb vesicles is unknown.

4.1.4 Physical Form of CKs on the Surface of Cultured Cells

As little is known about how CKs are released into cell culture medium there is only slightly more known about the form of CKs associated with the surface of cultured cells. The actual form of CKs on the cell surface is unknown since the epitopes recognized by commercial antibodies are unknown. Hembrough *et al.* (1996a) showed that at least the C-terminal portion of CK8 was expressed on the surface, using a monoclonal antibody raised against a C-terminal CK8 peptide. These authors reported preliminary data that suggested that cell surface CK8 was integrally associated with the lipid bilayer. This possibility is not without precedence as CKs, as well as other IFs, have been shown to associate with lipids both non-covalently and covalently (Asch *et al.*, 1993; Brunkener and Georgatos, 1992; Perides *et al.*, 1987).

How might CKs interact with lipids? Oullet *et al.* (1988) predicted that the CK8 head domain sequence was amphiphilic, similar to that of mitochondrial signal peptides, which could associate and form α-helices in lipid membranes. Interestingly, CK18 contains a glycine-rich domain in the head domain which

might participate in lipid interactions. For example, the glycine-rich domain of *Staphylococcus aureus* α-toxin is inserted into cell membranes and forms a pore in conjunction with six other α-toxin molecules (Lala and Raja, 1995). Interestingly, nucleolin, another cytoplasmic protein recently found to be expressed on the surface of HepG2 cells, also contains a glycine-rich domain (Leube *et al.*, 1986). As mentioned above CK18 has been found in a complex with uPAR and possibly LRP. In the present studies, trypsinization of HepG2 cells exposed more CK18 epitopes with a concomitant increase in TAT-binding. This seems to suggest that CK18 is found on the surface of hepatoma cells in complex with other proteins. These other proteins might even act as CK-binding proteins, a situation similar to that found for calmodulin (Houston *et al.*, 1997).

4.1.5 Biological Relevance of Surface-Expressed CKs

Although there is ample evidence that CKs are released into the culture medium and found on the surface of various cultured cells are these findings biologically relevant, i.e. is CK found extracellulary in vivo? As previously indicated, CK8 expressed on the surface of breast carcinoma cells, binds plasminogen and augments the tissue-plasminogen activator activation of plasminogen both on the cell surface and in the media of cultured breast carcinoma cells (Hembrough *et al.*, 1995; Hembrough *et al.*, 1996a; Hembrough *et al.*, 1996b). In addition, the transfection of mouse L fibroblasts with CK8 and CK18 resulted in their increased migration and invasion of matrigel (Chu *et al.*, 1993). This novel functional role for CKs is probably mediated by their acting as

cell surface receptors. CKs are known to be to be found in the sera of patients with carcinomas and are cell surface associated in vivo with carcinoma cells. This fact has lead to the use of anti-CK antibodies for immunoscintographic detection of carcinomas and for therapeutic use in radioimmunotherapy trials (De Jager *et al.*, 1993; LeTocha *et al.*, 1993; Taddei-Peters *et al.*, 1992; Riklund *et al.*, 1991). In sera, CKs are a major component of TPA, an in vivo marker of epithelial derived tumour cells (Sundstrom *et al.*, 1994). TPA has been demonstrated to be composed of CKs 8, 18, and 19 (Weber *et al.*, 1984). Interestingly, although TPA levels are high in patients with carcinomas, there is evidence that TPA and CKs are also expressed in normal humans and rats, providing an indication that CKs might be released from cells in non-pathological states (Mellerick *et al.*, 1990; Chan *et al.*, 1986). Furthermore, it has also been reported that a low level of anti-CK antibodies might exist in all individuals (Hintner *et al.*, 1983). This fact further supports the premise that CKs may be released in non-pathological situations in vivo. Experiments were done comparing the clearance and association of anti-CK18 antibodies and an equivalent preimmune IgG in a liver perfusion experiment to determine whether CK18 is expressed on the surface of hepatocytes in intact livers. These experiments showed a preferential clearance and association of the anti-CK18 IgG to the livers than that seen with preimmune IgG. This increased binding likely represents specific binding to CK18 as the anti-CK18 antibody was demonstrated to have high specificity for CK18 in Western blot analyses of RLPM, total rabbit liver homogenate, and also in solid-phase binding

assays to purified CK18. However, these data must be viewed with caution as it is likely that hepatocytes might have been dying over the period of perfusion with the resultant release or exposure of CK18 filaments. However, the livers appeared to be viable over the whole experimental time period as evident by the fact that the livers were still releasing glucose and protons.

At this time, the true role for CK18 in TAT removal from the circulation is unclear. However in this present study evidence is provided for the biochemical interaction between TAT and CK18 as well as the presence of CK18 on the surface of cultured hepatic cells and hepatocytes in liver perfusion experiments. These data thus support the hypothesis that CKs could represent cellular receptors, or receptor co-factors, at the hepatocyte cell surface. CK18 may thus be involved in the interaction of TAT, as well as other SEC, with hepatocytes. High sequence homology in the rod-domains of intermediate filaments indicate the necessity of these regions for the formation of filaments, yet the high sequence divergence of the head and tail regions suggests the possibility of functional differences between the different CKs unrelated to their cytoskeletal role. Such functions for IFs have only recently begun to be elucidated as demonstrated by CK8 binding with plasminogen and CK1 binding high molecular weight kininogen. Along with the growing body of evidence for surface expression of intracellular proteins, these data indicate potentially new and physiologically relevant roles for CKs as putative cellular receptors, and/or as co-factors of such cellular receptors.

4.2 Metabolism of VN-TAT

4.2.1 Characterization of VN-TAT

The impetus for these experiments was the finding that TAT was found as ternary complex with VN in human serum and later in plasma (Ill and Ruoslahti, 1985; de Boer *et al.*, 1993). Since the metabolism of the binary TAT complex had been well studied, I became interested in determining whether the addition of VN to TAT, to form a ternary complex, had any effect on TAT metabolism. Initially, the preparation of VN-TAT I hoped to use in experiments would be made simply by adding TAT to rabbit plasma. Unfortunately, I was unable to form VN-TAT in rabbit plasma using all combinations of ^{125}I-TAT formed with human thrombin, human AT, bovine thrombin or rabbit AT. Further experiments adding bovine or human ^{125}I-α-thrombin to defibrinogenated plasmas verified the experiments adding different combinations of TAT to plasma. Interestingly, VN-TAT formed rapidly in human plasma with TAT containing human thrombin and to a much smaller degree TAT containing bovine thrombin. These results suggest that some intrinsic property for the different species thrombin or vitronectin, or both, is necessary in forming VN-TAT. Moreover, although VN-TAT did not form in rabbit plasma with bovine or human thrombin, the fact that rabbit serum readily forms VN-TAT supports the premise of species-specificity playing a role in VN-TAT formation. Interestingly, de Boer *et al* (1995) reported that human TAT did not bind to purified mouse VN, that it bound to human VN with intermediate

affinity, but that it bound with high affinity to rat VN. In all, these data suggest the thrombin of some species and/or VN specificity affects VN-TAT formation. Alternatively other unknown factors may contribute to its formation in rabbit and mouse plasma.

To avoid these problems I purified human VN-TAT as described by de Boer *et al.* (1992). The purified VN-TAT possessed identical characteristics to that reported by de Boer *et al.* (1992), such as molecular mass and sensitivity to reducing agents. However, Western blot analysis revealed that HCII-thrombin-VN complexes were present in the preparation. This is not surprising since HCII was shown to form ternary complexes with thrombin and VN in vitro (Priessner and Sie, 1988) and that these ternary complexes have been found in human plasma along with VN-TAT (Liu *et al.*, 1995). Although I did not quantify the relative amounts of the two different ternary complexes in the purified VN-TAT, it has been reported that the content of HCII-thrombin-VN complexes in plasma are about 20% that of VN-TAT complexes (Liu *et al.*, 1995). The poor reactivity of anti-AT, anti-HCII, and especially anti-thrombin antibodies, indicate that in the ternary complexes there may be some conformational change of these moieties which could mask or alter epitope recognition. For example, based on the position of thrombin, in the modelled tertiary structure of TAT (Whisstock *et al.*, 1996; Introduction Figure 2.), thrombin is most likely sandwiched between VN and AT and thus some epitopes very well may be less accessible to some antibodies. Interestingly, thrombin-PN-1 complexes have also been found to form

multimeric complexes with thrombospondin from platelets (Detwiler *et al.*, 1992). Since thrombospondin would be released from platelets during the formation of serum from whole blood, it is possible that small amounts of thrombospondin-thrombin-PN-1 complexes could also be present in the purified VN-TAT mixture. Furthermore other SECs, containing thrombin or factor Xa, have been found to form ternary complexes with VN (see Introduction section 1.5.6). Based on such data it will be interesting to see whether other ternary VN complexes, if any, form with other SEC.

4.2.2 Plasma Clearance of VN-TAT is By Liver Receptors

These observations suggest that VN must play an important physiological role in the metabolism of various SEC and support the need to investigate the metabolism of these various VN-SEC complexes. de Boer *et al.* (1992) examined the binding of VN-TAT to endothelial cells on the basis that this interaction would be the first event of clearance. However, no clearance studies had been performed to support this premise. From the experiments performed in this present study, VN-TAT was found to be removed rapidly and degraded by a liver-specific mechanism(s). Similar observations were reported by de Boer *et al.* (1995b) showing that human VN-TAT is rapidly cleared in rats in a liver-specific fashion (de Boer *et al.*, 1995b). The VN-TAT results are similar to that observed during the clearance of binary serpin-enzyme complexes (i.e. TAT) in that VN-TAT clearance is best described by a two-compartment model and its removal is liver-specific. Furthermore, the clearance parameters for the α-phase of TAT and

VN-TAT clearance are very similar and suggest that both protein complexes are likely binding to the same initial hepatic binding sites. In comparison AT clearance was much slower with 75% of initially injected ^{125}I-AT remaining even at 60 min. Interestingly, the $t_{½\beta}$ for VN-TAT (85.35 ± 4.3 min) is significantly larger than that for TAT (42.78 ± 3.68 min). Since this slow phase of clearance most likely represents movement of VN-TAT out of the intravascular space into the subendothelium, it is possible that the reduced ß-phase clearance of VN-TAT could be due to its multimeric, and hence larger, size compared to TAT.

VN-TAT removal was shown to be liver-specific with 80% of ^{125}I-VN-TAT being found there after 60 min. The kidneys contained the next highest amount of radioactivity (~ 10%). The latter is most likely due to accumulation of degradation products coinciding with increased TCA-soluble radioactivity in the plasma. However, it could also be due to presence of specific receptors such as LRP or gp330. Finally, in other experiments, the total liver uptake was ~66% of the injected VN-TAT dose that had cleared from the circulation. Taken together, these data indicate that the rapid clearance of VN-TAT is mediated by liver-specific receptors.

4.2.3 Influence of Heparan Sulfate Proteoglycans on ^{125}I-VN-TAT Clearance

de Boer *et al.* (1992) found that VN-TAT bound to a heparinoid proteoglycan, most likely heparan sulfate, on the surface of HUVECs. In the present studies the coinjection of high doses of heparin or protamine sulfate completely reduced the initial rapid clearance of VN-TAT, such that VN-TAT

clearance in these experiments was best described by a single-compartment model. This suggests that the initial rapid phase of of VN-TAT removal from the circulation is by binding to heparan sulfate proteoglycans (HSPG). Competition experiments with heparin or a peptide, corresponding to the VN heparin-binding domain, were also reported to have similar effects on VN-TAT removal in rats (de Boer *et al.*, 1995b).

Furthermore, in the present studies heparin coinjection reduced liver specific uptake by 41% supporting the hypothesis that VN-TAT uptake in vivo, at least in part, is by liver-specific proteoglycans, most likely heparan sulfate proteoglycans. Narita *et al.* (1995) showed that ^{125}I-TFPI clearance in mice was inhibited by preinjection of the mice with protamine sulfate. This competition reduced the α clearance from < 1 minute to 1-2 min. Moreover, pre-injection of the LRP-antagonist, RAP, did not affect the α clearance but almost doubled the ß phase of clearance. These data suggest, that at least for TFPI, initial binding is to proteoglycans and that a secondary interaction with LRP occurs.

Heparin and protamine competition also reduced the degradation of VN-TAT by >50%, compared to animals which did not receive any competitors, indicating that HSPGs might be responsible directly for the internalization of VN-TAT in vivo. These data also suggest that the initial α-phase of clearance represents binding to cellular receptors versus that of the slower ß-phase. This conclusion is based on the fact that inhibition of the α-phase, by heparin or protamine, coincided with a reduction in VN-TAT degradation, as evident by a

reduction in TCA-soluble counts (Results section 3.2.9). Although decreased, some VN-TAT degradation still occurred during the ß-phase suggesting that some receptor-mediated degradation could have been occurring during this phase.

When I coinjected a large molar excess of TRAP with ^{125}I-VN-TAT, the clearance rate of ^{125}I-VN-TAT was not altered but its liver-specific uptake was reduced by 50%. However, this experiment was done with only one rabbit. If this experiment represents the true clearance of VN-TAT and TRAP then it suggests that LRP is also involved directly in VN-TAT clearance, since LRP has been shown to bind and internalize TRAP directly (Kounnas *et al.*, 1995). Furthermore this data also indicates that sites in other organs can also participate in VN-TAT catabolism. Another possibility is that TRAP complexes could associate with VN in vivo and bind to the same sites although there is no reported evidence to support the interaction between serpin-trypsin complexes with VN.

How does the present ^{125}I-VN-TAT clearance data fit into the context of VN-TAT binding to endothelial cells, as described by de Boer *et al.* (1992)? If endothelial cell HSPGs were important in VN-TAT binding then the organ profile of removal would be expected to be different from that seen in the present experiments, such that the lungs, with its large endothelial cell surface, would be a major site of removal. In the present studies this wasn't the case with the bulk of VN-TAT being liver-associated. In vivo, HSPGs are found on the luminal surface of endothelium but the amounts are relatively small compared to that found extravascularly. In this regard the liver is unique in that liver sinusoidal

endothelial cells lack a distinct basement membrane and contain large pores (De Leeuw *et al.*, 1990). Thus the plasma freely bathes the subendothelium in the liver. Therefore, the fact that VN-TAT would accumulate in the liver is not suprising since HSPGs are found abundantly in the space of Disse in the liver (the space between sinusoidal endothelial cells and the apical hepatocyte surface) (Geerts *et al.*, 1986).

In the liver there are two forms of HSPG: (1) Hepatocyte plasma membrane bound HSPG which is detergent-soluble; and (2) heparin-releasable HSPG which associates with the plasma membrane by its GAG side chains (Soroka and Farqhuar, 1991). Which of these HSPG forms are important in binding VN-TAT is unknown. Although membrane-bound HSPGs might seem like better candidates, since VN-TAT is internalized and degraded, the possibility of the releasable HSPGs binding VN-TAT and then transferring it to endocytic receptors is possible. Moreover, if the TRAP competition experiment is a true physiological effect then it would seem that HSPGs and LRP are both directly involved in VN-TAT clearance.

4.2.4 VN-TAT Binding to Hepatoma Cells

From competitive radioligand binding experiments, the affinity of VN-TAT for hepatoma cells was found to be low ($K_d \approx 1\mu M$). This is substantially lower than that found for binding to HUVECs by de Boer *et al.* (1992) (K_d= 16nM). This low affinity could be due to the fact that the ligand was a mixture of VN-SECs (VN-thrombin-HCII for example) and that the various forms of the different

VN-SECs had different affinities (ie monomeric versus dimeric versus trimeric etc.). A more likely explanation of the low apparent K_d is that the molecular mass of VN-TAT used in calculations was an underestimate. Due to the multimeric nature of VN-TAT I chose to use the molecular mass of monomeric VN-TAT (160 kDa). de Boer *et al.* (1992) also chose this value in their determinations. However, since multimeric VN-TAT makes up the bulk of the preparations, 160 kDa is most likely and underestimate. Indeed, VN has been shown to self-associate into multimers containing from 3 to 16 monomers (Stockmann *et al.*, 1993). Thus if the molecular mass of VN-TAT was only two to four-fold higher then the K_d could be at least a two to four fold overestimate which could place the K_d at ~250 nM. Relevantly, the K_d for thrombospondin 1, putatively interacting with proteoglycans, has been reported at 289 nM (Chen *et al.*, 1996).

Until recently, the ability of VN to bind heparin was believed to be linked to exposure of the cryptic C-terminal heparin-binding domain upon denaturation. However both monomeric VN and mVN have been demonstrated to bind heparin, with the mVN having higher heparin affinity due to multivalent interactions with heparin (Zhuang *et al.*, 1997; Sieffert, 1997). This observation implies that mVN-TAT should have higher affinity for HSPGs than monomeric VN-TAT. Thus the low affinity of binding found in the present experiments is surprising since the majority of the VN-TAT is multimeric (see Results 3.2.3). It is interesting to note that monomeric VN was found to have a K_d of ~ 5μM for heparin while mVN

(mass = 420,000) was determined to have a a $K_d \approx 200$ nM for heparin (Zhuang *et al.*, 1997). This latter value is similar to that estimated for VN-TAT if a higher molecular mass for VN-TAT is used for calculations, as mentioned above. In light of the recent data, it is surprising that a peptide, composing the heparin-binding domain of VN, competed for VN-TAT clearance in vivo (de Boer *et al.*, 1995b). This is particularly surprising in that the peptide represents the equivalent of native plasma VN and therefore would not be expected to compete for VN-TAT clearance (ie low heparin affinity). Another confounder is the fact two N-terminal domains of VN have been proposed to bind heparin, in addition to the well defined C-terminal binding domain (Liang *et al.*, 1997). Finally, it is possible that HepG2 cells lack the appropriate HSPG for higher affinity binding.

However, care must be taken in comparing mVN to VN-TAT. MVN has been found to be cleared rapidly from rabbits (Peake *et al.*, 1997). In these experiments ^{125}I-multimeric-VN accumulated mainly in the liver, lungs, spleen, and kidneys. The highest counts per gram of ^{125}I-mVN were found in the lungs, which suggests an endothelial cell-specific association. In the present studies ^{125}I-VN-TAT accumulated mainly in the liver, kidneys, and spleen, with lower counts per gram in the lungs. Kanse *et al.* (1996) found that ^{125}I-multimeric-VN associated specifically with uPAR on HUVECs. This association was inhibitable by heparin only at 37 °C and did not occur at 4 °C. Conversely, heparin competed ^{125}I-VN-TAT binding to HUVECs at 4 °C which suggests that different binding sites exist for VN-TAT and mVN on endothelial cells (de Boer *et al.*, 1992). These data

also suggest that different receptor-recognition sites exist on VN-TAT compared to that for mVN.

In further competition experiments, VN-TAT binding was inhibitable by VN-TAT, or with heparin. In comparison, VN-TAT binding was inhibited by TAT only slightly, indicating that the VN moiety of the complexes contains additional important binding residues. Furthermore, the LRP ligand, α_2M*, inhibited VN-TAT binding slightly. The inability of TAT and α_2M* to inhibit VN-TAT binding suggests that LRP plays a minimal role in VN-TAT binding to hepatoma cells.

The importance of HSPGs in VN-TAT binding in vitro is further supported by the fact that the pretreatment of HepG2 cells with heparinase reduced VN-TAT binding by ~ 50%. Furthermore incubation of HepG2 cells with ß-D-xyloside reduced VN-TAT binding to a similar extent. These effects are consistent with the previously reported results for VN-TAT binding to HUVEC proteoglycans (de Boer *et al.*, 1992). Finally, competition with heparin, but not the LRP-ligands, α_2M* and TRAP, significantly reduced the internalization and degradation of VN-TAT. Interestingly, four-fold more VN-TAT was degraded compared to α_2M* over a similar period of time further suggesting that LRP is not the primary binding protein on HepG2 cells. Indeed, these data suggest that HSPGs are the main proteins involved in the internalization of VN-TAT and is consistent with the data obtained from in vivo clearance experiments. Similarly, proteoglycans have been found to be responsible for the direct binding and internalization of lipoprotein lipase (Berryman and Bensadoun,1995) and factor

Xa-TFPI complexes (Ho *et al.*, 1997). In comparison, de Boer *et al.* (1995a) found that VN-TAT was was not degraded after internalization by HUVECs but was translocated to the subendothelium. These data suggest that endothelial HSPGs might have different functions on the surface of endothelial cells than that seen with hepatocytes and/or different receptor proteins are involved in internalizing VN-TAT after HSPG binding.

In recent years it has become apparent that cell surface HSPGs have biologically important roles regulating the cellular binding of ligands and their internalization. HSPGs have been reported to be involved in the cellular binding of growth factors (Coutts and Gallagher, 1995; Schlessinger *et al.*, 1995), hepatic lipase (Krapp *et al.*, 1996), thrombospondin-1 and 2 (Mikhailenko *et al.*, 1995; Godyna *et al.*, 1995; Chen *et al.*, 1997), factor Xa-TFPI (Ho *et al.*, 1997), lipoprotein lipase (Berryman and Bensadoun, 1995), and TFPI (Narita *et al.*, 1995). The true role of proteoglycans in each of these reactions is unknown. The most frequently proposed function for HSPGs is that they bind ligands and then present them to cellular receptors. For example proteoglycans likely bind TFPI (Warshawsky *et al.*, 1996), thrombospondin (Mikhailenko *et al.*, 1995), and lipoprotein lipase (Nykjaer *et al.*, 1993; Chappel *et al.*, 1993) and then present them to LRP for internalization. However, proteoglcyans have also been shown to bind factor Xa-TFPI and lipoprotein lipase and to internalize them without LRP being present (Ho *et al.*, 1997; Berryman and Bensadoun, 1995). In fact, cell-bound lipoprotein lipase was found to co-localize with HSPGs and not LRP.

Moreover, the investigators found an internalization pattern inconsistent with that of LRP-associated ligands (Fernandez-Borja *et al.*, 1996). Moreover, Schlessinger *et al.* (1995) disputed the presentation idea and suggested that proteoglycans function by reducing the three-dimensional diffusion of ligands to two-dimensions on the membrane surface, thereby increasing the chance of ligand-receptor interaction. Furthermore, HSPGs can localize proteins to areas of functional significance. For example TFPI has been proposed to bind to vascular endothelial HSPGs and then be released into the blood following heparinization (Hoppensteadt *et al.*, 1995). The importance of this vascular storage pool is demonstrated by the fact that there is no increase in thrombotic risk due to the greatly reduced plasma TFPI levels seen in abetalipoproteinemic patients (Novotny *et al.*, 1989).

The present data therefore suggest that liver-specific HSPGs are involved in the binding and degradation of VN-TAT in vivo and in vitro. However, these studies do not provide an indicaton as to the nature of the HSPGs specificity for VN-TAT. In comparison to other ligands, known to bind to cellular proteoglycans, it is possible other receptor proteins, like LRP or uPAR, could be involved. Thus the interactions between HSPGs, other cellular sites, and HSPG-binding ligands is very likely a complex set of interactions which require further study. Attempting to define these interactions will be complicated due to the different ligand binding abilities of monomeric versus mVN. Hopefully, further studies will advance our knowledge of these novel biological interactions.

5. FUTURE EXPERIMENTS

The findings that I have presented, in conjunction with other recent reports on the surface expression of other "intracellular" proteins, has opened the door to the discovery of new biological roles for these proteins. However, much remains to be determined concerning the true physiological relevance of these new findings. For example, it will be interesting to determine the relative contributions of CK18 and LRP to TAT metabolism. Below I propose some potential experiments that could shed some light on the proteins involved in TAT clearance.

1. For the determination of whether CK18 is part of a multi-protein receptor complex: cell-surface labelling experiments could be done (with ^{125}I or biotinylation) and immunoprecipitations done with anti-CK18, anti-LRP, and anti-HSPG antibodies. Any precipitated proteins could be visualized after separation on SDS-PAGE by autoradiography, or reaction with streptavidin-alkaline phosphatase.

2. I believe it is essential to demonstrate that CK18 is expressed on the surface of normal hepatocytes *in vivo*. To do this differentially labelled (fluorescein versus rhodamine) anti-CK18 and preimmune IgG could be injected into rabbits and then localized by fluorescence microscopy or immunocytochemistry.

3. A peptide library could be constructed, using phage display technology, and then peptides could be screened for their ability to inhibit binding or internalizaton of TAT or VN-TAT to hepatocytes.

6. REFERENCES

Abe, M. and Oshima, R.G. (1990) A single human keratin 18 gene is expressed in diverse epithelial cells of transgenic mice. J. Cell Biol. 111, 1197-1206.

Abilgaard, U. (1967) Purification of two progressive antithrombins of human plasma. Scand. J. Clin. Lab. Invest. 19, 190-195.

Abilgaard, U. (1969) Binding of thrombin to antithrombin III. Scand. J. Clin. Lab. Invest. 24, 23-27.

Abraham, C.R., Selkes, D.J., and Potter, H. (1988) Immunocytochemical identification of the serine protease inhibitor α_1-antichymotrypsin in the brain amyloid deposits of Alzheimer's disease. Cell 52, 487-501.

Albers, K. and Fuchs, E. (1989) Expression of mutant keratin cDNAs in epithelial cells reveals possible mechanisms for initiation and assembly of intermediate filaments. J. Cell Biol. 108, 1477-1493.

Albers, K.M., Davis, F.E., Perrone, T.N., Lee, E.Y., Liu, Y., and Vore, M. (1996) Expression of an epidermal keratin protein in liver of transgenic mice causes structural and functional abnormalities. J. Cell Biol. 128, 157-169.

Alhenc-Gelas, M.L., Aiach, M., Gorenflot, A., and Andreaux, J.P. (1985) Antithrombin III antigen in human platelets. Thromb. Haemostas. 54, 599-602.

Appella, E. Robinson, E.A., Ulrich, S.J., Stoppelli, M.P., Corti, A., Cassani, G., and Blasi, F. (1987) The receptor-binding sequence of urokinase. J. Biol. Chem. 262, 4437-4440.

Asch, H.L., Mayhew, E., Lazo, R.O., asnd Asch, B.B. (1993) Lipids covalently bound to keratins of mouse mammary epithelial cells. Biochem. Mol. Biol. Intern. 29, 1161-1169.

Ashcom, J.D., Tiller, S.E., Dickerson, K., Cravens, J.L., Argraves, W.S., and Strickland, D.K. (1990) The human α_2-macroglobulin receptor: identification of 420-kdD cell surface glycoprotein specific for the activated conformation of α_2-macroglobulin. J. Cell Biol. 110, 1041-1048.

Atha, D.H., Stephens, A.W., and Rosenberg, R.D. (1984a) Evaluation of critical groups required for the binding of heparin to antithrombin. Proc. Acad. Natl. Sci. USA 81, 1030-1034.

Atha, D.H., Brew, S.A., and Ingham, K.C. (1984b) Interaction and thermal stability of fluorescent labeled derivatives of thrombin and antithrombin III. Biochem. Biophys. Acta. 785, 1-6.

Atkins, H.L., Broudy, V.C., and Papayannopoulou, T. (1991) Characterization of the structure of the erythropoietin receptor by ligand blotting. Blood 77, 2577-2582.

Bachant, J.B. and Klymkowsky, M.W. (1996) A nontetrameric species is the major soluble form of keratin in *Xenopus* oocytes and rabbit reticulocyte lysates. J. Cell Biol. 132, 153-165.

Bader, B.L., Magin, T.M., Freudenmann, M., Stumpp, S., and Franke, W.W. (1991) Intermediate filaments formed de novo from tail-less cytokeratins in the cytoplasm and in the nucleus. J. Cell Biol. 115, 1293-1307.

Banda, M.J., Rice, A.G., Griffin, G.L., and Senior, R.M. (1988) α_1-proteinase inhibitor is a neutrophil chemoattractant after proteolytic inactivation by macrophage elastase. J. Biol. Chem. 263, 4481-4484.

Banda, M.J., Rice, A.G., Griffin, G.L., and Senior, R.M. (1988) The inhibitory complex of human α_1-proteinase inhibitor and human leukoycte elastase is a neutrophil chemoattractant. J. Exp. Med. 167, 1608-1615.

Bao, J., Sifers, R.N., Kidd, V.J., Ledley, P.D., and Woo, S.L. (1987) Molecular evolution of serpins: homologous structure of the human α_1-antichymotrypsin and α_1-antitrypsin genes. Biochemistry 26, 7755-7759.

Baribault, H., Price, J., Miyai, K., and Oshima, R.G. (1993) Mid-gestational lethality in mice lacking keratin 8. Genes and Development 7, 1191-1202.

Baribault, H., Penner, J., Iozzo, R.V., and Wilson-Heiner, M. (1994) Colorectal hyperplasia and inflammation in keratin 8-deficient FVB/N mice. Genes and Development 8, 2964-2973.

Bauer, P.I., Mandl, J., Machovich, R., Antoni, F., Garzo, T., and Horvath, I. (1982) Specific binding of thrombin-antithrombin III complex to hepatocytes. Thromb. Res. 28, 595-606.

Bauman, P.A., Dalton, W.S., Anderson, J.M., and Cress, A.E. (1994) Expression of cytokeratin confers multiple drug resistance. Proc. Natl. Acad. Sci. USA. 91, 5311-5314.

Behrendt, N. Ronne, E., and Dano, K. (1995) The structure and function of the urokinase receptor, a membrane protein governing plasminogen activation on the cell surface. Biol. Chem. Hoppe-Seyler 376, 269-279.

Bendayan, M. (1985) Ultrastructural localization of cytoskeletal proteins in pancreatic secretory cells. Can. J. Biochem. Cell Biol. 63, 680-690.

Bennett, Jr., J.P. and Yamamura, H.I. (1985) Neurotransmitter, hormone, or drug receptor binding methods, in Yamamura et al.(eds): Neurotransmitter receptor binding, 2nd Ed.. New York, Raven Press, pp. 62-89.

Berryman, D.E. and Bensadoun, A. (1995) Heparan sulfate proteoglycans are primarily responsible for the maintenance of enzyme acitivity, binding, and degradation of lipoprotein lipase in chinese hamster ovary cells. J. Biol. Chem. 270, 24525-24531.

Biemesderfer, D., Dekan, G., Aronson, P.S., and Farquhar, M.G. (1993) Biosynthesis of the gp330/44-kDa Heymann nephritis antigenic complex: assembly takes place in the ER. Am. J. Physiol. 264, F1011-1020.

Bird, T.A., Gearing, A.J.H., and Saklatvala, J. (1988) Murine interleukin 1 receptor: direct identification by ligand blotting and purification to homogeneity of an interleukin 1-binding glycoprotein. J. Biol. Chem. 263, 12063-12069.

Bjork, I., Danielsson, A., Fenton, J.W., and Jornvall, H. (1981) The site in human antithrombin for functional proteolytic cleavage by thrombin FEBS Lett. 126, 257-260.

Bjork, I., Jackson, C.M., Jornvall, H. Lavine, K.K., Nordling, K., and Salsgiver, W.J. (1982) The active site of antithrombin. Release of the same proteolytically cleaved form of the inhibitor from complexes with factor IXa, factor Xa and thrombin. J. Biol. Chem. 257, 2406-2411.

Bjork, I., Ylinenjarvi, K., Olson, S.T., and Bock, P.E. (1992) Conversion of antithrombin from an inhibitor of thrombin to a substrate with reduced heparin affinity and enhanced conformational stability by binding of a tetradecapeptide corresponding to the P1 to P14 region of the putative reactive bond loop of the inhibitor. J. Biol. Chem. 267, 1976-1982.

Bjork, I., Nordling, K., Larsson, I, and Olson, S.T. (1992) Kinetic characterization of the substrate reaction between a complex of antithrombin with a synthetic reactive-bond-loop tetradecapeptide and four target proteinases of the inhibitor. J. Biol. Chem. 267, 19047-19050.

Bleyl, H. (1981) Radioimmunologische antithrombin-bestimmiung im liquor cerebrospinalis. Urin, Dialysat and Thrombozyten, in Mikrozirulation and Prostaglandingstoffwerhsel, Blumel, G. and Haas, S (eds), Schattauer, New York, p. 433.

Bock, S.C., Wion, K.L., Vehar, G.A., and Lawn, R.M. (1982) Cloning and expression of the cDNA for human antithrombin III. Nucl. Acids Res. 10, 8113-8125.

Bock, S.C., Harris, F.J., Balazs, I., and Trent, J.M. (1985) Assignment of the human antithrombin III structural gene to chromosome 1q23-25. Cytogenet. Cell Genet. 39, 67-69.

Boland, K., Manias, K., and Perlmutter, D.H. (1995) Specificity in recognition of amyloid-ß peptide by the serpin-enzyme complex receptor in hepatoma cells and neuronal cells. J. Biol. Chem. 270, 28022-28028.

Boland, K., Behrens, M., Choi, D., Manias, K., and Perlmutter, D.H. (1996) The serpin-enzyme complex receptor recognizes soluble, nontoxic amyloid beta peptide but not aggregated, cytotoxic amyloid-beta peptide. J. Biol. Chem. 271, 18032-18044.

Borsodi, A., and Narasimhan, T.R. (1978) Microheterogeneity of human antithrombin III. Br. J. Haematol. 39, 121-127.

Bosch, F.X., Leube, R.E., Achtstatter, T., Moll, R., and Franke, W.W. (1988) Expression of simple epithelial type cytokeratins in stratified epithelia as detected by immunolocalization and hybridization in situ. J. Cell Biol. 106, 1635-1648.

Brennan, S.O., George, P.M., and Jordan, R.E. (1987) Physiological variant of antithrombin-III lacks carbohydrate side chain at Asn-135. Thromb. Res. 55, 471-480.

Brinkhous, K.M., Smith, H.P., Warner, E.D., and Seegers, W.H. (1939) The inhibition of blood clotting: an unidentified substance which acts in conjunction with heparin to prevent the conversion of prothrombin into thrombin. Am. J. Physiol. 125, 683-687.

Brunkener, M. and Georgatos, S.D. (1992) Membrane-binding properties of filensin, a cytoskeletal protein of the lens fiber cells. J. Cell Sci. 103, 709-718.

Bu, G., Williams, S., Strickland, D.K., and Schwartz, A.L. (1992) Low density lipoprotein receptor-related protein/alpha2-macroglobulin receptor is an hepatic receptor for tissue-type plasminogen activator. Proc. Natl. Acad. Sci. USA 89, 7427-7431.

Bu, G, Maksymovitch, E.A., and Schwartz, A.L. (1993) Receptor-mediated endoyctosis of tissue-type plasminogen activator by low density lipoprotein receptor-related protein on human hepatoma HepG2 cells. J. Biol. Chem. 268, 13002-13009.

Bu, G., Maksymovitch, E.A., Geuze, H., and Schwartz, A.L. (1994a) Subcellular localization and endocytic function of low density lipoprotein receptor-related protein in human glioblastoma cells. J.Biol. Chem. 269, 29874-29882.

Bu, G., Warshawsky, I., and Schwartz, A.L. (1994b) Cellular receptors for the plasminogen activators. Blood 83, 3427-3436.

Bu, G. and Rennke, S. (1996) Receptor-associated protein is a folding chaperone for low density lipoprotein receptor-related protein. J. Biol. Chem. 271, 22218-22224.

Cadrin, M. and Martinoli, M-G. (1995) Alterations of intermediate filaments in various histopathological conditions. Biochem. Cell Biol. 73, 627-634.

Carlson, T.H. and Atencio, A.C (1982) Isolation and partial characterization of two distinct types of antithrombin III from rabbit. Thromb. Res. 27, 23-24.

Carlson, T.H., Atencio, A.C., and Simon, T.L. (1984) In vivo behaviour of radioiodinated rabbit antithrombin III: demonstration of a noncirculating vascular compartment. J. Clin. Invest. 74, 191-199.

Carlson, T.H. (1989) Effect of heparin on the vascular distribution of *I-antithrombin III isoforms in rabbits. Thromb. Res. 55, 471-480.

Carrell, R.W. and Travis, J. (1985) α_1-Antitryspin and the serpins. Variation and countervariation. Trends Biol. Sci. 10,20-24.

Carrell, R.W., Christey, P.B., and Boswell, D.R. (1987a) Serpins: Antithrombin and other inhibitors of coagulation and fibrinolysis evidence from amino acid sequences, in Verstraete, M., Vermylen, J., Lijnen, R. et al. (eds): Thrombosis and Haemostasis. Leuven, Belgium, Leuven University Press, pp. 1-15.

Carrell, R.W., Pemberton, P.A., and Boswell, D.R. (1987b) The serpins: evolution and adaptation in a family of protease inhibitors, in: Cold Spring Harbour Symposia on Quantitative Biology, 52, 527-535.

Carrell, R.W., Evans, D.L.I., and Stein, P.E. (1991) Mobile reactive centre of serpins and the control of thrombosis. Nature 353, 576-578.

Carrell, R.W. and Evens, D.L.I. (1992) Serpins: mobile conformations in a family of proteinase inhibitors. Curr. Opin. Struct. Biol. 2, 438-446.

Carrell, R.W., Stein, P.E., Fermi, G., and Wardell, M. (1994) Biological implications of a 3 A structure of dimeric antithrombin. Structure 2, 257-270.

Carrell, R., Skinner, R., Jin, L., and Abrahams, J.P. (1997) Structural mobility of antithrombin and its modulation by heparin. Thromb. Haemostas. 78, 516-519.

Carson, E.R. and Jones, E.A. (1979) Use of kinetic analysis and mathematical modeling in the study of metabolic pathways in vivo: applications to hepatic organic anion metabolism (first of two parts). N. Eng. J. Med. 300, 1016-1027.

Caulin, C., Bauluz, C., Gandarillas, A., Cano, A., and Quintanilla, M. (1992) Changes in keratin expression during malignant progression of transformed mouse epidermal keratinocytes. Exp. Cell Res. 204, 11-21.

Chan, R., Rossitto, P.V., Edwards, B.F., and Cardiff, R.D. (1986) Presence of proteolytically processed keratins in th culture medium of MCF-7 cells. Cancer Res. 46, 6353-6359.

Chan, T.K., and Chan, V. (1981) Antithrombin III, the major modulator of intravascular coagulation is synthesized by human endothelial cells. Thromb. Haemostas. 46, 504-506.

Chan, V., Chan, T.K., Wang, V., Tso, S.C., and Todd, D. (1979) The determination of antithrombin III by radioimmunoassay and its clinical application. Br. J. Haematol. 41,563-572.

Chappel, D.A., Fry, G.L., Waknitz, M.A., Iverius, P-H., Williams, S.E., and Strickland, D.K. (1993) The low density lipoprotein receptor-related protein/α_2-macroglobulin receptor binds and mediates catabolism of bovine milk lipoprotein lipase. J. Biol. Chem. 267, 25674-25767.

Chen, H., Strickland, D.K., and Mosher, D.F. (1996) Metabolism of thrombospondin 2: binding and degradation by 3T3 cells and glycosaminoglycan-variant chinese hamster ovary cells. J. Biol. Chem. 271, 15993-15999.

Chen, M., Conn, K-J., and Festoff, B.W. (1993) A receptor for cathepsin G:α_1-antichymotrypsin complexes on mouse spinal cord astrocytes. Neurology 43, 1223-1227.

Chen, W-J., Goldstein, J.L., and Brown, M.S. (1990) NPXY, a sequence often found in cytoplasmic tails, is required for coated pit-mediated internalization of the low density lipoprotein receptor. J. Biol.Chem. 265, 3116-3123.

Cheng, Y. and Prusoff, W.H. (1973) Relationship between the inhibition constant (K1) and the concentration of inhibitor which causes 50 per cent inhibition (I50) of an enzymatic reaction. Biochem. Pharm. 22, 3099-3108.

Choay, J., Petitou, M., Lormeau, J.C., Sinay, P., Casu, B., and Gatti, G. (1983) Structure activity relationship in heparin: a synthetic pentasaccharide with high affinity for antithrombin III and eliciting high anti-factor Xa activity. Biochem. Biophys. Res. Commun. 116, 492-499.

Chou, C-F., Smith, A.J., and Omary, M.B. (1992) Characterization and dynamics of O-linked glycosylation of human cytokeratin 8 and 18. J. Biol. Chem. 267, 3901-3906.

Chou, C-F., Riopel, C.L., Rott, L.S., and Omary, M.B. (1993) A significant soluble keratin fraction in 'simple' epithelial cells: lack of an apparent phosphorylation and glycosylation role in keratin solubility. J. Cell Sci. 105, 433-444.

Christensen, L., Wiborg Simonsen, A.C., Heegaard, C.W., Moestrup, S.K., Andersen, J.A., and Andreasen, P.A. (1996) Immunohistochemical localization of urokinase-type plasminogen activator, type-1 plasminogen-activator inhibitor, urokinase receptor, amd α_2-macroglobulin receptor in human breast carcinomas. Int. J. Cancer 66, 441-452.

Chu, Y-W., Runyan, R.B., Oshima, R.G., and Hendrix, M.J.C. (1993) Expression of complete keratin filaments in mouse L cells augments cell migration and invasion. Proc. Natl. Acad. Sci. USA. 90, 4261-4265.

Chu, Y-W., Seftor, E.A., Romer, L.H., and Hendrix, M.J.C. (1996) Experimental coexpression of vimentin and keratin intermediate filaments in human melanoma cells augments motility. Am. J. Path. 148, 63-69.

Church, F.C., Pratt, C.W., and Hoffman, M. (1990) Leukocyte chemoattractant peptides from the serpin heparin cofactor II. J. Biol. Chem. 266, 704-709.

Collen, D., Schietz, J., De Cock, F., Holmer, E., and Verstraete, M. (1977) Metabolism of antithrombin III (heparin cofactor) in man: effects of venous thrombosis and of heparin administration. Eur. J. Clin. Invest. 7, 27-35.

Collen, D. and Wiman, B. (1979) Turnover of α_2-antiplasmin and of the plasmin α_2-antiplasmin complex. In:Collen, D., Wiman, B., and Verstraete, M.(eds): The physiological inhibitors of coagulation and fibrinolysis. Elvesier/North Holland Biomedical Press, Amsterdam. pp. 171-176.

Coulombe, P. and Fuchs, E. (1990) Elucidating the early stages of keratin filament assembly. J. Cell Biol. 111, 153-169.

Coulombe, P.A., Chan, Y.M., Albers, K., and Fuchs, E. (1990) Deletions in epidermal keratins leading to alterations in filament organization in vivo and in intermediate filament assembly in vitro. J. Cell Biol. 111, 3049-3064.

Coulombe, P.A. (1993) The cellular and molecular biology of keratins:beginning a new era. Curr. Opin. Cell Biol. 5, 17-29.

Conard, J., brosstad, F., Lie Larsen, F., Samama, M., and Abilgaard, U. (1983) Molar antithrombin concentration in normal human plasma. Haemostasis 13:363-368.

Conese, M., Olson, D., and Blasi, F. (1994) Protease nexin-1-urokinase complexes are internalized and degraded through a mechanism that requires both urokinase receptor and α_2-macroglobulin receptor. J. Biol. Chem. 269, 17886-17892.

Conway, J.F. and Parry, D.A.D. (1990) Structural features in the heptad substructure and longer range repeats of two-stranded alpha-fibrous proteins. Int. J. Biol. Macromol. 12, 328-334.

Cooperman, B.S., Stavridi, E., Nickbarg, E., Rescorla, E., Schechter, N.M., and Rubin, H. (1993) Antichymotrypsin interaction with chymotrypsin - partitioning of the complex. J. Biol. Chem. 268, 23616-23625.

Dahlback, B. and Podack, E.R. (1985) Characterization of human S-protein, an inhibitor of the membrane attack complexs fo complement. Demonstration of a free reactive thiol group. Biochemistry 24, 2368-2374.

Dainiak, N. (1991) Surface membrane-associated regulation of cell assembly, differentiation, and growth. Blood. 78, 264-276.

Daly, M., and Hallinan, F. (1985) Analysis of antithrombin III microheterogeneity by isoelectric focusing and immunoblotting. Thromb. Res. 40, 207-214.

Danishefsky, I., Zweben, A., and Slomiany, B.L. (1978) Human Antithrombin III: carbohydrate components and associated glycolipid. J. Biol. Chem. 253, 32-37.

de Boer, H.C. Preissner, K.T., Bouma, B.N., and de Groot, P.G. (1992) Binding of vitronectin-thrombin-antithrombin III complex to human endothelial cells is mediated by the heparin binding site of vitronectin. J. Biol. Chem. 267, 2264-2268.

de Boer, H.C., de Groot, P.G., Bouma, B.N., and Preissner, K.T. (1993) Ternary vitronectin-thormbin-antithrombin III complexes in human plasma. J. Biol. Chem. 268, 1279-1283.

de Boer, H.C., Preissner, K.T., Bouma, B.N., and de Groot, P.G. (1995a) Internalization of vitronectin-thrombin-antithrombin complex by endothelial cells leads to deposition of the complex into the subendothelial matrix. J. Biol. Chem. 270, 30733-30740.

de Boer, H.C., de Groot, P.G., Preissner, K.T., and Smit, M. (1995b) In vivo clearance of thrombin-antithrombin-vitronectin complex in rats. Thromb. Hemostas. 73, 936a.

De Jager, R., Abdel-Nabi, H., Serafini, A., Pecking, A., Klein, J.L., and Hanna, M.G. (1993) Current status of cancer immunodetection with radiolabelled human monoclonal antibodies. Seminars in nuclear medicine 23, 165-179.

De Leeuw, A.M., Brouwer, A., and Knook, D.L. (1990) Sinusoidal endothelial cells of the liver: fine structure and function in relation to age. J. Electron Microsc. Tech. 14, 218-236.

de Smet, B.J.G.L., de Boer, J-P., Agterberg, J., Rigter, G., Bleeker, W.K., and Hack, C.E. (1993) Clearance of human native, proteinase-complexed, and proteolytically inactivated C1-inhibitor in rats. Blood 81, 56-61.

de Swart, C.A.M., Nijmeyer, B., Andersson, L.O., Holmer, E., Sixma, J.J., and Bouma, B.N. (1984) Elimination of intravenously administered radiolabelled antithrombin III and heparin in humans. Thromb. Haemostas. 52, 66-70.

Denk, H., Lackinger, E., Zatloukal, J., and Franke, W.W. (1987) Turnover of cytokeratin polypeptides in mouse hepatocytes. Exp. Cell Res. 173, 137-143.

Detwiler, T.C., Chang, A.C., Speziale, M.V., Browne, P.C., Miller, J.J., and Chen, K. (1992) Complexes of thrombin with proteins secreted by activated platelets. Semin. Thromb. Hemostas. 18, 60-66.

Dixon, S.J., Pitaru, S., Bhargava, U., and Aubin, J.E. (1987) Membrane blebbing is associated with Ca^{+2}-activated hyperpolarizations induced by serum and α_2-macroglobulin. J. Cell. Physiol. 132, 473-482.

Doolittle, R.F. (1983) Angiotensinogen is related to the antitrypsin-antithrombin-ovalbumin family. Science 222, 417-419.

Downing, D.T. (1995) Molecular modeling indicates that homodimers form the basis for intermediate filament assembly from human and mouse epidermal keratins. Proteins: Structure, Function, and Genetics. 23, 204-217.

Dudani, A.K., Cummings,C. Hashemi, S., and Ganz, P. (1993) Isolation of a novel plasminogen receptor from human endothelial cells. Thromb. Research 69, 185-196.

D'Souza, S.E. and Mercer, J.F. (1987) Antithrombin III mRNA in adult rat liver and kidney and in rat liver during development. Biochem. Biophys. Res. Comm. 142, 417-421.

Egeberg, O. (1965) Inherited antithrombin deficiency causing thrombophilia. Thromb. Diath. Haemmorrh. 13, 516-530.

Eldering, E., Verpy, E., Roem, D., Meo, T., and Tosi, M. (1995) COOH-terminal substitutions in the serpin C1 inhibitor that cause loop overinsertion and subsequent multimerization. J. Biol. Chem. 270, 2579-2587.

Elliot, P.R., Lomas, D.A., Carrell, R.W., and Abrahams, J.P. (1996) Inhibitory conformation of the reactive centre loop of α_1-antitrypsin. Nature Struct. Biol. 3, 676-681.

Ellis, V., Wun, T.C., Behrendt, N., Ronne, E., and Dano, K. (1990) Inhibition of receptor-bound urokinase by plasminogen-activator inhibitors. J. Biol. Chem. 265, 9904-9908.

Enghild, J.J., Valnickova, Z., Thogersen, I.B., and Pizzo, S.V. (1994) Complexes between serpins and inactive proteinases are not thermodynamically stable but are recognized by serpin receptors. J. Biol. Chem. 269, 20159-20166.

Erdjument, H., Lane, D.A., Panico, M., DiMarzo, V., and Morris, H.R. (1988) Single amino acid substitutions in the reactive site of antithrombin leading to thrombosis. Congenital substitution of arginine 393 to cysteine in antithrombin Northwick Park and to histidine in antithrombin Glasgow. J. Biol. Chem. 263, 5589-5593.

Ernst, S., Langer, R., Cooney, C.L., and Sasisekharan, R. (1995) Enzymatic degradation of glycosaminoglycans. Crit. Rev. Biochem. Mol. Biol. 30, 387-444.

Fair, D.S., and Bahnak, B.R. (1984) Human hepatoma cells secrete single chain factor X, prothrombin, and antithrombin III. Blood 64, 194-204.

Fair, D.S. and Plow, E. F. (1986) Specific association of thrombin-antithrombin complexes with a human hepatoma cell line. Thromb. Res. 41, 67-78.

Fernandez-Borja, M., Bellido, D., Vilella, E., Olivecrona, G., and Vilaro, S. (1996) Lipoprotein lipase-mediated uptake of lipoprotein in human fibroblasts: evidence for an LDL-receptor-independent internalization pathway. J. Lipid Res. 37, 464-481.

Fish, W.W., Orre, K., and Bjork, I. (1979) Routes of thrombin action in the production of proteolytically modified, secondary forms of antithrombin-thrombin complex. Eur. J. Biochem. 101, 39-44.

Fleck, A. (1985) Computer models for metabolic studies on plasma proteins. Ann. Clin. Biochem. 22, 33-49.

Flink, I.L., Bailey, T.J., Gustafson, T.A., Markham, B.E., and Morkin, E. (1986) Complete amino acid sequence of human thyroxine-binding globulin deduced from cloned DNA:Close homology to the serine antiproteases. Proc. Natl. Acad. Sci. USA 83, 7708-7712.

Franke, W., Winter, W.S., Schmid, E., Sollner, P., Hammerling, G., and Achtstatter, T. (1987) Monoclonal cytokeratin antibody recognizing a heterotypic complex: immunological probing of conformational states of cytoskeletal proteins in filaments and in solution. Exp. Cell Res. 173, 17-37.

Franzen, L-E., Svensson, S., and Larm, O. (1980) Structural studies on the carbohydrate portion of human antithrombin III. J. Biol. Chem. 255, 5090-5098.

French, S.W., Kawahara, H., Katsuma, Y., Ohta, M., and Swierenga, S.H.H. (1989) Interaction of intermediate filaments with nuclear lamina and cell periphery. Electron Microsc. Rev. 2, 17-51.

Fuchs, E. (1994a) Intermediate filaments: structure, dynamics, function, and disease. Annu. Rev. Biochem. 63, 345-382.

Fuchs, E. (1994b) Intermediate filaments and disease: mutations that cripple cell

Fuchs, E. (1996) The cytoskeleton and disease: genetic disorders of intermediate filaments. Annu. Rev. Genet. 30, 197-231.

Fuchs, E. and Weber, K. (1994). Intermediate filaments:Structure, dynamics, function, and disease. Annu. Rev. Biochem. 63, 345-382. J. Cell. Biol. 125, 511-516.

Fuchs, H.E., Shifman, M.A., and Pizzo, S.V. (1982) In vivo catabolism of α_1-proteinase inhibitor-trypsin, antithrombin III-thrombin, and α2-macroglobulin-methylamine. Biochim. Biophys. Acta. 716, 151-157.

Fuchs, H.E., Michalopolous, and Pizzo, S.V. (1984) Hepatocyte uptake of α_1-proteinase inhibitor-trypsin complexes in vitro: evidence for a shared uptake mechanism for proteinase complexes of α_1-proteinase inhibitor and antithrombin III. J. Cell Biochem. 25, 231-243.

Furmiak-Kazmierczak, E., Nesheim, M.E., and Cote, G.P. (1995) Coagulation factor V_a is an actin filament binding and cross-linking protein. Biochem. Cell Biol. 73, 105-112.

Gassmann, M., Thommes, P., Wieser, T., and Hubscher, U. (1990) Efficient production of chicken egg yolk antibodies against a conserved mammalian protein. Faseb J. 4, 2528-2532.

Geerts, A., Geuze, H.J., Slot, J.W., Voss, B., Schuppan, D., Schellink, P., and Wisse, E. (1986) Immunogold localization of procollagen III, fibronectin, and heparan sulfate proteoglycan on ultrathin frozen sections of the normal rat liver. Histochemistry 84, 355-362.

George, J.N. (1978) Studies on platelet plasma membrane.IV.Quantitation analysis of platelet membrane glycoproteins by (^{125}I)-diazotized diiodosulfanilic acid labelling and SDS-polyacrylamide gel electrophoresis. J. Lab. Clin. Med. 92, 430-446.

Gettins, P., Patston, P.A., and Shapira, M. (1993) The role of conformational change in serpin structure and function. Bioessays 15, 461-467.

Gettins, P.G.W., Patston, P.A., and Olson, S.T. (1996) Serpins:structure, function and biology. New York, New York: R. G. Landes Co., pp. 1-202.

Godfroid, E., Geuskens, M., Dupressoir, T., Parent, I., and Szpirer, C. (1991) Cytokeratins are exposed on the outer surface of established mammary carcinoma cells. J. Cell Sci. 99, 595-607.

Godyna, S., Liau, G., Popa, H., Stefansson, S., and Argraves, W.S. (1995) Identification of the low density lipoprotein receptor-related protein (LRP) as an endocytic receptor for thrombospondin-1. J. Cell Biol. 129, 1403-1410.

Goldman, R.D., Khuon, S., Chou, Y.H., Opal, P., and Steinert, P.M. (1996) The function of intermediate filaments in cell shape and cytoskeletal integrity. J. Cell Biol. 134, 971-983.

Goldstein, J.L., Brown, M.S., Anderson, R.G.W., Russell, D.W., and Schneider, W.J. (1985) Receptor-mediated endocytosis: concepts emerging from the LDL receptor system. Ann. Rev. Cell Biol. 1, 1-39.

Gonias, S.L., Fuchs, H.E., and Pizzo, S.V. (1982) A unique pathway for the plasma elimination of α_2-antiplasmin-protease complexes in mice. Thromb. Haemostas. 48, 208-210.

Goodwin, R.L., Baumann, H., and Berger, F.G. (1996) Patterns of divergence during evolution of α_1-proteinase inhibitors in mammals. Mol. Biol. Evol. 13, 346-358.

Gouin-Thibault, I., Dewar, L., Kulczycky, M., Sternback, M., and Ofosu, F.A. (1996) Factor Xa-antithrombin III complexes in plasma: relationship to prothrombin activation in vivo. Br. J. Haematol. 90, 669-680.

Griffith, M.J. and Lundblad, R.L. (1981) Dissociation of antithrombin III-thrombin complex. Formation of active and inactive antithrombin III. Biochemistry 20, 105-110.

Griffith, M.J. (1982) Kinetics of the heparin-enhanced antithrombin III/thrombin reaction. Evidence for a template model for the mechanism of action of heparin. J. Biol. Chem. 257, 7260-7365.

Gursoy, A. and Ulutin, O.N. (1983) Platelet antithrombin III. Ann. Sarov. Med. Suppl. 3, 75-77.

Hajjar, K.A., Jacovina, A.T., and Chacko, J. (1994) An endothelial cell receptor for plasminogen/tissue plasminogen activator:I.Identity with annexin II. J. Biol. Chem. 269, 21191-21197.

Hamamoto, T., Foster, D.C., and Kisiel, W. (1996) The inhibition of human factor VIIa-tissue factor by antithrombin III-heparin is enhanced by factor X on a human carcinoma cell line. Int. J. Hematol. 63, 51-63.

Hammond.G.L., Smith C.L., Goping I.S., Underhill, D.A., Harley, M.J., Reventos, J., Musto, N.A., Gunsalus, G.L., and Bardin, C.W. (1987) Primary structure of human corticosteroid binding globulin, deduced from hepatic and pulmonary cDNAs, exhibits homology with serine protease inhibitors. Proc. Natl. Acad. Sci. USA 84, 5153-5157.

Hanukoglu, I., and Fuchs, E. (1982) The cDNA sequence of a human epidermal keratin: divergence of sequence but conservation of structure among intermediate filament proteins. Cell 31, 243-252.

Hanukoglu, I., and Fuchs, E. (1983) The cDNA sequence of a type II cytoskeletal keratin reveals constant and variable structural domains among keratins. Cell 33, 915-924.

Harlow, E. and Lane, D. (1988) Antibodies: a laboratory manual. Cold Spring Harbour Laboratory. Cold Spring Harbour, USA, pp. 630-631.

Hatton, M.W.C., Berry, L.R., and Regoeczi, E. (1978) Inhibition of thrombin by antithrombin III in the presence of certain glycosaminoglycans found in the mammalian aorta. Thromb. Hemostas. 13, 655-670.

Hatton, M.W.C., Southward, S., and Ross-Oullet,B. (1994) Catabolism of plasminogen glycoforms I and II in rabbits:relationship to plasminogen synthesis by the rabbit liver in vitro. Metabolism 43, 1430-1437.

Hatzfeld, M. and Weber, K. (1991) Modulation of keratin intermediate filament assembly by single amino acid exchanges in the consensus sequence at the C-terminal end of the rod domain. J. Cell Sci. 99, 351-362.

Heimburg, T., Schuenemann, J., Weber, K., and Geisler, N. (1996) Specific recognition of coiled coils by infrared spectroscopy: analysis of the three structural domains of type III intermediate filament proteins. Biochemistry 35, 1375-1382.

Herz, J., Kowal, R.C., Goldstein, J.L., and Brown, M.S. (1990) Proteolytic processing of the 600 kD low density lipoprotein receptor-related protein LRP occurs in a trans-golgi compartment. EMBO J. 9, 1769-1776.

Hembrough, T.A., Vasudevan, J., Allieta, M.M., Glass II, W.F., and Gonias, S.L. (1995) A cytokeratin 8-like plasminogen-binding activity is present on the external surfaces of hepatocytes, HepG2 cells and breast carcinoma cell lines. J. Cell Sci. 108, 1071-1082.

Hembrough, T.A., Li, L., and Gonias, S.L. (1996a) Cell-surface cytokeratin 8 is the major plasminogen receptor on breast cancer cells and is required for the accelerated activation of cell-associated plasminogen by tissue-type plasminogen activator. J. Biol. Chem. 271, 25684-25691.

Hembrough, T.A., Kralovich, K.R., Li, L., and Gonias, S. L. (1996b) Cytokeratin 8 released by breast carcinoma cells in vitro binds plasminogen and tissue-type plasminogen activator and promotes plasminogen activation. Biochem. J. 317, 763-769.

Herz, J., Clouthier, D.E., and Hammer, R.E. (1992) LDL receptor-related protein internalizes and degrades uPA-PAI-1 complexes and is essential for embryo implantation. Cell 71, 411-421.

Hintner, H., Steinert, P.M., and Lawley, T.J. (1983) Human upper epidermal cytoplasmic antibodies are directed against keratin intermediate filament proteins. J. Clin. Invest. 71, 1344-1351.

Hintner,H., Stanzl,U., Dahlback,K., Dahlback, B., Breathnach,S.M. (1989) Vitronectin shows complement-independent binding to isolated keratin filament aggregates. J. Invest. Derm. 93, 656-661.

Hirsh, J. (1991) Drug Therapy: Heparin. N. Engl. J. Med. 324, 1565-1574.

Hoffman, M., Fuchs, H.E., and Pizzo, S.V. (1986) The macrophage-mediated regulation of hepatocyte synthesis of antithrombin III and α_1-proteinase inhibitor. Thromb. Res. 41, 707-715.

Holmes, W.E., Lijnen, H.R., Nelles, L., Kluft, C., Nieuwenhuis, H.K., Rijken, D.C., and Collen, D. (1987) Alpha 2-antiplasmin Enschede: alanine insertion and abolition of plasmin inhibitory activity. Science 272, 209-211.

Hood, D.B., Huntington, J.A., and Gettins, P.G.W. (1994) α_1-Proteinase inhibitor variant T345R. Influence of P14 residue on substrate and inhibitory pathways. Biochemistry 33, 8538-8547.

Hook, V.Y.H., Purviance, R.T., Azaryan, A.V., Hubbard, G., and Krieger, T.J. (1993) Purification and characterization of α_1-antichymotrypsin-like protease inhibitor that regulates prohormone thiol protease involved in enkaphalin precursor processing. J. Biol. Chem. 268, 20570-20577.

Hopkins, P.C.R., Carrell, R.W., and Stone, S.R. (1993) Effects of mutations in the hinge region of serpins. Biochemistry 32, 7650-7657.

Hopkins, P.C.R. and Stone, S.R. (1995) The contribution of the conserved hinge region residues of α_1-antitrypsin to its reaction with elastase. Biochemistry 34, 15872-15879.

Hopkins, P.C.R., Chang, W-S.W., Wardell, M.R., and Stone, S.R. (1997) Inhibitory mechanism of serpins: mobility of the C-terminal region of the reactive-site loop. J. Biol. Chem. 272, 3905-3909.

Hoppensteadt, D.A., Walenga, J.M., Fasanella, A., Jeske, W., and Fareed, J. (1995) TFPI antigen levels in normal human volunteers after intravenous and subcutaneous administration of unfractionated heparin and a low molecular weight heparin. Thromb. Res. 77, 175-183.

Houston, D.S., Carson, C.W., and Esmon, C.T. (1997) Endothelial cells and extracellular calmodulin inhibit monocyte tumor necrosis factor release and augment neutrophil elastase release. J. Biol. Chem. 272, 11778-11785.

Howard, G.C., Misra, U.K., DeCamp, D.L., and Pizzo, S.V. (1996a) Altered interaction of *Cis*-dichlorodiammineplatinum(II)-modified α_2-macroglobulin (α_2M) with the low density lipoprotein receptor-related protein/α_2M receptor but not the α_2M signaling receptor. J. Clin. Invest. 97, 1193-1203.

Howard, G.C., Yamaguchi, Y., Misra, U.K., Gawdi, G., Nelsen, A., DeCamp, D.L., and Pizzo, S.V. (1996b) Selective mutations in cloned and expressed α-macroglobulin receptor binding fragment alter binding to either the α_2-macroglobulin signaling receptor or the low density lipoprotein receptor-related protein/α_2-macroglobulin receptor. J. Biol. Chem. 271, 14105-14111.

Hubbard, A.L., Wall, D.A., and Ma, A. (1983a) Isolation of rat hepatocyte plasma membranes. I. Presence of the three major domains. J. Cell Biol. 96,217-229.

Hubbard, A.L. and Ma, A. (1983b) Isolation of rat hepatocyte plasma membranes. II. Identification of membrane associated cytoskeletal proteins. J. Cell Biol. 96, 230-239.

Huber, R. and Carrell, R.W. (1992) Implications of the three-dimensional structure of α_1-antitrypsin for structure and function of serpins. Biochemistry 28, 8951-8966.

Hunt, L.T. and Dayhoff, M.O. (1980) A surprising new protein superfamily containing ovalbumin, antithrombin-III, and alpha 1-proteinase inhibitor. Biochem. Biophys. Res. Commun. 95, 864-871.

Huntington, J.A., Olson, S.T., Fan, B., and Gettins, P.G.W. (1996) Mechanism of heparin activation of antithrombin. Evidence for reactive centre loop preinsertion with expulsion upon heparin binding. Biochemistry 35, 8495-8503.

Ill, C.R. and Ruoslahti, E. (1985) Association of thrombin-antithrombin III complex with vitronectin in serum. J. Biol. Chem. 260, 15610-15615.

Izumi, M., Yamada, K.M., and Hayashi, M. (1989) Vitronectin exists in two structurally and functionally distinct forms in human plasma. Biochim. Biophys. Acta 990, 101-108.

Jardi. M., Ingeles-Esteve, J., Burgal, M., Azqueta, C., Velasco, F., Lopez-Pedrera, C., Miles, L., and Felez, J. (1996) Distinct patterns of urokinase receptor (uPAR) expression by leukemic cells and peripheral blood cells. Thromb. Hemostas. 76, 1009-1019.

Jensen, P.H., Moestrup, S.K., and Gliemann, J. (1988) Purification of the human placental alpha 2-macroglobulin receptor. FEBS Lett. 255, 275-280.

Jensen, P.H., Gliemann, J., and Orntoft, T. (1992) Characterization of carbohydrates in the α_2-macroglobulin receptor. FEBS Lett. 305, 129-132.

Jesty, J. (1979) Dissociation of complexes and their derivatives formed during inhibition of bovine thrombin and activated factor X by antithrombin III. J. Biol. Chem. 254, 1044-1049.

Jordan, R.E., Oosta, G.M., Gardner, W.T., and Rosenberg, R.D. (1980) The kinetics of hemostatic enzyme-antithrombin interactions in the presence of low molecular weight heparin. J. Biol. Chem. 255, 10081-10090.

Jornvall, H., Fish, W.W., and Bjork, I. (1979) The thrombin cleavage site in bovine antithrombin. FEBS Lett. 106, 358-362.

Joslin, G., Fallon, R.J., Bullock, J., Adams, S.P., and Perlmutter, D.H. (1991a) The SEC receptor recognizes a pentapeptide neodomain of α_1-antitrypsin-protease complexes. J. Biol. Chem. 266, 11282-11288.

Joslin, G., Krause, J.E., Hershey, A.D., Adams, S.P., Fallon, R.J., and Perlmutter, D.H. (1991b) Amyloid-ß peptide, substance P, and bombesin bind to the serpin-enzyme complex receptor. J. Biol. Chem. 266, 21897-21902.

Joslin, G., Griffin, G.L., August, A.M., Adams, S., Fallon, R.J., Senior, R.M., and Perlmutter, D.H. (1992) The serpin-enzyme complex (SEC) receptor mediates the neutrophil chemotactic effect of α_1-antitrypsin-elastase complexes and amyloid-ß peptide. J. Clin. Invest. 90, 1150-1154.

Joslin, G., Wittwer, A., Adams, S., Tollefsen, D.M., August, A., and Perlmutter, D.H.(1993) Cross-competition for binding of α_1-antitrypsin (α_1-AT)-elastase complexes to the serpin-enzyme complex receptor by other serpin-enzyme complexes and by proteolytically modified α_1-AT*. J. Biol. Chem. 268, 1886-1893.

Kalaria, R.N., Golde, T., Kroon, S.N., and Perry, G. (1993) Serine protease inhibitor antithrombin III and its messenger RNA in the pathogenesis of Alzheimer's disease. Am. J. Path. 143, 886-893.

Kanse, S.M., Kost, C., Wilhelm, O.G., Andreasen, P.A., and Preissner, K.T. (1996) The urokinase receptor is a major vitronectin-binding protein on endothelial cells. Exp. Cell Res. 224, 344-353.

Kao, F.T., Morse, H.G., Law, M.L., Lidsky, A., Chandra, T., and Woo, S.L.C. (1984) Genetic mapping of the structural gene for antithrombin III to human chromosome 1. Hum. Genet. 67, 34-36.

Kawahara, H., Cadrin, M., Perry, G., Autilio-Gambetti, L., Swierienga, S.H., Metuzals, J., Marceau, N., and French, S.W. (1990) Role of cytokeratin intermediate filaments in transhepatic transport and canalicular secretion. Hepatology 11, 435-448.

Klymkowsky, M.W. (1995) Intermediate filaments: new proteins, some answers, more questions. Curr. Opin. Cell Biol. 7, 46-54.

Knapp, A.C., Bosch, F.X., Hergt, M., Kuhn, C., Winter-Simanowski, S., Schmid, E., Regauer, S., Bartek, J., and Franke, W.W. (1989) Cytokeratins and cytokeratin filaments in subpopulations of cultured human and rodent cells of nonepithelial origin: modes and patterns of formation. Differentiation 42, 81-102.

Knauer, M.F., Hawley, S.B., and Knauer, D.J. (1997) Identification of a binding site in protease nexin 1 (PN1) required for the receptor-mediated internalization of PN1-thrombin complexes. J. Biol. Chem. 272, 12261-12264.

Knoller, S. and Savion, N. (1991) Characterization of the cellular binding domain and the effects of monoclonal antibodies and thrombin inhibitors on the binding and internalization of the antithrombin III-thrombin complex by cultured cells. Eur. J. Biochem. 195, 801-806.

Knot, E.A.R., de Jong, E., ten Cate, J.W., Iburg, A.H.C., Hennry, Ch.P., Bruin, T., and Stibbe, J. (1986) Purified rabiolabelled antithrombin III metabolism in three families with hereditary AT III deficiency:Application of a three-compartment model. Blood 67, 93-98.

Koide, T. (1979) Isolation and characterization of antithrombin III from human, porcine, and rabbit plasma, and rat serum. J. Biochem. 86, 1841-1850.

Komiyama, T., Ray, C.A., Pickup, D.J., Howard, A.D., Thornberry, N.A., Peterson, E.P., and Salvesen, G. (1994) Inhibition of interleukin-1ß converting enzyme by the cowpox virus serpin CrmA. An example of cross-class inhibition. J. Biol. Chem. 269, 19331-19337.

Kounnas, M.Z., Moir, R.D., Rebeck, G.W., Bush, A.I., Argraves, W.S., Tanzi, R.E., Hyman, B.T., and Stickland, D.K. (1995) LDL receptor-related protein, a multifunctional ApoE receptor, binds secreted ß-amyloid precursor protein and mediates its degradation. Cell 82, 331-340.

Kounnas, M.Z., Church, F.C., Argraves, W.S., and Strickland, D.K. (1996) Cellular internalization and degradation of antithrombin III-thrombin, heparin-cofactor II-thrombin, and α_1-antitrypsin-trypsin complexes is mediated by the low denstiy lipoprotein receptor-related protein. J. Biol. Chem. 271, 6523-6529.

Kovacs, T., Kalapos, P., Mandl, J., Spolarics, Z., Garzo, T., Antoni, F., and Machovich, R. (1987) Interaction of thrombin, antithrombin III and their complex with hepatocytes: comparison of the molecular components of human and mouse origin. Thromb. Res. 46, 875-880.

Kowal, R.C., Herz, J., Goldstein, J.L., Esser, V., and Brown, M.S. (1989) Low density lipoprotein receptor-related protein mediates uptake of cholesteryl esters derived from apoprotein E-enriched lipoproteins. Proc. Natl. Acad. Sci. USA 86, 5810-5814.

Kristensen, T., Moestrup, S.K., Gliemann, J., Bendtsen, L., Sand, O., and Sottrup-Jensen, L. (1990) Evidence that the newly cloned low-density-lipoprotein receptor related protein (LRP) is the alpha 2-macroglobulin receptor. FEBS Lett. 276, 151-155.

Ku, N-O. and Omary, M.B. (1994) Identification of the major physiologic phosphorylation site of human keratin 18: potential kinases and a role in filament reorganization. J. Cell Biol. 127, 161-171.

Ku, N-O. and Omary, M.B. (1995) Identification and mutational analysis of the glycosylation sites of human keratin 18. J Biol. Chem. 270, 11820-11827.

Ku, N-O., Michie, S., Oshima, R.G., and Omary, M.B. (1995) Chronic hepatitis, hepatocyte fragility, and increased soluble phosphoglycokeratins in transgenic mice expressing a keratin 18 conserved arginine mutant. J. Cell Biol. 131, 1303-1314.

Ku, N-O., Michie, S.A., Soetikno, R.M., Resurrection, E.Z., Broome, R.L., Oshima, R.G., Omary, M.B. (1996) Susceptibility to hepatoxicity in transgenic mice that express a dominant-negative human keratin 18 mutant. J. Clin. Invest. 98, 1034-1046.

Kuiper, J., Rijken, D.C., de Munk, G.A.W., and van Berkel, T.J.C. (1992) In vivo and in vitro interaction of high and low molecular weight singl-chain urokinase-type plasminogen activator with rat liver cells. J. Biol. Chem. 267, 1589-1595.

Kulesh, D.A. and Oshima, R.G. (1988) Cloning of the human keratin 18 gene and its expression in nonepithelial mouse cells. Mol. Cell. Biol. 8, 1540-1550.

Kulesh, D.A., Cecena, G., Darmon, Y.M., Vasseur, M., and Oshima, R.G. (1989) Posttranslational regulation of keratins: degradation of mouse and human keratins 18 and 8. Mol. Cell. Biol. 9, 1553-1565.

Laemmli, U.K. (1970) Cleavage of structural proteins during the assembly of the head of the bacteriophage T4. Nature 227, 680-685.

Lala, A.K. and Raja, S.M. (1995) Photolabeling of a pore-forming toxin with the hydrophobic probe 2-[^{3}H]Diazofluorene: Identification of membrane-inserted segments of *Staphylococcus aureas* α-toxin. J. Biol. Chem. 270, 11348-11357.

Lane, D.A., Denton, J., Flynn, A.M., Thunberg, L., and Lindahl, U. (1984) Anticoagulant acitivities of heparin oligosaccharides and their neutralization by platelet factor 4. Biochem. J. 218, 725-732.

Lane, D.A., Olds, R.J., Boisclair, M., Chowdhury, V., Thein, S.L., Cooper, D.N., Blajchman, M.A., Perry, D., Emmerich, J., and Aiach, M. (1993) Antithrombin III mutation database:first update. Thromb. Haemostas. 70, 361-369.

Lawson, J.H., Butenas, S., Ribarik, N., and Mann, K.G. (1993) Complex-dependent inhibition of factor VIIa by antithrombin and heparin. J. Biol. Chem. 268, 767-770.

Lechner, K., Niessner, H., and Thaler, E. (1977) Coagulation abnormalities in liver disease. Semin. Thromb. Haemostas. 4, 40-56.

Lee, C., Levin, A., and Branton, D. (1987) Copper staining: a five-minute protein stain for sodium dodecyl sulfate-polyacrylamide gels. Anal. Biochem. 166, 308-312.

Leon, M., Aiach, M., Coezy, E., Guennec, J-Y., and Fiessinger, J-N. (1983) Antithrombin III synthesis in rat liver parenchymal cells. Thromb. Res. 30, 369-382.

Letocha, H., Nilsson, S., Silen, A., Ekblom, J., Arnberg, H., Wiklund, B., and Westlin, J. (1993) Immunotargeting with monoclonal cytokeratin 8 antibodies of human urothelial cancer transplanted to nude mice. Acta Oncologica 32, 793-800.

Leube, R.E., Bosch, F.X., Romano, V., Zimbelmann, R., Hofler, H., and Franke, W. (1986) Cytokeratin expression in simple epithelia III: detection of mRNAs encoding human cytokeratins nos. 8 and 18 in normal and tumor cells by hybridization with cDNA sequences in vitro and in situ. Differentiation 33, 69-85.

Lee, A.K.Y., Chan, V., and Chan, T.K. (1979) The identification and localization of antithrombin III in human tissues. Thromb. Res. 14, 209-217.

Li, Y., Wood, N., Parsons, P.G., Yellowlees, D., and Donnelly, P.K. (1997) Expression of alpha2-macroglobulin receptor/low density lipoprotein receptor-related protein on surfaces of tumor cells: a study using flow cytometry. Canc. Lett. 111, 199-205.

Liang, O.D., Rosenblatt, S., Chhatwal, G.S., and Preissner, K.T. (1997) Identification of novel heparin-binding domains of vitronectin. FEBS Letts. 407, 169-172.

Liao, J., Lowthert, L.A., Ku, N-O., Fernandez, R., and Omary, M.B. (1995) Dynamics of human keratin 18 phosphorylation: polarized distribution of phosphorylated keratins in simple epithelial tisses. J. Cell Biol. 131, 1291-1301.

Lindo, V.S., Kakkar, V.V., and Melissari, E. (1995) Cleaved antithrombin (ATc) a new marker for thrombin generation and activation of the coagulation system. Brit. J. Haematol. 89, 157-162.

Liu, L., Dewar, L., Song, Y., Kulczycky, K., Blajchman, M.A., Fenton II, J.W., Andrew, M., Delorme, M., Ginsberg, J., Preissner, K.T., and Ofosu, F.A. (1995) Inhibition of thrombin by antithrombin III and heparin cofactor II in vivo. Thromb. Haemostas. 73, 405-412.

Loeberman, H., Tokuoka, R., Deisenhofer, J., and Huber, R. (1984) Human α_1-proteinase inhibitor: crystal structure analysis of two crystal modifications, molecular model and preliminary analysis of the implications for function. J. Mol. Biol. 177, 531-556.

Loewinger, L. and McKeon, F. (1988) Mutations in the nuclear lamin proteins resulting in their aberrant assembly in the cytoplasm. Eur. Mol. Biol. Organ. J. 7, 2301-2309.

Longas, M.O., and Finlay, T.H. (1980) The covalent nature of the human antithrombin III-thrombin bond. Biochem. J. 189, 481-487.

Luomu, J., Hiltunen, T., Sarkioja, T., Moestrup, S.K., Gliemann, J., Kodama, T., Nikkari, T., and Yla-Herttuala, S. (1994) Expression of α_2-macroglobulin recptor/low density lipoprotein receptor-related protein and scavenger receptor in human atherosclerotic lesions. J. Clin. Invest. 93, 2014-2021.

Lupu, F., Heim, D., Bachmann, F., and Kruithof, E.K. (1994) Expression of LDL-receptor-related protein in human normal and atherosclerotic arteries. Arterio. Thromb. 14, 1438-1444.

Maekawa, H. and Tollefsen, D.M. (1996) Role of the proposed serpin-enzyme complex receptor recognition site in binding and internalization of thrombin-heparin cofactor II complexes by hepatocytes. J. Biol. Chem. 271,18604-18609.

Malek, R., Aulak, K.S., and Davis, A.E. (1996) The catabolism of intact, reactive-centre cleaved and proteinase-complexed C1 inhibitor in the guinea pig. Clin. Exp. Immunol. 105, 191-197.

Marceau, N. and Loranger, A. (1995) Cytokeratin expression, fibrillar organization, and subtle function in liver cells. Biochem. Cell Biol. 73, 619-625.

Mast, A.E., Enghild, J.J., Pizzo, S.V., and Salvesen, G. (1991) Analysis of the plasma elimination kinetics and conformational stabilities of the native, proteinase-complexed, and reactive site cleaved serpins: comparison of α_1-proteinase inhibitor, α_1-antichymotrypsin, antithrombin III, and α_2-antiplasmin, angiotensinogen, and ovalbumin. Biochemistry 30, 1723-1730.

Mazar, A.P., Buko, A., Petros, A.M., Barnathan, E.S., and Henkin, J. (1992) Domain analysis of urokinase plasminogen activator (u-PA): preparation and characterization of intact A-chain molecules. Fibrinolysis 6, Suppl. 1, 49-55.

McLachlan, A.D. (1978) Coiled coil formation and sequence regularities in the helical regions of alpha-keratin. J. Mol. Biol. 124, 297-304.

Medjoub, H., Leret, M., Boulanger, Y., Mamman, M., Choay, J., and Rheinbolt, J. (1991) The complete amino acid sequence of bovine antithrombin (AT-III) J. Protein Chem. 10, 205-212.

Meiklejohn, B., Nagle, R.B., McDaniel, K.M., and Wilson, G.S. (1990) Improved methods for separation of human cytokeratins. Life Sci. 47, 637-645.

Mellerick, D.M., Osborn, M., and Weber, K. (1990) On the nature of serological tissue polypeptide antigen (TPA);monoclonal keratin 8,18, and 19 antibodies react differently with TPA prepared from human cultured carcinoma cells and TPA in human serum. Oncogene 5, 1007-1017.

Menache, D., O'Malley, J.P., Schorr, J.B., Wagner, B., Williams, C., and the Cooperative Study Group (1990) Evaluation of the safety, recovery, half-life and clinical efficacy of antithrombin III (human) in patients with hereditary antithrombin III deficiency. Blood 75, 33-39.

Meng, J-J., Khan, S., and Ip, W. (1996) Intermediate filament protein domain interactions as revealed by two-hybrid screens. J. Biol. Chem. 271, 1599-1604.

Mikhailenko, I., Kounnas, M.Z., and Strickland, D. (1995) Low density lipoprotein receptor-related protein/α_2-macroglobulin receptor mediates the cellular internalization and degradation of thrombospondin. J.Biol. Chem. 270, 9543-9549.

Miller-Andersson, M., Borg, H., and Andersson, L-O. (1974) Purification of antithrombin III by affinity-chromatography. Thromb. Res. 5, 439-452.

Mimuro, J. and Loskutoff, D.J. (1989) Purification of a protein from bovine plasma that binds to type 1 plasminogen activator inhibitor and prevents its interaction with extracellular matrix. J. Biol. Chem. 264, 936-939.

Mizuochi, T., Fuji, J., Kurachi, K., and Kobata, A. (1980) Structural studies of the carbohydrate moiety of human antithrombin III. Arch. Biochem. Biophys. 203, 458-465.

Moll, R., Franek, W.W., Schiller, D.L., Geiger, B., and Krepler, R. (1982) The catalog of human cytokeratins in normal epithelia, tumors, and cultured cells.Cell 31, 11-24.

Moestrup, S.K. and Gliemann, J. (1989) Purification of the rat hepatic α_2-macroglobulin receptor as an approximately 440 kDa single chain protein. J. Biol. Chem. 264, 15574-15577.

Moestrup, S.K., Gliemann, J., and Pallesen, G. (1992) Distribution of the α_2-macroglobulin receptor/low density lipoprotein receptor-related protein in human tissues. Cell Tissue Res. 269, 375-382.

Moestrup, S.K., Nielsen, S., Andreasen, P., Jorgensen, K.E., Nykaer, A., Roigaard, H., Gliemann, J., and Christensen, E.I. (1993) Epithelial glycoprotein-330 mediates endocytosis of plasminogen activator-plasminogen activator inhibitor type-1 complexes. J.Biol. Chem. 268, 16564-15570.

Morawitz, P. (1905) Die Chemie der Blutgerinnung. Ergeb. Physiol. 4, 307.

Moroianu, J.W., Fett, J.W., Riordan, J.F. and Vallee, B.L. (1993) Actin is a surface component of calf pulmonary artery endothelial cells in culture. Proc. Natl. Acad. Sci. USA 90, 3815-3819.

Mourey, L., Samama, J.P., Delarue, M., Petitou, M., Choay, J., Moras, D. (1990) Crystal structure of cleaved bovine antithrombin-III at 3.2 Angstrom resolution. J. Mol. Biol. 218, 595-606.

Narita, M., Bu, G., Olins, G.M., Higuchi, D.A., Herz, J., Broze Jr., G.J., Schwartz, A.L. (1995) Two receptor systems are involved in the plasma clearance of tissue factor pathway inhibitor in vivo. J. Biol. Chem. 270, 24800-24804.

Nielsen, K.L., Holtet, T.L., Etzerodt, M., Moestrup. S.K., Gliemann, J., Sottrup-Jensen, L., and Thogersen, H.C. (1996) Identification of residues in α-macroglobulins important for binding to the α_2-macroglobulin receptor/low density lipoprotein receptor-related protein. J. Biol. Chem. 271, 12909-12912.

Niessen, R.W.L.M., Sturk, A., Hordijk, P., Michiels, F., and Peters, M. (1992) Sequence characterization of a sheep cDNA for antithrombin III. Biochem. Biophys. Acta 1171, 207-210.

Novotny, W.F., Brown, S.G., Miletich, J.P., Rader, D.J., and Broze Jr., G.J. (1991) Plasma antigen levels of the lipoprotein-associated coagulation inhibitor in patient samples. Blood 78, 387-393.

Nykjaer, A., Petersen, C.M., Moller, B., Jensen, P.H., Moestrup, S.K., Holtet, T.L., Etzerodt, M., Thogersen, H.C., Munch, M., Andreasen, P.A., and Gliemann, J. (1992) Purified alpha$_2$-macroglobulin receptor/LDL receptor-related protein binds urokinase plasminogen activator inhibitor type-1 complex. Evidence that the alpha2-macroglobulin receptor mediates cellular degradation of urokinase receptor-bound complexes. J. Biol. Chem. 267, 14543-14546.

Nykjaer, A., Bengtsson-Olivecrona, G., Lookene, A., Moestrup, S.K., Petersen, C.M., Weber, W., Beisiegel, U., and Gliemann, J. (1993) The α_2-macroglobulin receptor/low density lipoprotein receptor-related protein binds lipoprotein lipase and ß-migrating very low density lipoprotein associated with the lipase. J. Biol. Chem. 268, 15048-15055.

Ohlsson, K., Ganrot, P.O., and Laurell, C.B. (1971) In vivo interaction between trypsin and some plasma proteins in relation to the tolerance to intravenous trypsin infusion in dog. Acta Chir. Scand. 137, 113-121.

Ohlsson, K. (1971) Elimination of ^{125}I-Trypsin α-macroglobulin complexes from blood by reticuloendothelial cells in dog. Acta Physiol. Scand. 81, 269-272.

Ohlsson, K. and Laurell, C.B. (1976) The disappearance of enzyme-inhibitor complexes from the circulation of man. Clin. Sci. Mol. Med. 51, 87-92.

Okanoue, T., Ohta, M., Fushiki, S., Ou, O., Kachi, K., Okuno, T., Takino, T., and S. French, S.W. (1985). Scanning electron microscopy of the liver cell cytoskeleton. Hepatology 5, 1-6.

Olds, R.J., Lane, D.A., Chowdhury, V., De Stefano, V., Leone, G., and Lay Thein, S. (1993) Complete nucleotide sequence of the antithrombin gene: evidence for homologous recombination causing thrombophilia. Biochemistry 32, 4216-4224.

Olson, S.T., and Bjork, I. (1991) Predominant contribution of surface approximation to the mechanism of heparin acceleration of the antithrombin-thrombin reaction. Elucidation from salt concentration effects. J. Biol. Chem. 266, 6353-6364.

Olson, S.T., Bjork, I., Sheffer, R., Craig, P.A., Shore, J.D., and Choay, J. (1992) Role of the antithrombin-binding pentasaccharide in heparin acceleration of antithrombin-proteinase reactions. Resolution of the antithrombin conformational change contribution to heparin rate enhancement. J. Biol. Chem. 267, 12528-12538.

Olson, S.T., Stephens, A.W., Hirs, C.W., Bock, P.E., and Bjork, I. (1995) Kinetic characterization of the proteinase binding defect in a reactive site variant of the serpin,antithrombin. Role of the P1' residue in transition state stabilization of antithrombin-proteinase complex formation. J. Biol. Chem. 270, 9717-9724.

O'Malley, K.M., Nair, S.A., Rubin, H., and Cooperman, B.S. (1997) The kinetic mechanism of serpin-proteinase complex formation: an inermediate between the michaelis complex and the inhibited complex. J. Biol. Chem. 272, 5354-5359.

Orth, K., Madison, E.L., Gething, M-J., Sambrook, J.F., and Herz, J. (1992) Complexes of tissue-type plasminogen activator and its serpin inhibitor plaminogen-activator inhibitor type 1 are internalized by means of the low density lipoprotein receptor-related protein/α_2-macroglobulin receptor. Proc. Natl. Acad. Sci. USA. 89, 7422-7426.

Oshima, R.G., Millan J.L., and Cecena, G. (1986) Comparison of mouse and human keratin 18: a component of intermediate filaments expressed prior to implantation. Differentiation 33, 61-68.

Oshima, R.G., Trevor, K., Shevinksy, L.H., Ryder, O.A., and Cecena, G. (1988) Identification of the gene coding for the Endo B murine cytokeratin and its methylated, stable inactive state in mouse nonepithelial cells. Genes Dev. 2, 505-516.

Owen, M.C. (1975) Evidence for the formation of an ester between thrombin and heparin cofactor. Biophys. Biochem. Acta 405, 380-387.

Pang, S.Y-Y., Schermer, A., Yu, J., and Sun, T-T. (1993) Suprabasal changes and subsequent formation of disulfide-stabilized homo- and hetero-dimers of keratins during esophageal epithelial differentiation. J. Cell Sci. 104, 727-740.

Pankov, R., Umezawa, A., Maki, R., Der, R.J., Hauser, C.A., Oshima, R.G. (1994) Oncogene activation of human keratin 18 transcription via the Ras signal transduction pathway. Proc. Natl. Acad. Sci. USA. 91, 873-877.

Patston, P.A., Gettins, P., Beechem, J., and Schapira, M. (1991) The mechanism of serpin action: evidence that C1-inhibitor functions as a suicide substrate. Biochemistry 30, 8876-8882.

Patston, P.A., Medcalf, R.L., Kourteva, Y., and Schapira, M. (1993) C1-inhibitor-serine proteinase complexes and the biosynthesis of C1-inhibitor by Hep G2 and U 937 cells. Blood 82, 3371-3379.

Patston, P.A., Gettins, P., and Schapira, M. (1994) The mechanism by which serpins inhibit thrombin and other serine proteinases. Ann. N.Y. Acad. Sci. 714, 13-20.

Peake, P.W., Greenstein, J.D., Pussell, B.A., and Charlesworth, J.A. (1997) The behaviour of human vitronectin in vivo: effects of complement activation, conformation, and phosphorylation. Clin. Exp. Immunol. 106, 416-422.

Perides, G., Harter, C., and Traub, P. (1987). Electrostatic and hydrophobic interactions of the intermediate filament protein vimentin and its amino terminus with lipid bilayers. J. Biol. Chem. 262, 13742-13749.

Perlmutter, D.H., and Punsal, P.I. (1988) Distinct and additive effects of elastase and endotoxin on expression of α_1 proteinase inhibitor in mononuclear phagocytes. J. Biol. Chem. 263, 16499-16503.

Perlmutter, D.H., Travis, J., and Punsal, P.I. (1988) Elastase regulates the synthesis of its inhibitor, α_1-proteinase inhibitor, and exaggerates the defect in homozygous PiZZ α_1PI deficiency. J. Clin. Invest. 81, 1774-1780.

Perlmutter, D.H., Glover, G.I., Rivetna, M., Schasteen, C.S., and Fallon, R.J. (1990) Identification of a serpin-enzyme complex receptor on human hepatoma cells and human monocytes. Proc. Natl. Acad. Sci. U.S.A. 87, 3753-3757.

Perlmutter, D.H. (1994) The SEC receptor: a possible link between neonatal hepatitis in α_1-antitrypsin deficiency and Alzheimer's disease. Ped. Res. 36, 271-277.

Perry, D.J. and Carrell, R.W. (1992) Identification of antithrombin mRNA in peripheral blood lymphocytes and its use in the characterization of antithrombin variants. Br. J. Haematol. 80, 2a.

Perry, D.J. (1994) Antithrombin and its inherited deficiences. Blood Rev. 8, 56-62.

Peterson, C.B., and Blackburn, M.N. (1985) Isolation and characterization of a antithrombin-III variant with reduced carbohydrate content and enhanced heparin binding. J. Biol. Chem. 260, 1723-1729.

Peterson, C.B., Noyes, C.M., Pecon, J.M., Church, F.C., and Blackburn, M. (1987) Identification of a lysyl residue in antithrombin which is essential for heparin binding. J. Biol. Chem. 262, 8061-8065.

Peterson, T.E., Dudek-Wojciechowska, G., Sottrup-Jensen, L., plus others. (1979) Primary structure of antithrombin III (heparin cofactor). Partial homology between α_1-antitrypsin and antithrombin III, in Collen, D., Wiman, B. and Verstraete, M. (eds): The Physiological Inhibitors of Coagulation and Fibrinolysis. Amsterdam, The Netherlands, Elsevier, North-Holland Biomedical Press pp 43-54.

Pike, C.J., Walencewicz-Wasserman, A.J., Kosmoski, J., Cribbs, D.H., Glabe, C.G., and Cotman, C.W. (1995) Structure-activity analyses of beta-amyloid peptides: contributions of the beta 25-35 region to aggregation and neurotoxicity. J. Neurochem. 64, 253-265.

Pizzo, S.V., Mast, A.E., Feldman, S.R., and Salvesen, G. (1988) In vivo catabolism of α_1-antichymotrypsin is mediated by the serpin receptor whichs binds α_1-proteinase inhibitor, antithrombin III, and heparin cofactor II. Biochim. Biophys. Acta. 967, 158-162.

Pizzo, S.V. (1990) Serpin receptor 1: a hepatic receptor that mediates the clearance of antithrombin III-proteinase complexes. Am. J. Med. 87, 10S-14S.

Plotnick, M.I., Mayne, L., Schechter, N.M., and Rubin, H. (1996) Distortion of the active site of chymotrypsin complexed with a serpin. Biochemistry 35, 7586-7590.

Podack, E.R., Kolb, W.P., and Muller-Eberhard, H.J. (1977) The SC5b-7 complex: formation, isolation, properties, and subunit composition. J. Immunol. 119, 2024-2029.

Podack, E.R., Dahlback, B., and Griffin, J.H. (1986) Interaction of S-protein of complement with thrombin and antithrombin during coagulation, Protection of thrombin by S-protein from antithrombin III inactivation. J.Biol. Chem. 261, 7387-7392.

Poller, W., Willnow, T.E., Hilpert, J., and Herz, J. (1995) Differential recognition of α_1-anitrypsin-elastase and α_1-antichymotrypsin-cathepsin G complexes by the low density lipoprotein receptor-related protein. J. Biol. Chem. 270, 2841-2845.

Polson, A. (1990) Isolation of IgY from the yolks of eggs by a chloroform polyethylene glycol procedure. Immun. Invest. 19, 253-258.

Pratt, C.W., Church, F.C., and Pizzo, S.V. (1988) In vivo catabolism of heparin cofactor II and its complex with thrombin: evidence for a common receptor-mediated clearance pathway for three serine proteinase inhibitors. Arch. Biochem. Biophys. 262, 111-117.

Preissner, K.T. and Muller-Berghaus, G. (1987) Neutralization and binding of heparin by S-protein/vitronectin in the inhibition of factor Xa by antithrombin III. J. Biol. Chem. 262, 12247-12253.

Preissner, K.T. and Sie, P. (1988) Modulation of heparin cofactor II function by S protein (vitronectin) and formation of a ternary S protein-thrombin-heparin cofactor II complex. Thromb. Haemostas. 60, 399-406.

Preissner, K.T. and Jenne, D. (1991) Structure of vitronectin and its biological role in haemostasis. Thromb. Hemostas. 66, 123-132.

Preissner, K.T., de Boer, H., Pannekoek, H., and de Groot, P.G. (1996) Thrombin regulation by physiolgical inhibitors: the role of vitronectin. Semin. Thromb. Hemostas. 22, 165-172.

Prochownik, E.V., Markham, A.F., and Orkin, S.H. (1983) Isolation of a cDNA clone for human antithrombin III. J. Biol. Chem. 258, 8389-8394.

Rao, L.V., Williams, T., and Rapaport, S.I. (1996) Studies of the activation of factor VII bound to tissue factor. Blood 88, 3664-3666.

Ratnoff, O.D. (1982) Disordered hemostasis in hepatic disease, in Schiff, L. Schiff, E.R. (eds): Diseases of the Liver. Philadelphia, J.B. Lippincott, pp. 237-258.

Rebeck, G.W., Harr, S.D., Strickland, D.K., and Hyman, B.T. (1995) Multiple, diverse senile plaque-associated proteins are ligands of an apolipoprotein E receptor, the α_2-macroglobulin receptor/low-density-lipoprotein receptor-related protein. Ann. Neurol. 37, 211-217.

Remold-O'Donnell, E. (1993) The ovalbumin family of serpin proteins. FEBS Lett. 315, 105-108.

Riklund, K.E., Makiya, R., Sundstrom, B., Back, O., Henriksson, R., Hietala, S-O., and Stigbrand, T. (1991) Inhibition of growth of Hela cell tumours in nude mice by ^{125}I-labelled anticytokeratin and antiPLAP monoclonal antibodies. Anticancer Res. 11, 555-560.

Riopel, C.L., Butt, I., and Omary, M.B. (1993) Method of cell handling affects leakiness of cell surface labeling and detection of intracellular keratins. Cell Motil. Cytoskel. 26, 77-78.

Romano, V., Hatzfeld, M., Magin, T.M., Zimbelmann, R., Franke, W., Maier, G., and Ponstingl, H. (1986) Cytokeratin expression in simple epithelia I: identification of mRNA coding for human cytokeratin no. 18 by a cDNA clone. Differentiation 30, 244-253.

Rosenberg, R.D., and Damus, P.S. (1973) The purification and mechanism of action of human antithrombin-heparin cofactor. J. Biol. Chem. 248, 6490-6505.

Rosenblatt, D.E., Geula, C., and Mesulam, M-M. (1989) Protease nexin I immunostaining in Alzheimer's disease. Ann. Neurol. 26, 628-634.

Rovelli, G., Stone, S.R., Preissner, K.T., and Monard, D. (1990) Specific interaction of vitronectin with the cell-secreted protease inhibitor glia-derived nexin and its thrombin complex. Eur. J. Biochem. 192, 797-803.

Savion, N. and Farzame, N. (1984) Binding uptake and degradation of antithrombin III-protease complexes by cultured corneal endothelial cells. Exp. Cell. Res. 153, 50-60.

Savion, N. and Farzame, N. (1986) Comparative study of antithrombin III-protease complex metabolism by fibroblasts and vascular endothelial cells. Thromb. Res. 41, 459-471.

Sahyoun, N., Stenbuck, P., Levine III, H., Bronson, D., Moncharmont, B., Henderson, C., and Cuatrecasas, P. (1982) Formation and identification of cytoskeletal components from liver cytosolic precursors. Proc. Natl. Acad. Sci. USA. 79, 7341-7345.

Schechter, I. and Berger, A. (1967) On the size of the active site in proteinases. I. Papain. Biochem. Biophys. Res. Comm. 27, 157-162.

Schmaier, A.H. (1997) Contact activation: a revision. Thromb. Haemostasis 78, 101-107.

Schreuder, H.A., de Boer, B., Dijkema, R., Mulders, I., Theunissen, H.I.M., Grootenhuis, P.D.I., and Hol, W.G.J. (1994) The intact and cleaved antithrombin III complex as a model for serpin-proteinase interactions. Nature Struct. Biol. 1, 48-54.

Schwartz. A.L. (1995) Receptor cell biology: receptor mediated endocytosis. Pediatric Res. 38, 835-843.

Schulze, A.J., Baumann, U., Knof, S., Jaeger, E., Huber, R., and Laurell, C.B. (1992) Structural transition of α_1-antitrypsin by a peptide sequentially similar to ß-strand s4A. Eur. J. Biochem. 194, 51-56.

Schulze, A.J., Huber, R., Bode, W., and Engh, R.A. (1994). Structural aspects of serpin inhibition. FEBS Letters 344,117-124.

Schuster, M.G., Enriquez, P.M., Curran, P., Cooperman, B.S., and Rubin, H. (1992) Regulation of neutrophil superoxide by antichymotrypsin-chymotrypsin complexes. J. Biol. Chem. 267, 5056-5059.

Seegers, W.H., Johnson, J.F., and Fall, C. (1954) An antithrombin reaction related to prothrombin activation. Am. J. Physiol. 176, 97-103.

Sheffield, W.P., Brothers, A.B., Wells, M.J., Hatton, M.W.C., Clarke, B.J., and Blajchman, M.A. (1992) Molecular cloning and expression of rabbit antithrombin III. Blood 79, 2330-2339.

Sheffield, W.P., Wu, Y., and Blajchman, M.A. (1995) Antithrombin: structure and function, In High, K.A. and Roberts, H.R. (eds): Molecular Basis of Thrombosis and Hemostasis. Marcel Dekker Inc., New York. pp. 355-377.

Shifman, M.A. and Pizzo, S.V. (1988) The in vivo metabolism of antithrombin III and antithrombin III complexes. J. Biol. Chem. 257, 3243-3248.

Sie, P., Lansen, J., Lachertez, F., Verschuere, B., and Boneu, B. (1986) Comparative turn-over of heparin cofactor II and antithrombin III in baboons. Thromb. Haemostas. 56, 302-307.

Simon, D. I., Xu, H., and Vaughan, D.E. (1995) Cathepsin D-like aspartyl protease activity mediates the degradation of tissue-type plasminogen activator/plasminogen activator inhibitor-1 complexes in human monocytes. Biochem. Biophys. Acta. 1268, 143-151.

Singer, P.A., Trevor, K., and Oshima, R.G. (1986) Molecular cloning and characterization of the Endo B cytokeratin expressed in preimplantation mouse embryos. J. Biol. Chem. 261, 538-547.

Soellner, P., Quinlan, R.A., and Franke, W. (1985) Identification of a distinct soluble subunit of an intermediate filament protein: tetrameric vimentin from living cells. Proc. Natl. Acad. Sci. USA. 82, 7929-7933.

Soroka, C.J. and Farqhuar, M.G. (1991) Characterization of a novel heparan sulfate proteoglycan found in the extracellular matrix of liver sinusoids and basement membranes. J. Cell Biol. 113, 1231-1241.

Splarics, Z., Kalapos, M.P., Lerant, I., Garzo, T., Antoni, F., Mandl, J., and Machovich, R. (1989) Association of thrombin, plasmin, thrombin-antithrombin III complex, and plasmin-antithrombin III complex with isolated hepatocytes. Biochim. Biophys. Acta. 1012, 231-236.

Stackhouse, R., Chandra, T., Robson, K.J.H., and Woo, S.L.C. (1983) Purification of antithrombin III mRNA and cloning of its cDNA. J. Biol. Chem. 258, 703-706.

Stavridi, E.S., O'Malley, K., Lukacs, C.M., Moore, W.T., Lambris, J.D., Christianson, D.W., Rubin, H., and Cooperman, B.S. (1996) Structural change in α-chymotrypsin induced by complexation with α_1-antichymotrypsin as seen by enhanced sensitivity to proteolysis. Biochemistry 35, 10608-10615.

Stefansson, S., Kounnas, M.Z., Henkin, J., Mallampalli, R.K., Chappell, D.A., Strickland, D.K., and Argraves, W.S. (1995) gp330 on type II pneumocytes mediates endocytosis leading to degradation of pro-urokinase, plasminogen activator inhibitor-1 and urokinase-plasminogen activator inhibitor-1 complex. J. Cell Sci. 108, 2361-2368.

Stefansson, S., Lawrence,D.A., and Argraves, W.S. (1996) Plasminogen activator inhibitor-1 and vitronectin promote the cellular clearance of thrombin by low density lipoprotein receptor-related proteins 1 and 2. J. Biol. Chem. 271, 8215-8220.

Stein, P.E. and Carrell, R.W. (1995) What do dysfunctional serpins tell us about molecular mobility and disease? Nat. Struct. Biol. 2, 96-113.

Steinert, P.M., Idler, W.W., and Zimmerman, S.B. (1976) Self-assembly of bovine epidermal keratin filaments *in vitro*. J. Mol. Biol. 108, 547-576.

Steinert, P.M. (1990) The two-chain coiled-coil molecule of native epidermal keratin intermediate filaments is a type-I-type-II heterodimer. J. Biol. Chem. 265, 8766-8774.

Steinert, P.M. (1991) Organization of coiled-coil molecules in native mouse keratin 1/keratin 10 intermediate filaments: evidence for alternating rows of antiparallel in-register and antiparallel staggered molecules. J. Struct. Biol. 107, 157-174.

Steinert, P.M. (1993) Structure, function, and dynamics of keratin intermediate filaments. J. Invest. Derm. 100, 729-734.

Stephens, A.W., Siddiqui, A., and Hirs, C.H.W. (1988) Site-directed mutagenesis of the reactive centre (serine 394) of antithrombin III. J. Biol. Chem. 263, 15849-15852.

Stephens, A.W., Thalley, B.S., and Hirs, C.H.W. (1987) Antithrombin-III-Denver, a reactive site variant. J. Biol. Chem. 262, 1044-1048.

Stockmann, A., Hess, S., Declerck, P., Timpl, R., and Preissner, K.T. (1993) Multimeric vitronectin. Identification and characterization of conformation-dependent self-association of the adhesive protein. J. Biol. Chem. 268,22874-22882.

Strickland, D.K., Ashcom, J.D., Williams, S., Burgess, W.H., Migliorini, M., and Argraves, W.S. (1990) Sequence identity between the α2-macroglobulin receptor and low density lipoprotein receptor-related protein suggests that this molecule is a multifunctional receptor. J.Biol. Chem. 265, 17401-17404.

Strickland, D.K., Kounnas, M.Z., and Argraves, W.S. (1995) LDL receptor-related protein: a multiligand receptor for lipoprotein and proteinase catabolism. FASEB 9, 890-897.

Strittmatter, W.J., Saunders, A.M., Schmechel, D., Pericak-Vance, M., Enghild, J., Salvesen, G.S., and Roses, A.D. (1993) Apolipoprotein E: high avidity binding to ß-amyloid and increased frequency of type 4 allele in late-onset familial Alzheimer's locus. Proc. Natl. Acad. Sci. USA 90, 1977-1981.

Stump, D.C., Kieckens, L., de Cock, F., and Collen, D. (1987) Pharacokinetics of single chain forms of urokinase-type plasminogen activator. J. Pharm. Exp. Ther. 242, 245-250.

Sudhof, T.C., Goldstein, J.L., Brown, M.S., and Russell, D.W. (1985) The LDL receptor gene: a mosaic of exons shared with different proteins. Science 23, 815-822.

Sun, X.-J., and Chang, J.-Y. (1989) Heparin binding domain of human antithrombin III inferred from the sequential reduction of its three disulfide linkages. J. Biol. Chem. 264, 11288-11293.

Sundstrom, B.E. and Stigbrand, T.I. (1994) Cytokeratins and tissue polypeptide antigen. Int. J. Biol. Markers 9, 102-108.

Taddei-Peters, W.C., Haspel, M.V., Vente, P., Murray, J.L, Cleary, K.R., Levin, B., Paris, E.M., Pomato, N., Murray, J.H., Weidman, D., Hanna Jr., M.G., and McCabe, R.P. (1992) Quantitation of human tumor-reactive monoclonal antibody 16.88 in the circulation and localization of 16.88 in colorectal metastatic tumor tissue using murine antiidiotypic antibodies. Cancer Res. 52, 2603-2609.

Takeda, A., Yamamoto, T., Nakamura, Y., Takahashi, T., Hibino, T. (1985) Squamous cell carcinoma antigen is a potent inhibitor or cysteine proteinase cathepsin L. FEBS Lett. 359, 78-80.

Takenouchi, T. and Munekata, E. (1995) ß-amyloid peptide, substannce P, and SEC receptor ligand activate cytoplasmic Ca^{+2} in neutrophil-like HL-60 cells:effect of chemotactic peptide antagonist BocMLF. Peptides 16, 1019-1024.

Takeya, H., Hamada, T., Kume, M., and Suzuki, K. (1994) Receptor mediated endocytosis of thrombin-antithrombin III complex by the human monocytoid cell line U937. Biochem. Biophys. Res. Commun. 200, 1334-1340.

Tejada, M.L. and Deeley, R.G. (1995) Cloning of an avian antithrombin: developmental and hormonal regulation of expression. Thromb. Haemostas. 73, 654-661.

Theunissen, H.J.M., Dijkema, R., Grootenhuis, P.D.J., Swinkels, J.C., de Poorter, T.L., Carati, P., and Visser, A. (1993) Dissociation of heparin-dependent thrombin and factor Xa inhibitory activities of antithrombin-III by mutations in the reactive site. J. Biol. Chem. 268, 9035-9040.

Tokunaga, F., Goto, T., Wakabayashi, S., and Koide, T. (1994) Amino acid sequence of porcine antithrombin III. J. Biochem. 116, 1164-1170.

Tomasini, B.R. and Mosher, D.F. (1986) On the identity of vitronectin and S-protein: immunological crossreactivity and functional studies. Blood 68, 737-742.

Tomasini, B.R. and Mosher, D.F. (1990) Vitronectin. Prog. Hemost. Thromb. 10, 269-305.

Traub, P., Kuhn, S., and Grub, S. (1993) Separation and characterization of homo and hetero-oligomers of the intermediate filament proteins desmin and vimentin. J. Mol. Biol. 230, 837-856.

Trevor, K. and Oshima, R.G. (1985) Preimplantation mouse embryos and liver express the same type I keratin gene product. J. Biol. Chem. 260, 15885-15891.

van Boeckel, C.A.A., Grootenhuis, P.D.J., and Visser, A. (1994) A mechanism for heparin-induced potentiation of antithrombin III. Nature Struct. Biol. 1, 423-425.

van der Kaaden, M.E., Rijken, D. C., Kruijt, J.K., van Berkel, T.J.C., and Kuiper, J. (1997) The role of the low-density lipoprotein receptor-related protein (LRP) in the plasma clearance and liver uptake of recombinant single-chain urokinase-type plasminogen activator in rats. Thromb. Haemostas. 77, 710-717.

Van Eyken, P. and Desmet, V.J.(1993). Cytokeratins and the liver. Liver 13, 113-122.

van Meijer, M., Stoop, A., Smilde, A., Preissner, K.T., van Zonneveld, A.J., and Pannekoek, H. (1997) The composition of complexes between plasminogen activator inhibitor 1, vitronectin, and either thrombin or tissue-type plasminogen activator. Thromb. Hemostas. 77, 516-521.

Vassalli, J.D., Baccino, D., and Belin, D. (1985) A cellular binding site for the M_r 55,000 form of the human plasminogen activator, urokinase. J. Cell. Biol. 100, 86-92.

Vassar, R., Coulombe, P.A., Degenstein, L., Albers, K., and Fuchs, E. (1991) Mutant keratin expression in transgenic mice causes marked abnormalities resembling a human genetic skin disease. Cell 64, 365-380.

Vercaigne-Marko, D., Carrere, J., Ducourouble, M.P., Davril, M., Laine, A., Amouric, M., Figarella, C., and Hayem, A. (1987) "In vivo" and "in vitro" inhibition of human pancreatic chymotrypsin by serum inhibitors. Biol. Chem. Hoppe-Seyler. 368, 37-45.

Villanueva, G.B. (1984) Predictions of the secondary structure of antithrombin III and the location of the heparin-binding site. J. Biol. Chem. 259, 2531-2536.

Vogel, C.N., Kingdon, H.S., and Lundblad, R.L. (1979) Correlation of in vivo and in vitro inhibition of thrombin by plasma inhibitors. J. Lab. Clin. Med. 93, 661-673.

Voorschuur, A.H., Kuiper, J., Neelissen, J.A.M., Boers, W., and Van Berkel, T.J.C. (1994) Diiferent zonal distribution of the asialoglycoprotein receptor, the α_2-macroglobulin receptor/low-density-lipoprotein receptor-related protein and the lipoprotein-remnant receptor of rat liver parenchymal cells. Biochem. J. 303, 809-816.

Warshawsky, I., and Schwartz, A.L. (1996) The 39-kDa protein regulates LRP activity in cultured endothelial and smooth muscle cells. Eur. J. Cell Biol. 69, 156-165.

Warshawsky, I., Herz, J., Broze Jr., G.J., and Schwartz, A.L. (1996) The low density lipoprotein receptor-related protein can function independently from heparan sulphate proteoglycans in tissue factor pathway inhibitor endocytosis. J. Biol. Chem. 271, 25873-25879.

Watada, M., Nagakawa, M., Kitani, T., Okajima, Y., Maeda, Y., Urano, S., and Ijichi, H. (1981) Identification of the AT III synthesizing hepatocytes by immunofluorescent technique. Thromb. Haemostas. 46, 284a.

Whisstock, J., Lesk, A.M., and Carrell, R. (1996) Modelling of serpin-protease complexes: antithrombin-thrombin, α_1-antitrypsin (358met-arg)-thrombin, α_1-antityrpsin (358met-arg)-trypsin, and antitrysin-elastase. Proteins:Structure, Function, and Genetics 26, 288-303.

Williams, S.E., Ashcom, J.D., Argraves, W.S., and Strickland, D.K. (1992) A novel mechanism for controlling the activity of α2-macroglobulin receptor/low density lipoprotein receptor-related protein. Multiple regulatory sites for 39-kDa receptor-associated protein. J. Biol. Chem. 267, 9035-9040.

Willnow, T.E., Goldstein, J.L., Orth, K., Brown, M.S., and Herz, J. (1992) Low density lipoprotein receptor-related protein and gp330 bind similar ligands including plasminogen activator-inhibitor complexes and lactoferrin, an inhibitor of chylomicron remnant clearance. J. Biol. Chem. 267, 26172-26180.

Willnow, T.E., Rohlmann, A., Horton, J., Otani, H., Braun, J.R., Hammer, R.E., and Herz, J (1996) RAP, a specialized chaperone, prevents ligand-induced ER retention and degradation of LDL receptor-related endocytic receptors. EMBO J. 15, 2632-2639.

Wilson, A.K., Coulombe, P.A., and Fuchs, E. (1992) The roles of K5 and K14 head, tail and R/KLLEGE domains in keratin filament assembly in vitro. J. Cell Biol. 119, 401-414.

Witmer, M.R. and Hatton, M.W.C. (1991) Antithrombin III-ß associates more readily than -α with the uninjured and de-endothelialized aorta wall in vitro and in vivo. Arterio. Thromb. 11, 530-539.

Wright, H.T., Qian, H.X., and Huber, R. Crystal structure of plakalbumin, a proteolytically nicked form of ovalbumin. Its relative relationship to the structure of cleaved α-1-proteinase inhibitor. J. Mol. Biol. 213, 513-528.

Wright, H.T. and Scarsdale, J.N. (1995) Structural basis for serpin inhibitor activity. Proteins:structure, function, and genetics. 22, 210-225.

Wu, J.K., Sheffield, W.P., and Blajchman, M.A. (1992) Molecular cloning and cell-free expression of murine AT-III. Thromb. Haemostas. 68, 291-296.

Wu, S.M. and Pizzo, S.V. (1996) Low density lipoprotein receptor-related protein/α_2-macroglobulin receptor on murine peritoneal macrophages mediates the binding and catabolism of low-density lipoprotein. Arch. Biochem. Biophys. 326, 39-47.

Wuillemin, W.A., Bleeker, W.K., Agterberg, J., Rigter, G., ten Cate, H., and Hack, C.E. (1996) Clearance of human factor X1a-inhibitor complexes in rats. Brit. J. Haematol. 93, 950-954.

Xiong, W., Tang, C.Q., Zhou, G.X., Chao, L., and Chao, J. (1991) In vivo catabolism of human kallikrein-binding protein and its complex with tissue kallikrein. J. Lab. Clin. Med. 119, 514-521.

Yankner, B.A., Duffy, L.K., and Kirschner, D.A. (1990) Science 25, 279-282.

Zheng, G., Bachinsky, D.R., Stamenkovic, I., Strickland, D.K., Brown, D., Andres, G., and McCluskey, R.T. (1994) Organ distribution in rats of two members of the low-density lipoprotein receptor gene family, gp330 and LRP/α_2-macroglobulin receptor, and the receptor-associated protein (RAP). J. Histochem. Cytochem. 42, 531-542.

Zou, Z., Anisowicz, A., Hendrix, M.J.C, Thor, A., Neveu, M., Sheng, S., Rafidi, K., Seftor, E., and Sager, R. (1994) Maspin, a serpin with tumor-suppressing activity in human mammary epithelial cells. Science 263, 526-529.

605 Third Avenue
New York, NY 10158-0012
212 850.6000
FAX 212. 850.6088

John Wiley & Sons, Inc.

Publishers Since 1807

December 10, 1997

Mike Wells
McMaster University
Dept. of Pathology
Fax: 905 527 4866

Dear Mr. Wells :

RE: Your letter dated December 10, 1997, requesting permission to reuse up to a maximum of 5 figures or 300 words in print media only from PROTEINS: STRUCTURE, FUNCTION AND GENETICS, a work published by Wiley-Liss, Inc., a subsidiary of John Wiley & Sons, Inc.

1. Permission is granted for this use, except that you must obtain authorization from the original source to use any material that appears in our work with credit to another source.
2. Permitted use is limited to the original edition of your forthcoming work described in your letter and does not extend to future editions of your work. In addition, permission does not include the right to grant others permission to photocopy or otherwise reproduce this material except for versions made by non-profit organizations for use by blind or physically handicapped persons.
3. Appropriate credit to our publication must appear on every copy of your work, either on the first page of the quoted text or in the figure legend. The following components must be included: Title, author(s) and /or editor(s), journal title (if applicable), Copyright © (year and owner). Reprinted by permission of John Wiley & Sons, Inc.
4. This permission is for non-exclusive world rights in the English language only. (For translation, please contact our Subsidiary Rights Department.)
5. This permission is for print rights only. If you wish permission for non-print media rights, please contact Judith Spreitzer, for requests for material from our books, and Neil Adams, for requests for material from our journals, when you have firm plans for publishing your book in a specific non-print medium.
6. **If your published work contains more than 8 figures and/or 300 words from our title, this permission shall be void.**

Sincerely yours,

Christopher Sheridan
John Wiley & Sons, Inc.
Permissions Department

If you have any questions regarding permissions, please call (212) 850-6011.
VISIT OUR WEBSITE @ "HTTP://WWW.WILEY.COM" FOR PERMISSIONS INFORMATION AND REQUEST FORMS.

CS210N23.DOC